PROGRAMA DE DOCTORADO EN
BIOMEDICINA Y FARMACIA

SEARCH FOR NEW IMMUNE PLAYERS IN PRIMARY HYPERCHOLESTEROLEMIA AND ATHEROSCLEROSIS DEVELOPMENT

TESIS DOCTORAL PRESENTADA POR:

ELENA DOMINGO PÉREZ

DIRECTORA:

MARÍA JESÚS SANZ FERRANDO

VALENCIA, ABRIL 2023

VNIVERSITAT DE VALÈNCIA Facultat de Medicina i Odontologia

Dña. María Jesús Sanz Ferrando, Catedrática del Departamento de Farmacología de la *Universitat de València*

HACE CONSTAR:

Que el trabajo titulado "*Search for new immune players in Primary Hypercholesterolemia and Atherosclerosis Development*", presentado por **Elena Domingo Pérez** para obtener el título de doctor, ha sido realizado en el Departamento de Farmacología de la Facultad de Medicina y Odontología de la *Universitat de València*, bajo mi dirección y asesoramiento.

Concluido el trabajo experimental y bibliográfico, autorizo la presentación y defensa de esta Tesis Doctoral para que sea juzgada por el Tribunal correspondiente.

Valencia, abril de 2023

MARIA JESUS| SANZ| FERRANDO

Firmado digitalmente por MARIA JESUS| SANZ|FERRANDO
Fecha: 2023.05.10 12:51:02 +02'00'

Fdo. **Dra. María Jesús Sanz Ferrando** (Directora)

La presente Tesis Doctoral ha sido financiada por las siguientes ayudas:

PROYECTOS

- Título del proyecto: Modulación Inmunofarmacológica de la Inflamación Sistémica asociada a Desordenes Metabólicos. Búsqueda de nuevas dianas terapéuticas y síntesis de fármacos novedosos. Entidad financiadora: Ministerio de Economía y Competitividad (SAF2014- 57845-R). Duración: De enero 2015 hasta junio 2018. Investigadores responsables: **Dra. María Jesús Sanz Ferrando** y Dr. Juan Francisco Ascaso Gimilio.

- Título del proyecto: Modulación farmacológica del sistema inmune como diana clave en la prevención de la enfermedad cardiovascular asociada a desórdenes metabólicos. Síntesis de fármacos novedosos. Entidad financiadora: Ministerio de Economía y Competitividad (SAF2017-89714-R). Duración: De julio 2018 hasta agosto 2021. Investigadores responsables: **Dra. María Jesús Sanz Ferrando** y Dr. Juan Francisco Ascaso Gimilio.

- Título del proyecto: Una aproximación traslacional desde la clínica a la experimentación animal: Estudio del papel del eje CCL11/CCR3 y la inflamación eosinofílica en la patología cardiovascular asociada a desórdenes metabólicos. Entidad financiadora: Conselleria de Educación, Cultura y Deporta (PROMETETO/2019/032). Duración: De enero 2020 hasta abril 2023. Investigador principal: **Dra. María Jesús Sanz Ferrando**.

- Título del proyecto: Modulación de la inflamación metabólica en la prevención de la patología cardiovascular: Identificación de nuevas dianas terapéuticas y desarrollo de fármacos novedosos. Entidad financiadora: Ministerio de Ciencia e Innovación (PID2020-120336RB-I00). Duración: De Septiembre 2021 hasta Agosto 2024. Investigador principal: **Dra. María Jesús Sanz Ferrando**.

BECAS

- Beca Predoctoral del Programa ACIF concedida por la Conselleria de Educación, Investigación, Cultura y Deporte de la Generalitat Valenciana. ACIF2018/037. Duración: septiembre 2018 hasta diciembre de 2021.

- Contrato Predoctoral. : Modulación de la inflamación metabólica en la prevención de la patología cardiovascular: Identificación de nuevas dianas terapéuticas y desarrollo de fármacos novedosos. Entidad financiadora: Ministerio de Ciencia e Innovación (PID2020-120336RB-I00). Duración: De Septiembre 2021 hasta Agosto 2024. Investigador principal: **Dra. María Jesús Sanz Ferrando**.

- Beca intramural INCLIVA para estancias formativas en centros de prestigio 2022. Entidad financiadora: Fundación Instituto de Investigación del Hospital Clínico de Valencia (INCLIVA). Duración: De septiembre 2022 hasta diciembre 2022. Lugar de estancia: Karolinska Institutet, Estocolmo, Suecia. Investigador principal: **Dr. John Pernow.**

A lo largo de esta Tesis Doctoral se han obtenido las siguientes publicaciones:

- Collado A†, Marques P†, Escudero P, Rius C, **Domingo E,** Martínez-Hervas S, Real JT, Ascaso JF, Piqueras L and Sanz MJ. *Functional role of endothelial CXCL16/CXCR6-platelet-leukocyte axis in angiotensin II-associated metabolic disorders. Cardiovascular Research*. 2018;114(13): 1764-75.

- Collado A†, Marques P†, **Domingo E†** , Perello E, Gonzalez-Navarro H, Martinez-Hervas S, Real JT, Piqueras L, Ascaso JF and Sanz MJ. *Novel Immune Features of the Systemic Inflammation Associated with Primary Hypercholesterolemia: Changes in Cytokine/Chemokine Profile, Increased Platelet and Leukocyte Activation. Journal of Clinical Medicine*. 2018;8(1):18.

†These authors have contributed equally to this work as first authors

- Marques P, Collado A, Martinez-Hervas S, **Domingo E**, Benito E, Piqueras L, Real JT, Ascaso JF and Sanz MJ. *Systemic Inflammation in Metabolic Syndrome: Increased Platelet and Leukocyte Activation, and Key Role of CX_3CL1/CX_3CR1 and CCL2/CCR2 Axes in Arterial Platelet-Proinflammatory Monocyte Adhesion. Journal of Clinical Medicine*. 2019;8(5):708.

- Collado A†, **Domingo E†**, Marques P†, Perelló E, Martinez-Hervas S, Piqueras L, Ascaso JF, Real JT and Sanz MJ. *Oral Unsaturated Fat Load Impairs Postprandial Systemic Inflammation in Primary Hypercholesterolemia Patients. Frontiers in Pharmacology.* 2021; 12:656244.

†These authors have contributed equally to this work as first authors

- Collado A, **Domingo E**, Piqueras L, and Sanz MJ. *Primary hypercholesterolemia and development of cardiovascular disorders: Cellular and molecular mechanisms involved in low-grade systemic inflammation and endothelial dysfunction. The International Journal of Biochemistry and Cell Biology*. 2021; 139:106066.

- Marques P, **Domingo E**, Rubio A, Martinez-Hervas S, Ascaso JF, Piqueras L, Real JT and Sanz MJ. *Beneficial effects of PCSK9 inhibition with alirocumab in familial hypercholesterolemia involve modulation of new immune players. Biomedicine and Pharmacotherapy* 2022; 145:112460.

- Corro-Morón M, Granell A, Ivanova V, **Domingo E**, Beltrán-Debón R, Barril X, Sanz MJ, Matheu MI, Castillón S and Diaz Y. *Revealing 2-dimethylhydrazino-2-alkyl alkynyl sphingosine derivatives as sphingosine kinase 2 inhibitors: Some hints on the structural basis for selective inhibition. Bioorganic Chemistry.* 2022; 121:105668.

- Marques P, Francisco V, Martínez-Arenas L, Carvalho-Gomes A, **Domingo E**, Piqueras L, Belenguer M and Sanz MJ. *Overview of Cellular and Soluble Mediators in Systemic Inflammation Associated with Non-Alcoholic Fatty Liver Disease. International Journal of Molecular Biosciences.* 2023;24(3):2313.

AGRADECIMIENTOS

En primer lugar, agradecer a mi directora de tesis, la Dra. María Jesús Sanz por guiarme en mi carrera científica desde mi trabajo de fin de carrera. Muchas gracias por el tiempo dedicado a mi formación y confiar en mis aptitudes.

Es imposible no agradecer en segundo lugar a mis compañeros de laboratorio en todos estos años. Muchos de nosotros hemos realizado la tesis juntos en el mismo laboratorio desde el principio: Luisa, Rebeca, Patrice, Mireia, Paqui, Samantha, Rosa, Laura Vila, Laura Pérez y Aida Collado, junto a la cual hemos abarcado y solucionado los problemas de este proyecto. A todos los estudiantes que han realizado sus trabajos con nosotros y me han ayudado a seguir avanzando en mis experimentos. A las nuevas incorporaciones del laboratorio, Inés y José, por desarrollar entre todos, un nuevo proyecto. Por supuesto, agradecer a las investigadoras principales Dra. Laura Piqueras, Dra. Nuria Cabedo y Dra. Vera Francisco, por sus enseñanzas y consejos. Y por último, pero no menos importantes, a la Dra. Guadalupe Herrera por invertir conmigo muchas horas junto al citómetro y por no negarme la ayuda cada vez que la he necesitado, y a Ana Díaz y todo el equipo del animalario por las enseñanzas y el tiempo invertido en el desarrollo de esta tesis.

Del mismo modo querría agradecer de nuevo a Aida Collado por su involucramiento en mi estancia predoctoral. Gracias a ella, pude disfrutar y conocer a los integrantes del laboratorio del Dr. Pernow en el *Karolinska Institutet,* en Estocolmo, Suecia. *I would like to thank my colleagues at Karolinska: Effy, Bo, Tong, Zhichao, Pauline and Julia for accompanying me many hours in the lab, making me feel like one more from the very first day and counting on me in all plans. I loved the experience. Of course, I would* also like to thank Dr. Pernow for allowing me to stay in his laboratory.

También quiero dar la gracias a todos mis amigos que han estado animándome en el desarrollo de esta tesis: Alejandra, Victoria, Mar Villanueva, Álex, Carlos(s), Amparo, Paula, Marta, Lidia

Quiero dar las gracias, asimismo, a mi familia, en especial a mis padres María José y Luis, porque han estado en cada mínimo detalle y en cada ayuda que he necesitado. Porque he llegado a donde estoy gracias a ellos. Y, por supuesto, a mi hermana Marta, que, con su punto de vista objetivo, siempre me ha dicho las palabras que necesitaba escuchar. Gracias a los que desgraciadamente ya no están, en especial, a mis abuelos, porque he llegado aquí por todos los consejos y las enseñanzas que me han inculcado.

Por último, y no por ello menos importante, un enorme gracias a Jaime porque durante estos últimos tres años, ha sufrido las consecuencias de mis peores y mis mejores días, me ha acompañado al laboratorio, y aunque no pertenece a este mundo, me ha escuchado y me ha dado los mejores consejos.

¡Gracias!

TABLE OF CONTENTS

LIST OF ABBREVIATIONS

APC	Allophycocyanin
ApoB	Apolipoprotein B
ApoE	Apolipoprotein E
AAM	Alternatively activated macrophages
BM	Bone marrow
BMC	Bone marrow cells
BMI	Body mass index
BSA	Bovine serum albumin
BUV	Brilliant ultraviolet
BV	Brilliant violet
CAMs	Cell adhesion molecules
CCLs/CXCLs	Chemokines ligands
CCRs/CXCRs	Chemokines receptors
CD	Cluster differentiation
CF	5-Carboxyfluorescein
CVDs	Cardiovascular diseases
Cys	Cysteine
DAB	3,3-Diaminobenzidine
DBP	Diastolic blood pressure
ECs	Endothelial cells
ECP	Eosinophil cation protein
EDN	Eosinophil-derived neurotoxin
EDTA	Ethylenediaminetetraacetic acid
ELISA	Enzyme-linked immunosorbent assay
eNOS	Endothelial nitric oxide synthase
EPX	Epoperoxidase
ESAM	Endothelial cell-selective adhesion molecule
ESL-1	E-selectin ligand-1
FACS	Fluorescent activated cell sorter
FBS	Fetal bovine serum
FcεR1α	High affinity IgE receptor
FH	Familial hypercholesterolemia
FITC	Fluorescein isothiocyanate
FSC	Forward scatter
GAGs	Glycosaminoglycans
GlyCAM-1	Glycosylation-dependent cell adhesion molecule-1
GM – CSF	Granulocyte Macrophage Colony-Stimulating Factor
GOT	Glutamic-oxalacetic transaminase
GPCR	G protein-coupled receptors
GPT	Glutamate-pyruvate transaminase
GRO-α	Growth-regulated oncogene-α/CXCL1
HUAEC	Human umbilical artery endothelial cells
HBSS	Hank's balanced salt solution
HCC	Hemofiltrate CC Chemokine
HDL	High-density lipoprotein
HeFH	Heterozygous familial hypercholesterolemia
HEPES	N-(2-Hydroxyethyl)piperazine-N'-(2-ethanesulfonic acid)
HMG-CoA	3-Hydroxy-3-methylglutaryl-CoA
HoFH	Homozygous familial hypercholesterolemia
HRP	Horseradish peroxidase
HS	Heparan sulfate
Hs – CRP	High-sensitivity C-reactive protein
ICAMs	Intercellular adhesion molecules
iE	inflammatory eosinophil
IFN-γ	Interferon-γ
Ig	Immunoglobulin
IL	Interleukin

IL-Rs	Interleukin receptors
IP	Interferon-gamma inducible protein
JAMs	Junctional adhesion molecules
LAMP-2	Lysosomal associated membrane protein-2
LDL	Low-density lipoprotein
LDLR	Low-density lipoprotein receptor
LDLRAP-1	Low density lipoprotein receptor adaptor protein 1
LFA-1	Lymphocyte function-associated antigen 1
LGSI	Low grade systemic inflammation
LOX-1	Lectin-Like Oxidized Low-Density Lipoprotein Receptor 1
LPAM-1	Lymphocyte Peyer's patch adhesion molecule-1
LPS	Lipopolysaccharides
mAb	Monoclonal antibody
Mac-s	Macrophage antigens
MAdCAM-1	Mucosal vascular addressin cell adhesion molecule-1
MBP	Myelin basic protein
M – CSF	Macrophage colony-stimulating factor
MCP-1	Monocyte chemoattractant protein-1/CCL2
MIPs	Macrophage inflammatory proteins
MMPs	Metalloproteinases
Mon(s)	Monocyte types
NIH	National Institutes of Health
NO	Nitric oxide
NOS	Nitric oxide synthase
OCT	Optimal cutting temperature compound
OUFL	Oral unsaturated fat load
ox-LDL	Oxidized low-density lipoprotein
pAb	Polyclonal antibody
PB	Pacific blue
PBS	Phosphate-buffered saline
PCSK9	Proprotein convertase subtilisin/kexin type 9
PE	Phycoerythrin
PECAMs	Platelet-endothelial cell adhesion molecules
PFA	Paraformaldehyde
PH	Primary hypercholesterolemia
PLT	Platelet
PMTs	Photomultiplier tubes
PSGL-1	P-selectin glycoprotein ligand-1
PCR	Quantitative polymerase chain reaction (also known as Real-time PCR)
RANTES	Regulated on activation, normal T cell expressed and secreted/CCL5
rE	resident eosinophil
ROS	Reactive oxygen species
SBP	Siastolic blood pressure
SEM	Standard error of the mean
sP-selectin	Soluble P-selectin
SSC	Side scatter
SMCs	Smooth muscle cells
TAE	Tris-acetate EDTA
TBS	Tris-buffered saline
Tc	T cytotoxic lymphocytes
TFG-β	Transforming growth factor-β
Th	T helper lymphocytes
TNF-α	Tumor necrosis factor-α
Tregs	Regulatory T cells
VCAM	Vascular cell adhesion molecule
VLA-4	Very late antigen-4
VLDL	Very-low density lipoprotein
VSMCs	Vascular smooth muscle cells
WHO	World Health Organization

LIST OF FIGURES

LIST OF TABLES

RESUMEN / ABSTRACT

RESUMEN

La hipercolesterolemia primaria (HP) es un trastorno lipídico caracterizado por niveles elevados de colesterol y lipoproteínas de baja densidad (LDL). Se asocia con una inflamación sistémica de bajo grado que probablemente sea la principal desencadenante de aterosclerosis prematura. Por ello, el primer objetivo de esta Tesis fue caracterizar el comportamiento de diferentes células inmunes en HP y sus posibles consecuencias. Para ello, sangre entera de 22 pacientes con HP y 21 controles de la misma edad se analizó mediante citometría de flujo para determinar el porcentaje de inmunofenotipos de leucocitarios, su estado de activación y los agregados de plaquetas y leucocitos. Los marcadores plasmáticos se determinaron mediante ensayo inmunoabsorbente ligado a enzimas (ELISA). La adhesión de los agregados de plaquetas y leucocitos al endotelio arterial estimulado por el factor de necrosis tumoral-α (TNF-α) se investigó utilizando el modelo dinámico de la cámara de flujo en placa paralela. Los pacientes con HP presentaron mayor porcentaje de monocitos Mon 3, linfocitos Th2 y Th17, plaquetas y leucocitos activados que los controles. Los porcentajes más elevados se dieron en los de agregados de plaquetas-neutrófilos, -monocitos y -linfocitos circulantes de los pacientes que fueron responsables de una mayor adhesión de los agregados plaquetas-leucocitos al endotelio arterial disfuncional. Además, los niveles circulantes de IL-8/CXCL8, MCP-1/CCL2, fratalquina/CX_3CL1 e IL-6 se correlacionaron positivamente con las características lipídicas clave de la HP, mientras que se encontraron correlaciones negativas para IL-4 e IL-10. De esta manera, mostramos la primera evidencia de que el aumento de la activación de plaquetas y leucocitos conduce a un aumento de los agregados de plaquetas y leucocitos en la HP y aumenta la adhesividad de los leucocitos al endotelio arterial, evento clave en la aterogénesis. Por tanto, la modulación del comportamiento del sistema inmunitario podría constituir una importante diana terapéutica en el control del desarrollo de enfermedades cardiovasculares asociadas a la HP.

A continuación, en el segundo objetivo de esta Tesis, se evaluó el efecto de una carga oral de grasas insaturadas (OUFL) sobre diferentes parámetros inmunológicos y sus consecuencias funcionales en pacientes con HP en estado posprandial. Se administró una preparación líquida comercial de triglicéridos de cadena larga (Supracal®; relación ω6/ω3 >20/1, OUFL) a 20 pacientes con HP y 10 controles de la misma edad. Se recolectó sangre entera antes (estado de ayuno) y 4 h después de la administración (estado posprandial) y usamos las mismas técnicas descritas anteriormente. El grupo con HP presentó un porcentaje más bajo de plaquetas activadas y monocitos tipo 1 circulantes, así como una activación de neutrofílica atenuada después de la OUFL, acompañada de un aumento significativo en el porcentaje de linfocitos T reguladores. En este grupo (pacientes con HP), la OUFL condujo a una disminución significativa de la adhesión leucocitria al endotelio arterial disfuncional (estimulado con TNF-α) y redujo los niveles plasmáticos de P-selectina soluble, factor plaquetario-4 (PF-4)/ CXCL4, CXCL8, CCL2, CCL5 y TNF-α. En conclusión, la OUFL presenta un impacto beneficioso en el estado protrombótico y proinflamatorio de los pacientes con HP y podría constituir una prometedora aproximación para atenuar la inflamación sistémica asociada con la HP y el consiguiente desarrollo de eventos cardiovasculares.

Finalmente, en el tercer objetivo de esta Tesis, el papel del eje eotaxina-1 (CCL11)/CCR3 en la inflamación sistémica asociada a la HP y el desarrollo de aterosclerosis fue investigado. La hipercolesterolemia primaria está asociada con el desarrollo de arteriosclerosis y la enfermedad cardiovascular, predominantemente infarto de miocardio y accidente cerebrovascular, siguen siendo la principal causa de muerte en todo el mundo, y la aterosclerosis se considera la patología subyacente más común. Se ha detectado expresión de eotaxina-1 (CCL11) en aortas ateroscleróticas humanas y de ratón, sin embargo, su papel en el desarrollo de lesiones ateroscleróticas sigue estando inexplorado. Sorprendentemente, se detectaron niveles circulantes más altos de eotaxina-1/CCL11 en pacientes con HP que en controles sanos de la misma edad. Dado que esta quimiocina señala exclusivamente a través del receptor CCR3, que se expresa constitutivamente en los eosinófilos, se detectó un aumento de los porcentajes circulantes de leucocitos que expresan CCR3, principalmente eosinófilos, en pacientes con HP, una característica hematológica no descrita previamente en esta enfermedad. De igual forma, se detectaron niveles plasmáticos más elevados de eotaxina-1/CCL11 y del porcentaje de eosinófilos circulantes en ratones *apoE*$^{-/-}$ sometidos a una dieta hipercolesterolémica. Estos efectos fueron acompañados por desarrollo de placa de ateroma, mayor expresión de eotaxina-1/ CCL11 en la lesión aterosclerótica junto con una mayor infiltración de macrófagos y linfocitos T. Asimismo, se ha descrito, por primera vez la infiltración clara de eosinófilos en el ateroma de animales *apoE*$^{-/-}$ en este entorno hipercolesterolémico. Por lo tanto, se generaron ratones deficientes en *apoE* y en el receptor de eotaxina-1/ (CCL11), CCR3, y se determinó el impacto de una dieta aterogénica en la formación de lesiones en ratones *apoE*$^{-/-}$*CCR3*$^{+/+}$ frente a *apoE*$^{-/-}$*CCR3*$^{-/-}$. Ratones *apoE*$^{-/-}$*CCR3*$^{+/+}$ o *apoE*$^{-/-}$*CCR3*$^{-/-}$ de dos meses de edad fueron sometidos o no a una dieta hipercolesterolémica (10,8% grasa, 0,75% colesterol) durante dos meses más. Los ratones *apoE*$^{-/-}$*CCR3*$^{+/+}$ y *apoE*$^{-/-}$*CCR3*$^{-/-}$ sometidos a una dieta hipercolesterolémica mostraron una clara formación de lesión aterosclerótica caracterizada por una mayor infiltración de macrófagos y linfocitos T, colágeno y núcleo necrótico que los sometidos a una dieta control. Sin embargo, los ratones *apoE*$^{-/-}$*CCR3*$^{-/-}$ mostraron una mayor lesión, mayor infiltración de macrófagos y linfocitos T y contenido en colágeno en la lesión que los ratones *apoE*$^{-/-}$*CCR3*$^{+/+}$. La expresión de eotaxina-1 en la lesión de ratones *apoE*$^{-/-}$*CCR3*$^{+/+}$ en este escenario hipercolesterolémico fue mucho mayor que la detectada en ratones *apoE*$^{-/-}$*CCR3*$^{-/-}$. Cabe señalar que, aunque se detectaron eosinófilos en la lesión aterosclerótica de ratones *apoE*$^{-/-}$*CCR3*$^{+/+}$, éstos estaban ausentes en la lesión de los animales *apoE*$^{-/-}$*CCR3*$^{-/-}$. Es más, no se detectaron eosinófilos en la circulación, el tejido adiposo o el intestino de los ratones *apoE*$^{-/-}$*CCR3*$^{-/-}$. Por el contrario, se detectó un mayor contenido de eosinófilos en la médula ósea de ratones *apoE*$^{-/-}$*CCR3*$^{-/-}$ en comparación con los *apoE*$^{-/-}$*CCR3*$^{+/+}$. Experimentos adicionales revelaron que los eosinófilos ejercen un papel beneficioso al mitigar la infiltración de monocitos CCR2^{+} a través de la generación adicional de eotaxina-1/CCL11 dentro del ateroma y aumentar la cantidad de macrófagos antiinflamatorios tipo M2, siendo ambos eventos mediados por la liberación de IL-4 y activación de la señalización de la *signal transducer and activator of transcription* 6 (STAT6). Todos los hallazgos antes mencionados están siendo refrendados con los estudios que actualmente se realizan con trasplantes de médula ósea (MO). En conjunto, estos hallazgos sugieren que en un entorno aterogénico, los eosinófilos se movilizan desde la médula ósea a través del eje eotaxina-1 (CCL11)/CCR3, lo que ha arrojado luz sobre un mecanismo aún no explorado y favorable de los eosinófilos en el desarrollo de la lesión aterosclerótica.

ABSTRACT

Primary hypercholesterolemia (PH) is a lipid disorder characterized by elevated levels of cholesterol and low-density lipoprotein (LDL) and is associated with a low grade systemic inflammation that is likely the main driver of premature atherosclerosis. Accordingly, the firt objective of this Thesis was to characterize the immune cell behaviour in PH and its potential consequences. Whole blood from 22 PH patients and 21 age-matched controls was analysed by flow cytometry to determine the percentage of leukocyte immunophenotypes, activation, and platelet-leukocyte aggregates. Plasma markers were determined by Enzyme-Linked ImmunoSorbent Assay (ELISA). The adhesion of platelet-leukocyte aggregates to tumor necrosis factor-α (TNFα)-stimulated arterial endothelium was investigated using the dynamic model of the parallel-plate flow chamber. PH patients presented greater percentage of Mon 3 monocytes, Th2 and Th17 lymphocytes, activated platelets, and leukocytes than controls. The higher percentages of circulating platelet-neutrophil, monocyte and lymphocyte aggregates in patients caused increased platelet-leukocyte adhesion to dysfunctional arterial endothelium. Circulating IL-8/CXCL8, MCP-1/CCL2, fractalkine/CX_3CL1, and IL-6 levels positively correlated with key lipid features of PH, whereas negative correlations were found for IL-4 and IL-10. We provide the first evidence that increased platelet and leukocyte activation leads to elevated platelet-leukocyte aggregates in PH and augmented arterial leukocyte adhesiveness, a key event in atherogenesis. Accordingly, modulation of immune system behavior might be a powerful target in the control of further cardiovascular disease in PH.

Next, in the second objective of this Thesis, the effect of an oral unsaturated fat load (OUFL) on different immune parameters and functional consequences in patients with PH in postprandial state was evaluated. A commercial liquid preparation of long-chain triglycerides (Supracal®; $\omega 6/\omega 3$ ratio >20/1, OUFL) was administered to 20 patients and 10 age-matched controls. Whole blood was collected before (fasting state) and 4 h after administration (postprandial state) and we used the same techniques as described above. The PH group had a lower percentage of activated platelets and circulating type 1 monocytes, and blunted neutrophil activation after the OUFL, accompanied by a significant increase in the percentage of regulatory T lymphocytes. In this group, the OUFL led to a significant impairment of leukocyte adhesion to the dysfunctional [tumor necrosis factor-α (TNFα)-stimulated] endothelium and reduced the plasma levels of soluble P-selectin, platelet factor-4 (PF-4)/CXCL4, CXCL8, CCL2, CCL5, and TNF-α. As a conclusion, the OUFL has a beneficial impact on the pro-thrombotic and pro-inflammatory state of PH patients and might be a promising macronutrient approach to dampen the systemic inflammation associated with PH and the development of further cardiovascular events.

Finally, in the third objective of this Thesis, the role of the eotaxin-1 (CCL11)/CCR3 axis in the systemic inflammation associated with PH and the development of atherosclerosis was investigated. Primary hypercholesterolemia is associated with arteriosclerosis development and cardiovascular disease,

predominantly myocardial infarction and stroke, remains the main cause of death worldwide, with atherosclerosis considered to be the most common underlying pathology. Eotaxin-1 (CCL11) expression has been detected in human and mouse atherosclerotic aortas, however, its role in the atherosclerotic lesion development remains elusive. Unexpectedly, higher circulating levels of eotaxin-1/CCL11 were detected in PH patients than in aged-matched healthy controls. Since this chemokine signals exclusively through the CCR3 receptor, which is constitutively expressed on eosinophils, increased circulating percentages of CCR3-expressing leukocytes, mainly eosinophils, were detected in PH patients, a hematological feature not previously described in this disease. Similarly, higher plasma levels of eotaxin-1/CCL11 and percentage of circulating eosinophils were detected in *apoE*$^{-/-}$ mice subjected to a hypercholesterolemic diet. These effects were accompanied by significant development of an atheroma plaque, increased eotaxin-1/CCL11 expression in the lesion together with enhanced infiltration of macrophages and T lymphocytes. Surprisingly, clear eosinophil infiltration in the atheroma of *apoE*$^{-/-}$ animals in this hypercholesterolemic setting was described for first time. Therefore, mice deficient in *apoE* and the eotaxin-1/ (CCL11) receptor, CCR3, were generated and the impact of an atherogenic diet in the lesion formation in *apoE*$^{-/-}$*CCR3*$^{+/+}$ *versus apoE*$^{-/-}$*CCR3*$^{-/-}$ mice was evaluated. Two months old *apoE*$^{-/-}$*CCR3*$^{+/+}$ or *apoE*$^{-/-}$*CCR3*$^{-/-}$ mice were subjected or not to an hypercholesterolemic diet (10.8% fat, 0.75% cholesterol) during two additional months. *ApoE*$^{-/-}$*CCR3*$^{+/+}$ and *apoE*$^{-/-}$*CCR3*$^{-/-}$ mice under an atherogenic diet showed clear atherosclerotic lesion formation characterized by enhanced macrophage and T lymphocyte infiltration, collagen and necrotic core than those subjected to a control diet. However, *ApoE*$^{-/-}$*CCR3*$^{-/-}$ mice showed increased lesion formation, augmented macrophage and T lymphocyte infiltration and collagen content within the lesion than *apoE*$^{-/-}$*CCR3*$^{+/+}$ mice. Eotaxin-1 expression within the lesion of *apoE*$^{-/-}$*CCR3*$^{+/+}$ mice in a hypercholesterolemic scenario was much higher than that detected in *apoE*$^{-/-}$*CCR3*$^{-/-}$mice. Of note, while eosinophils were detected in the atherosclerotic lesion of *apoE*$^{-/-}$ *CCR3*$^{+/+}$ mice they were absent in the lesion of *apoE*$^{-/-}$*CCR3*$^{-/-}$ animals. Inasmuch, no eosinophils were detected in the circulation, fat tissue or the gut of *apoE*$^{-/-}$*CCR3*$^{-/-}$ mice. In contrast, increased eosinophil content was detected in the bone marrow of *apoE*$^{-/-}$*CCR3*$^{-/-}$ mice compared with *apoE*$^{-/-}$*CCR3*$^{+/+}$. Additional experiments revealed that eosinophils exert a beneficial role mitigating CCR2^{+} monocyte infiltration through additional eotaxin-1/CCL11 generation within the atheroma and increasing the numbers of M2-like anti-inflammatory macrophages being both events mediated through the release of IL-4 and activation of signal transducer and activator of transcription 6 (STAT6) signalling pathway. All the above-mentioned findings are being endorsed with the studies that are currently performed with bone marrow (BM) transplants. Taken together, these findings suggest that in an atherogenic environment, eosinophils are mobilized from the bone marrow through eotaxin-1 (CCL11)/CCR3 axis which has shed mechanistic light to a yet unexplored and favourable effects of eosinophils in atherosclerosis lesion formation.

INTRODUCTION

1. THE INFLAMMATORY RESPONSE

Inflammation is an adaptative response to defend the organism against harmful stimuli that cause disruptions in homeostasis. It is a biological process that includes numerous molecular reactions to restore or repair the damaged tissue and eliminate damaging factors (Medzhitov, 2008). This complex mechanism usually begins with an insult that provokes the vasodilation of venules and arterioles, increased in vascular permeability, and the transmigration of leukocytes towards the inflammatory focus (Ley, Laudanna, Cybulsky, & Nourshargh, 2007).

Inflammation can be classified based on the duration of the process and the immune factors involved (Germolec, Shipkowski, Frawley, & Evans, 2018). Acute inflammation consists in a short response in which the innate immune system is mainly involved. The vasculature plays a crucial role since it is responsible for supplying circulating inflammatory mediators and cells to the injured area. It is characterized by the presence of platelets and neutrophils, increased blood flow, and edema formation in the inflammatory focus (Moro-García, Mayo, Sainz, & Alonso-Arias, 2018; Sherwood & Toliver-Kinsky, 2004). The classic symptoms of inflammation appear at this stage, such as swelling, redness, pain, warmth, and organ loss of function.

However, when all the organism's defense mechanisms fail, the state of chronic inflammation is triggered which is led by both, the innate and the adaptive immunity. It usually occurs when infections or tissue damage have not been resolved favourably. This stage is characterized by the action of other biochemical factors and cell types such as monocytes, macrophages and lymphocytes. The causes of chronic inflammation can be the consequence of the persistence of specific pathogenic organisms, the continuous exposure to chemical agents, such as tobacco, or repeated acute inflammation (Germolec et al., 2018; Moro-García et al., 2018).

Recent studies have shown that chronic inflammation underlies the development of many diseases or disorders such as diabetes, cancer or cardiovascular diseases, among others. For this reason, in the last two centuries, inflammation has become one of the greatest areas of research in diseases that were not previously be considered as inflammatory (Germolec et al., 2018; Ley et al., 2007).

1.1. Inflammatory process

1.1.1. Endothelial dysfunction

The vascular endothelium is a multifunctional organ composed by a monolayer of endothelial cells that lines the inner surface of blood vessels which border the vascular lumen. It plays an important role in vascular homeostasis since it regulates vascular tone, structure and permeability, as well as coagulation

processes (Cho, Lee, Chang, Lee, & Kim, 2018; Incalza et al., 2018). In addition, it produces a wide range of mediators involved in leukocyte adhesion in inflammatory processes, such as cell adhesion molecules (CAMs), cytokines, chemokines and other inflammatory mediators. Any alteration in the physiology of the endothelium leads to its activation and to a proinflammatory and prothrombotic state commonly known as endothelial dysfunction. These changes are accompanied by an imbalance in the bioavailability of nitric oxide (NO), an anti-inflammatory free radical produced by the enzyme nitric oxide synthetase (NOS); and abnormal blood vessels growth (Cyr, Huckaby, Shiva, & Zuckerbraun, 2020; Gavriilaki et al., 2020; Rajendran et al., 2013). This imbalance may be due to reduced expression of endothelial nitric oxide synthase (eNOS) and/or increased formation of reactive oxygen species (ROS) (Cyr et al., 2020; Gavriilaki et al., 2020).

Endothelium activation can be induced by the release of proinflammatory molecules such as histamine (stored in the granules of mast cells), cytokines such as tumor necrosis factor-α (TNF-α), interleukin-1β (IL-1β), and prostaglandins, among others, from damaged tissue (Schnoor, Alcaide, Voisin, & van Buul, 2015). In this activated state, the CAM expression, cytokine production and proinflammatory chemicals are increased, which are responsible of the leukocyte recruitment to the inflammatory focus (McEver, 2010).

1.1.2. *The leukocyte recruitment cascade*

As a consequence of the detection of a foreign agent or tissue injury, the organism initiates a cascade of molecular signalling reactions, whose objective is the repair of the tissue and/or the elimination of the causal agent through the generation and release of mediators of inflammation. These mediators are molecules, usually of low molecular weight, that regulate all the steps of these cascade reactions (Ley et al., 2007).

Leukocyte infiltration is a biological process of homeostatic maintenance of the organism that occurs in the inflammatory processes. This process consists in an adhesion cascade involving complex interactions between circulating leukocytes and the vascular endothelium (L. Chen et al., 2018; Filippi, 2019). As a consequence of these interactions, inflammatory signalling mechanisms are activated through the release of proinflammatory cytokines, chemokines and other chemoattractants (Soehnlein & Lindbom, 2010).

Cytokines are important mediators involved in leukocyte infiltration (J. M. Zhang & An, 2007). Among them, proinflammatory cytokines such as IL-1, IL-6 or TNF-α, despite not having chemotactic activity, they induce the increased expression of endothelial CAMs and the generation and release of chemoattractants including chemokines from different immune cells (Propper & Balkwill, 2022).

In this line, circulating leukocytes adhere to the activated vascular endothelium through the interaction of different cell adhesion molecules (CAMs). These CAMs are surface ligands, usually glycoproteins, that play a critical role in maintaining tissue integrity and cell migration. Therefore, these CAMs promote direct interaction between leukocytes and endothelial cells (Nourshargh & Alon, 2014).

On the other hand, the release and activity of different chemotactic factors are also crucial in the development of the inflammatory process (Propper & Balkwill, 2022). Chemotactic factors are locally produced soluble chemical mediators and molecular guidance cues whose function is to attract and guide leukocytes to the inflammatory site partly through the regulation of the expression of some CAMs (Hughes & Nibbs, 2018). Chemoattractants can be divided into four families: lipids, *N*-formylated peptides, complement anaphylotoxins, and chemokines (Petri & Sanz, 2018).

1.1.3. *Steps of leukocyte infiltration*

Leukocyte infiltration requires the movement of cells through the vascular wall. Currently, the leukocyte infiltration process consists in four steps: primary adhesion or leukocyte rolling, leukocyte activation, firm adhesion, and finally, transendothelial migration (Ley et al., 2007).

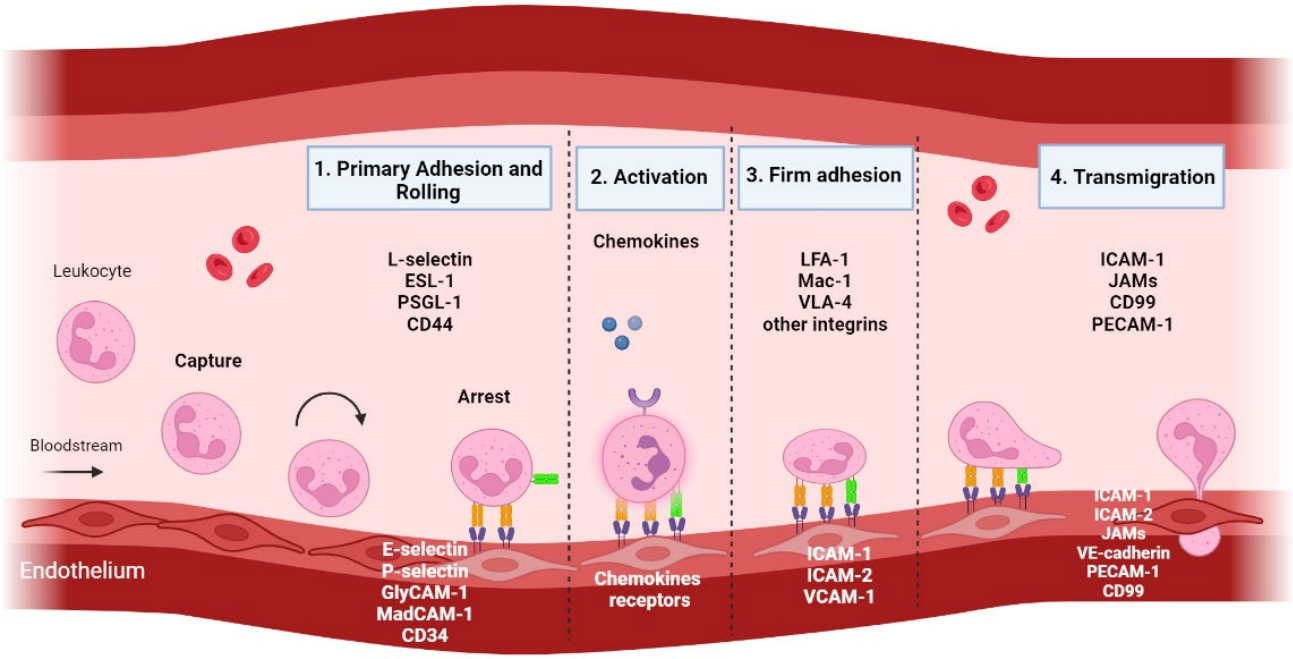

Figure 1. Steps of leukocyte recruitment and extravasation.

Under inflammatory conditions, endothelial cells and leukocytes express diverse CAMs that contribute to leukocyte rolling, which is the first step in the leukocyte infiltration process. Then, leukocytes become activated, and they firmly attach to the endothelium. After the adhesion stage, leukocytes migrate to the inflammatory focus. Only the most remarkable cell adhesion molecules are shown. Created with BioRender.com.

1.1.3.1. *Primary adhesion: leukocyte rolling*

Leukocyte rolling is first step and considered the limiting step for leukocyte infiltration into the subendothelial or extravascular space. This first interaction between leukocytes and the endothelium allows further contacts with chemokines and other chemoattractants immobilized on the surface or presented by endothelial cells. The combined expression of different CAMs and chemokine receptors determines the leukocyte subpopulation that enters into the tissue (Ley et al., 2007). Leukocyte rolling is a reversible and weak interaction mainly mediated by selectins (**Figure 1**).

Once the endothelium is activated through the recognition of a causal inflammatory agent, increased expression of some selectins take place. Selectins are transmembrane glycoproteins with the ability to establish interactions with carbohydrates. To date 3 are described: E-selectin (located in the endothelium), P-selectin (located in the endothelium and platelets) and L-selectin (located on the leukocyte surface). These CAMs facilitate interactions between the ligands present on leukocytes and the endothelium (Langer & Chavakis, 2009). The main ligands of selectins are sialylated, fucosylated or sulfated carbohydrates.

Among the selectin ligands, the P-selectin glycoprotein ligand-1 (PSGL-1) is a transmembrane mucin, which was originally described as a P-selectin ligand. However, currently, it has been shown to have the ability to bind to all three selectins. PSGL-1 is expressed on endothelial cells and on most leukocytes, but it is only functional when is glycosylated. E-selectin ligand-1 (ESL-1) and glycosylated CD44, both expressed on leukocytes, have affinity for E-selectin (Ley et al., 2007). Finally, the glycosylation-dependent cell adhesion molecule-1 (GlyCAM-1), the mucosal vascular addressin cell adhesion molecule-1 (MAdCAM-1) and the mucin-like protein CD34, expressed on endothelial cells, can interact with L- selectin (Hintermann & Christen, 2019) (**Table 1**).

Table 1 – CAMs: Selectins, adapted from (Hintermann & Christen, 2019)

Name	Expressed by	Ligand(s)	Function(s)
E-selectin/CD62E	Endothelial cells	PSGL-1/ ESL-1/ CD44	Leukocyte Rolling
L-selectin/CD62L	Leukocytes	PSGL-1/MAdCAM-1/CD34	Leukocyte Rolling and signalling
P- selectin/CD62P	Endothelial cells and activated platelets	PSGL-1	Leukocyte rolling and tethering

CD: Cluster of Differentiation; PSGL-1: P-Selectin Glycoprotein Ligand-1; ESL-1: E-Selectin Ligand-1; MAdCAM-1: Mucosal vascular Addressin Cell Adhesion Molecule-1

Depending on the intensity of the inflammatory response, the leukocytes may adhere firmly to the endothelium or may return to the bloodstream.

1.1.3.2. *Leukocyte activation*

As previously described (***Section 1.1.2 The leukocyte recruitment cascade***), leukocytes require to be activated before firmly adhere to the endothelium. Rolling leukocyte can detect chemoattractans such as lipid mediators and chemokines. This chapter will be only focused on the role of chemokines on leukocyte activation.

Chemokines

Chemokines or chemotactic cytokines are a family of cytokines with chemotactic properties. They are widely generated by cytokines, a large family of low molecular weight proteins (~5-20 kDa) that regulate cell communication and are involved in autocrine, paracrine and endocrine signalling as immunomodulating agents. One of the most relevant cytokines in atherosclerosis is tumor necrosis factor-α (TNF-α). Although it does not exert chemotactic properties, it causes increased CAM expression and chemokine production (Wakefield, James, Samlaska, & Meltzer, 1991). In addition, it induces endothelial dysfunction, and is considered one of the major contributors to the initiation and progression of the atherosclerotic process. It is produced by macrophages, endothelial cells, lymphocytes and many other immune cells (Dimitrov et al., 2013; Mehta, Gracias, & Croft, 2018; Wakefield et al., 1991). TNF-α is involved in many pathological disorders such as rheumatoid arthritis, obesity, atherosclerosis, metabolic syndrome and familial hypercholesterolemia, etc. (Aggarwal, Gupta, & Kim, 2012; Croft & Siegel, 2017).

Chemokines can modulate leukocyte trafficking and their selective migration to the inflammatory focus. For this purpose, they are usually immobilized by glycosaminoglycans (GAGs) or heparan sulfate (HS) in particular on the lumenal membrane of endothelial cells. These mediators of ~8-12 kDa are composed by 70-130 amino acids (Ozga, Chow, & Luster, 2021). In addition to exert homeostatic functions such as leukocyte maturation, trafficking and tissue repair, chemokines are associated to pathological conditions, including metastasis and autoimmune diseases, among others (Blanchet, Langer, Weber, Koenen, & von Hundelshausen, 2012). Additionally, they are necessary to mediate leukocyte adhesion to the vascular endothelium and transmigration through a paracrine or autocrine pathway. All of them share a structural homology since intramolecular disulfide bonds are established, which gives them an essential structure to establish interactions with their receptors (Miller & Mayo, 2017).

Currently, there are two classifications to designate chemokines. The first classification is based on the number and arrangement of their amino terminal cysteine residues (Zernecke & Weber, 2010). All chemokines have four cysteine residues at the N-terminus except α and β lymphoactins, which have only two. These residues form disulfide bonds that allow the tertiary fold to be established/adopted. According to this classification, there are four subfamilies of chemokines: C-C, C-X-C, C-X_3-C and C (**Figure 2**) (Miller & Mayo, 2017). The first three families are characterized for having four conserved cysteine residues (Cys), while those of the C family have only two at the N-terminus. The CC group has two adjacent cysteines at

the N-terminus (e.g. monocyte chemoattractant protein-1 or MCP-1/CCL2); the CXC group has an amino acid in between the two cysteines (e.g IL-8/CXCL8); the CX_3C group has 3 amino acids between them (e.g. fractalkine or CX_3CL1) and the C group has just one cysteine residue at the N-terminus (e.g XCL1 or XCL2/ lymphotactins-α and -β) (M. Zhang et al., 2018; Zlotnik & Yoshie, 2012). Except CX_3CL1 and CXCL16, which are normally expressed as membrane-bound, all other chemokines are soluble.

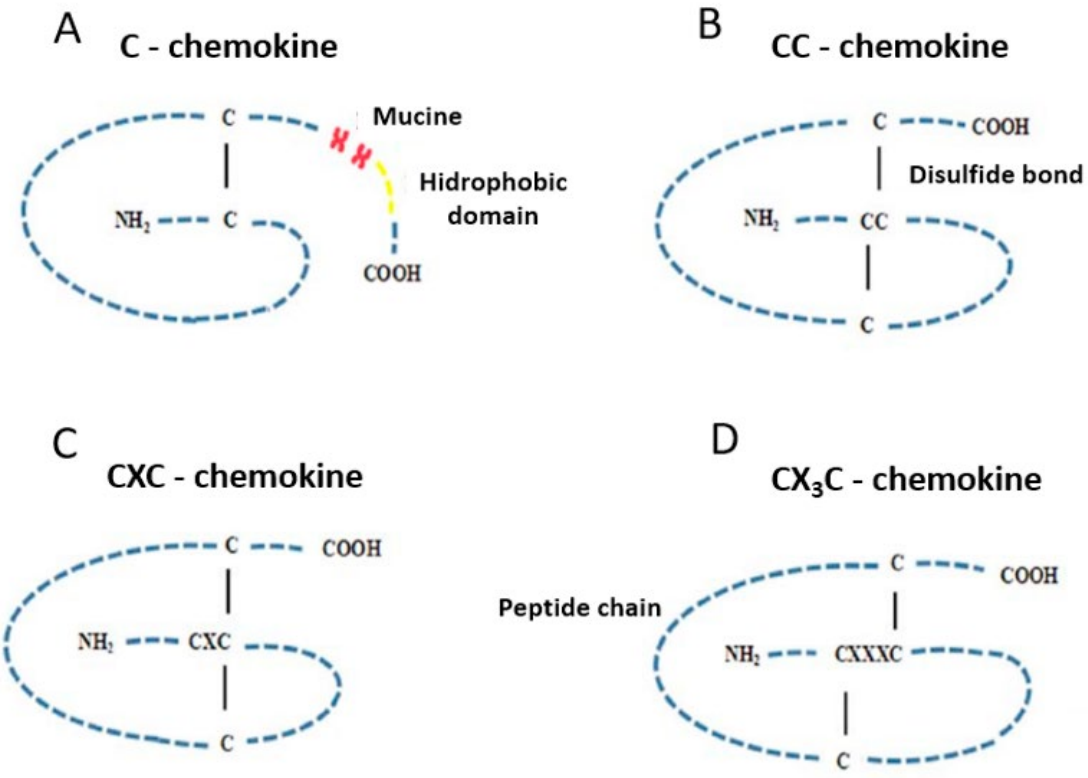

Figure 2. Structure of different chemokine families.

According to the conserved N-terminal cysteine-containing motif, chemokines can be classified into four subfamilies: chemokines type C (**A**), chemokines type C-C (**B**), chemokines type C-X-C (**C**) and chemokines type C-X_3-C (**D**). Letter C refers to a cysteine amino acid and letter X refers to any amino acid different from cysteine. Discontinuous lines represent peptide chain and continuous lines refer to disulfide bonds. Adapted from (M. Zhang et al., 2018).

Alternatively, chemokines can be classified according to their functional activity. This classification groups chemokines into three families: proinflammatory chemokines, involved in the inflammatory process; homeostatic chemokines, constitutively expressed and involved in leukocyte migration in non-pathological conditions; and chemokines with mixed functions (Zlotnik & Yoshie, 2012).

As mentioned above, chemokines are potent mediators of leukocyte adhesion and migration through their interaction with G protein-coupled receptors (GPCR) (L. Chen et al., 2018). The receptors are composed by seven transmembrane α-helices surrounding a central cleft and connected to three intracellular and three extracellular loops. The N-terminus and the C-terminus are located in the extracellular and intercellular part, respectively (**Figure 3**) (Crijns, Vanheule, & Proost, 2020; Hilger, Masureel, & Kobilka, 2018). These receptors are further classified into subfamilies: rhodopsin, secretin/glucagon receptors, and the metabotropic receptor family for glutamate/calcium sensing. The intracellular region is the one that is bound to the G protein, which in turn can be subjected to regulatory phosphorylation (Vass et al., 2018).

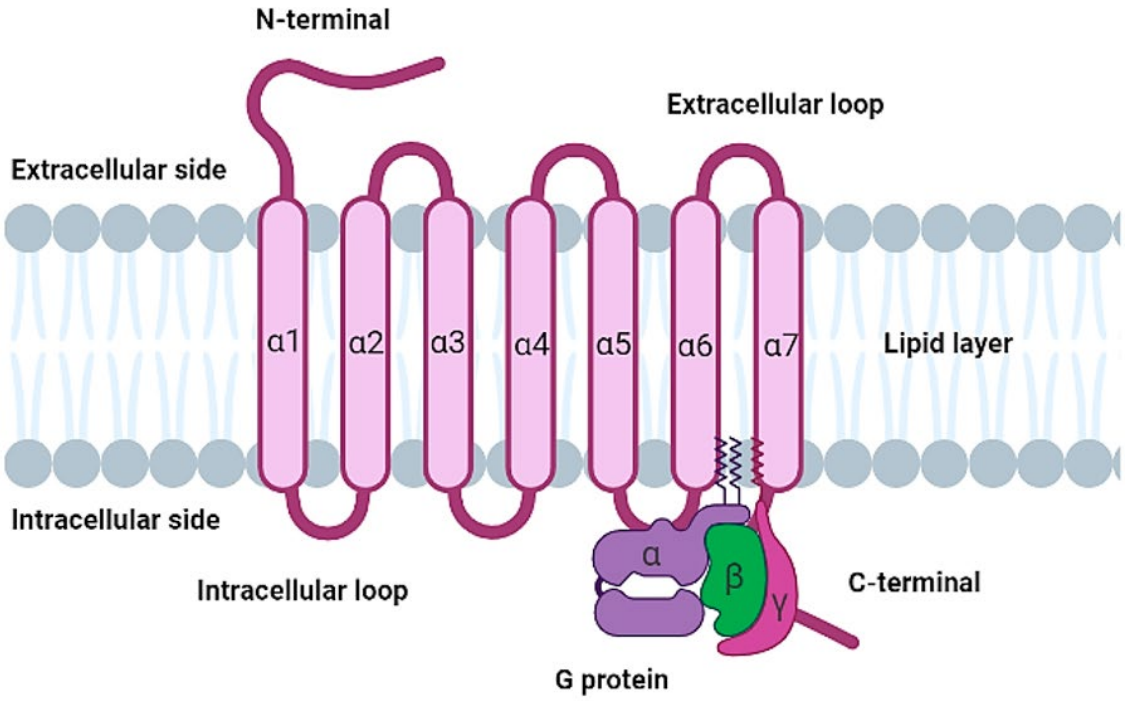

Figure 3. Generic structure of G protein-coupled receptors.

G protein-coupled receptors are composed by seven transmembrane α-helices (α) connected by three intracellular and three extracellular loops. The N-terminus and the C-terminus are in the extracellular and intracellular parts, respectively. Created with BioRender.com.

To date, 48 human chemokines have been identified (Roy, Evans, & Dwinell, 2014) but only 23 receptors have been described, which means that the same receptor can recognize several chemokines. Likewise, a chemokine can interact with several receptors.

1.1.3.3. *Firm adhesion*

Rolling Leukocyte rolling can detect chemokines and through their engagement to cognate GPCR "inside-out" signals are triggered which lead to the activation of leukocyte integrins (β_2 and/or α_4 integrins), responsible for firm adhesion to the vascular endothelium. Integrins are a family of glycosylated transmembrane proteins composed by two subunits: α and β. They are involved in numerous cellular functions and expressed on the cell surface of leukocytes (Bednarczyk, Stege, Grabbe, & Bros, 2020). Basally, circulating leukocytes maintain their integrins in an inactive state. When they are activated by the interaction of selectins and chemokines, the affinity of integrins for their ligands is increased. Integrins are classified according to the β subunit in: β_1 (CD29), β_2 (CD18), and β_3 (CD61) (Guenther, 2022). Among them, the most important integrins in leukocyte adhesion are β_2 and α_4 integrins. β_2 integrins are coupled to different α subunits (**Table 2**).

Table 2 – CAMs: β_2 Integrins, adapted from (Guenther, 2022)

Name	Expressed by	Ligand(s)	Function(s)
$\alpha_L\boldsymbol{\beta_2}$/ LFA-1/ CD11a/CD18	Granulocytes, Monocytes, Lymphocytes	ICAM-1,-2 ICAM-3, -5	Locomotion leukocyte tethering
$\alpha_M\boldsymbol{\beta_2}$/ Mac-1/ CD11b/CD18	Granulocytes, Monocytes	ICAM-1 ICAM-2	Locomotion, leukocyte tethering, activation and transmigration
$\alpha_X\boldsymbol{\beta_2}$/ CD11c/CD18	Granulocytes, Monocytes, Macrophages	ICAM-1 ICAM-4	Leukocyte adhesion and migration
$\alpha_D\boldsymbol{\beta_2}$/ CD11d/CD18	Dendritic cells, Macrophages, CD8 lymphocytes	ICAM-3 VCAM-1	Leukocyte tethering

LFA-1: Lymphocyte Function-associated Antigen-1, CD: Cluster of Differentiation, ICAM: Intercellular Adhesion Molecule; Mac-1: Macrophage-1 antigen; VCAM-1: Vascular Cell Adhesion Molecule-1.

Another family of integrins relevant for leukocyte adhesion are α_4 integrins which are coupled to different β subunits (**Table 3**).

Table 3 – CAMs: α_4 Integrins, adapted from (Guenther, 2022)

Name	Expressed by	Ligand(s)	Function(s)
$\boldsymbol{\alpha_4}\beta_1$/ VLA-4/CD49d/CD29	Leukocytes, except neutrophils	VCAM-1 and CS-1 fragment of fibronectin	Leukocyte tethering, and firm adhesion
$\boldsymbol{\alpha_4}\beta_7$/LPAM-1	Lymphocytes	VCAM-1, MAdCAM-1, and CS-1 fragment of fibronectin	Locomotion, leukocyte tethering, activation and transmigration

VLA-4: Very Late Antigen-4, CD: Cluster of Differentiation, LPAM-1: Lymphocyte Peyer's patch Adhesion Molecule-1; VCAM-1: Vascular Cell Adhesion Molecule-1, MAdCAM-1: Mucosal vascular Addressin Cell Adhesion Molecule-1.

Activated integrins bind with relatively high affinity to their counter endothelial ligands that belong to the immunoglobulin (Ig)-like superfamily including intercellular adhesion molecule-1 (ICAM-1) for β_2-integrins, and vascular cell adhesion molecule-1 (VCAM-1) for α_4-integrins, resulting in firm adhesion and arrest. They are especially expressed on endothelial cells, although they can also be found on the surface of leukocytes, platelets, and other cells. The most prominent immunoglobulins are ICAM-1, -2 and -3, VCAM-1, MAdCAM-1 and platelet-endothelial cell adhesion molecule-1 (PECAM-1) (Hintermann & Christen, 2019) (**Table 4**). Some immunoglobulins are constitutively expressed, while others require *de novo* synthesis in response to different stimuli such as cytokines or bacterial toxins.

The integrins are not only responsible for the attachment of leukocytes to the endothelium, they are also able to transfer signals from the extracellular domain into the cell (outside-in signaling) (Ginsberg, Partridge, & Shattil, 2005). These signals strengthen adhesion and induce crawling after leukocytes flatten and extend pseudopods across the endothelial surface (Giagulli et al., 2006; Ginsberg et al., 2005; Ley et al., 2007).

Table 4 – CAMs: Important Immunoglobulin-like CAMs, adapted from (Guenther, 2022)

Name	Expressed by	Ligand(s)	Function(s)
ICAM-1	Macrophages, EC, other cells	$\alpha_M\beta_2$, $\alpha_L\beta_2$	T-cell responses,leukocyte adhesion to EC
ICAM-2	EC	$\alpha_L\beta_2$	Leukocyte adhesion to EC
ICAM-3	Leukocytes	$\alpha_L\beta_2$	T-cell responses, leukocyte aggregation
ICAM-4	Erythroid precursors	$\alpha_4\beta_1$, $\alpha_V\beta_3$, $\alpha_{IIb}\beta_3$	Regulate erythropoiesis
VCAM-1	Activated EC, SMC	$\alpha_4\beta_1$, $\alpha_4\beta_7$	Mononuclear cell adhesion to EC
PECAM-1	Leukocytes, platelets and EC	PECAM-1	EC junctions, leukocyte transmigration, cell signaling
MAdCAM-1	EC of Peyer patches	$\alpha_4\beta_7$	Lymphocyte homing

ICAMs: Intercellular Adhesion Molecules; EC: Endothelial Cell; VCAM-1: Vascular Cell Adhesion Molecule-1; SMC: Smooth Muscle Cell; PECAM-1: Platelet-Endothelial Cell Adhesion Molecule-1; MAdCAM-1: Mucosal vascular Addressin Cell Adhesion Molecule-1.

1.1.3.4. *Transmigration to inflammatory focus*

Both integrins and their ligands can interact with components of the extracellular matrix, which means their involvement in cell-cell mechanisms and matrix-cell interactions, crucial in the process of transmigration of leukocytes to the inflammatory focus (Hintermann & Christen, 2019).

Once leukocytes are firmly attached to the endothelium, leukocyte transmigration occurs. This is the last step of the leukocyte recruitment cascade that allows the migration of leukocytes to the inflammatory focus. In this process, the extension of the cell cytoplasm occurs, promoted by a rearrangement of the cytoskeleton induced by integrins, and followed by a crawling guided by intravascular chemotactic gradients along the endothelium in the search for the ideal site to transmigrate. It is the least understood step and involves platelet-endothelial cell adhesion molecule-1 (PECAM-1 or CD31), junctional adhesion molecules (JAM), CD99, endothelial cell-selective adhesion molecule (ESAM) and intercellular adhesion molecules (ICAMs). These mechanisms reduce leukocyte adhesion, facilitate diapedesis and migration through a chemotactic gradient.

2. ATHEROSCLEROSIS AND CARDIOVASCULAR RISK

Cardiovascular diseases (CVDs) are the leading cause of morbidity and mortality in Western societies, accounting for 17.9 million deaths between 2017-2019, (32% of annual deaths) (Collado, Domingo, Piqueras, & Sanz, 2021; Hilger et al., 2018; "World Health Organization cardiovascular disease risk charts: revised models to estimate risk in 21 global regions," 2019). According to the World Health Organization (WHO), the pathology with the highest mortality is the ischemic heart disease, since it represents the 16% of the total deaths in 2019, followed by cerebrovascular accidents. Despite all the technological advances in medicine and the emergence of new pharmacological therapies, poor lifestyle habits are the main cause of the increased incidence of diabetes and obesity, pathologies that are closely associated to cardiovascular disease development (Libby, 2021). Many factors contribute significantly to CVDs development, but chief amongst these is atherosclerosis, which is considered as the cardinal underlying pathology and its prevalence has increased in the last years (Libby, Ridker, & Hansson, 2011; Moore, 2019).

Atherosclerosis is a lipid-driven inflammatory disease of the arterial intima in which the balance of proinflammatory mechanisms and resolution of inflammation dictates the ultimate clinical outcome (Bäck, Yurdagul, Tabas, Öörni, & Kovanen, 2019). It is a chronic vascular and inflammatory pathology, characterized by the presence of high plasma concentrations of low-density lipoproteins (LDL), which causes an accumulation of lipids such as cholesterol and cholesterol crystals in the artery wall, known as atherosclerotic plaque or atheroma (Wolf & Ley, 2019). This accumulation of lipids is accompanied by an infiltration immune cells, calcium accumulation, and a lining of fibrous tissue, such as collagen fibres and vascular smooth muscle cells. This deposition can cause a narrowing of the aortic lumen, which increases the risk of developing associated cardiovascular pathologies (Libby et al., 2019).

Atherosclerosis occurs in regions in which the vasculature describes complex geometric shapes, such as curves or bifurcations. At these points, the blood flow rate slows down and allows the deposition of the atherosclerotic plaque (Tabas, García-Cardeña, & Owens, 2015). Normally, it develops in the subendothelial space or intima of intermediate-caliber elastic arteries, medium-sized muscular arteries, and large-caliber vessels. The largest area of the aortic arch and the carotid bifurcations are those where blood flow is modified and causes an increase in endothelial dysfunction.

Atherosclerosis is not a uniform pathology in the population. It is considered a multifactorial disease since it has a genetic and an environmental component. One of the main risk factors is dyslipidemia, a series of pathological conditions that have in common the alteration of lipid metabolism, which modifies the concentrations of lipids and lipoproteins. Furthermore, it has been shown that CVDs are predicted by

a low degree of systemic inflammation, a clear driver of the atherosclerotic process. Another feature of atherosclerosis is its asymptomatology, because normally patients do not suffer any symptoms until the severity is notorious (Badimon & Vilahur, 2014).

2.1. Atherogenesis

Atherogenesis is the process of the atherosclerotic lesion formation. Initially, atherogenesis was thought to be characterized by the deposition of fats in the arterial wall (Libby et al., 2011). Currently, it is known that this pathology involves highly specific biochemical and molecular responses with constant interactions between several cellular mediators. Furthermore, this process involves immune cells, mainly macrophages and T lymphocytes, and is induced by insults to the endothelial cells linning the vascular bed (Gisterå & Hansson, 2017; Libby, 2021; Libby et al., 2019). Accumulating scientific evidence relates inflammation and its effector mechanisms with the pathogenesis of atherosclerosis.

2.1.1. *Onset of atherosclerotic lesion formation*

The onset of atherosclerosis occurs in the presence of an excess low-density lipoprotein (LDL) (Kamstrup, 2021). These lipoproteins are protein carriers of lipid oxidation products, components that stimulate the atherosclerotic process. Two of the most important lipoproteins are: low-density lipoprotein particles (LDL), which transports its products to peripheral tissues, and high-density lipoprotein particles (HDL), which transports them to the liver (Ahotupa, 2017). LDL are rich in cholesterol, surrounded by a phospholipid shell and apolipoprotein B that transport water-insoluble cholesterol through the blood (Bäck et al., 2019; Libby, 2021).

Recent studies have shown that LDL concentrations in the range of 20 – 30 mg/dL are enough to maintain good health. However, the concentrations of cholesterol in the blood prevailing in most societies far exceed the biological needs of the organism, a fact that allows the atherosclerosis development. The duration and extent of exposure to the above-ideal concentrations of LDL are associated with atherosclerotic disease development (Libby, 2021).

The structure of the arterial wall comprises three layers: adventitia, media, and intima. The furthest layer from the aortic lumen is the lamina adventitia. This layer contains nerve endings, vascular adipose tissue and connective elements (collagen fibres and fibroblasts) that ensure adherence with the rest of the organs (**Figure 4**). Adventitia components are also involved in vascular development and remodelling, immune surveillance, and signal exchanges between the blood vessel and the tissue in which it resides (Zhao, Vanhoutte, & Leung, 2015).

The middle layer lies between the adventitial layer and the innermost layer, the media layer. The middle lamina consists of vascular smooth muscle cells (VSMCs), which regulate the constriction and dilation of blood vessels (**Figure 4**). These constrictions increase the intercellular concentration of calcium, which binds to calmodulin and cause a smooth contraction of the muscles (Zhao et al., 2015).

The innermost layer is composed primarily by endothelial cells that function as a barrier between the vessel lumen and the blood (**Figure 4**). The vascular endothelium plays a key role in the basal and dynamic regulation of blood vessels with the release of different mediators such as nitric oxide (NO) or prostacyclin among others.

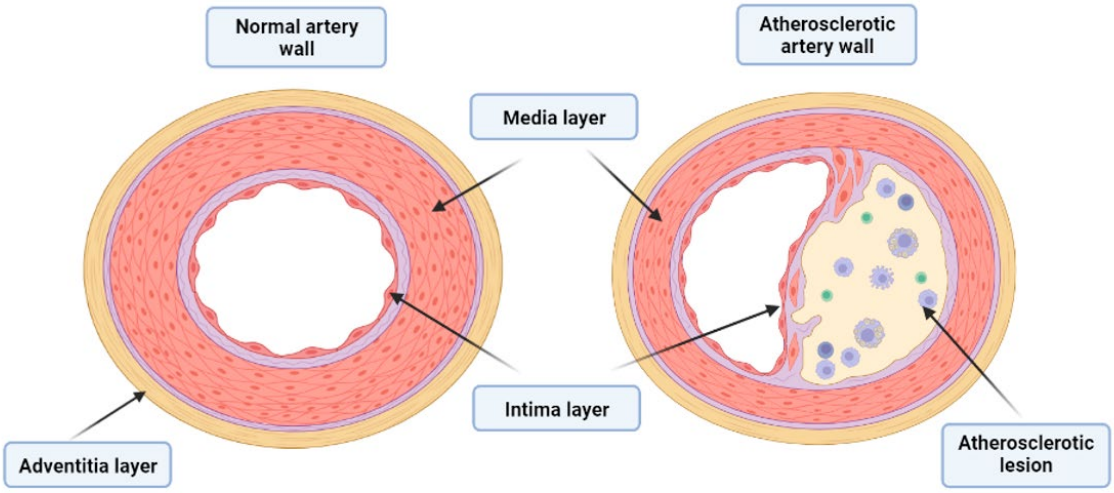

Figure 4. Trilaminar structure.

The outermost layer, the adventitia, contains nerve endings, mast cells, and vasa vasorum, microvessels that nourish the outer layer of the media. The tunica media consists in smooth muscle cells and an extracellular matrix comprising elastin, collagen and other macromolecules. The atherosclerotic plaque forms in the innermost layer, the intima. Created with BioRender.com.

As previously indicated, atherosclerosis is an inflammatory disease and its onset occurs when the endothelium reaches an activated state leading to endothelial dysfunction. This activation is manifested by an alteration in the bioavailability of NO due to either a reduction in the production by endothelial NO synthase (eNOS), or more frequently, through an increased production of reactive oxygen species (ROS) (Zhao et al., 2015). NO normally exerts a protective effect on the vessel wall. The imbalance in NO bioavailability leads to an alteration in the arterial vasomotor properties which can alter LDL transport and promote its accumulation in the intima (Incalza et al., 2018). In addition, endothelial cell activation leads to an increased expression and activation of CAMs and generation and release of chemoattractants such as chemokines that mediate the recruitment of immune cells, mainly monocytes and T cells, and their subendothelial transmigration (**Figure 5**).

Monocytes, macrophages, endothelial cells and SMCs generate free radicals that undergo enzymatic modifications oxidizing LDL particles (ox-LDL) (Bartlett, Ludewick, Misra, Lee, & Dwivedi, 2019). Then, a proinflammatory and prothrombotic phenotype of the endothelium takes place with the increased expression of CAMs and chemokine synthesis leading to endothelial dysfunction, a process that precedes the atherosclerotic lesion development (Landmesser, Hornig, & Drexler, 2004).

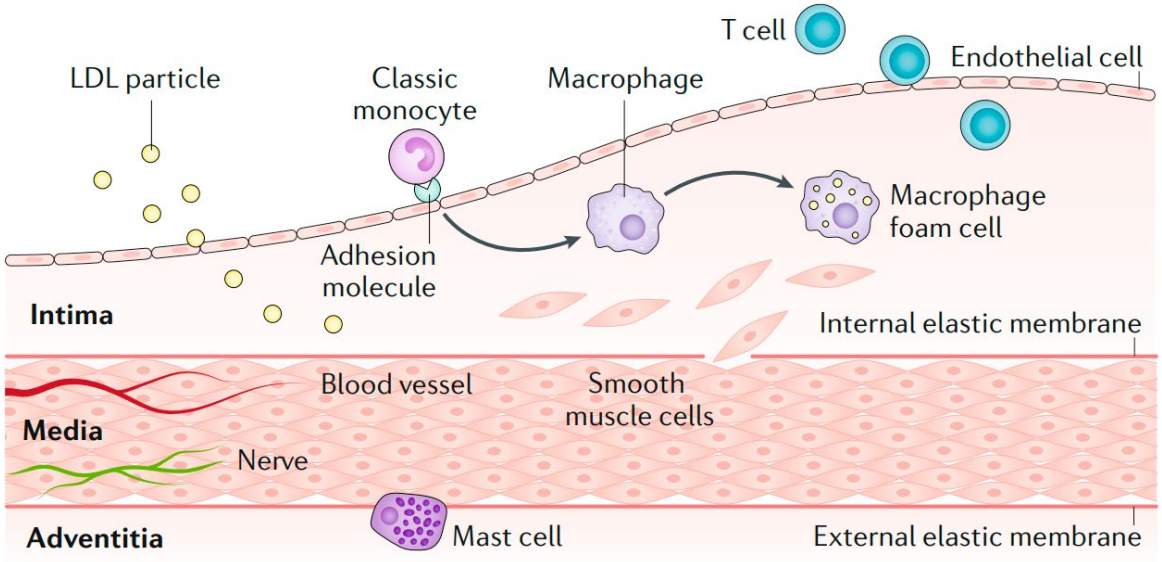

Figure 5. Initiation and progression of atherosclerosis.

In the early stage of lesion initiation, low-density lipoprotein (LDL) particles accumulate in the intima and undergo enzymatic modifications that can cause a pro-inflammatory and immunogenic state. Circulating monocytes can bind to adhesion molecules expressed by activated endothelial cells. Chemokines can promote the migration of bound monocytes into the artery wall. Once in the intima, monocytes can mature into macrophages. These cells express scavenger receptors that allow them to bind and engulf lipoprotein particles becoming in foam cells. T lymphocytes also enter the intima and regulate functions of the innate immune cells as well as the endothelial and smooth muscle cells. Adapted from (Libby et al., 2019).

2.1.2. *Fatty streak formation*

Once in the intima, monocytes mature into macrophages that express scavenger receptors. In an attempt to eliminate oxidized LDL particles (ox-LDLs), macrophages recognize, uptake and accumulate these particles in their cytoplasm through interaction with these receptors. Since macrophages are unable to eliminate ox-LDLs, they transform into foam cells (**Figure 6**). This ox-LDLs accumulation activates macrophages which in turn start releasing additional inflammatory and chemotactic factors that in combined action with other inflammatory mediators such as TNF-α, IL-1β or IL-6, among others, promote the further infiltration of leukocytes into the subendothelial space (Gisterå & Hansson, 2017; Libby, 2021; Libby et al., 2019; Libby et al., 2011).

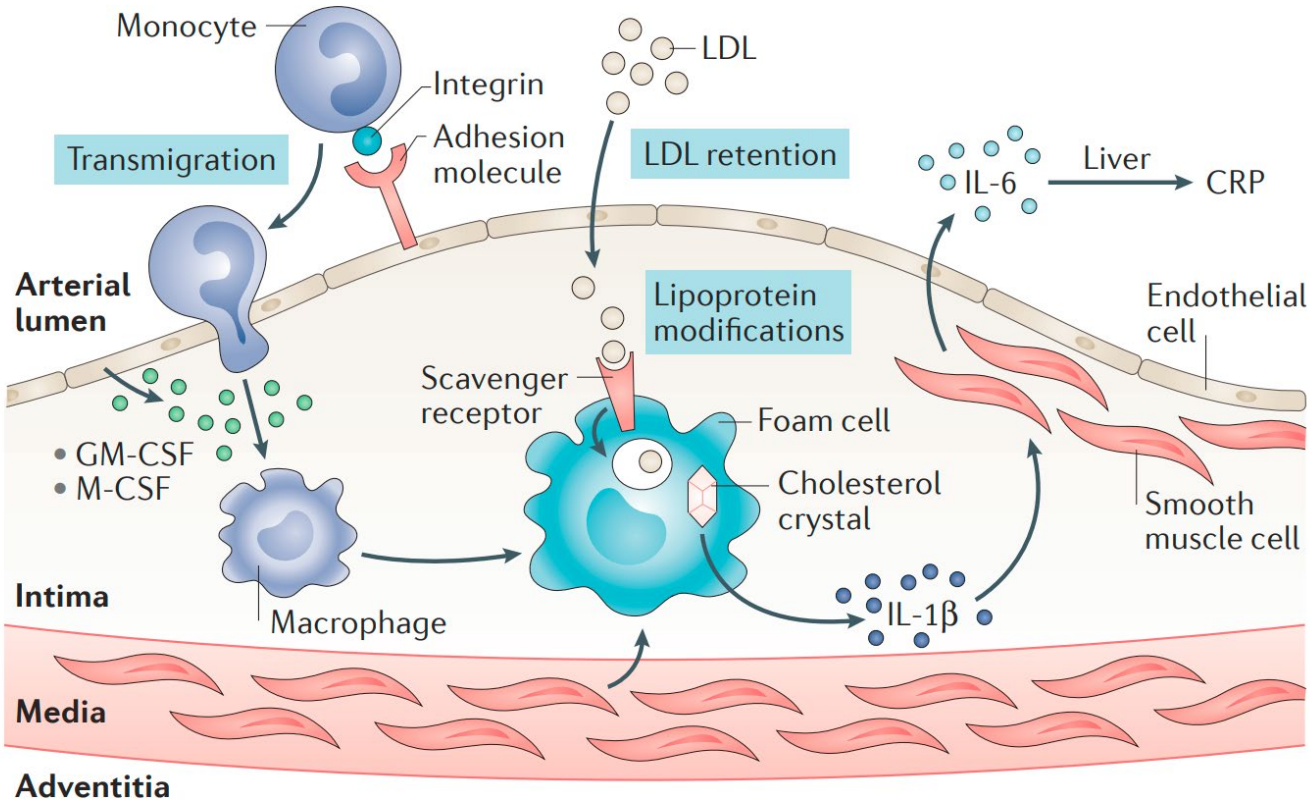

Figure 6. Innate immune responses in atherosclerosis.

Monocytes transmigrate into the intima and differentiate into macrophages in response to macrophage-colony stimulating factor (M-CSF) and granulocyte–macrophage colony stimulating factor (GM-CSF). Scavenger-receptor-mediated uptake of lipoproteins by macrophages leads to the formation of foam cells. This process results in the release of IL-1β and other cytokines, which stimulates smooth muscle cells to produce IL-6 and create a proinflammatory environment. Adapted from (Gisterå & Hansson, 2017).

Furthermore, these cytokines stimulate the local production of fibroblast and platelet growth factor, essential for plaque formation and progression. Specifically, TNF-α promotes SMC migration from the media to the intima. Once the leukocytes accumulate in the inner arterial membrane, the inflammatory process is intensified, producing reactive oxygen species (ROS), additional cytokines, chemokines and metalloproteases at the local level, which accelerate the progression of the pathology. This accumulation of immune cells, especially foam cells and T lymphocytes, gives rise to the so-called early plaque or fatty streak (Rafieian-Kopaei, Setorki, Doudi, Baradaran, & Nasri, 2014).

2.1.3. *Transformation of fatty streak into fibrous plaque*

TNF-α synthesized by activated vascular endothelium promotes migration of SMCs to the intima. Another mediator synthesized by the endothelium is lipoprotein lipase, responsible for degrading lipoprotein, which promotes SMC proliferation. This process involves the activation of protein kinase C, which regulates the production of extracellular matrix elements by SMCs and macrophages, and allow the progression to a stable plaque (P. Y. Chen, Qin, Li, Tellides, & Simons, 2016). Another cytokine, TGF-β promotes collagen production, SMC differentiation, and inhibition of SMC proliferation by interferon-γ (IFN-γ). All these factors lead to the formation of a thick layer of connective tissue with a lipid core. Indeed, recent studies have shown that destruction of SMCs may be beneficial, while their cell death causes inflammation (Bennett, Sinha, & Owens, 2016).

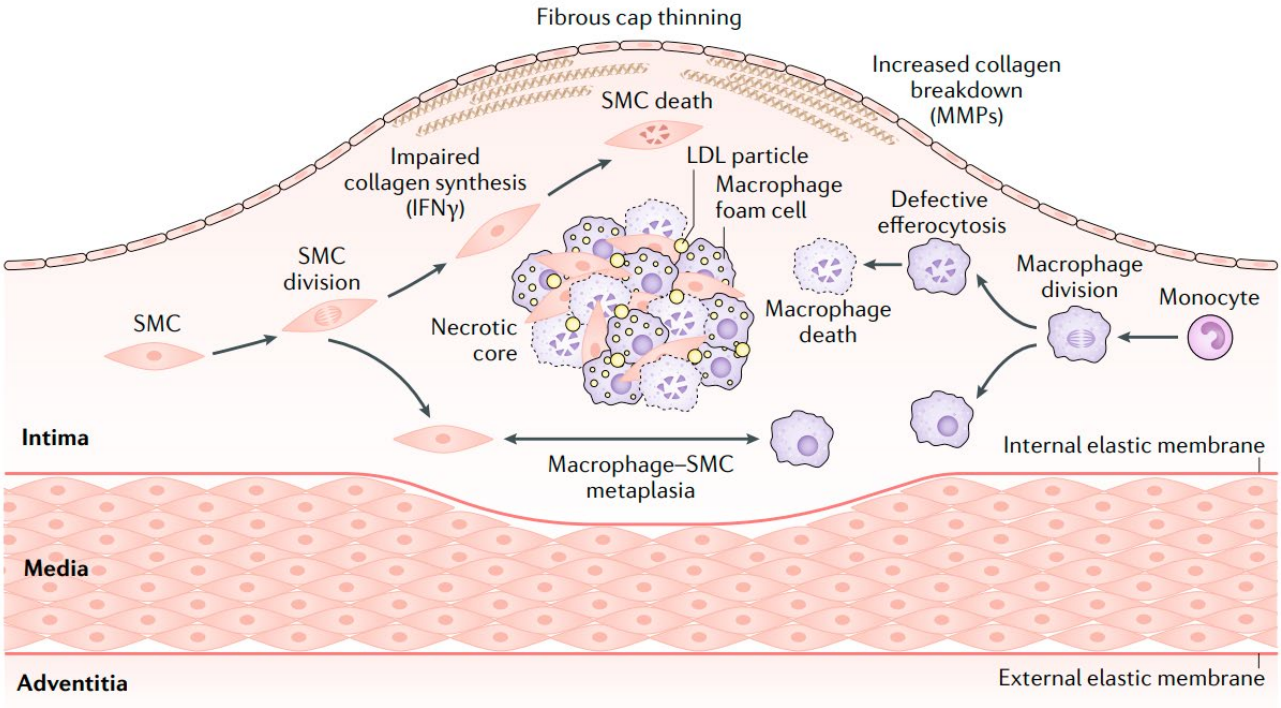

Figure 7. The progression of atherosclerotic lesions.

During the evolution of the atherosclerotic plaque, smooth muscle cells (SMCs) produce extracellular matrix molecules that contribute to the thickening of the intimal layer. However, cytokines such as IFN-γ can affect the ability of the SMC to synthesize interstitial collagen and thereby damage the function of T lymphocytes to repair the fibrous cap that overlies to the necrotic core. Furthermore, activated macrophages show increased production of enzymes of the matrix metalloproteinases (MMPs) family that degrade the interstitial collagen that lends strength to the fibrous cap. SMCs and macrophages in the evolving lesion can divide and undergo cell death in advance lesions. The debris accumulates, forming the necrotic lipid-rich core of the atheroma. Adapted from (Libby et al., 2019).

With the arrival of SMCs in the atherosclerotic plaque, extracellular matrix molecules are released, such as collagen, elastin, proteoglycans, and glycosaminoglycans that contribute to plaque thickening, giving rise to a fibrous plaque (Libby et al., 2019). These advanced lesions are characterized by the accumulation of lipids, apoptotic macrophages, apoptotic SMC and apoptotic endothelial cells, cellular debris and extracellular material, forming the necrotic core, which favours chronic inflammation (**Figure 7)** (Camaré, Pucelle, Nègre-Salvayre, & Salvayre, 2017; de Vries & Quax, 2016). This thickening is initially offset by gradual dilation. However, narrowing of the aortic lumen is not avoided, and it can cause ischemic episodes (Bennett et al., 2016).

Another feature of the advanced plaque is neovascularization. The entire atherosclerotic process requires oxygen demand, but its diffusion is hampered by intimal thickening and inflammation. Hypoxia is one of the most potent angiogenic factors (de Vries & Quax, 2016). In this way, neovascularization is stimulated in atherosclerotic lesions, which allows nutrients to be supplied to the atherosclerotic plaque, vascular thickening, lipid deposition, inflammation, and lesion progression.

Over time, the atherosclerotic plaque becomes weak due to the activity of inflammatory cells and the activation of extracellular matrix metalloproteases (MMPs), which cause the rupture in the most prone sites (Camaré et al., 2017). MMPs are proteolytic enzymes secreted by macrophages, endothelial cells and inflammatory cells, capable of degrading extracellular matrix proteins, that facilitate cell migration and release of growth factors embedded in the matrix (Libby et al., 2019). In addition, they are also responsible for the degradation of collagen fibres. At the same time, chronic inflammation also causes collagen degradation due to the presence of apoptotic SMCs. All this process causes the rupture of the internal elastic lamina and thus, the integrity and resistance of the fibrous plate.

The vulnerable (weakened) lesion differs from the stable fibrous plaque in its necrotic core, since the former is larger, acellular, and composed by lipids, fibrin, and apoptotic macrophages. As mentioned above, the fibrous layer becomes thin due to the action of MMPs and neovascularization, producing small haemorrhages and increased microcalcifications (Chistiakov, Orekhov, & Bobryshev, 2015).

Finally, the sudden rupture of the vulnerable lipid-rich plaque exposes its content to the circulation, allowing the activation of the coagulation cascade and the recruitment of platelets, with the consequent thrombi formation and triggering ischemic events.

2.2. Main cellular components involved in the atherosclerotic process

2.2.1. *Macrophages*

Macrophages are the main effector cells of innate immunity, and have a key role in the detection, phagocytosis and main degradation of necrotic cells and bacteria. In addition, this cell type is essential in the development of the pro-inflammatory cascade.

As discussed above (***Section 2.1.2 Fatty streak formation***), macrophages play a key role in the development of atherosclerosis (Wolfs, Donners, & de Winther, 2011). The presence of increased LDL particles in the blood initiates the atherosclerotic process. Monocytosis derived from hematopoietic cells in the bone marrow or a transdifferentiation of smooth muscle cells (SMCs) into macrophages is induced (Bartlett et al., 2019; Pan et al., 2020). Indeed, recent studies have shown the loss of SMC-specific markers and the expression of macrophage-specific markers (CD68, LAMP-2, Mac-2, CD11b) (Barrett, 2020). These macrophage-differentiated from SMCs represent 40% of the macrophages within the lesion and they can turn into foam cells since they can uptake lipids (Barrett, 2020; Bartlett et al., 2019).

This process results in an increase in circulating blood monocytes, which enter into the atherosclerotic lesions and differentiate into macrophages. This differentiation promotes the atherosclerosis progression through their cytokine, chemokine and ROS, production, maintaining a local pro-inflammatory environment (Bartlett et al., 2019). Monocyte/macrophage infiltration is mainly mediated, among other chemokines, by monocyte chemoattractant protein-1 (MCP-1)/CCL2, which interacts with its receptor, CC-chemokine receptor 2 (CCR2). This chemical is overexpressed in the atheroma, which induces the recruitment and accumulation of monocytes/macrophages in the nascent atheroma (Libby, 2002).

The LDL accumulation and retention in the arterial wall is mediated by the binding of apoB to proteoglycans present in the vascular endothelium. These particles undergo enzymatic modifications such as oxidation leading to ox-LDL formation. Macrophages express scavenger receptors, such as CD36, LOX-1 and SR-A1, among others, which recognize ox-LDL and are internalized in their cytosol. Given that macrophages can not eliminate them, they turn into foam cells, key immune players in the initial phases of the atherosclerotic process (Bartlett et al., 2019).

Macrophages are traditionally classified as M1 or M2. Both types were identified in the atherosclerotic plaques of humans and mice. While M1 macrophages are involved in the atherosclerotic lesion progression, M2 ($CD206^{+}$) exert an atheroprotective role (**Figure 8**) (Pello, Silvestre, De Pizzol, & Andrés, 2011).

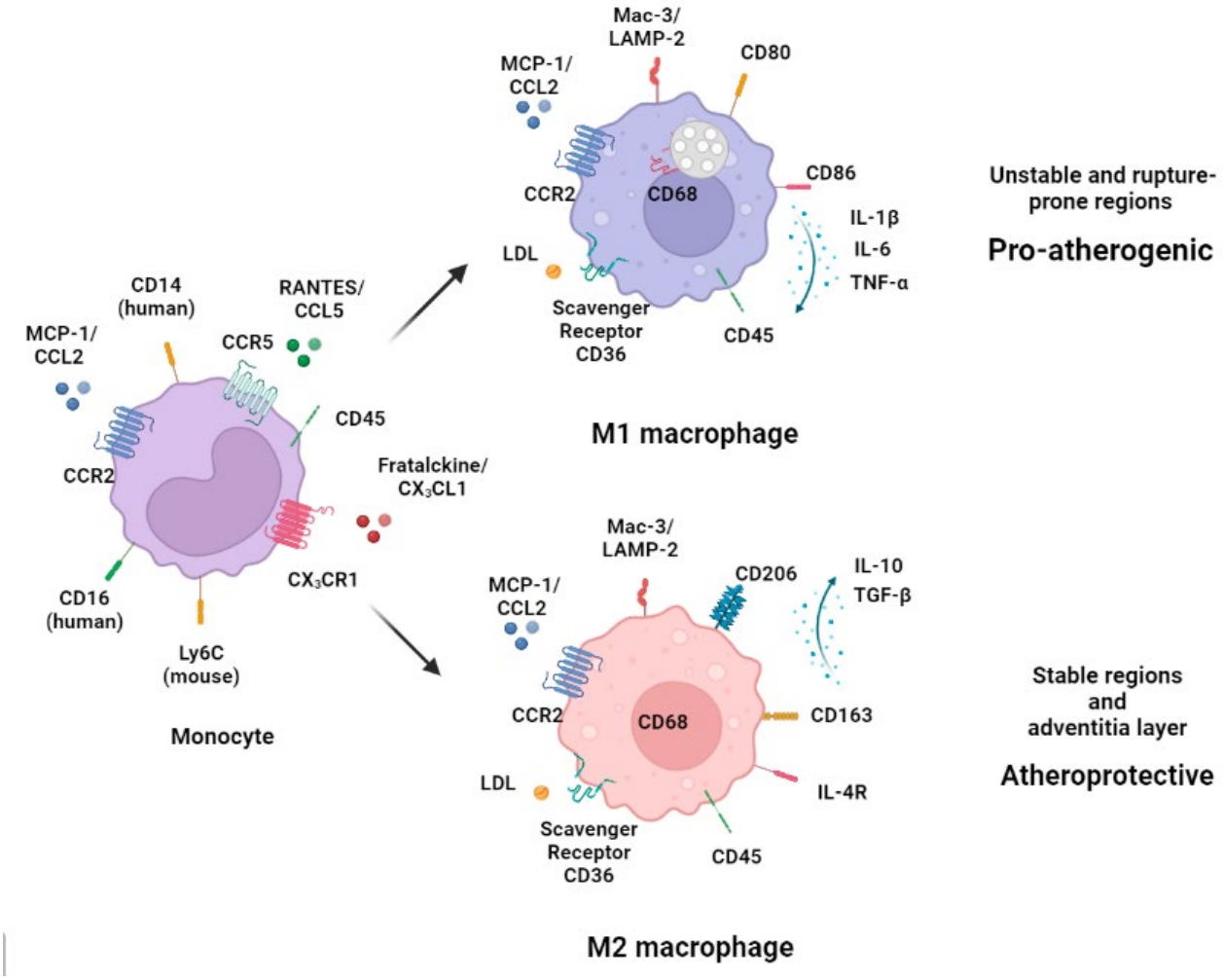

Figure 8. Specific markers of monocytes/macrophages
(Y. Chen et al., 2019). Created by Biorrender.com.

M1 macrophages

M1 or "classically activated" macrophages contribute to tissue destruction and secrete proinflammatory cytokines such as IL-1β, TNF-α or IL-6. In the atherosclerotic context, the M1 type is the predominant phenotype, approximately 40%, and is mostly found in unstable and rupture-prone regions (Barrett, 2020; Bartlett et al., 2019) (**Figure 8**). M1 macrophages are induced by bacterial components such as lipopolysaccharide (LPS) or inflammatory cytokines like TNF-α or IFN-γ and have a key role increasing the ongoing inflammatory response (Wolfs et al., 2011).

M2 macrophages

The polarization of M1 macrophages towards a M2 phenotype is mainly mediated by cytokines such as IL-4, IL-10 and IL-13 (Bhargava & Lee, 2012). M2 macrophage role in atherosclerosis has been associated to the regression of the plaque. More specifically, with the reduction of the plaque size, pro-inflammatory macrophages and cholesterol content. It seems that this favourable state is partly mediated by the secretion of anti-inflammatory factors such as IL-10 and collagen (Barrett, 2020).

Additionally, recent studies support a role of M2 type macrophages in plaque stabilization (Barrett, 2020). Unlike M1 macrophages, M2 macrophages are located in the adventitial layer. As opposed to M1 macrophages, M2 macrophages promote tissue repair (Wolfs et al., 2011). Nevertheless, previous evidence pointed out that macrophages display remarkable plasticity and that the M1/M2 macrophage classification is an oversimplification of the macrophage heterogeneity. In fact, some studies in mice have confirmed the existence of a distinct proatherogenic phenotype, referred to as Mox macrophages or M4 macrophages that express pro-inflammatory mediators such as TNF-α and IL-6, MMP-7, and MMP-12 and the calcium binding protein S100A8 (Bartlett et al., 2019).

2.2.2. *T lymphocytes*

T lymphocytes are one of the main cellular mediators of the adaptive immunity and play an important role in atherosclerosis. These cells are originated in the bone marrow from a hematopoietic stem cell from the lymphoid lineage. T cells continue their development in the bone marrow and subsequently migrate to the thymus, where they will be processed and differentiated into helper T lymphocytes (Th, $CD4^+$), whose main function is the secretion of cytokines, or cytotoxic T lymphocytes ($CD8^+$), that lyse cells that present foreign antigens on their membrane (Tse, Tse, Sidney, Sette, & Ley, 2013).

Recruitment of T lymphocytes to the atherosclerotic plaque occurs through chemokine (CCLs/CXCLs)-chemokine receptor (CCRs/CXCRs) interactions. Many axes chemokine/chemokine receptor axes are involved in their infiltration into the atherosclerotic lesion: CCL5/CCR1 and CCL5/CCR5; CXCL10/CXCR3; CX_3CL1/ CX_3CR1, etc. (Saigusa, Winkels, & Ley, 2020). Several studies indicate that between 25-38% of the total leukocytes in atherosclerotic plaques of mice and humans are T cells ($CD3^+$), both $CD4^+$ and $CD8^+$ (Saigusa et al., 2020).

$CD4^+$ T lymphocytes are commonly found in atherosclerotic plaques. In general, their presence is related with the progression of the disease; however, when the different subpopulations of $CD4^+$ T lymphocytes were studied separately, it has been observed that they can exert different effects, either accelerating or attenuating atherosclerosis (Saigusa et al., 2020). The predominant T helper (Th) lymphocytes are Th1, Th2, and Th17, which differ in the cytokines generated and, therefore, exert different functions (Hedrick, 2015). A substantial body of evidence indicates that Th1 cells are the most common Th cell subtype and

play a pro-atherogenic role (Poznyak, Bezsonov, Popkova, Starodubova, & Orekhov, 2021). In contrast, the role of the other effector Th cells – Th2 and Th17 – in atherogenesis is controversial and remains unclear, and they are less abundant in atherosclerotic plaque (Hedrick, 2015; Saigusa et al., 2020). On the other hand, regulatory T cells (Tregs) represent 1-5% of the total T lymphocytes present in the atherosclerotic lesions. This leukocyte subpopulation seems to exert atheroprotective effects through the secretion of the anti-inflammatory cytokine IL-10 and the key cytokine in vascular repair, Transforming Growth Factor-β (TGF-β) (Sharma et al., 2020). Inasmuch, in unstable atheroma plaques, the percentage of Tregs is even lower, making disease resolution more difficult (Poznyak et al., 2021).

Regarding $CD8^+$ T lymphocytes, their function in the context of atherosclerosis has been scarcely studied. In experimental settings, both their proatherogenic or atheroprotective role have been described (van Duijn et al., 2019). These cells are not as common as $CD4^+$ T cells; however, in advanced lesions, $CD8^+$ T cells outnumber $CD4^+$ T lymphocytes (Poznyak et al., 2021; Saigusa et al., 2020).

3. PRIMARY HYPERCHOLESTEROLEMIA

Hypercholesterolemia is a lipid metabolism disorder characterized by high plasma levels of cholesterol and low-density lipoproteins (LDL), which trigger atherosclerotic cardiovascular diseases. Chronic exposure to high circulating levels of cholesterol is a clear risk factor that characterizes several hypercholesterolemias (Mytilinaiou, Kyrou, Khan, Grammatopoulos, & Randeva, 2018). There are two major subtypes of primary and secondary hypercholesterolemia. Primary hypercholesterolemia (PH) is a pathology whose origin is unknown. At the genetic level, PH is a heterogeneous metabolic disorder and includes heterozygous familial hypercholesterolemia (FH), homozygous FH, and non-familial polygenic hypercholesterolemia, which is the most common (Langslet, Emery, & Wasserman, 2015). In contrast, secondary or acquired hypercholesterolemia is a lipid disorder that occurs as a consequence of other pathologies, such as diabetes, metabolic syndrome, renal dysfunction, and medications (Cicero & Cincione, 2022).

One of the best characterized primary hypercholesterolemias is Familial Hypercholesterolemia (FH) caused by a mutation in a gene (LDLR, ApoB, PCSK9 or ApoE) with an autosomal codominant inheritance pattern, that causes an extreme rise in LDL lipoprotein and an early ischemic heart disease (Jarauta, Bea-Sanz, Marco-Benedi, & Lamiquiz-Moneo, 2020). The underlying cause of FH is a genetic defect in both the LDL receptor and proteins that regulate their metabolism, that results in abnormal uptake of LDL by the liver. Consequently, this leads to the accumulation of cholesterol in the circulation, which explains the associated high cardiovascular risk (Mytilinaiou et al., 2018). Currently, it is estimated that approximately 1.5 billion people in the world suffer from this pathology (Tokgozoglu & Kayikcioglu, 2021).

FH is a heterogenous disease, depending on the gene mutation and the levels of LDL. As such, inheritance of a single mutant allele results in Heterozygous Familial Hypercholesterolemia (HeFH) leading to a 2- to 3-fold increase in circulating LDL levels. On the other hand, a genotype with both alleles mutated, either with the same mutation (true homozygosity, pathogenic variant) or with different mutations (compound heterozygosity) leads to a Homozygous Familial Hypercholesterolemia (HoFH) and translates into a total absence or total defect of the LDL receptor (LDLR). This leads to a worse prognosis due to decreased LDLR functionality (Mytilinaiou et al., 2018). Furthermore, HoFH patients are known to have 3 to 6 times higher circulating levels of cholesterol than a healthy individual. These genetic misalignments of lipid metabolism induce atherogenesis, and therefore, premature CVD. Fortunately, the HoFH with the worst prognosis has a prevalence of 1:300,000 - 1:400,000 in the world (Butt & Yee, 2022; Tokgozoglu & Kayikcioglu, 2021), 1:1,000,000 in Europe (Taylan & Weber, 2022) compared to HeFH with an estimated prevalence of 1:200 - 1:300 in the world (Butt & Yee, 2022; Tokgozoglu & Kayikcioglu, 2021) and 1:500 in Europe (Taylan & Weber, 2022)).

It is now clear that the underlying pathological mechanism are defective clearance of LDL particles. The three most common pathogenic variants are mutations in the LDL receptor gene, the apolipoprotein B gene, and the proprotein convertase subtilisin/kexin type 9 (PCSK9) gene (Butt & Yee, 2022; Jarauta et al., 2020; Mytilinaiou et al., 2018).

LDL receptor is a hepatocyte membrane receptor, and its main function is the removal of LDL by endocytosis of the ligand-receptor complex (Mytilinaiou et al., 2018). This receptor is synthesized as a precursor protein. Upon maturation by glycosylation, it is externalized to the membrane where it binds to ApoB and ApoE – lipoproteins. The complex is internalized and migrates to endosomes, where cholesterol is released and degraded by lysosomes (De Castro-Orós, Pocoví, & Civeira, 2010; Libby, 2021; Libby et al., 2019). These receptors are recycled several times to repeat this process until they are eliminated.

FH caused by mutations in the LDL receptor accounts for 90% of all cases (Pirillo, Catapano, & Norata, 2021). These mutations can be classified into five classes with one common result: a failure of hepatocytes in LDL clearance (**Table 5**) (De Castro-Orós et al., 2010).

Table 5 – **Main genetic defects of LDLR, adapted from (De Castro-Orós et al., 2010)**

Type	Genetic defect
Class 1	LDLR not synthesized
Class 2	Alteration in LDLR transport to the cell surface
Class 3	Alteration in LDL-LDLR binding
Class 4	Alteration in LDL-LDLR complex internalization
Class 5	Alteration in LDLR recycling

LDL: Low Density Lipoprotein; LDLR: Low Density Lipoprotein Receptor

Familial defective apolipoprotein B-100 is an autosomal dominant genetic disorder of lipid metabolism associated with hyperlipidemia and increased risk of atherosclerosis. Apolipoprotein B is a protein that participates in the transport of cholesterol and fatty acids, insoluble in water, to the liver or other tissues. It is the component of very low-density lipoproteins (VLDL) and LDL and allows the binding to the LDL receptor regulating their elimination. Mutations in this gene cause a reduction in receptor affinity to ApoB. It is the second most prevalent FH, since it represents between 2-5% of all cases (Mytilinaiou et al., 2018).

Mutations in the PCSK9 gene constitute the third gene involved in FH. The PCSK9 protein is the enzyme responsible for the removal of LDLR from the hepatocyte surface. Pathogenic variants of gain or loss of function alter the availability of LDL in the bloodstream. It represents less than 1% of FH cases (Mytilinaiou et al., 2018).

Although these three pathogenic variants are the most common, mutations have been recently found in genes such as low density lipoprotein receptor adaptor protein-1 (LDLRAP-1) (Mytilinaiou et al., 2018; Tokgozoglu & Kayikcioglu, 2021) and ApoE (Jarauta et al., 2020; Tokgozoglu & Kayikcioglu, 2021). In addition, the non-familial polygenic hypercholesterolemia, can be attributed to small additive effect of having single nucleotide variants throughout the genome. Non-familial polygenic hypercholesterolemia is clinically similar to FH, being hard to differentiate in most cases (Sharifi, Futema, Nair, & Humphries, 2019). It represents 20-30% of patients diagnosed with clinical FH, in which the genetic cause is not identified. The increased levels of cholesterol could be due to polygenic, environmental, or unknown monogenic causes (Trinder, Francis, & Brunham, 2020). Currently, its diagnosis, prevalence and cardiovascular risk are not fully established (Jarauta et al., 2020).

Despite being a widespread disease, only a minority of patients are identified and treated. Early diagnosis is extremely important, since those subjects with HeFH could suffer cardiovascular events between 30-50 years old in men and 40-60 years old in women. Patients with HoFH have a worse prognosis, since they could die before the age of 30 if they are not treated (Tokgozoglu & Kayikcioglu, 2021).

During the last decades, there have been important developments in genetic diagnosis and treatment. However, FH continues to be an underdiagnosed and undertreated pathology worldwide (Tokgozoglu & Kayikcioglu, 2021).

3.1. Clinical manifestations, treatment and future prospects

Given that the possibility of suffering cardiovascular events at an early age, a quick diagnosis and a rapid start of lipid-lowering therapy is crucial to reduce cardiovascular risk in these individuals (Gencer & Nanchen, 2016). Among the clinical manifestations that could be highlighted for FH diagnosis are the presence of tendon and corneal arch xanthomas, which are linked to the storage of cholesterol in macrophages and may progress to thicker deposits. However, not all patients manifest these symptoms (Mytilinaiou et al., 2018). Diagnosis can be also based on plasma LDL levels, presence of lipid accumulations, premature coronary artery disease, and family history. A genetic diagnosis is very useful to detect mutations and stabilize a diagnosis. However, a negative result is not enough to discard the disease. Once diagnosed, it should be treated immediately, since the goal is to reduce plasma levels by 50%. Adopting good lifestyle habits such as reducing the intake of a high-fat diet, implementing physical exercise and quitting smoking are necessary to achieve this goal. Despite these good habits, pharmacological treatment is needed (Cartier & Goldberg, 2016; Mytilinaiou et al., 2018; Onorato & Sturm, 2016). Statins are selective inhibitors of HMG-coA reductase, which leads to a reduction in cholesterol biosynthesis (Libby et al., 2011). However, in HoFH patients these treatments are insufficient, and other pharmacological alternatives are used. If these approaches do not work, apheresis is required to reduce LDL levels by 60%. However, this treatment is expensive and requires hospital treatment every two weeks.

Currently, PCSK9 inhibitors (monoclonal antibodies or antisense oligonucleotides against PCSK9) are currently used as alternative lipid-lowering therapies. In fact, drastic reductions of up to 75% of LDL particles in the blood have been observed (Baum & Cannon, 2018; Chlebus et al., 2022). For this reason, these treatments together with new approved drugs in the market (bempedoic acid or evinacumab) are becoming good approaches to treat this metabolic disease.

3.2. Low-grade Systemic inflammation (LGSI)

LGSI is a chronic and subclinical state that contributes to the pathogenesis of many cardiometabolic diseases, such as atherosclerosis, type 2 diabetes, metabolic syndrome, and obesity, and it has been recently reported in patients with PH (Barale, Frascaroli, Senkeev, Cavalot, & Russo, 2018; Langslet et al., 2015). LGSI is characterized by the enhanced production of inflammatory mediators including cytokines, chemokines, and acute-phase proteins within the circulation, as well as by changes in the activation state of different immune players (Cho et al., 2018).

Recent evidence suggests that CVD might arise in patients with PH as a consequence of LGSI accompanied by a pro-thrombotic state, with heightened platelet activation and levels of associated circulating soluble markers (Hansen et al., 2019; von Hundelshausen & Schmitt, 2014). In fact, increased levels of different soluble inflammatory markers, such as TNF-α, IL-1, IL-6, IFN-γ, and high sensitivity C reactive protein (hs-CRP) have been detected in patients with hypercholesterolemia (Barale et al., 2018; Hansen et al., 2019). Likewise, elevated circulating levels of chemokines including MCP-1/CCL2, macrophage inflammatory protein (MIP)-1α/CCL3, MIP-1β/CCL4, IL-8/CXCL8, and IFNγ-inducible protein-10 (IP-10)/CXCL10 have also been detected in these patients (Cortes et al., 2016; Hansen et al., 2019).

In regard to cellular markers, hypercholesterolemia has been previously associated with platelet activation (Barale et al., 2018; Chironi et al., 2006) and *in vitro* studies showed increased leukocyte activation in patients with hyperlipidemia (Mazor et al., 2008). In addition, there is evidence to support that adults with PH have a pro-inflammatory imbalance in the circulating type 1 monocyte subpopulation (Mon 1, classical, $CD14^{+}CD16^{-}CCR2^{+}$) (Fadini et al., 2014) and an increase in this population is related to CVD (Kratofil, Kubes, & Deniset, 2017); however, other studies have indicated that the levels of type 2 monocyte subpopulation (Mon 2, intermediate, $CD14^{+}CD16^{+}CCR2^{+}$) and/or type 3 monocyte subpopulation (Mon 3, nonclassical, $CD14^{+}CD16^{+}CCR2^{-}$) subtypes were increased in hyperlipidemia and were associated with atherosclerosis development (H. Wu & Ballantyne, 2017). Nevertheless, recent studies in mice suggest that the populations responsible for atherosclerosis development are Mon 1 and Mon 3 (Kratofil et al., 2017).

As explained in ***Section 1.1 Inflammatory process***, LGSI is also associated to endothelial dysfunction, a prothrombotic and pro-inflammatory state of the endothelium that causes the adhesion and subsequent migration of leukocytes to the subendothelial space (Landmesser et al., 2004). As a summary of this section, it is concluded that endothelial dysfunction can be caused by different atherogenic factors such as ox-LDL, cytokines, tobacco smoke, among others. Endothelial dysfunction has not only been detected in patients with hypercholesterolemia, but also in relatives who have not yet developed the pathology (T. Rahman et al., 2017). This alteration causes increased expression of CAMs such as VCAM-1 or ICAM-1, as well as the synthesis and release of chemokines such as CCL2, CCL3, CXCL8, CX_3CL1, etc. These cellular and molecular mediators are also capable of amplifying the inflammatory response and promote the growth and rupture of the atherosclerotic plaque.

4. THE CCL11/CCR3 AXIS

4.1. Chemokine receptor CCR3

CC chemokine receptor type 3 (CD193/CCR3) is a G protein-coupled receptor that belongs to the class A subfamily of rhodopsin-like receptors. It is expressed in different leukocytes such as eosinophils, mast cells, basophils, and a subset of Th2 lymphocytes, as well as in cells such as keratinocytes, epithelial airway cells, microglia and endothelial cells (Cheng, Lukacs, & Kunkel, 2002; Erin, Williams, Barnes, & Hansel, 2002; Kodali et al., 2004). Unlike eosinophils, basophils, and the subpopulation of Th2 lymphocytes in which CCR3 is expressed on the cell surface, mast cells have the receptor stored in their cytoplasmic granules. Once mast cells are activated through the high-affinity IgE receptor (FcεRIα), CCR3 receptor is transported to the cell membrane and expressed on its surface (Willems & Ijzerman, 2010).

However, CCR3 predominates in eosinophils whose antigenic density is 5 x 10^4 receptors per cell (Erin et al., 2002; Willems & Ijzerman, 2010). Its expression is constitutive in eosinophils, basophils and in a subset of Th2 cells (Conroy & Williams, 2001) or can be induced by cytokines such as IL-4 (Willems & Ijzerman, 2010).

As a G protein-coupled receptor, it is constituted by 7 transmembrane α-helix proteins and recognizes several ligands, although the potency and affinity differ between them (Erin et al., 2002). Currently it is known that *Regulated upon Activation, Normal T Cell Expressed and Presumably Secreted* (RANTES)/ CCL5, eotaxin-1/CCL11, eotaxin-2/CCL24, eotaxin-3/CCL26 (only in humans), MCP-3/CCL7, MCP-2/CCL8, MCP-4/ CCL13, HCC-1/CCL14, MIP-1δ/CCL15 and mucosae-associated epithelial chemokine (MEC)/CCL28 are ligands for CCR3 (Willems & Ijzerman, 2010). These ligands, in addition to producing the recruitment of $CCR3^+$ cells, in eosinophils, they induce actin polymerization, increases intracellular calcium levels and degranulation promoting the release of ROS and cytotoxic molecules (Willems & Ijzerman, 2010).

Among all of these chemokines, the three eotaxins: eotaxin-1/CCL11, eotaxin-2/CCL24, and eotaxin-3/CCL26, solely interact with CCR3 receptor and the highest level of CCR3 receptor expression is found in eosinophils (Conroy & Williams, 2001). CCR3 has been shown to be required for the migration of eosinophils from the bone marrow into the bloodstream and the intestine (Humbles et al., 2002; Matthews et al., 1998). This receptor has been mainly implicated in allergic diseases and asthma (Grozdanovic et al., 2019; Pease, 2006).

4.2. Eotaxin-1/ CCL11

The CCL11 chemokine is also called eotaxin-1 and belongs to the CC chemokine family. As previously mentioned, (***Section 1.1.3.2. Leukocyte activation. Chemokines*****),** this family is characterized by the presence of two adjacent cysteines at its N-terminus (Menzies-Gow et al., 2002). It is released by various cell types including epithelial cells, endothelial cells, smooth muscle cells or mast cells (Menzies-Gow et al., 2002; Rabin, 2003). Other studies have shown that it is also released by eosinophils (Blanchet et al., 2012), chondrocytes and fibroblasts (Wakabayashi, Isozaki, Tsubokura, Fukuse, & Kasama, 2021). Although it belons to the eotaxin family, it maintains low homology (34-38%) with eotaxin-2/CCL24 and eotaxin-3/CCL26 (Rabin, 2003). All of these chemokines can be induced in response to IL-4 or IL-13, cytokines associated with the Th2 response through the activation of signal transducer and activator of transcription factor-6 (STAT-6) (Rabin, 2003). Nevertheless, it can also be induced by TNF-α (Wakabayashi et al., 2021).

Eotaxin-1/CCL11 binds to CCR3 receptor with high affinity. However, it is also a ligand for the CCR2 and CCR5 receptors which are involved in monocyte recruitment, but it behaves as an antagonist of these receptors (Ogilvie, Bardi, Clark-Lewis, Baggiolini, & Uguccioni, 2001). Through its interaction with CCR3 receptor, CCL11 promotes the migration and recruitment of different leukocyte subsets, mainly eosinophils and basophils (Menzies-Gow et al., 2002). In addition, it seems that eotaxin-1 can also induce endothelial cell chemotaxis and angiogenesis (Korbecki et al., 2020; Park et al., 2017; Salcedo et al., 2001).

In general, the entire family of eotaxins are considered to be potent basophil and eosinophil chemotactic factors (Rabin, 2003; Suzuki et al., 2021). Indeed, they increase intracellular calcium concentrations, cause actin polymerization, and eosinophil effector functions such as leukotriene production, activation of CAMs, release of eosinophil cytotoxic granules and IL-4, as well as CCR3 receptor internalization (Rabin, 2003).

Although eotaxin-1 is a widely studied chemokine in the field of allergic disorders and asthma (Suzuki et al., 2021), other and more recent studies suggest that this chemokine is involved in several pathological conditions, such as cardiovascular disorders (Li et al., 2020; Lieschke et al., 2019; Xing et al., 2016), ulcerative colitis (Ahrens et al., 2008; Loktionov, 2019; Polosukhina et al., 2021) or cancer (Tian et al., 2016; Xing et al., 2016), among others.

4.3. Eosinophils

Eosinophils are bone marrow-derived granulocytes with different roles in innate and adaptive immunity. It is a non-abundant cell under normal conditions since it represents between 1-5% of the total leukocytes in human blood (Jung & Rothenberg, 2014; McBrien & Menzies-Gow, 2017) and 1-2% in total murine blood (Reichman, Rozenberg, & Munitz, 2017). They are also tissue-resident cells, being the main reservoir the intestine where they represent the 20-30% of the total leukocyte populations (Jung & Rothenberg, 2014). In addition to the intestine, several studies have shown that there is a migration of eosinophils from the bloodstream to other organs such as the adipose tissue or the lung where they can play a homeostatic role (Kanda et al., 2021; Marichal, Mesnil, & Bureau, 2017; Xenakis et al., 2018). They also contribute to glucose homeostasis, tissue and muscle remodeling or liver tissue repair (Gevaert et al., 2022; Marichal et al., 2017).

Eosinophils are highly pro-inflammatory leukocytes in different diseases and seem to be involved in the pathogenesis of allergic disorders, asthma and helminth infections (Grozdanovic et al., 2019; Jung & Rothenberg, 2014; Marichal et al., 2017). However, its role in cardiovascular disorders remains controversial since some studies indicate that they can be deleterious while others protective (C. L. Liu et al., 2021; J. Liu et al., 2020; Marx et al., 2019)

Eosinophil differentiation in the bone marrow is a complex and organized process, where hematopoietic stem cells ($CD34^+$) undergo a maturation process with the intervention of different cytokines and transcription factors, rising the number of granulocyte/monocyte progenitors. The differentiation of eosinophil precursor cells is regulated by the transcription factors GATA-1 (a member of the zinc finger family), PU.1 (a member of the ETS family) and c/EBP (CCAAT promoter binding protein family), being the most important the role of GATA-1 (Jacobsen et al., 2021) (**Figure 9**). Three cytokines, IL-3, IL-5, and GM-CSF are particularly important in the regulation of eosinophil development (Germic et al., 2021; J. Liu et al., 2020; Rothenberg & Hogan, 2006; Tao et al., 2022). Among these three cytokines, IL-5 is the most specific in this process being responsible of eosinophil release from the bone marrow to the peripheral circulation (Guthier & Zimmermann, 2022; Rothenberg & Hogan, 2006). In addition, IL-5 increases the pool of eotaxin-responsive cells and primes eosinophils to respond to CCR3 ligands. The finding that IL-4 and IL-13 are potent inducers of the eotaxin chemokines by a STAT6-dependent pathway, provides an integrated mechanism that may explain the eosinophilia associated to Th2 responses (Bhargava & Lee, 2012).

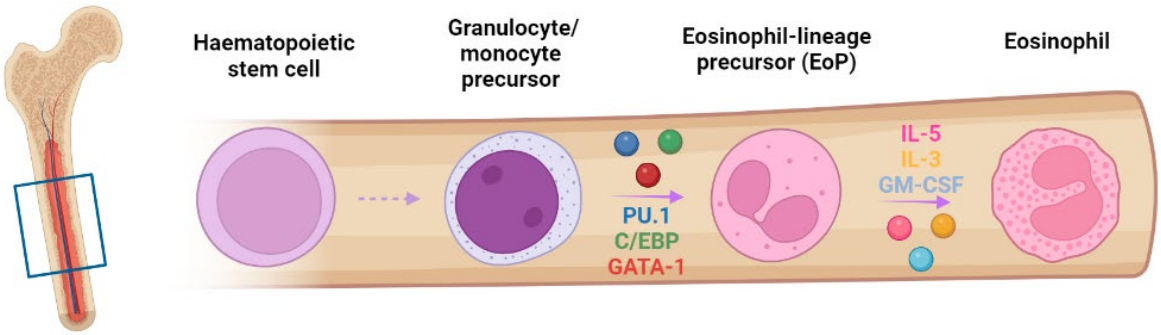

Figure 9. **Eosinopoiesis.**

The mature eosinophil is derived from the pluripotent $CD34^+$ stem cell via IL-5 in the bone marrow. The differentiation and release into the circulation of the eosinophil is directed by IL-5, IL-3, GM-CSF (Rosenberg, Dyer, & Foster, 2013). Created by Biorrender.com.

One of the distinguishing features of eosinophils is the presence of specific large granules, which differentiates them from other granulocytes such as neutrophils and basophils. These granules are enriched with highly cationic proteins. The four predominant cytotoxic cationic proteins are: major basic protein (MBP), eosinophil peroxidase (EPX), eosinophil-derived neurotoxin (EDN), and eosinophil cationic protein (ECP) (Jacobsen et al., 2021; Xu et al., 2022). In addition, these granules also contain cytokines such as IL-2, IL-4, IL-5, IL-10, IL-12, IL-13, IL-16, and IL-18, chemokines, growth factors, and enzymes, which induce inflammation and/or tissue damage (Lacy, Rosenberg, & Walsh, 2021; Rothenberg & Hogan, 2006).

In spite of being discovered in 1879 by Paul Ehrlich, differential functions have been detected which suggest the existence of different eosinophil subpopulations (Jacobsen et al., 2021; Kanda et al., 2021; O'Sullivan & Bochner, 2018). Furthermore, it seems that they are not a uniform population in the same individual given that they appear to behave differently in healthy and pathological conditions (Rosenberg et al., 2013). Indeed, recent studies have highlighted the phenotypic diversity of eosinophils even within the same organism (Carlens et al., 2009). In fact, it seems that their surface markers are dissimilar when resident (rE) are compared with inducible or inflammatory eosinophils (iE with a higher expression of Siglec-F) (Kanda et al., 2021; O'Sullivan & Bochner, 2018).

4.3.1. *Eosinophils markers*

The detection of eosinophils has always been a challenge to overcome given their low circulating levels. However, with the wide variety of surface molecules and receptors which are currently known, a proper eosinophil selection is straightforward through the use of markers such as CD193/CCR3 (***Section 4.1 Chemokine receptor CCR3***), CD125/IL-5Rα and Siglec-8/Siglec-F (Hassani et al., 2020).

4.3.1.1. *CD125/IL-5Rα*

The IL-5 heterodimeric receptor (IL-5R) is one of the most relevant in the eosinophilic population. Its α subunit (IL-5Rα, also known as CD125) is expressed on eosinophils (McBrien & Menzies-Gow, 2017) and mature B cells (Kawano et al., 2010). Its expression is constitutive during all stages of maturation, but the highest expression is on mature eosinophils in the bone marrow and circulation (Hassani et al., 2020). As mentioned above, this receptor is crucial for eosinophil differentiation and their migration from the bone marrow to the peripheral blood.

4.3.1.2. *Siglec-8/Siglec-F*

Eosinophils also express on their surface the marker Siglec-8 (humans) and Siglec-F (mouse), that belongs to the family of immunoglobulin-type lectins (Bochner, 2009; M. Zhang et al., 2007). Siglec-8, so named because it is the eighth family member identified at the time, is prominently present in eosinophils but also in other cell types such as mast cells and, to a lesser extent, in basophils. Its function in eosinophils has been associated to the induction of apoptosis (Bochner, 2009). Siglec-F, was later identified as a functionally convergent paralogue of Siglec-8 and is expressed predominantly in murine eosinophils (J. Q. Zhang, Biedermann, Nitschke, & Crocker, 2004; M. Zhang et al., 2007). It is not found in murine mast cells but it is present in a range of cells including alveolar macrophages and, at very low levels, on neutrophils and T cells (Bochner, 2009). Based on these data, Siglec-F has emerged as a reliable distinguishing marker for eosinophils in the mouse when granulocytes are analyzed.

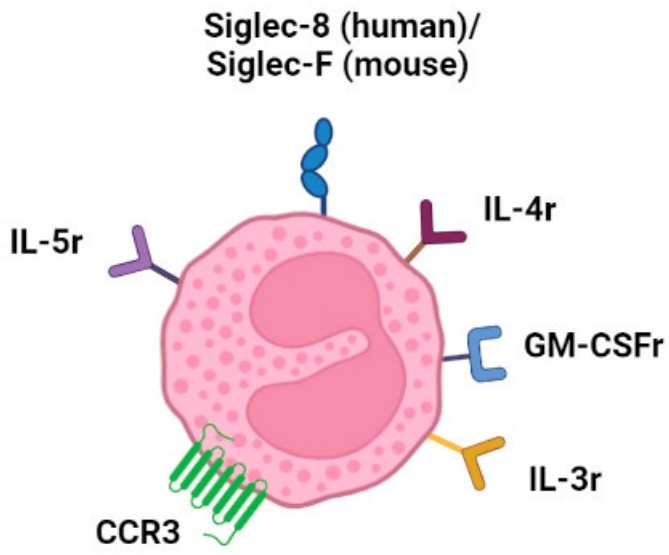

Figure 10. **Eosinophils main markers.**
Created by Biorrender.com

OBJECTIVES

5. OBJECTIVES

1. Since Primary hypercholesterolemia (PH) is associated with a low-grade of systemic inflammation and a higher risk of suffering cardiovascular diseases, **the first objective** of this Thesis was to study the systemic inflammation associated to PH. Specifically, the activation state of platelets and different leukocyte populations and the presence of platelet-leukocyte aggregates were evaluated. Additionally, several soluble mediators were determined as well as the functional consequences of the systemic inflammation in PH patients compared with healthy age-matched controls.

2. Once the first study was established, **the second objective** of this Thesis was to evaluate the effect of the administration of an oral unsaturated fat load (OUFL) with a commercial preparation of long-chain triglycerides (the ω6/ω3 ratio is >20/1). Different immunological parameters were investigated as well as its potential beneficial consequences after 4h of its administration to patients with PH or healthy age-matched control subjects.

3. Finally, **the third and last objective** of the Thesis was to characterize the role of the CCL11/CCR3 axis in the systemic inflammation associated with PH and the development of atherosclerosis. For this purpose, different immune parameters of CCL11/CCR3 axis were analyzed in whole blood from PH patients and healthy age-matched controls. Additionally, similar parameters were evaluated in mice deficient in apolipoprotein E (*apoE*$^{-/-}$) subjected to an atherogenic diet. Lastly, *apoE*$^{-/-}$ mice were crossed with mice lacking CCR3 receptor to generate *apoE*$^{-/-}$*CCR3*$^{-/-}$ mice. The role of CCL11/CCR3 axis was investigated in an atherogenic environment in *apoE*$^{-/-}$*CCR3*$^{-/-}$ and *apoE*$^{-/-}$*CCR3*$^{+/+}$ mice.

MATERIAL AND METHODS

6. HUMAN STUDIES AND ETHICAL COMMITTEE APPROVAL

The study protocol was performed following the principles detailed in the Declaration of Helsinki and was approved by The Clinical Research Ethics Committee of the University Clinic Hospital of Valencia (Valencia, Spain). All participating subjects had signed the appropiate written informed consent.

6.1. Blood samples from age-matched controls and primary hypercholesterolemia (PH) patients

A total of 22 subjects with Primary Hypercholesterolemia (PH) were recruited by the Endocrinology and Nutrition Service of the University Clinic Hospital of Valencia (Valencia, Spain). Their medical histories were evaluated and different anthropomorphic and biochemical parameters, and blood pressure, were measured. The criteria for the diagnosis of patients were defined as follows: 1) Total cholesterol content (TC) > 260 mg/dL and/or LDL > 160 mg/dL; 2) Total triglyceride content (TG) > 150 mg/dL.

A total of 21 healthy individuals were recruited by our center. Their medical records were evaluated, and the same parameters were measured. The inclusion criteria for healthy subjects were defined by the following features: 1) Total cholesterol content (TC) < 200 mg / dL and apoB < 120 mg/dL; 2) Total triglyceride content (TG) < 150 mg/dL; 3) Blood glucose level (fasting) < 100 mg/dL; 4) Absence of dyslipidemia, cardiovascular diseases, or diabetes. Genetic testing for *APOE* was performed in both groups and only those subjects who presented the *E3/E3* genotype participated.

The exclusion criteria for both groups were: 1) Presence of cardiovascular diseases, hypertension, diabetes, chronic diseases or cancer; 2) Smoking or alcohol consumption> 30 g/day; 3) Presence of renal or hepatic insufficiency and hypothyroidism; 4) Pregnancy or lactation; 5) Presence of infections and inflammatory diseases (including asthma, allergies and autoimmune deficiencies); 6) Presence of drugs that can alter the inflammatory profile six weeks before the study, and 7) the use of drugs capable of modifying the lipid profile or inflammation that cannot be withdrawn 6 weeks before starting the study.

Blood from all subjects was drawn by venipuncture after a fasting period of at least 12 hours in BD Vacutainer tubes (BD Biosciences, San José, CA) containing 3.2% sodium citrate, or in BD Vacutainer PST™ tubes II with lithium heparin as an anticoagulant agent (17 IU/mL; BD Biosciences). The study of different analytical determinations was performed including a complete biochemical analysis with lipid and glycemic profile.

6.2. Oral unsaturated fat load (OUFL) test

The study started at 8:30 a.m. and blood was drawn by venipuncture after a fasting period of at least 12 hours. Anthropometric parameters and blood pressure were measured using standardized procedures: body mass index (BMI; kg/m^2), waist circumference (midpoint between the edge lower rib and iliac crest; cm) and blood pressure (mmHg). Blood samples from PH patients and age-matched controls were taken and collected in Vacutainer® blood collection tubes containing sodium citrate (3.2%), or in Vacutainer® PST II tubes with lithium/heparin (17 IU/mL) as anticoagulant agents (BD Biosciences, San Jose, CA) and subsequently subjected to different analytical determinations including complete biochemistry with glycemic and lipid profile, and quantification of creatinine as a measure of renal function.

After the first blood sampling (time 0; T0), both patients and controls ingested a commercial OUFL of 25 g of a high-fat meal per m^2 of body surface area, prepared with a commercial long-chain triglycerides (TG) liquid preparation (Supracal®; SHS International, Liverpool, UK). Each 100 mL of the formula contained 50 g of fat (450 kcal), of which 9.6 g was saturated, 28.2 g monounsaturated and 10 g polyunsaturated, with a ω6/ω3 ratio >20/1. Fatty acid content and the complete composition are detailed in **Table 6**, as explained previously (Pedro et al., 2013) . Subjects were only allowed to drink mineral water during the test. Blood samples were taken before and four hours after the OUFL challenge for the various measurements.

Table 6 - Fatty acid composition of Supracal® (Pedro et al., 2013)

Composition	g/100g fatty acids
Lauric (C_{12})	<1
Myristic (C_{14})	<1
Palmitic (C_{16})	10
Stearic (C_{18})	3
Oleic ($C_{18:1}$)	58
Linoleic ($C_{18:2}$)	20
α-linoleic ($C_{18:3}$)	<1
Arachidonic (C_{20})	1
Eicosanoic ($C_{20:1}$)	1
Behenic (C_{22})	3
Lignoceric (C_{24})	1

6.3. Immunophenotyping by flow cytometry

6.3.1. *General points*

Flow cytometry is one of the most used tools, especially in immunology. One of the most common applications is cell sorting based on subtype or expression marker. This process is known as FACS (*Fluorescence-activated cell sorting*) analysis (Biosciences, 2000).

When samples are run into the cytometer (BD FACSVerse™ or BD FACSFortessa x20, BD Biosciences), particles are randomly arranged in space, and subsequently aligned due to a fluid system, so that they can be detected and analyzed individually using a laser to obtain information from each particle.

To perform a basic analysis of particles, two parameters are important: the *Forward Scatter Channel* (FSC) and the *Side Scatter Channel* (SSC). The first provides information on the size of particles, allowing to distinguish living cells from dead ones, while the second analyzes cell complexity or granular content. If particles are associated with different fluorochromes (with different wavelengths) (**Table 7**), a quantitative and identifying analysis can be carried out that reinforces the basic analysis. When it is irradiated with the laser, the fluorochrome is excited and emits radiation collected in a detector (Biosciences, 2000).

6.3.2. *Flow cytometry experimental protocol*

Whole blood from all subjects was drawn by venipuncture after a fasting period of at least 12 hours in BD Vacutainer tubes (BD Biosciences, San José, CA) containing 3.2% sodium citrate, or in BD Vacutainer PST™ tubes II with lithium heparin as an anticoagulant agent (17 IU/mL; BD Biosciences).

Saturating concentrations of each fluorochrome-conjugated antibody (**Table 7**) were used according to the manufacturer's instructions to detect different cell surface markers. Next, 20 µL of blood was added to each tube, gently shaken and incubated 30 min at room temperature and in the dark. Following the incubation period, 1X lysis buffer (BD FACS Lysing Solution 10X, BD Bioscience, CA) was added to each tube to lyse erythrocytes. Finally, samples were run into a the FACSVerse BD cytometer (BD Biosciences) and analyzed using FlowJo®v.10.0.7 software (FlowJo, Ashland, OR).

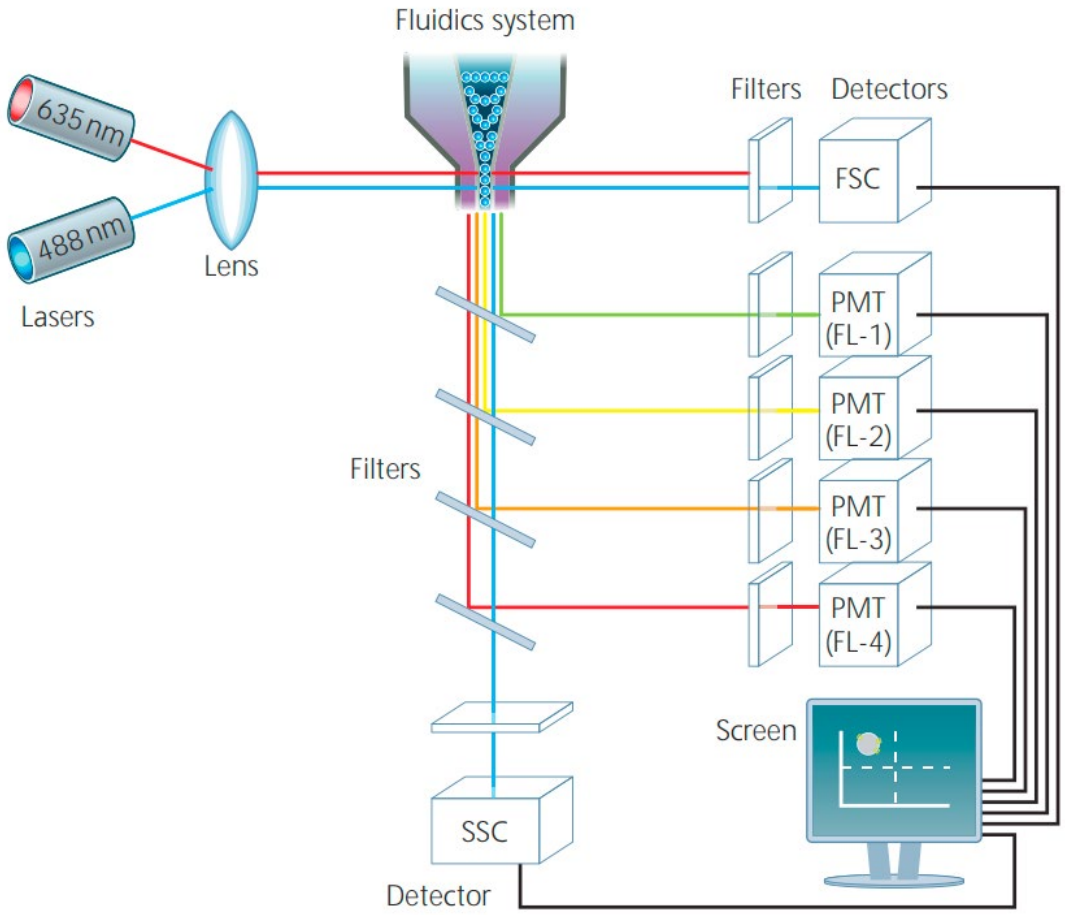

Figure 11. Schematic of a cytometer setup.

Once particles pass through the fluid system, the laser excites them. Radiation from each molecule passes through various filters to eliminate unwanted wavelengths and it is sent to detectors. Modified from (M. J. A. s. Rahman, 2006).

Table 7 – Antibodies used in flow cytometry assays

Antibody- Fluorochrome	Clone	Isotype	Supplier	Immune cell
CD41 – CF-Blue™	HIP8	IgG	Immunostep	Platelets
PAC-1 – FITC	PAC-1	Mouse IgM	BD Biosciences	
P- selectin (CD62P) – APC	HI62P	IgG_1	Immunostep	
CD41 – PE/Cy7™	HIP8	Mouse IgG_1	BioLegend	
CD45 – PB™	HI30	Mouse IgG_1	BioLegend	Leukocytes
CD69- PE	FN50	IgG_1	Immunostep	Leukocyte activation
CD69 – APC	FN50	Mouse IgG_1	BD Biosciences	
CD11b – PerCP/Cy™5.5	ICRF44	Mouse IgG_1	BioLegend	Myeloid lineage
CD11b – PE	CBRM1/5	Mouse IgG_1	BioLegend	Myeloid activation
CD193/CCR3 – PE	5E8	Mouse IgG_{2B}	BD Biosciences	Eosinophils
CD16 – FITC	3G8	Mouse IgG_1	BD Biosciences	
CD16 – APC	3G8	Mouse IgG_1	Immunostep	
CD14 – APC	47-3D6	Mouse IgG_{2A}	Immunostep	Monocytes
CD192 (CCR2) – BV421™	K036C2	Mouse IgG_{2A}	BioLegend	
CX_3CR1 – PE	2A9-1	Rat IgG2B	BioLegend	
CD8 – FITC	SK1	Mouse IgG_1	BD Biosciences	Tc lymphocytes
CD4 – PerCP/Cy™5.5	RPA-T4	Mouse IgG_1	BD Biosciences	Th lymphocytes
CD183 / CXCR3 – AF488	IC6/CXCR3	Mouse IgG_1	BD Biosciences	
CD196 / CCR6 – BV421™	11A9	Mouse IgG_1	BD Biosciences	
CD4 – FITC	SK3	Mouse IgG_1	BD Biosciences	Treg lymphocytes
CD127 – Alexa Fluor® 647	HIL-7R-M21	Mouse IgG_1	BD Biosciences	
CD25 – PE/Cy™7	2A3	Mouse IgG_1	BD Biosciences	

Tc: T citotoxic; Th: T helper; Treg: T regulatory

6.3.3. *Platelet analysis*

6.3.3.1. *Measurement of platelet activation*

To assess platelet activation, PAC-1$^+$ platelets (detecting activated integrin $\alpha_{IIb}\beta_{3/}$GPIIb/IIIa) and P-selectin (CD62P) expression were measured in platelets (CD41$^+$ population) from PH patients and age-matched controls by flow cytometry. Samples of citrated blood, diluted 1:10 in glucose buffer (1 mg/mL glucose in phosphate-buffered saline; PBS containing 0.35% of bovine serum albumin, BSA; Sigma-Aldrich) (Murugappa & Kunapuli, 2006), were incubated in the dark for 30 min with a 5-carboxyfluorescein (CF)-Blue™-conjugated monoclonal antibody (mAb) against human CD41 (clone HIP8, IgG_1; Immunostep, Salamanca, Spain) and a fluorescein isothiocyanate (FITC)-conjugated mouse mAb against the human integrin $\alpha_{IIb}\beta_{3/}$GPIIb/IIIa (clone PAC-1, IgM; BD Biosciences) or with an allophycocyanin (APC)-conjugated mAb against human P-selectin (CD62P, clone HI62P, IgG_1; Immunostep).

Samples were run into the cytometer. The morphology was determined using the FSC vs SSC channels followed by a selection of the CD41$^+$ population (platelets), as shown in **Figure 12**. Results were expressed as a percentage of positive platelets.

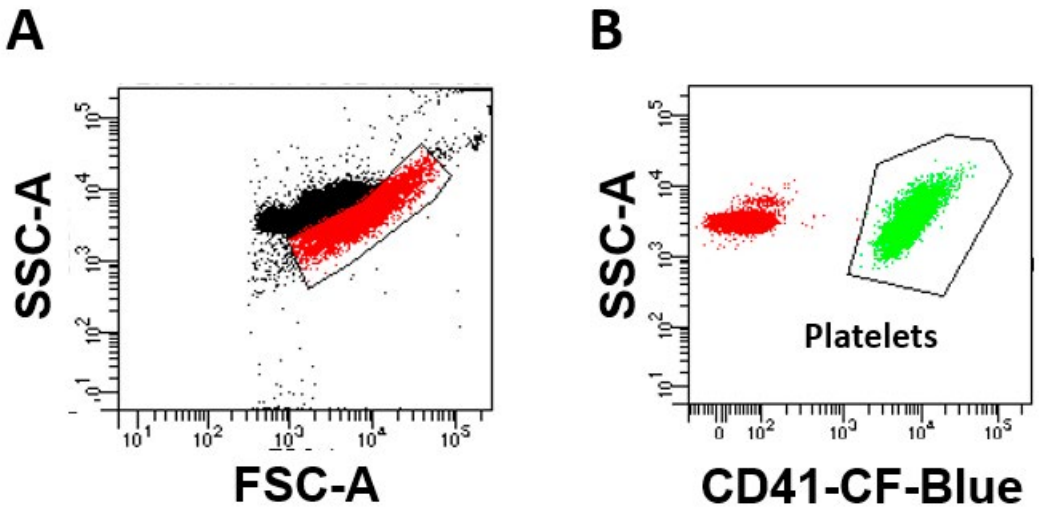

Figure 12. Flow cytometry detection and morphologic gating of human platelets in whole blood.

Platelets were gated according to the *side scatter* (SSC-A) and *forward scatter* (FSC-A, **A**) in the logarithmic scale and defined as CD41$^+$ population (**B**).

6.3.3.2. *Determination of CCR3 expression in platelets*

To determine the expression of CCR3 in platelets, both from healthy individuals and from patients with PH, 20 µL of citrate blood was incubated with 1 µL of phycoerythrin (PE)- conjugated mouse mAb against human CD193/CCR3 (clone 5E8, IgG_{2B}, BD Biosciences) and with 1 µL of 5-carboxyfluorescein (CF)-Blue™ conjugated mAb against human CD41 (clone HIP8, IgG_1, Immunostep, Salamanca, Spain). Samples were incubated for 30 min at room temperature in the dark. Subsequently, the erythrocytes were lysed with 1X lysis buffer (*BD FACS Lysing Solution* 10X, BD Biosciences, CA).

6.3.4. *Leukocyte studies*

6.3.4.1. *Neutrophils and eosinophils*

To assess the polymorphonuclear population present in the blood samples, the Pacific Blue (PB)-conjugated mouse mAb against human CD45 (clone HI30, IgG_1; BioLegend, San Diego, CA) and an elevated SSC were used to discard the erythrocytes and select the neutrophilic and eosinophilic populations. These cells correspond to the population with the highest granular content. To distinguish these two populations, the analysis was carried out with the fluorescein isothiocyanate (FITC)- conjugated mouse mAb against human CD16 (clone 3G8, IgG_1; BD Biosciences). Subsequently, an analysis of the expression of the CCR3 receptor was performed using the phycoerythrin (PE)- conjugated mouse mAb against human CD193/CCR3 (clone 5E8, IgG_{2B}, BD Biosciences).

In some experiments, heparinized blood samples were incubated with EDTA (10 mM, for 15 min at 37ºC) to promote platelet dissociation as described (Postea et al., 2012). This disaggregation was measured using the marker CD41 in circulating leukocyte subsets. To do this, heparinized whole blood or EDTA samples were incubated in the dark for 30 min with saturated amounts of a PE/Cy™7-conjugated mouse mAb against human CD41 (clone HIP8, IgG_1, Biolegend). Subsequently, an analysis determined the activation state in these cell populations with a PE-conjugated mAb against human CD69 (clone FN50, IgG_1; Immunostep) or an APC-conjugated mAb against human integrin CD11b (clone M1/70, IgG_{2B}, BD Biosciences).

Table 8 – Antibodies for the detection of polymorphonuclear cells

Antibody	Cellular population
$CD16^+$	Neutrophils
$CD16^-CCR3^+$	Eosinophils

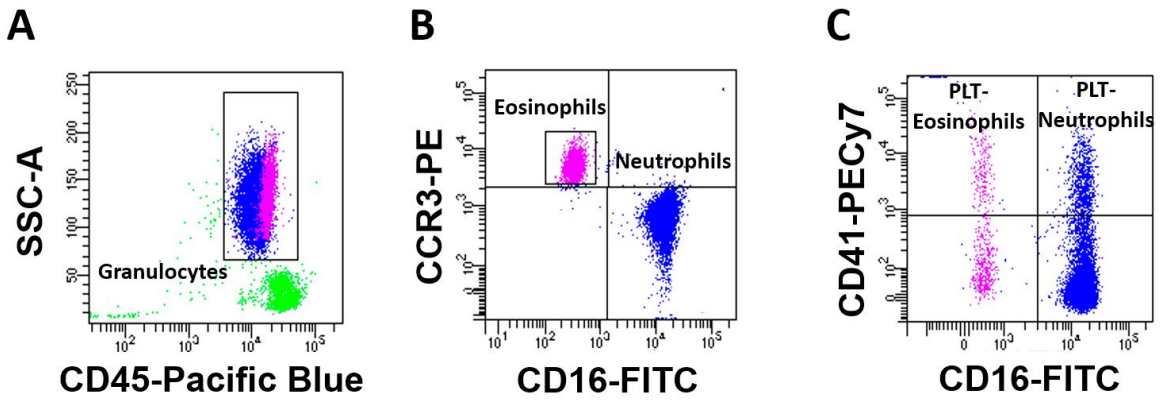

Figure 13. Flow cytometry detection and morphologic gating of human neutrophils and eosinophils in whole blood.

Population were selected by CD45 labeling and morphology (high SSC; **A**). To differentiate cell population, CD16 and CCR3 antibodies were used, being neutrophils $CD16^+$ and eosinophils $CD16^-$ (**B**). Neutrophil-platelet (PLT) complexes were selected as $CD16^+CCR3^-CD41^+$ population from heparinized whole blood (**C**), and platelet-free neutrophils were gated as $CD16^+CCR3^-CD41^-$ from blood incubated with EDTA (**C**). Eosinophil-platelet (PLT) complexes were selected as $CD16^-CCR3^+CD41^+$ population from heparinized whole blood (**C**), and platelet-free eosinophils were gated as $CD16^-CCR3^+CD41^-$ from blood incubated with EDTA (**C**).

6.3.4.2. *Monocytes*

To select the monocyte population, an APC-conjugated mouse mAb against human CD14 (clone 47-3D6, IgG_{2A}; Immunostep) was used. Previous studies (Jaipersad, Lip, Silverman, & Shantsila, 2014) demonstrated the existence of three subpopulations of monocytes differentiated by the surface markers CD16 and CCR2. Therefore, the CD14 antibody was confronted with the antibodies FITC-conjugated mouse mAb against human CD16 (clone 3G8, IgG_1; BD Biosciences) and to BV421™-conjugated mouse mAb against human CD192 (CCR2, clone K036C2, IgG_{2A}; Biolegend) (**Figure 14**). Subsequently, leukocyte-platelet aggregates were analyzed using the marker CD41 – PE/Cy7™ (clone HIP8, Mouse IgG_1; BioLegend) as described in the previous section. To detect monocyte activation, an APC-conjugated mouse mAb against human integrin CD11b (clone ICRF44, IgG_1, Biolegend, San Diego, CA). Similarly, the fractalkine receptor (CX_3CR1) expression was also determined in these three subpopulations using a PE-conjugated rat mAb against human CX_3CR1 (clone 2A9-1, IgG_{2B}; Biolegend).

Table 9 – Antibodies for the detection of monocyte subpopulations (Shantsila et al., 2011)

Antibody	Cellular subpopulation
$CD14^{+}CD16^{-}CCR2^{+}$	Type 1 monocytes (Mon 1)
$CD14^{+}CD16^{+}CCR2^{+}$	Type 2 monocytes (Mon 2)
$CD14^{+}CD16^{+}CCR2^{-}$	Type 3 monocytes (Mon 3)

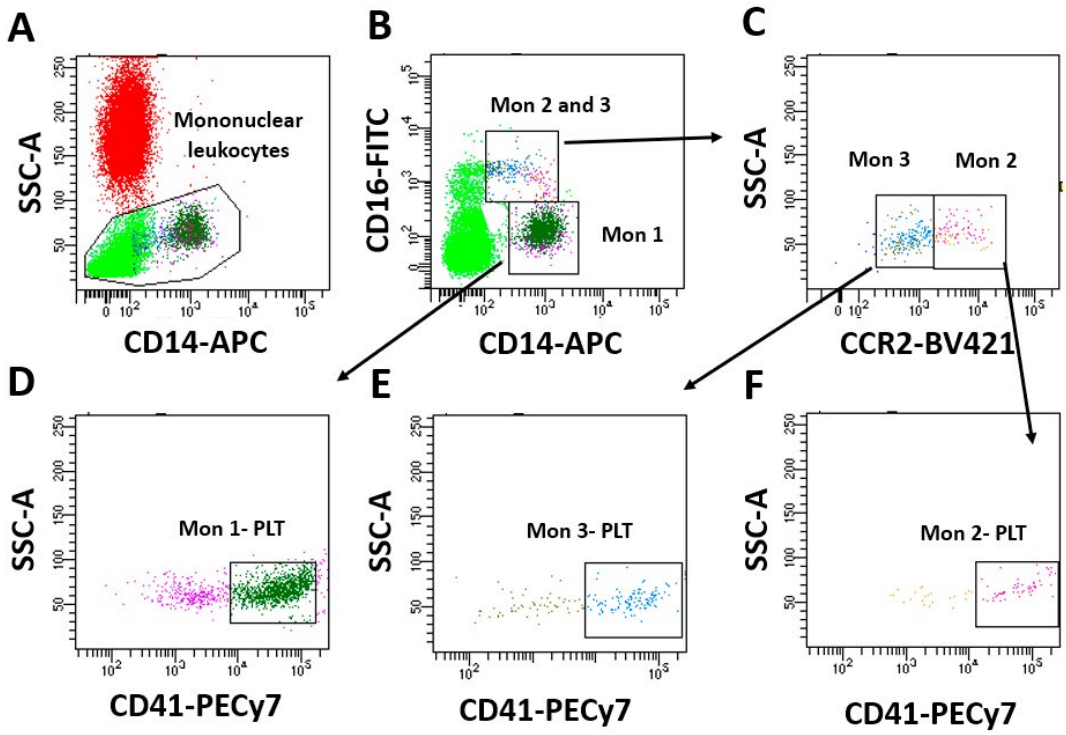

Figure 14. Flow cytometry detection and morphologic gating of human monocytes in whole blood.

Monocytes were selected by CD14 labeling and morphology (medium SSC-A, **A**). For the detection of monocyte subpopulations, CD16 and CCR2 markers were used (**B – F**). Monocytes-platelets (PLT) complexes were selected as $CD14^{+}CD41^{+}$ populations in heparinized whole blood, and platelet-free monocytes were gated as $CD14^{+}CD41^{-}$ from blood incubated with EDTA (**D** - **F**).

6.3.4.3. *T lymphocytes*

CD3, CD4 and CD8 markers were used to identify the population of T lymphocytes ($CD3^+$), the T helper (Th, $CD4^+$) and T cytotoxic subpopulations (Tc, $CD8^+$), respectively, present in the peripheral blood. The gating strategy consisted in the selection of T lymphocytes using an APC-conjugated mouse mAb against CD3 (CD3 – APC, clone 33-2A3, Mouse IgG_{2A}; Immunostep), a V450-conjugated mouse mAb against human CD4 (clone RPA-T4, IgG_1; BD Bioscences) and finally, a FITC-conjugated mouse mAb against human CD8 (clone SK1, IgG_1; BD Biosciences). Subsequently, the possible contribution of platelets was studied as previously described (***Section 5.3.4.1 Leukocyte studies. Neutrophils and eosinophils***). Then, an analysis of activation state was determined by using a PE-conjugated mAb against human CD69 to detect lymphocyte activation (clone FN50; IgG_1; Immunostep).

Table 10 – Antibodies for the detection of lymphocytes

Antibody	Cellular subpopulation
$CD3^+$	T lymphocytes
$CD3^+CD4^+$	T helper lymphocytes
$CD3^+CD8^+$	T cytotoxic lymphocytes

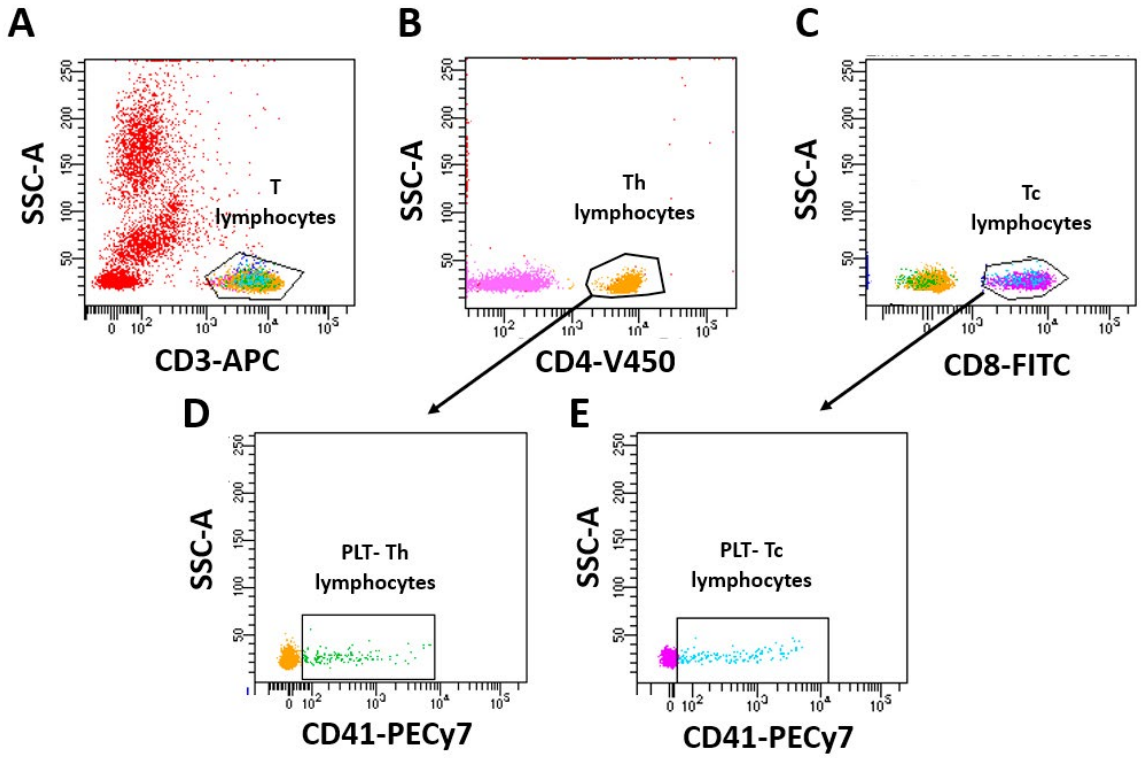

Figure 15. Flow cytometry detection and morphologic gating of human T lymphocytes in whole blood.

T lymphocytes were selected as $CD3^+$ population and with a low SSC (**A**). T helper (Th) lymphocytes were the $CD3^+CD4^+$ population (**B**) and cytotoxic T lymphocytes (Tc) were selected as $CD3^+CD8^+$ (**C**). Th lymphocyte-platelet (PLT) complexes were selected as $CD3^+CD4^+CD41^+$ population from heparinized whole blood (**D**), and platelet-free were gated as $CD3^+CD4^+CD41^-$ from blood incubated with EDTA (**D**). Tc lymphocytes-platelet (PLT) complexes were selected as $CD3^+CD8^+CD41^+$ population from heparinized whole blood (**E**), and platelet-free Tc lymphocytes were gated as $CD3^+CD8^+CD41^-$ from blood incubated with EDTA (**E**).

6.3.4.4. Th lymphocytes

To identify the T helper lymphocyte population present in blood samples, the PerCP/Cy5.5™ - conjugated mouse mAb against human CD4 (clone RPA-T4, IgG_1, BD Biosciences) was used. The different subpopulations of T helper lymphocytes were identified by Alexa Fluor® 488 - conjugated mouse mAb against human CD183/CXCR3 (clone IC6/CXCR3, IgG_1, BD Biosciences) and the BV421™-conjugated mouse mAb against human CD196/CCR6 (clone 11A9, IgG_1, BD Biosciences). Subsequently, the expression of CCR3 was evaluated by the phycoerythrin (PE)- conjugated mouse mAb against human CD193/CCR3 (clone 5E8, IgG_{2B}, BD Biosciences). Leukocyte-platelet aggregates were analyzed using the marker CD41 – PE/Cy7™ (clone HIP8, Mouse IgG_1; BioLegend) and activation was determined employing an APC-conjugated mouse mAb against human CD69 (clone FN50, IgG_1, BD Biosciences).

Table 11 – Antibodies for Th lymphocyte subtype detection

Antibody	Cellular subpopulation
$CD4^+CXCR3^+CCR6^-$	T helper 1 (Th1)
$CD4^+CXCR3^-CCR6^-$	T helper 2 (Th2)
$CD4^+CXCR3^-CCR6^+$	T helper 17 (Th17)

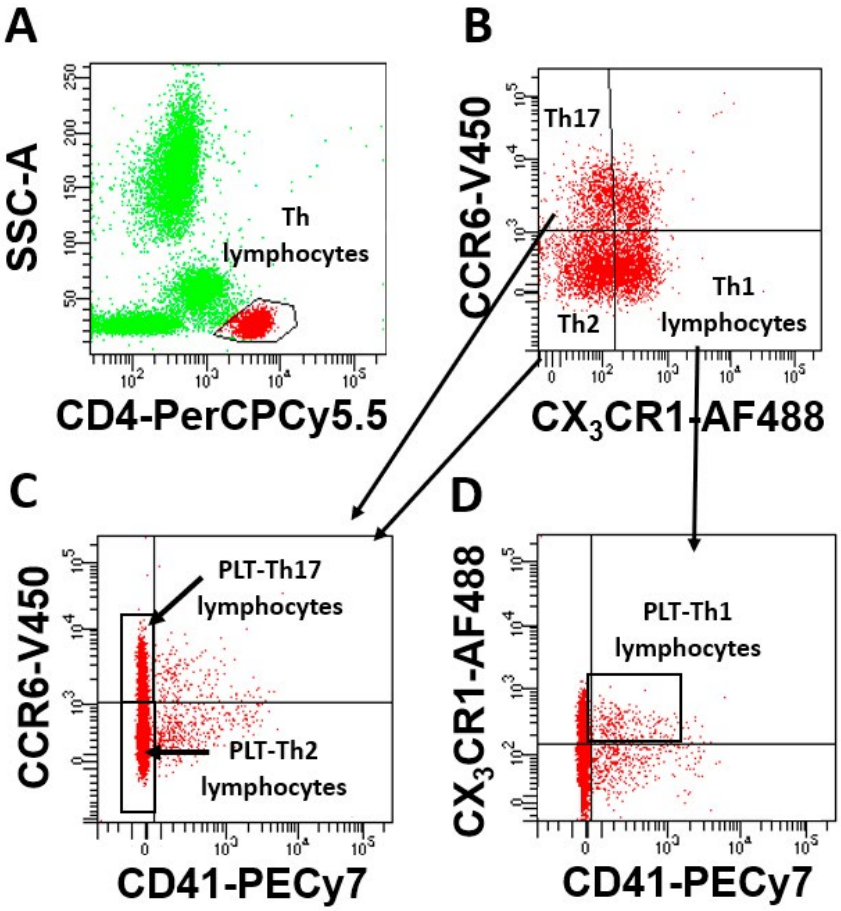

Figure 16. Flow cytometry detection and morphologic gating of human $CD4^+$ lymphocytes in whole blood, as well as Th1, Th2 and Th17 populations.

Th lymphocytes were selected as $CD4^+$ population and with a low SSC (**A**). Th lymphocyte subpopulatios were detected with markers CXCR3 and CCR6 (**B**). Th1-, Th2- and Th17-platelet complexes were selected as $CCR6^-CXCR3^+CD41^+$, $CCR6^-CXCR3^-CD41^+$ or $CCR6^+CXCR3^-CD41^+$ respectively, whereas platelet-free Th1, Th2 and Th17 cells were selected as $CCR6^-CXCR3^+CD41^-$, $CCR6^-CXCR3^-CD41^-$ or $CCR6^+CXCR3^-CD41^-$ respectively (**C** and **D**).

6.3.4.5. *Regulatory T lymphocytes (T reg)*

To identify the Treg population, a human regulatory T cell cocktail (BD Pharmingen™ Human Regulatory T Cell Cocktail; BD Biosciences) was used. Th lymphocytes were firstly identified with the marker CD4 (FITC-conjugated mouse mAb, against human CD4, clone SK3, IgG_1; BD Biosciences). An Alexa Fluor® 647-conjugated mouse mAb against human CD127 (clone HIL-7R-M21, IgG_1; BD Biosciences) and a PE/Cy™7-conjugated mouse mAb against human CD25 (clone 2A3, IgG_1; BD Biosciences) were used to determine the natural Treg cells (**Figure 17**). Two experiments were carried out in parallel: one with heparinized whole blood and the other with EDTA-treated blood, to determine Treg lymphocyte-platelet aggregates. For that purpose, a CF-Blue™-conjugated mAb against human CD41 (clone HIP8, IgG_1; Immunostep) was employed.

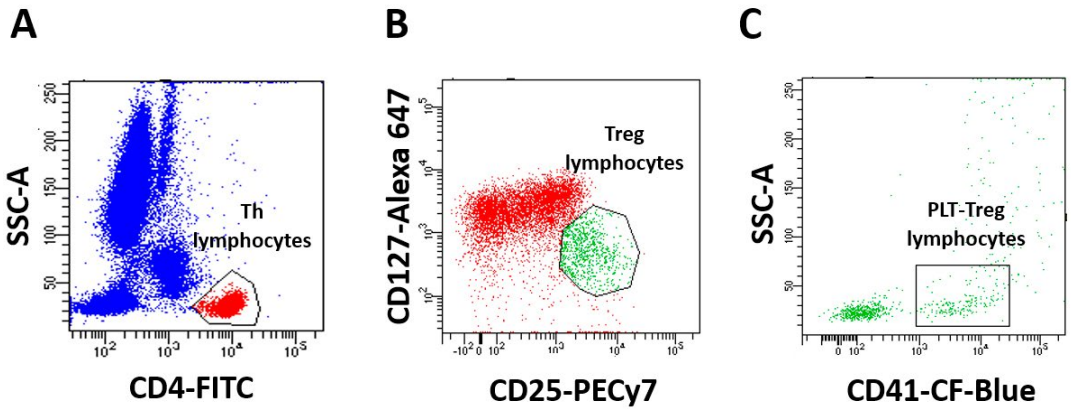

Figure 17. Flow cytometry detection and morphologic gating of human Treg lymphocytes in whole blood.

Treg lymphocytes were selected as $CD4^+$ population and with a low SSC (**A**). Treg were detected with the markers CD127 and CD25 (**B**). Treg lymphocyte-platelet complexes were selected as $CD4^+CD25^+CD127^+CD41^+$ population from heparinized whole blood (**C**), and platelet-free Treg lymphocytes were gated as $CD4^+CD25^+CD127^+CD41^-$ from blood incubated with EDTA (**C**).

6.4. Parallel-plate flow chamber studies

In order to study the leukocyte adhesion to the dysfunctional arterial endothelium, a parallel-plate flow chamber assay was employed.

6.4.1. *General points*

Parallel-plate flow chamber procedure allows the visualization of cell adhesion under dynamic flow conditions, mimicking the physiological milieu. As shown in **Figure 18**, the parallel flow chamber system

consists in a base plate with an entrance and exit port through which cells and media are perfused. Coupled to this base plate there are a vacuum pump and a gasket. At the base plate, there is a 35 mm diameter culture plate, on which the endothelial cell monolayer is grown. As a result, a flow channel is generated over the endothelial monolayer, with the infusion rate being regulated by a suction pump, thus emulating the blood flow over the human endothelium.

To measure leukocyte adhesion, HUAEC were seeded on 35 mm diameter culture plates pre-coated with 5.5 µg/mL fibronectin. Once confluence was reached and after the corresponding treatment of the cells, the plates were placed in a dynamic flow assay using a parallel flow chamber (GlycoTech flow, Gaithersburg, MD). The GlycoTech flow chamber was assembled and placed onto an inverted microscope stage, and diluted whole blood was then perfused through the HUAEC monolayers. Leukocyte adhesion was determined after 7 min at 0.5 dyn/cm^2. Cells interacting on the surface of the endothelium were visualized and recorded (x20 objective, x10 eyepiece) using a phase-contrast microscope (Axio Observer A1, Carl Zeiss microscope, Oberkochen, Germany) connected to a video camera (SSC-DC80P, Sony, Tokio, Japan). At least 5 fields were recorded for 10 s each. Those leukocytes that established a stable contact with the endothelial monolayer for at least 10 s were considered adherent. Adherent cells were counted while the perfusion medium remained in continuous infusion.

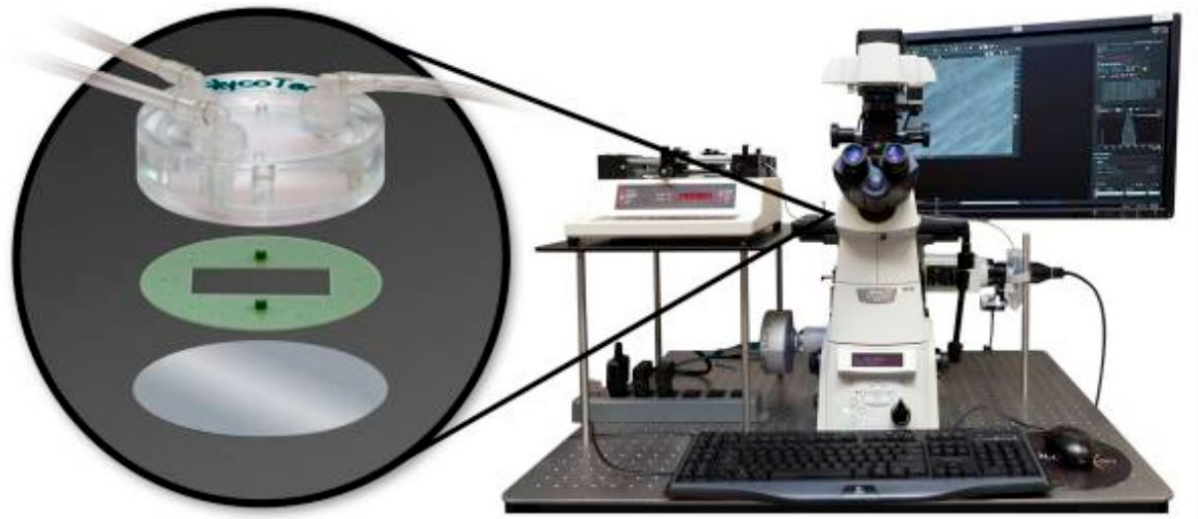

Figure 18. Parallel-plate flow chamber system.
Adapted from (Palange et al., 2012).

6.4.2. *Experimental design*

HUAEC were cultured on 35 mm culture dishes. Cells were stimulated, or not, with recombinant human TNF-α (20 ng/mL, Sigma-Aldrich, Madrid, Spain) for 24h. Before starting each assay, HBSS (Lonza, Verviers,

Belgium), tempered at 37ºC, was perfused in order to adjust the flow at a rate of 0.156 mL/min (corresponding to a shear stress of 0.5 dyn/cm^2). Then whole blood (1:10 dilution in Hank's balanced salt solution, HBSS) was perfused across HUAEC monolayers using a Glycotech flow chamber (GlycoTech, Gaithersburg, MD) assembled and placed onto an inverted microscope. To determine the platelet contribution to leukocyte adhesion, some experiments were carried out with whole blood incubated with EDTA (10 mM, for 15 minutes at 37ºC), as previously described. In all experiments, leukocyte-endothelial cell interactions were determined as described before.

6.5. Immunofluorescence studies

To visualize adherent platelet-leukocyte complexes to endothelial cells, immunofluorescence analysis was performed. HUAEC were grown to confluence on glass coverslips and stimulated with TNF-α (20 ng/mL; Sigma-Aldrich) for 24 h. Cells were incubated for 1 h at 37ºC with heparinized whole blood from patients with PH and age-matched controls, treated or not with EDTA as described before in ***Section 5.3.4.1 Leukocyte studies. Neutrophils and eosinophils***. Then, cells were fixed with 4% paraformaldehyde (PFA; PanReac AppliChem GmbH) and blocked in PBS containing 1% BSA (Sigma-Aldrich). Subsequently, cells were incubated at room temperature for 2 h with an Alexa Fluor® 488-conjugated mouse mAb against human CD45 (1:50 dilution, clone HI30, IgG_1; BioLegend) and an APC-conjugated mAb against human CD41 (1:50 dilution, clone HIP8, IgG_1; Immunostep) in 0.1% BSA- PBS. Nuclei from endothelial cells and leukocytes were counterstained with Hoechst dye (1:4000 dilution; Sigma-Aldrich). Images were captured with an Axio Observer A1 fluorescence microscope (ZEISS International).

6.6. Quantification of soluble metabolic and inflammatory markers

Blood from patients with PH and controls was drawn by venipuncture after a fasting period of at least 12 hours in BD Vacutainer PST™ II tubes with lithium heparin as anticoagulant agent (17 IU/mL; BD Biosciences) and was centrifuged to obtain the plasma, which was stored at -80 ° C. Soluble human cytokines interleukin human soluble interleukin (IL)-4, IL-5, IL-6, IL-10, IL-12 IL-13, IL-25, IL-33, TNF-α, IFN-γ, growth-regulated oncogene-α (GRO-α/CXCL1), platelet factor-4 (PF-4/CXCL4), IL-8/CXCL8, MCP-1/CCL2, regulated on activation normal T cell expressed and secreted chemokine (RANTES/CCL5), eotaxin-1/CCL11, eotaxin-2/CCL24, eotaxin-3/CCL26 fractalkine/CX_3CL1, soluble P-selectin (sP-selectin), adiponectin, leptin and ghrelin were measured in plasma samples using the technique known as ELISA (*Enzyme-Linked Immunosorbent assay*; Human DuoSet® ELISA; R&D Systems, Inc., Minneapolis, MN) following the manufacturer's instructions. Results were expressed as pg/mL or ng/mL of the plasma mediator.

7. ANIMAL STUDIES

All experiments carried out with animals comply with the principles detailed in the "*Guide for the Care and Use of Laboratory Animals*", 8th edition and published by the National Institutes of Health (NIH, Department of Health and Human Services) of the United States (NIH publication No. 85-23, revised in 2011) and approved by the Ethical Committee on Animal Experimentation of the University of Valencia (Valencia, Spain).

Animals were bred and maintained under specific pathogen-free conditions, fed with a control or atherogenic autoclaved diet and with free access to water during the entire experimental period, with a humidity of 60-65% and a constant temperature of 22 ± 2 ° C with 12h dark / light cycles. All protocols and corrective measures have been used to avoid animal suffering.

7.1. ApoE$^{-/-}$ mice: A model of aterosclerosis

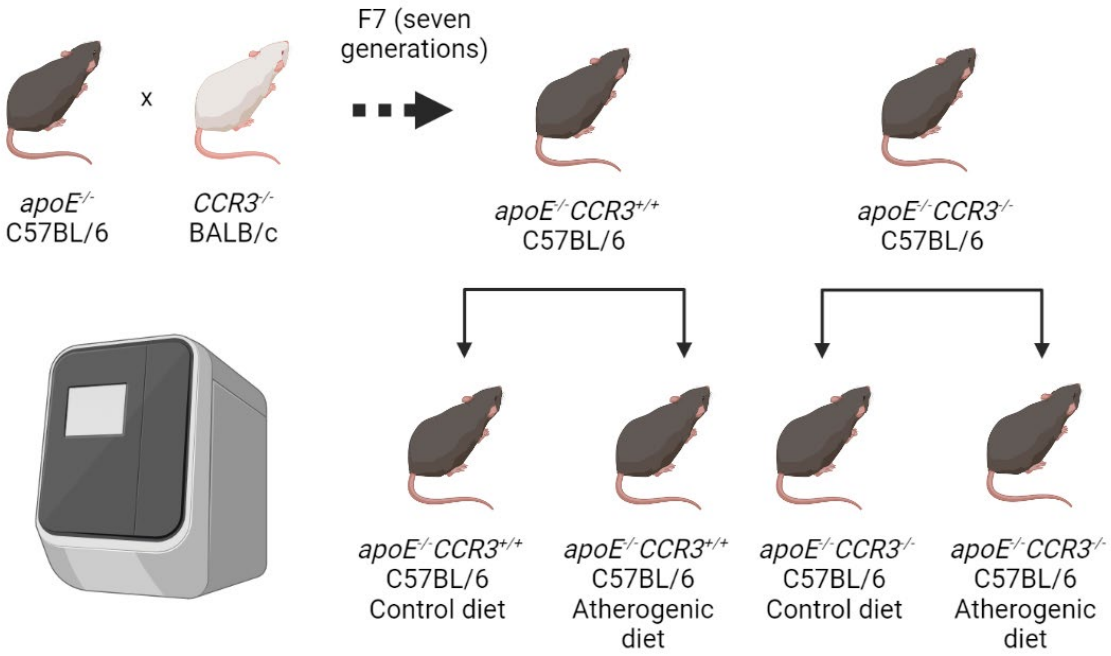

Figure 19. Generation of double transgenic apoE$^{-/-}$CCR3$^{-/-}$.

After seven generations, the different genotypes were obtained. Animals were fed with control diet during their first eight weeks. Then, one group of each genotype remained with this diet for additional eight weeks and another group of both genotypes was fed an atherogenic diet for the same period of time.

ApoE$^{-/-}$ C57BL/6 and *CCR3*$^{-/-}$ BALB/c mice were supplied by Charles River Laboratories. To obtain the double transgenic mice, *apoE*$^{-/-}$*CCR3*$^{-/-}$ C57BL/6 mice were generated by crossing *apoE*$^{-/-}$ C57BL/6 with *CCR3*$^{-/-}$ BALB/c for seven generations. Therefore, the genotypes obtained were: *apoE*$^{-/-}$ *CCR3*$^{-/-}$ and *apoE*$^{-/-}$ *CCR3*$^{+/+}$. Genotyping was carried out with mouse-tail DNA using the Maxwell® 16 Mouse Tail DNA purification kit (Promega, Madison, WI) following manufacturer´s instructions. For that purpose, the Maxwell® 16 Instrument (Promega) was employed.

7.1.1. *Polymerase Chain Reaction (PCR) analysis for genotype confirmation*

To confirm the genotype, a polymerase chain reaction analysis was performed using specific primers (5'-3' sequences) (**Table 12**). The oIMR primers 180, 181 and 182 were used to determine the presence or absence of the *Apoe* gene while the Ex2p5 FW and RV primers verified the absence of the *Ccr3* gene. To ensure the presence of *Ccr3*, primers oIMR 3896 and 3897 were utilized. All primers were designed by Sigma – Aldrich.

Table 12 – Sequences of specific primers for *Apoe* and *Ccr3* genes

Gen	Primer	Sequence [5' – 3')
Mouse Apoe	oIMR 180	GCCTAGCCGAGGGAGAGCCG
	oIMR 181	TGTGACTTGGGAGCTCTGCAGC
	oIMR 182	GCCGCCCCGACTGCATCT
Mouse Ccr3	Ex2p5 FW	CTTGCTGACCGCTTCCTCGTG
	Ex2p5 RV	CATCATGTTGCCCAGGAGGCC
Mouse Ccr3	oIMR 3896	TGGCATTCAACACAGATGAAA
	oIMR 3897	CATGACCCCAGCTCTTTGAT

For each PCR sample, the following reagents were used (**Table 13**).

Table 13 – Reagents used in PCR assay

Stock reagent	Volumen (µL)/sample
Promega™ GoTaq™ Master Mix	12.5
Forward Primer	0.2
Reverse Primer	0.2
Nuclease-free Water	9.1
DNA sample	2

Finally, the PCR tubes were placed in the SimpliAmp ™ Thermal Cycler (Applied Biosystems, Thermo

Fisher Scientific, Waltham, MA) and the following PCR program (**Table 14**) was used.

Table 14 – Cycle conditions for PCR

Cycle step	Temperature (°C)	Time (min)
Initial denaturalization	94	5
Denaturalization	94	0.5
Annealing	62	0.5
Extension	72	0.5
(Denaturalization + Anneling + Extension) repeated for 38 cycles		
Final extension	72	2
Hold	4	∞

Gels were prepared with 2% agarose dissolved in 1x Tris acetate-EDTA (TAE) buffer. After solidification, the gel was placed inside the electrophoresis chamber and covered with TAE buffer before loading the samples. Gels were run at 120V for 30 minutes. A molecular weight marker (Generuler™ 1 Kb Plus SNA Ladder; Thermo Fisher Scientific, Waltham, MA) was used to establish the weight of the DNA.

Table 15 – TAE 50x

Stock reagent	Measure units
Tris free base	242 g
Disodium EDTA	22.6 g
Glacial Acetic Acid	57.1 mL
ddH_20	to 1 L

7.1.2. *Induction of atherosclerosis by diet*

Male *apoE*$^{-/-}$, *apoE*$^{-/-}$*CCR3*$^{+/+}$ and *apoE*$^{-/-}$*CCR3*$^{-/-}$ mice were fed with a control diet during their first eight weeks (2.8% fat; Panlab, S.L, Harvard Apparatus, Barcelona, Spain). Then, one group of each genotype remained with this diet for additional eight weeks and another group of both genotypes was fed with an atherogenic diet for the same period of time (10.8% fat, 0.75% cholesterol, S4892-E010; Ssniff Spezialdiäten, Soest, Germany). Finally, six groups of animals were analyzed: *apoE*$^{-/-}$ fed a control diet, *apoE*$^{-/-}$ fed an atherogenic diet, *apoE*$^{-/-}$*CCR3*$^{+/+}$ fed a control diet, *apoE*$^{-/-}$*CCR3*$^{+/+}$ fed an atherogenic diet, *apoE*$^{-/-}$*CCR3*$^{-/-}$ fed a control diet and *apoE*$^{-/-}$*CCR3*$^{-/-}$ fed an atherogenic diet (**Figure 19**).

7.2. Quantification of the atherosclerotic lesion

After 8 weeks with control or atherogenic diet, the mice investigated (*apoE*$^{-/-}$, *apoE*$^{-/-}$*CCR3*$^{+/+}$ and *apoE*$^{-/-}$*CCR3*$^{-/-}$) were sacrificed by an anaesthetic overdose with an intraperitoneal administration of a mixture of medetomidine hydrochloride (1mg/mL; Orion Corporation, Espoo, Finland) and ketamine (50 mg/mL; Orion Corporation) and cut open ventrally. Left cardiac ventricles were perfused with 10 mL of PBS in order to remove the blood from the aortas with its exit through the severed right atrium. Aortas were isolated and cleaned *in situ* with PBS, and fixed with 4% PFA *overnight* at 4 ° C.

Next day, aorta samples were stained with Oil Red-O (0.2% Oil Red-O in 78% methanol; Sigma-Aldrich) following the protocol previously described (Avogaro & de Kreutzenberg, 2005; Landmesser et al., 2004). Images were obtained (Axio Observer A1 inverted microscope; ZEISS International), digitized and analysed (ImageJ software, Windows free version; NIH, Bethesda, MD). Scoring was blindly performed on coded slides.

7.3. Histological analysis

During sacrifice, different murine organs and tissues were removed, washed with PBS and processed. Hearts were fixed in 4% PFA *overnight*. The following day, they were dehydrated and embedded in paraffin to obtain 5 µm histological sections using a microtome (Leica RM2245; Leica Biosystems, Wetzlar, Germany) and mounted on Superfrost plus slides (J1800AMNZ, Fisher Scientific). Other organs were embedded in specific moulds (1120, Thermo Fisher Scientific) in *Optimal Cutting Temperature* (OCT, 22-118, DDK, Vigenavo, Italy) medium. These samples were deep frozen with isopentane and liquid nitrogen and kept at -80ºC until the obtention of histological sections in silane slides (631-1163, VWR, Leuven, Belgium) using a cryostat microtome (Thermo Shandon FE A78900102, Thermo Fisher).

Once the samples of sigmoid aortic valves were dried, the area of interest was selected using a digital microscope (Leica DMD108, Leica Biosystems) and the following histological studies were performed:

7.3.1. *Hematoxylin and eosin staining*

Samples were hydrated and immersed in filtered Harris hematoxylin (Sigma-Aldrich) and continuously washed in running water. Samples were then rapidly immersed in differentiation solution (0.25 mL of concentrated HCl in 100 mL of 70% ethanol) followed by continuous washing with running water. Samples were first immersed in 95% ethanol and then in a 1: 1 dilution of eosin in 95% ethanol. After a third wash, samples were dehydrated in solutions with increasing concentrations of ethanol and finally immersed in

xylene. Staining was completed with the assembly of the coverslips on the slides with the help of Bio-Mount synthetic based mounting media for histology and cytology (Bio-Optica, Milan, Italy).

7.3.2. *Masson's trichrome staining*

This staining defines the area of connective tissue present in the atherosclerotic lesion, which is related to the stability of the atheroma plaque. It is also useful to determine the necrotic core that correlates with the crystallization of cholesterol in the lesion (Luo et al., 2016).

Samples were immersed in Weigert's Hematoxylin (Merck Millipore, Burlington, MA) and continuously washed in running water. Next, histological sections were stained with a fuchsin solution (1:10 dilution; Sigma-Aldrich) followed by a wash with 1% acetic acid. Subsequently, samples were immersed in a 5% phosphotungstic acid solution followed by an immersion in Light Green solution (Sigma-Aldrich) and an additional wash in 1% acetic acid. As in the previous staining, slides were assembled with their coverslips with Bio-Mount (Bio-Optica).

7.4. Immunohistochemical studies

Immunohistochemistry is a widely used technique to detect cell surface markers, cytokines or even transcription factors in tissues or cells.

7.4.1. *Immunohistochemistry assays in aortic sigmoid valves*

Samples were hydrated and the endogenous peroxidase was inactivated with 3% H_2O_2. Subsequently, non-specific binding was blocked with horse serum (5% in PBS, Abcam, Cambridge, UK) for for 1.5 h. Samples were incubated *overnight* at 4°C with different primary antibodies. The signal was amplified with a biotin-conjugated goat anti- rat secondary antibody (1:400 dilution, Santa Cruz Biotechnology, Inc.,) or a biotin-conjugated goat anti-rabbit secondary antibody (1:200, Invitrogen, Thermo Fisher Sicentific) (**Table 16**), and HRP-Streptavidin (1:2 dilution, Large Volume Streptavidin Peroxidase (Ready-To-Use), Thermo Fisher Scientific). Then, a solution with 3.3'-diamonobenzine (1:1000, DAB; Dako, Agilent Technologies, Santa Clara, CA) was used and samples were counterstained with Harris Hematoxylin (Sigma-Aldrich), dehydrated and mounted as described in ***Section 6.3. Histological studies.***

Table 16 – Immunohistochemistry assays (IHQ) of aortic sigmoid valves

IHQ	Blocking buffer	Antigen Retrieval	Primary Ab	Secondary Ab
Mac-3	Horse Serum (5%)	-	Rat mAb Mac-3 (1:100)	Biotin-Ab (1:400)
CCL11	Horse Serum (5%)	-	Rat mAb CCL11 (1:40)	Biotin-Ab (1:400)
IL-4	Horse Serum (5%)	Citrate Buffer	Rb mAb IL-4 (1:20)	Biotin-Ab (1:200)
PSTAT-6	Horse Serum (5%)	Citrate Buffer	Rb mAb PSTAT-6 (1:1000)	Biotin-Ab (1:200)

Rb: rabbit ; mAb: monoclonal antibody

7.4.2. *Immunohistochemistry of α-actin in aortic sigmoid valves*

Samples were hydrated and then blocked with horse serum (5% in PBS, Abcam) for 1 h. Subsequently, they were incubated with the alkaline phosphatase-conjugated mouse mAb against murine α-smooth muscle actin (1:60 dilution, clone 1A4, Sigma-Aldrich) *overnight* at 4°C, followed by the Fast Red (SigmaFast™, Fast Red TR / Naphthol AS-MX Alkaline Phosphatase Substrate Tablets Set, Sigma-Aldrich) according to manufacturer's instructions. Samples were mounted without dehydration with glycerol / gelatine.

7.4.3. *Immunofluorescences of aortic sigmoid valves*

Samples were heated at 60°C for 30 min to remove the wax. Then, they were deparaffinized and antigens were unmasked heating them in 10 mM citrate buffer (pH 6.0; **Table 17**) or 1 mM Tris-EDTA buffer (pH 9.0; Ta**ble 18**) for 20 min. Once at room temperature, non-specific binding was blocked with goat or house normal serum (**Table 19**) (5% in PBS-BSA 1%, Abcam). Next, samples were incubated with different primary antibodies at 4°C *overnight*. Specific labelling was detected after incubation for 1 h with Alexa Fluor 488 (1:1000 dilution; Molecular Probes, Thermo Fisher Scientific) or Alexa Fluor 594 (1:500 dilution, Molecular Probes, Thermo Fisher Scientific) secondary antibodies. Cell nuclei were counterstained with Hoechst 33344 dye (1:4000, Sigma-Aldrich). Then, coverslips were assembled with SlowFade® Gold antifade reagent (Molecular Probes, Thermo Fisher Scientific).

Table 17 – Composition of Citrate Buffer

Stock reagent	Measure units
$C_6H_5Na_3O_7 \cdot 2\ H_2O$	5.88 g
dH_2O	2 L
Tween 20	1 mL

Table 18 – Composition of Tris-EDTA Buffer

Stock reagent	Measure units
$C_4H_{11}NO_3$	2.42 g
EDTA tetrasodium salt 4-hydrate	0.74 g
dH_2O	2 L
Tween 20	1 mL

Different immunofluorescence assays were carried out to characterize the atherosclerotic plaque in this study. All their specifications are detailed in **Table 19.**

Table 19 – Reagents used for immunofluorescence assays (IF) in the aortic sigmoid valves

Epitope	Blocking buffer	Antigen Retrieval	Primary Ab	Secondary Ab
CD4	HS (5%)	Citrate buffer	Rat mAb CD4 (1:100)	AF488 anti-rat (1:1000)
CD8	HS (5%)	Citrate buffer	Rb pAb CD8 (1:500)	AF488 anti-rb (1:1000)
Siglec-F	HS (5%)	Citrate buffer	Rat mAb Siglec-F (1:20)	AF488 anti-rat (1:1000)
CCR3			Gt pAb CCR3 (1:200)	AF594 anti-goat (1:500)
Siglec-F	GS (5%)	Citrate buffer	Rat mAb Siglec-F (1:20)	AF594 anti-rat (1:500)
CD125			Rb pAb CD125 (1:50)	AF488 anti-rb (1:1000)
Siglec-F	GS (5%)	Tris-EDTA buffer	Rat mAb Siglec-F (1:20)	AF594 anti-rat (1:500)
Ly6G			Rb mAb Ly6G (1:2000)	AF488 anti-rb (1:1000)
EPX	HS(5%)	Citrate buffer	Rb pAb EPX (1:200)	AF488 anti-rb (1:100)
CCR3			Gt pAb CCR3 (1:200)	AF594 anti-goat (1:500)
CD68	HS(5%)	Citrate buffer	Rt pAb CD68 (1:50)	AF488 anti-rb (1:1000)
CD206			Rb pAb CD206 (1:100)	AF594 anti-goat (1:500)

HS: Horse Serum; GS: Goat Serum; mAb: monoclonal antibody; pAb: polyclonal antibody; Rb: rabbit; Gt: goat; AF: Alexa Fluor.

7.4.4. *Immunofluorescence for epoperoxidase (EPX^+) $CCR3^+$ cells in small intestine*

Samples at -80°C were warm up at room temperature for 15 min. Then, sections were fixed with 4% PFA for 7.5 min, antigens were unmasked and permeabilized with 0.5% PBS-Tween 20 for 10 min. Non-specific binding was blocked with horse serum (10% in PBS-BSA 1%, Abcam) for 1h. Samples were incubated with two primary antibodies, a rabbit mAb against murine EPX (1:200 dilution, IgG, Abcam) and a goat pAb against murine CCR3 (1:200 dilution, IgG, Abcam) *overnight* at 4°C. Specific labelling was detected with Alexa Fluor 488 donkey anti-rabbit (1:1000 dilution, Invitrogen) and Alexa Fluor 594 chicken anti-goat (1:500 dilution, Invitrogen) for 1 h. Cell nuclei were counterstained with Hoechst 33342 dye (1:4000, Sigma-Aldrich). Finally, coverslips were assembled with SlowFade® Gold antifade reagent (Molecular Probes, Thermo Fisher Scientific).

All the antibodies used in immunohistochemical studies are listed in the following table:

Table 20 – Antibodies used in immunohischemical and immunofluorescence assays

Antibody	Clone	Isotype	Supplier
Rat mAb against LAMP-2	M3/84	IgG_1	Santa Cruz Biotechnology
Rat mAb against CCL11	42285	IgG_{2a}	R&D Systems
Mouse mAb against α-actin.	1A4		Sigma- Aldrich
Rat mAb against CD4	4SM95	IgG_1	ThermoFisher
Rabbit pAb against CD8	-	IgG	ThermoFisher
Rat mAb against Siglec-F	E50-2440	LOU/M IgG_{2a}	BD Biosciences
Goat pAb against CCR3	-	IgG	Abcam
Rabbit pAb against IL5RA	-	IgG	Abcam
Rabbit mAb against Ly6G	EPR22909-135	IgG	Abcam
Rabbit pAb against EPX	-	IgG	Abcam

mAb: monoclonal antibody; pAb: polyclonal antibody

7.5. Measurement of lipid and glycemic profile

Total cholesterol (TC) and triglyceride (TG) levels were measured by enzymatic methods (Wako Pure Chemicals Industries, Ltd., Cape Charles, VA, USA). High-density lipoprotein cholesterol (HDL-c) was determined by the same method used for TC content quantification after apolipoprotein B (apoB) precipitation of with a combination of dextran sulfate and magnesium chloride ($MgCl_2$; Sigma-Aldrich) as previously described (Zieske et al., 2005).

Blood glucose levels were measured using a Contour next USB glucometer (Bayer HealthCare Pharmaceuticals LLC, Berlin, Germany).

7.6. Quantification of soluble metabolic and inflammatory markers

Heparinized whole blood from *apoE*$^{-/-}$, *apoE*$^{-/-}$*CCR3*$^{+/+}$ and *apoE*$^{-/-}$*CCR3*$^{-/-}$ mice was collected and centrifuged to obtain plasma samples and then stored at -80 °C. Murine cytokines and chemokines (IL-4, IL-5, eotaxin-1/CCL11) were measured in plasma samples using ELISA (*Enzyme-Linked Immunosorbent assay*; Mouse DuoSet® ELISA; R&D Systems, Inc.) following the manufacturer's instructions. Results were expressed as pg/mL or ng/mL of the mediator in plasma.

7.7. Flow cytometry studies

7.7.1. *Whole blood*

For these studies, 20 µL of heparinized blood and 20 µL of Brilliant Violet (BV) buffer (RUO, BD Biosciences) were incubated for 30 min at room temperature with saturated concentrations of different antibodies (**Table 22**). After incubation, erythrocytes were lysed with a Buffer Lysis solution (1:10 dilution; RMC Lysis Buffer Multispecies, Invitrogen, Thermo Fisher) for 10 min. After 5 min centrifugation at 500 g, samples were washed with PBS and again centrifuged for 5 min at 1,500 rpm. The supernatant was removed and samples were resuspended in 600 µL of Flow Cytometry Buffer (Invitrogen, Thermo Fisher). Then, the samples were run in a LSR20x-Fortessa cytometer and the results analyzed using the FlowJO v10.0.7 (FlowJO LLC) software.

7.7.1.1. Leukocyte populations

Neutrophils and eosinophils

For polymorphonuclear leukocytes, a BV510-conjugated rat mAb against murine CD45 (clone 30-F11, IgG_{2B}, BD Biosciences), a BUV395-conjugated rat mAb against murine Ly6G (clone 1A8, IgG_{2A}, BD Biosciences), and a PerCPCy5.5-conjugated rat mAb against murine CD11b (clone M1/70, IgG_{2B}, BD Biosciences) were used. For eosinophil detection different combinations of fluorochrome-labelled antibodies were used: a BV421-conjugated rat mAb against murine SiglecF (clone E50-2440, IgG_{2A}, BD Biosciences), a PE/Cy7-conjugated rat mAb against murine CD125 (clone DIH37, IgG_{2A}, Biolegend) and a APC-conjugated rat mAb against murine CCR3 (clone J073E5, IgG_{2A}, Biolegend).

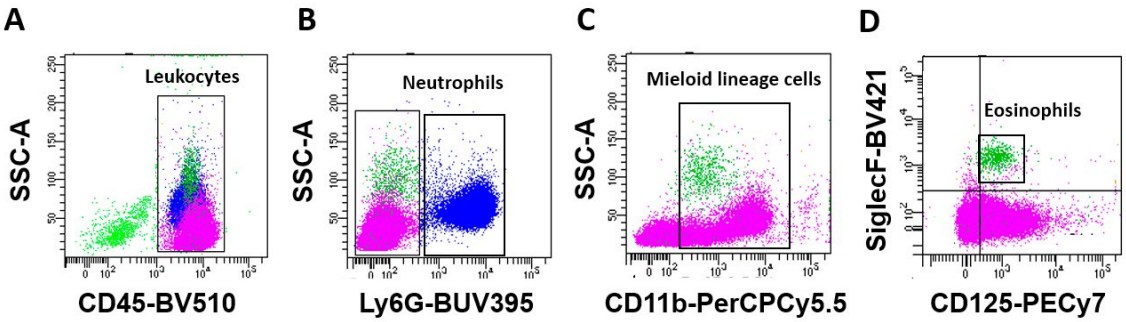

Figure 20. Gating strategy for murine neutrophils and eosinophils in whole blood by flow cytometry.

Populations were selected by CD45 labelling and morphology (high SSC-A, **A**). A Ly6G antibody was used to differentiate neutrophils ($Ly6G^+$) from eosinophils and monocytes ($Ly6G^-$, **B**). To detect only myeloid line, a CD11b antibody was selected ($CD11b^+$, **C**). Eosinophils were detected with Siglec-F and CD125 antibodies ($Siglec\text{-}F^+CD125^+$, **D**).

Monocytes

To detect the monocyte population, a BV510-conjugated rat mAb against murine CD45 (clone 30-F11, IgG_{2B}, BD Biosciences), a BUV395-conjugated rat mAb against murine Ly6G (clone 1A8, IgG_{2A}, BD Biosciences), and a PerCPCy5.5-conjugated rat mAb against murine CD11b (clone M1/70, IgG_{2B}, BD Biosciences) were used to select the myeloid lineage. To specifically detect monocytes, a BV650-conjugated rat mAb against murine CD115 (clone AFS98, IgG_{2A}, BD Biosciences) was additionally employed. The different subpopulations of monocytes were distinguished using an Alexa Fluor 488®-conjugated goat mAb against murine CX_3CR1 (clone Q9Z0D9, IgG_1, R&D Systems) and a PE-conjugated rat mAb against murine CCR2 (clone 475301, IgG_{2B}, R&D Systems).

Table 21 – **Abs for the detection of monocyte subpopulations in mice (Kratofil et al., 2017)**

Antibody	Cellular subpopulation
$CD115^+CX_3CR1^{low}CCR2^{hi}$	Pro-inflammatory monocytes
$CD115^+CX_3CR1^{hi}CCR2^{low}$	Patrolling monocytes

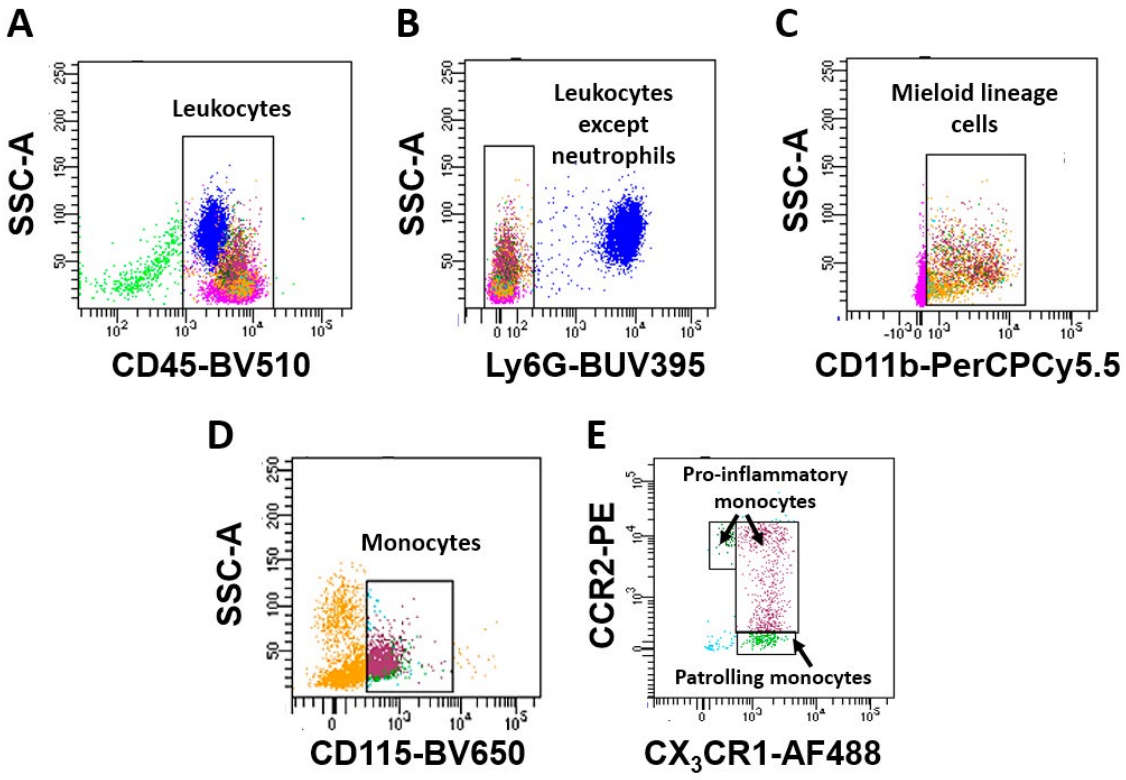

Figure 21. Gating strategy for murine monocytes in whole blood by flow cytometry.

The populations were selected by CD45 labelling (**A**). A Ly6G antibody was used to differentiate neutrophils ($Ly6G^+$) from eosinophils and monocytes ($Ly6G^-$, **B**). To detect the myeloid lineage, a CD11b antibody was employed ($CD11b^+$, **C**). Monocytes were detected as $CD115^+$ cells (**D**) and the different monocyte subpopulations were selected based on their surface expression of CCR2 and CX_3CR1 (**E**).

Lymphocytes

To identify the T lymphocyte population the following fluorochrome labelled antibodies were used: a BV510-conjugated rat mAb against murine CD45 (clone 30-F11, IgG_{2B}, BD Biosciences) and a FITC-conjugated hamster mAb against murine CD3e (clone 145-2C11, Armenian Hamster IgG_1, BD Biosciences). The different T cell subpopulations were identified using a PE-conjugated rat mAb against murine CD8 (clone 53-6.7, IgG_{2A}, Biolegend), and a PerCP/Cy5.5™ - conjugated rat mAb against murine CD4 (clone RM4.5, IgG_{2A}, BD Biosciences). In parallel, the expression of CD69 which reveals the T cell activation, was detected with a BV650-conjugated hamster mAb against murine CD69 (clone H1.2F3, IgG_1, BD Biosciences).

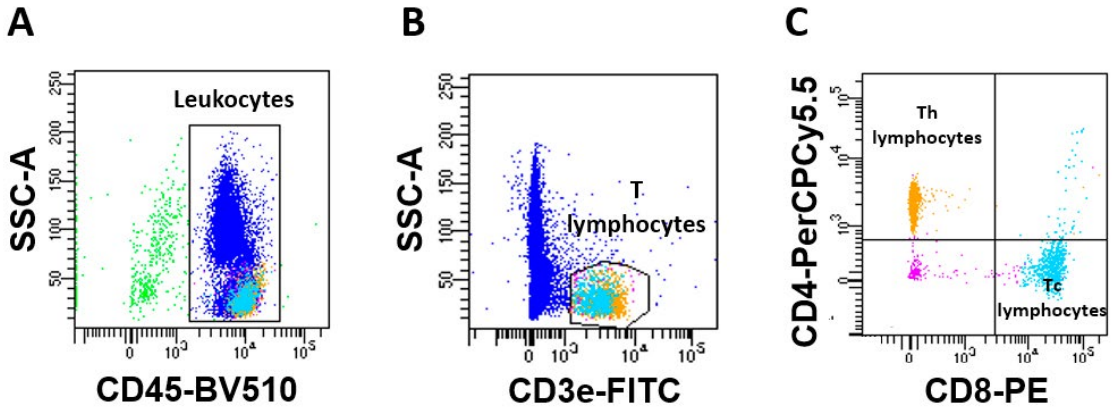

Figure 22. Gating strategy for murine lymphocytes in whole blood by flow cytometry.

Populations were selected by CD45 labelling (**A**). A CD3e antibody was used to detect T lymphocytes ($CD3e^+$, **B**). The subpopulations of T lymphocytes were selected using fluorochrome labelled antibodies against CD4 and CD8 ($CD4^+$ or $CD8^+$, **C**).

7.7.2. *Bone marrow*

First, bone marrow was extracted from the femur. The content was centrifuged to obtain whole bone marrow cells (BMC). Erythrocytes from the resulting pellet were lysed with a Buffer Lysis solution (1:10 dilution; RMC Lysis Buffer Multispecies, Invitrogen). Subsequently, the cell suspension was centrifuged at 500 g for 5 min. The pellet was resuspended in 1 mL PBS. Then 20 µL of bone marrow from each mouse and 20 µL of Brilliant Violet (BV) Buffer (RUO, BD Bioscience) were incubated for 30 min at 4°C with saturated concentrations of different antibodies. After incubation, samples were washed twice with PBS to remove the excess of antibodies (1,500 rpm for 5 min). Then the pellet was resuspended in 400 µL of Flow Cytometry Buffer (Invitrogen) and run in a LSR20x-Fortessa cytometer. Analysis was performed with FlowJO v10.0.7 software (FlowJO LLC). The panels, antibodies and gating strategy are the same as those employed for blood samples analysis.

7.7.3. *White adipose tissue (WAT)*

For white adipose tissue (WAT) cytometry study, inguinal subcutaneous WAT (scWAT) and gonadal visceral AT (vWAT) were extracted from each mouse. Tissues were digested by gentle agitation for 1 h at 37°C with Collagenase Type II (Gibco, Thermo Fisher Scientific) at a concentration of 1 mg/mL in 0.5% HBSS-BSA. To stop the reaction, samples were incubated with 20 mM EDTA for 8 min under gentle shaking. After digestion, samples were filtered and centrifuged several times at 500 g for 10 min at 4°C and erythrocytes lysed with Buffer Lysis solution (1:10 dilution; RMC Lysis Buffer Multispecies, Invitrogen). Non-specific binding was blocked with 15 min incubation with a CD16/CD32 antibody (clone 2.4G2, Rat IgG_{2B}).

Samples were next incubated with the Zombie NIR dyes (BioLegend) for the eosinophil panel and Zombie UV (BioLegend) for the remainder leukocyte subpopulation panels to discriminate living cells from dead cells. Subsequently, the excess of dye was removed by centrifugation. 100 µL of the final product was placed in each microtube with the respective antibodies and incubated for 30 minutes at room temperature in the dark. Afterwards, samples were washed several times to remove the excess of antibodies. Finally, the samples were resuspended in 400 µL of Flow Cytometry Buffer (Invitrogen) and run in the LSR20x-Fortessa cytometer (BD Biosciences). Eosinophils were analyzed in both adipose tissues. FlowJO v10.0.7 software (FlowJO LLC) was used for the analysis of the flow cytometry results.

All the antibodies used for the detection of murine leukocytes are listed in the following table:

Table 22– Antibodies for the detection of murine leukocytes by flow cytometry

Antibody-Fluorochrome	Clone	Isotype	Supplier	Immune cell
CD45 – BV510	30-F11	IgG_{2B}	BD Biosciences	Leukocyte
CD69 – BV650	H1.2F3	IgG_1	BD Biosciences	Leukocyte activation
CD11b – PerCP/ $Cy^{TM}5.5$	M1/70	IgG_{2B}	BD Biosciences	Myeloid activation
Ly6G-BUV395	1A8	IgG_{2A}	BD Biosciences	Neutrophils
CCR3 – APC	J073E5	IgG_{2A}	BioLegend	Eosinophils
SiglecF-BV421	E50-2440	IgG_{2A}	BD Biosciences	
CD125-PECy7	DIH37	IgG_{2A}	BioLegend	
CD115-BV650	AFS98	IgG_{2A}	BD Biosciences	Monocytes
CCR2-PE	475301	IgG_{2B}	R&D Systems	
CX_3CR1- Alexa Fluor 488	IC6/CXCR3	IgG_1	R&D Systems	
CD3e – FITC	145-2C11	IgG_1	BD Biosciences	T lymphocytes
CD4 – PerCP/CyTM5.5	RM4.5	IgG_{2A}	BD Biosciences	
CD8 – PE	53-6.7	IgG_{2A}	BioLegend	
F4/80-APC	BM8	IgG_{2A}	BioLegend	Macrophages
CD11c-BV785	N418	Hamster IgG	BioLegend	
CD206-BV711	CO68CR	IgG_{2A}	BioLegend	

7.8. Bone marrow (BM) transplantation

To confirm the results obtained, we generated BM chimeras by transferring whole BM from *apoE*$^{-/-}$ *Ly5.1* or *apoE*$^{-/-}$*CCR3*$^{-/-}$ mice to whole-body irradiated *apoE*$^{-/-}$ *Ly5.1* or *apoE*$^{-/-}$*CCR3*$^{-/-}$ mice. Mice with an *apoE*$^{-/-}$ *Ly5.1* genotype were donated by Dr. Gonzalez-Navarro (Department of Biochemistry, Faculty of Medicine and Odontology, University of Valencia). The panleukocyte cell marker CD45 is known to have two isoforms: CD45.1 and CD45.2 and the use of *apoE*$^{-/-}$ *Ly5.1* genotype, which has a single isoform, creates a genetic fingerprint that allow us to trace the success of the BM transplant.

7.8.1. *Experimental design*

One week before irradiation, antibiotics and antifungals: neomycin (10 mg/mL, Sigma-Aldrich) and polymyxin B sulfate (25 mg/mL) were administered to recipient mice. *ApoE*$^{-/-}$ *Ly5.1* or *apoE*$^{-/-}$*CCR3*$^{-/-}$ recipient mice were irradiated in a pie cage (Braintree Scientific Inc, Braintree, MA, USA) to limit mobility

and ensure equal dose of irradiation, and were exposed to two radiation doses of 5.5 Gy spaced 4 hours apart to achieve myeloablation using an X-RAD 225 XL Optimax Irradiator (Precision X-Ray irradiation, Madison, CT, USA). The irradiation dose was selected based on previous studies in order to minimize potentially confounding gastrointestinal side effects of radiation, but still achieve efficient myeloablation (typically less than 0.5% recipient WBCs could be detected 4 weeks post-transplantation). After the second irradiation, each recipient mouse was injected with cell suspensions of 10^7 bone marrow cells (BMCs) i.v from the appropriate donor. Sterilized caging, food, and water were provided during the first 14 days post-transplant and water was supplemented with antibiotics (neomycin and polymyxin B sulfate). Three weeks later, mice were subjected to a control or atherogenic diet for eight additional weeks.

7.8.2. *BM cell (BMC) isolation*

BMCs were isolated from femurs of 8 week-old donor mice after euthanasia. Femurs of each mouse were removed and placed in a Petri dish with 1x PBS on ice. The condyles were cut from the bone and femurs were perfused with 25G needles with RPMI 1640 medium (Lonza) containing 2% fetal bovine serum (FBS, Biowest, Nuaillé, France), 10 IU/mL of heparin (Sigma-Aldrich) and 2% penicillin and streptomycin (Lonza). The entire content was well resuspended and then filtered through a 40 µm filter to retain bone chips and tissue debris in the filter. Cells were then centrifuged at 900 g for 10 min at 4 ° C. Supernatant was discarded and the pellet was washed twice with RPMI 1640 medium with 2% streptomycin/penicillin, and 20 mM HEPES (Sigma-Aldrich). After the second centrifugation at 900 g for 5 min at 4 ° C, cells were resuspended in 25 mL of the RPMI medium with HEPES. Cell content was quantified in a Neubauer chamber. Samples were centrifuged again to obtain the proper BMCs suspension for transplantation which were iv. injected through the tail vein. A minimum of 1 x 10^7 BMCs/mouse were administered. After BM transplantation, neomycin and polymyxin B sulfate were administered to recipient mice for two weeks to prevent infections. Donor CD45.2$^+$ cells were obtained from *apoE*$^{-/-}$*CCR3*$^{-/-}$, whereas donor CD45.1$^+$ cells were obtained from *apoE*$^{-/-}$ *Ly5.1* mice.

7.8.3. *Follow up of BM recovery*

To carry out a proper BM recovery of the generated chimeric mice, 20 µL of whole blood was obtained few days before and one day after irradiation and transplantation of donor BMCs, blood count analysis was performed using an automatic hemocytometer Element H5 (Heska, United States). As expected, while blood cells were detected before irradiation, no circulating cells were found one day after irradiation (**Figure 23**). Similarly, blood counts were again quantified three weeks later and before starting the administration of the diets, as well as eight weeks after the administration of the diets to confirm the recovery of the whole leukocyte populations.

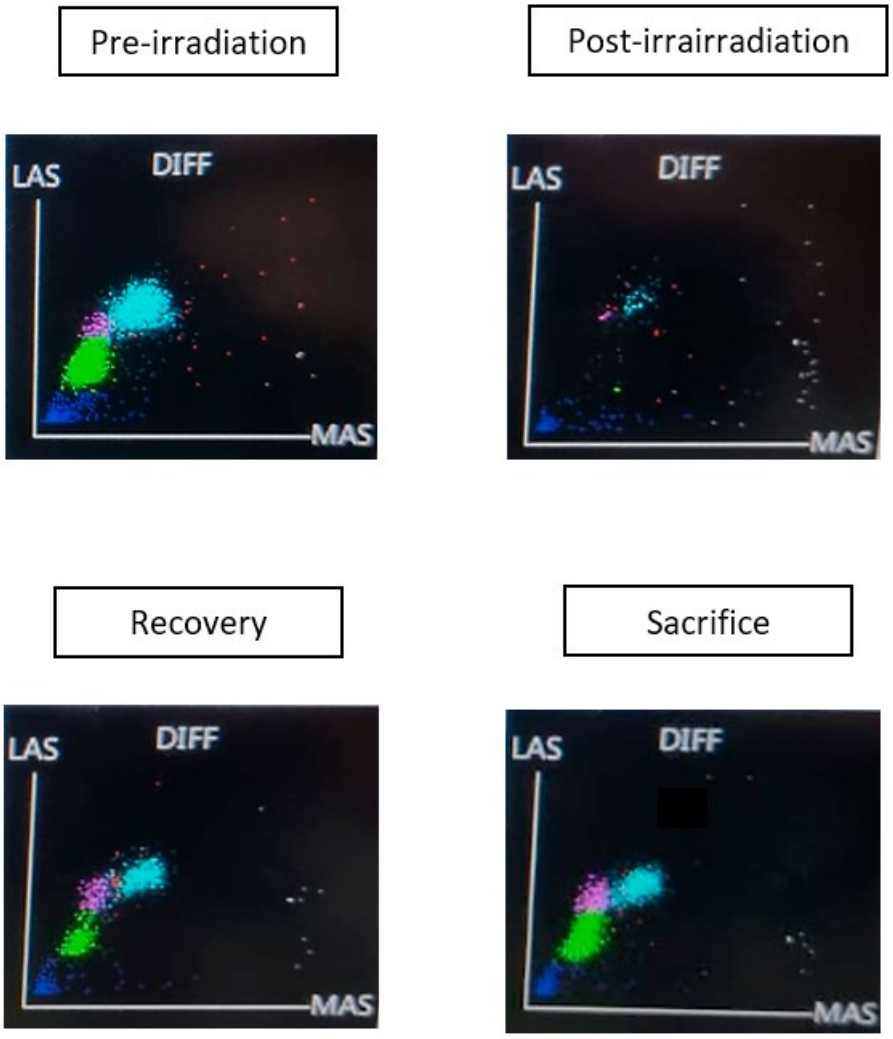

Figure 23. **Gating strategy to follow up myeloablation after irradiation and leukocyte recovery to confirm BM transplantation success.**

7.8.4. *Confirmation of transplant success by flow cytometry studies*

To follow up the traceability of BM transplanted cells in recipient animals, different antibodies against leukocyte surface markers were employed. More precisely, specific antibodies against the panleukocyte marker CD45, CD45.1 and CD45.2 were used. To determine the percentage of $CD45.1^+$ cells in *apoE*$^{-/-}$ *Ly5.1* or *apoE*$^{-/-}$*CCR3*$^{-/-}$ recipient mice a BV510-conjugated antibody against CD45.1 (clone A20, IgG_{2A}, BD Biosciences) was employed. Similarly, to detect the percentage of $CD45.2^+$ cells in *apoE*$^{-/-}$ Ly5.1 or *apoE*$^{-/-}$*CCR3*$^{-/-}$ recipient mice a BUV737-conjugated antibody against CD45.2 (clone 104, IgG_{2A}, BD Biosciences) was used. Eosinophil (**Figure 24**), monocyte (**Figure 25**) and lymphocyte (**Figure 26**) $CD45.1^+$ or $CD45.2^+$ were detected as illustrated in the **Figures 24 - 26** in blood and bone marrow samples.

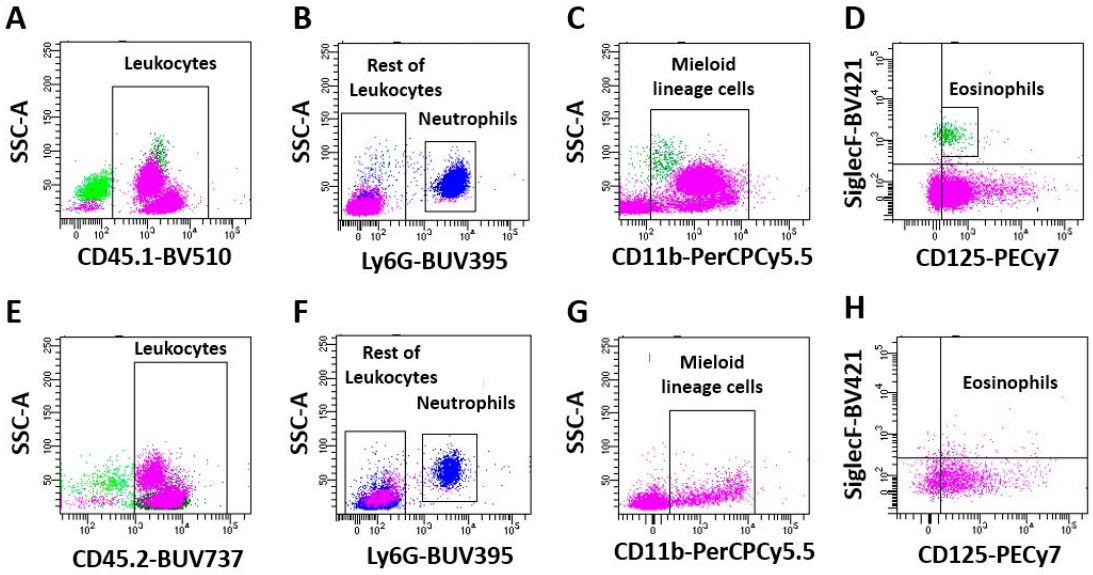

Figure 24. Gating strategy for murine eosinophils in whole blood by flow cytometry.

Populations were selected by morphology and CD45.1 or CD45.2 staining (high SSC-A, **A** and **E**). An antibody against Ly6G was used to differentiate neutrophils ($Ly6G^+$) from eosinophils and monocytes ($Ly6G^-$, **B** and **F**). To detect solely the myeloid lineage from lymphocytes, an antibody against CD11b was used ($CD11b^+$, **C** and **G**). Eosinophils (green population) were detected with antibodies against Siglec-F and CD125 ($Siglec\text{-}F^+CD125^+$, **D** and **H**).

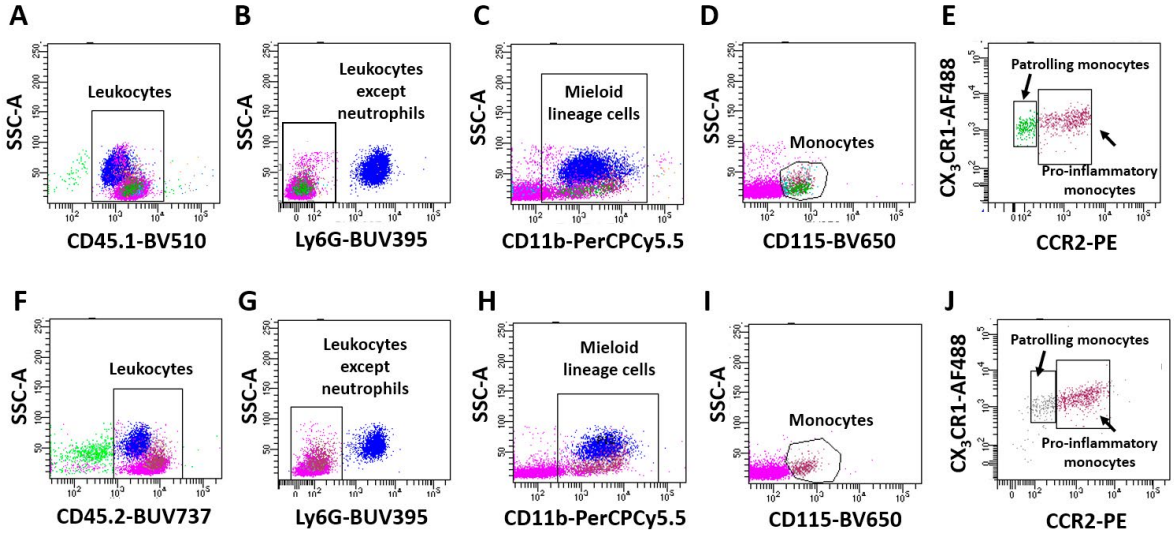

Figure 25. Gating strategy for murine monocytes in whole blood by flow cytometry.

Populations were selected by morphology and CD45.1 or CD45.2 staining (high SSC-A, **A** and **F**). An antibody against Ly6G was used to differentiate neutrophils ($Ly6G^+$) from eosinophils and monocytes ($Ly6G^-$, **B** and **G**). To detect solely the myeloid lineage from lymphocytes, an antibody against CD11b was used ($CD11b^+$, **C** and **H**). Monocytes (green and brown populations) were detected with an antibody against CD115 ($CD115^+$, **D** and **I**) and the different monocyte subpopulations through the use of antibodies against CCR2 and CX_3CR1. (**E** and **J**).

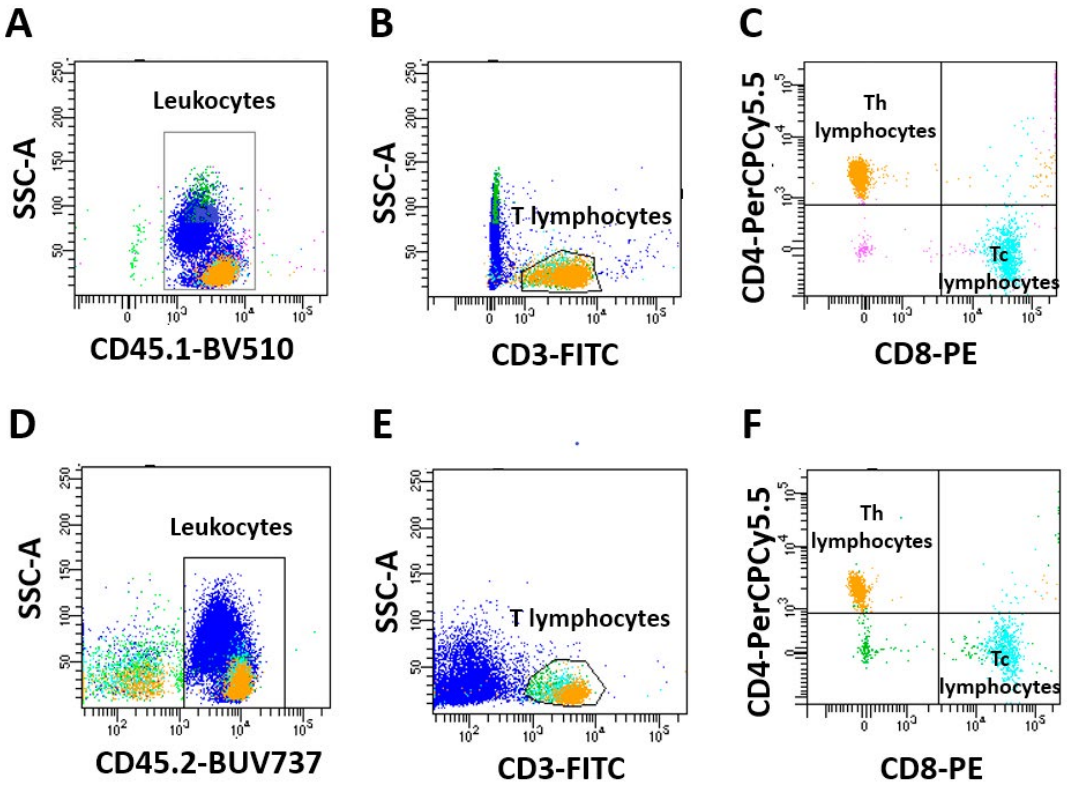

Figure 26. **Gating strategy for murine lymphocytes in whole blood by flow cytometry.**

Populations were selected by morphology and CD45.1 or CD45.2 staining (high SSC-A, **A** and **D**). An antibody against CD3e was used to detect T lymphocyte population ($CD3e^+$, **B** and **E**). T lymphocyte subtypes were identified using antibodies against CD4 and CD8 ($CD4^+$ or $CD8^+$, **C** and **F)**

7.8.5. *Experimental protocol and induction of atherosclerosis*

$ApoE^{-/-}$ Ly5.1 mice or *$apoE^{-/-}CCR3^{-/-}$ mice* were irradiated and transplanted either with BMCs from *$ApoE^{-/-}$* Ly5.1 mice or *$apoE^{-/-}CCR3^{-/-}$* mice following the scheme depicted in **Figure 27**. After three weeks for recovery, chimeric mice were subjected to a control diet (2.8% fat; Panlab, S.L, Harvard Apparatus, Barcelona, Spain) or to an atherogenic diet (10.8% fat, 0.75% cholesterol, S4892-E010; Ssniff Spezialdiäten, Soest, Germany) for 8 additional weeks (See the scheme in **Figure 28** with whole protocol). Then animals were sacrificed by an overdose of anesthesia with an i.p. injection of a mixture of medetomidine hydrochloride (1mg/mL; Orion Corportation) and ketamine (50 mg/mL; Orion Corporation). Then blood, aortas, bone marrow and different organs were extracted, processed and analyzed as described in ***Sections 6.2 Quantification of the atherosclerotic lesion - 6.7 Flow cytometry studies.***

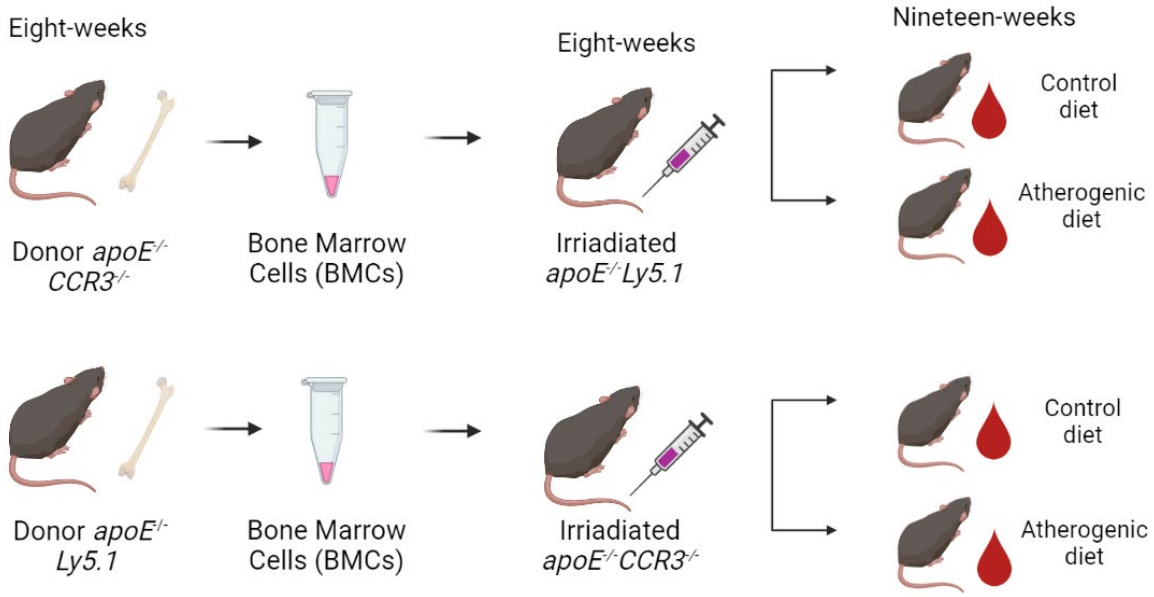

Figure 27. Graphic scheme of bone marrow transplantation procedure

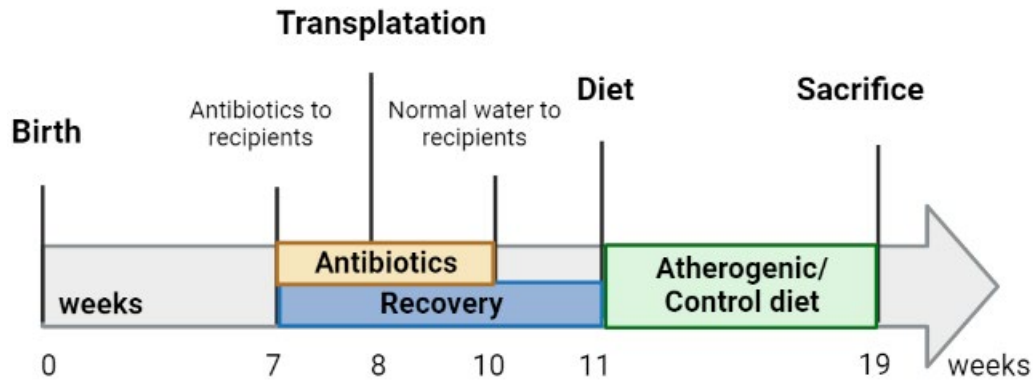

Figure 28. Time chart scheme of bone marrow transplantation and atherosclerosis induction

7.9. Statistical analysis

Values are expressed as individual data points, percentages or mean ± standard error of the mean (SEM) when appropriate. For comparisons of two unpaired groups, unpaired Student´s t test was used in data that passed both normality (Kolmogorov-Smirnov test) and equal variance (Levene test); otherwise, a non-parametric Mann Whitney U test was performed. For comparisons of two paired groups, paired Student´s t test was used in data that passed both normality (Kolmogorov-Smirnov test) and equal variance (Levene test); otherwise, a non-parametric Wilcoxon matched-pairs test was performed. For comparisons among multiple groups, two-way analysis of variance (ANOVA) followed by post hoc analysis (Bonferroni test) was used in data that passed both normality and equal variance.

Data were considered statistically significant at $P < 0.05$. In addition, some correlations between experimental findings and clinical features were calculated using Pearson and Spearman correlation methods. All statistical studies were performed with GraphPad Prism 8 (GraphPad Software, La Jolla, CA).

RESULTS

8. STUDY OF SYSTEMIC INFLAMMATION IN PATIENTS WITH PH

8.1. Clinical features of studied subjects

A total number of 43 individuals, 22 patients with Primary Hypercholesterolemia (PH) (4 males and 18 females) and 21 healthy age-matched individuals (5 males and 16 females) were recruited by the Endocrinology and Nutrition Service at University Clinic Hospital of Valencia (Valencia, Spain) for the present study. Blood samples were extracted from all subjects and collected in blood collection tubes containing sodium citrate or lithium/heparin as anticoagulant agents. All individuals who did not comply the requirements detailed in ***Section 5.1 Blood samples from age-matched controls and primary hypercholesterolemia (PH) patients*** were eliminated from the analysis. All clinical, demographic, and biochemical characteristics of all participants are shown in the following table (**Table 23**)

No statistically significant differences were found regarding as age, gender, body mass index (BMI) or waist circumference between the two groups. However, four characteristic parameters of PH; total cholesterol (TC), triglycerides (TG), low-density lipoprotein (LDL) and ApoB showed a significant increase in patients compared to the control group, as expected (**Table 23**).

Table 23 – Clinical features of studied subjects

Parameters	Control volunteers (n = 21)	PH subjects (n = 22)
Age (years)	48.8 ± 2.7	49 ± 3.1
Gender M/F (%)	5/16 (23.8/76.2)	4/18 (18.2/81.8)
BMI (kg/m2)	25.4 ± 0.7	25.7 ± 0.9
Waist circumference (cm)	85.3 ± 1.9	85.7 ± 2.2
SBP (mmHg)	115.9 ± 2.0	124.7 ± 3.6 *
DBP (mmHg)	71.6 ± 1.8	78.5 ± 2.6 *
Glucose (mg/dL)	86.7 ± 1.5	88.1 ± 1.9
TC levels (mg/dL)	206.1 ± 6.8	264.6 ± 8.9 **
LDL levels (mg/dL)	130.6 ± 5.4	182.8 ± 6.2 **
TG (mg/dL)	80.9 ± 7.3	109.7 ± 8.5 **
HDL levels (mg/dL)	65.9 ± 2.5	63.4 ± 2.9
ApoB (mg/dL)	92.5 ± 4.1	127.4 ± 5.0 **
GOT (U/L)	21.7 ± 0.9	22.8 ± 1.1
GPT (U/L)	18.3 ± 1.8	18.5 ± 1.1
Creatinine (mg/dL)	0.7 ± 0.0	0.7 ± 0.0
IgG (mg/dL)	966.7 ± 41.1	968.5 ± 34.4
IgM (mg/dL)	100.4 ± 7.6	125.8 ± 14.1
IgE total (IU/L)	42.6 ± 12.0	50.4 ± 16.9

*M, male; F, female; BMI, body mass index; SBP, systolic blood pressure; DBP, diastolic blood pressure; TC, total cholesterol; LDL, low-density lipoprotein; TG, triglycerides; HDL, high-density lipoprotein; ApoB, apolipoprotein B; GOT, glutamic-oxalacetic transaminase; GPT, glutamate- pyruvate transaminase; Ig, immunoglobulin. Data are presented as mean ± SEM. *p <0.05 or **p<0.01 relative to values in the control group.*

8.2. Platelet activation is enhanced in patients with PH

By flow cytometry and ELISA, we first determined the percentage of circulating platelets, the platelet activation state, and plasma levels of several mediators released by the activated platelets. No significant differences were found in the number of circulating platelets between the two study groups (**Figure 29A**). However, the percentage of activated platelets expressing PAC-1 and P-selectin (CD62P) was significantly higher in patients than in control subjects (**Figures 29B** and **C**).

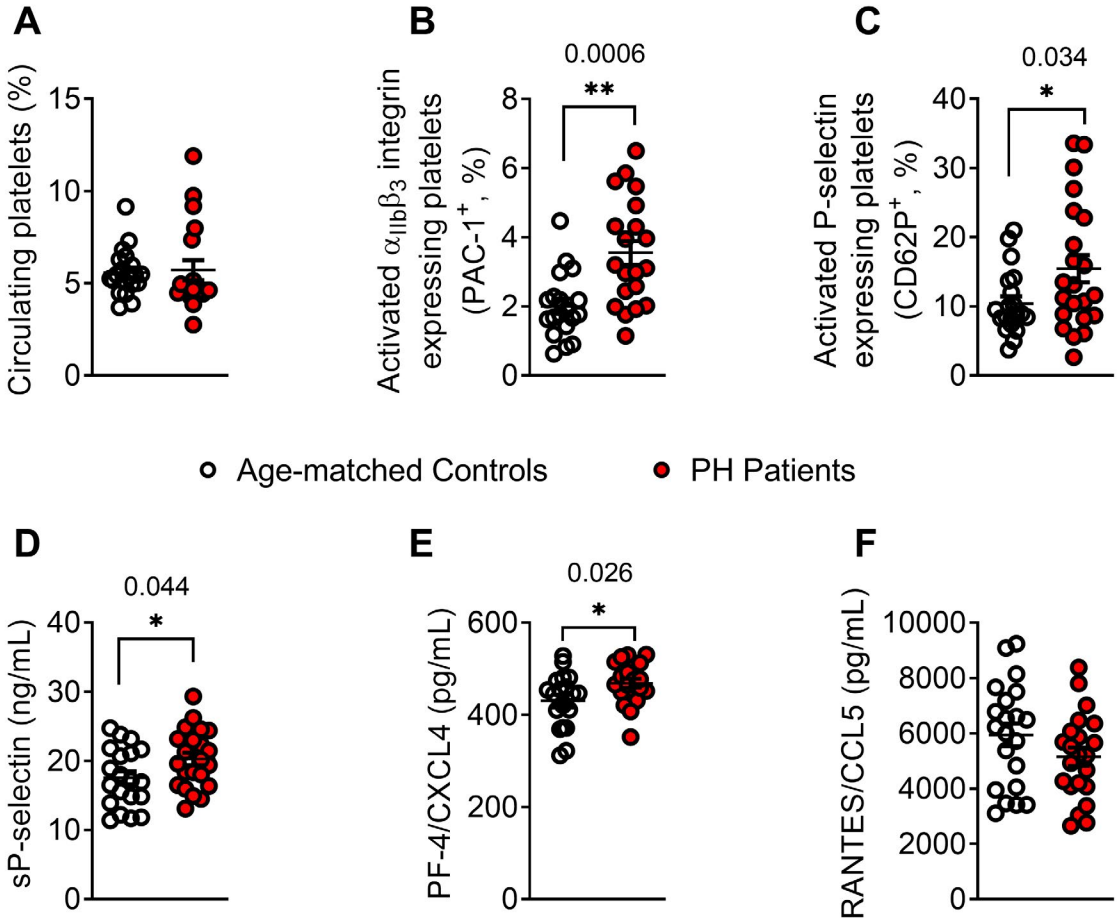

Figure 29. Platelet activation and related soluble markers are elevated in patients with PH.

Flow cytometry analysis of platelets stained with conjugated antibodies against CD41 (**A**), CD41 and PAC-1 (**B**), and CD41 and CD62P (**C**). Results are expressed as the percentage of positive cells. Soluble P-selectin (sP-selectin, **D**), PF-4/CXCL4 (**E**) and RANTES/CCL5 (**F**) plasma levels (ng or pg/mL) were measured by ELISA (n= 21 control subjects and n=22 PH patients). Values are expressed as mean ± SEM. * $p < 0.05$ or ** $p < 0.01$ relative to values in the control group.

P-selectin is a mediator that translocates to the cell surface when cells are activated, where it can be cleaved and released into circulation as soluble P-selectin (sP-selectin). For this reason, these circulating plasma levels were also determined, finding significantly increased levels in the PH group than in the control (**Figure 29D**). Similarly, plasma levels of PF-4/CXCL4, a chemokine released upon platelet activation, also showed a significant increase in PH patients (**Figure 29E**). However, no differences were demonstrated between PH patients and controls for levels of the chemokine RANTES/CCL5, a chemokine released by platelet activation and other immune cells (**Figure 29F**).

8.3. The percentage of platelet-neutrophils aggregates, activated neutrophils, and circulating levels of IL-8, are elevated in patients with PH

Next, some parameters related to the activation of different leukocyte subsets were evaluated. Regarding circulation, no differences were found in the circulating percentage of neutrophils in the heparinized blood between both groups (**Figure 30A**); however, both the percentage of neutrophil-platelet aggregates and the percentage of activated neutrophils ($CD69^+$) were significantly higher in PH patients compared to controls (**Figures 30B** and **C**). Regarding neutrophil-related mediators, chemokine GRO-α/CXCL1 and interleukin IL-8/CXCL8 can induce activation and chemotaxis of human neutrophils, and their levels were quantified in plasma. While no differences were found in plasma levels of GRO-α/CXCL1 (**Figure 30D**), a significant increase in plasma levels of IL-8/CXCL8 was observed in patients with PH (**Figure 30E**). A positive correlation was also detected between the circulating levels of IL-8 and the three clinical PH parameters in the patient group: ApoB, LDL, and TC (**Figure 30F - H**).

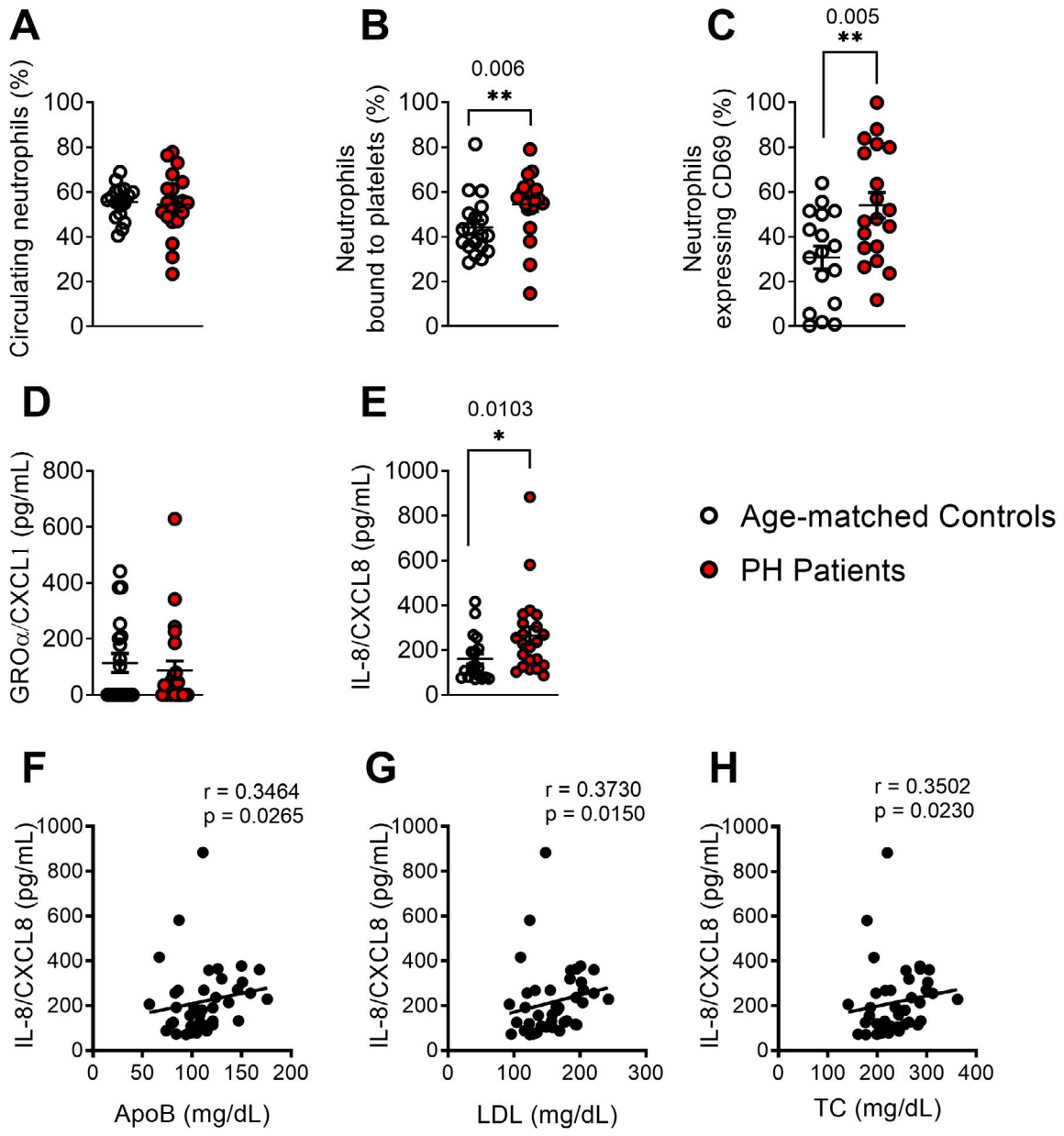

Figure 30. The percentage of platelet-neutrophil aggregates, activated neutrophils, and IL-8 circulating levels, are higher in patients with PH.

Flow cytometry analysis of heparinized whole blood co-stained with specific markers for platelets and neutrophils (**A** and **B**). Neutrophils were also stained for CD69 (**C**). Results are expressed as the percentage of positive cells. GRO-α/CXCL1 (**D**) and IL-8/CXCL8 (**E**) plasma levels (pg/mL) were measured by ELISA (n = 21 control subjects and n=22 PH patients). Values are expressed as mean ± SEM. * $p < 0.05$ or ** $p < 0.01$ relative in the control group. Correlations between circulating IL-8 and ApoB (**F**), LDL (**G**) and TC (**H**) plasma levels.

8.4. Circulating Mon 3 monocytes, platelet-Mon 1 and Mon 3 aggregates, activated Mon 1 and Mon 2 monocytes and plasma levels of CCL2 and CX_3CL1, are all elevated in patients with PH

Three monocyte subpopulations have been described in peripheral blood based on their differential expression on the cell surface markers CD14, CD16 and CCR2 (Jaipersad et al., 2014; Shantsila et al., 2011). While the percentage of circulating monocytes type 1 (Mon 1) and type 2 (Mon 2) did not differ between the different study groups, the percentage of type 3 monocytes (Mon 3) was significantly elevated in patients with PH compared to the control group (**Figure 31A, D** and **G**). When platelet-monocyte aggregates were analysed, those platelet aggregates and Mon 1 and Mon 3 monocytes were significantly increased in patients with PH (**Figures 31B** and **H**), but there was no difference in Mon 2 aggregates (**Figure 31E)**. In addition, the expression of the CD11b marker determined by fluorescence intensity by flow cytometry was significantly higher in Mon 1 and Mon 2 monocytes, but not Mon 3 monocytes of patients compared to controls, indicating their activation state (**Figures 31C, F** and **I**). The fluorescence intensity of the fractalkine/CX_3CL1 receptor (CX_3CR1) in the different subtypes of monocytes in heparinized blood was also measured by flow cytometry. This analysis revealed that the percentage of Mon 1 monocytes expressing this receptor was significantly higher in patients than in controls (**Figure 31J**). After the dissociation of platelets with EDTA, it was concluded that all subtypes of receptor-positive monocytes were significantly increased in patients than in controls, with the highest expression in Mon 1 monocytes (**Figure 31K**).

Table 24 – Differential markers of monocyte subpopulations (Shantsila et al., 2011)

Markers	Cellular subpopulation
$CD14^+CD16^-CCR2^+$	Type 1 monocytes (Mon 1)
$CD14^+CD16^+CCR2^+$	Type 2 monocytes (Mon 2)
$CD14^+CD16^+CCR2^-$	Type 3 monocytes (Mon 3)

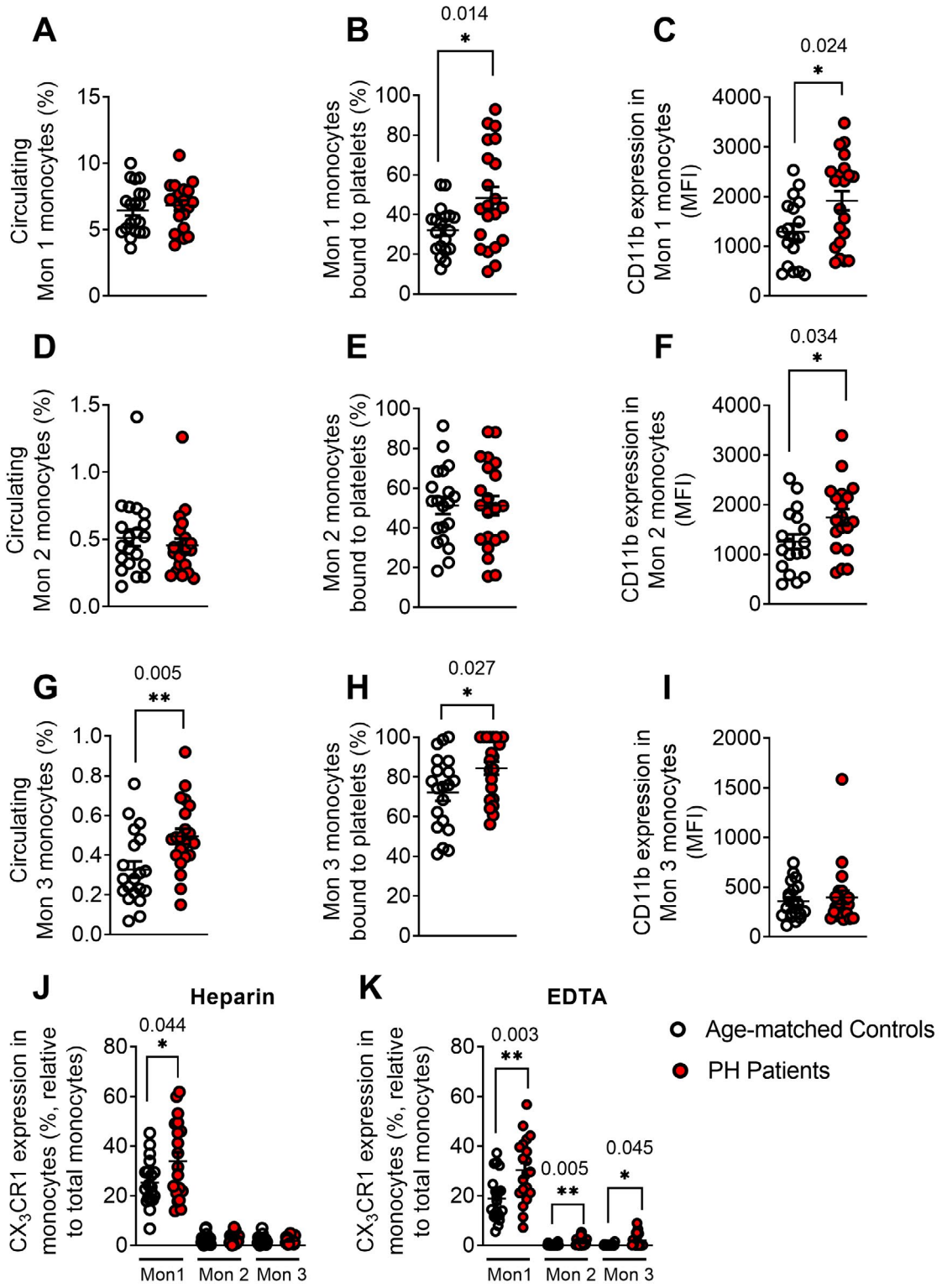

Figure 31. The percentage of circulating Mon 3 monocytes, platelet-Mon 1 and 3 aggregates, and activated Mon 1 and 2 monocytes are elevated in patients with PH.

Flow cytometry analysis of heparinized whole blood co-stained with specific markers for platelets and Mon 1, 2 and 3 monocytes (**A**, **B**, **D**, **E**, **G**, **H**), CD11b integrin (**C**, **F** and **I**), and also for CX_3CR1 in heparinized and EDTA-treated whole blood (**J** and **K**). Results are expressed as the percentage of positive cells or mean fluorescence intensity (MFI, n = 21 control subjects and n = 22 patients with PH). * $p < 0.05$ or ** $p > 0.01$ relative to values in the control group.

In addition, the circulating levels of MCP-1/CCL2 and soluble fractalkine/CX_3CL1, ligands of CCR2 and CX_3CR1 receptors respectively which are involved in mononuclear cell recruitment, were significantly higher in patients (**Figures 32A** and **B**), and a positive correlation was found between the circulating concentration of both chemokines and ApoB, LDL and TC levels in patients (**Figures 32C - H**).

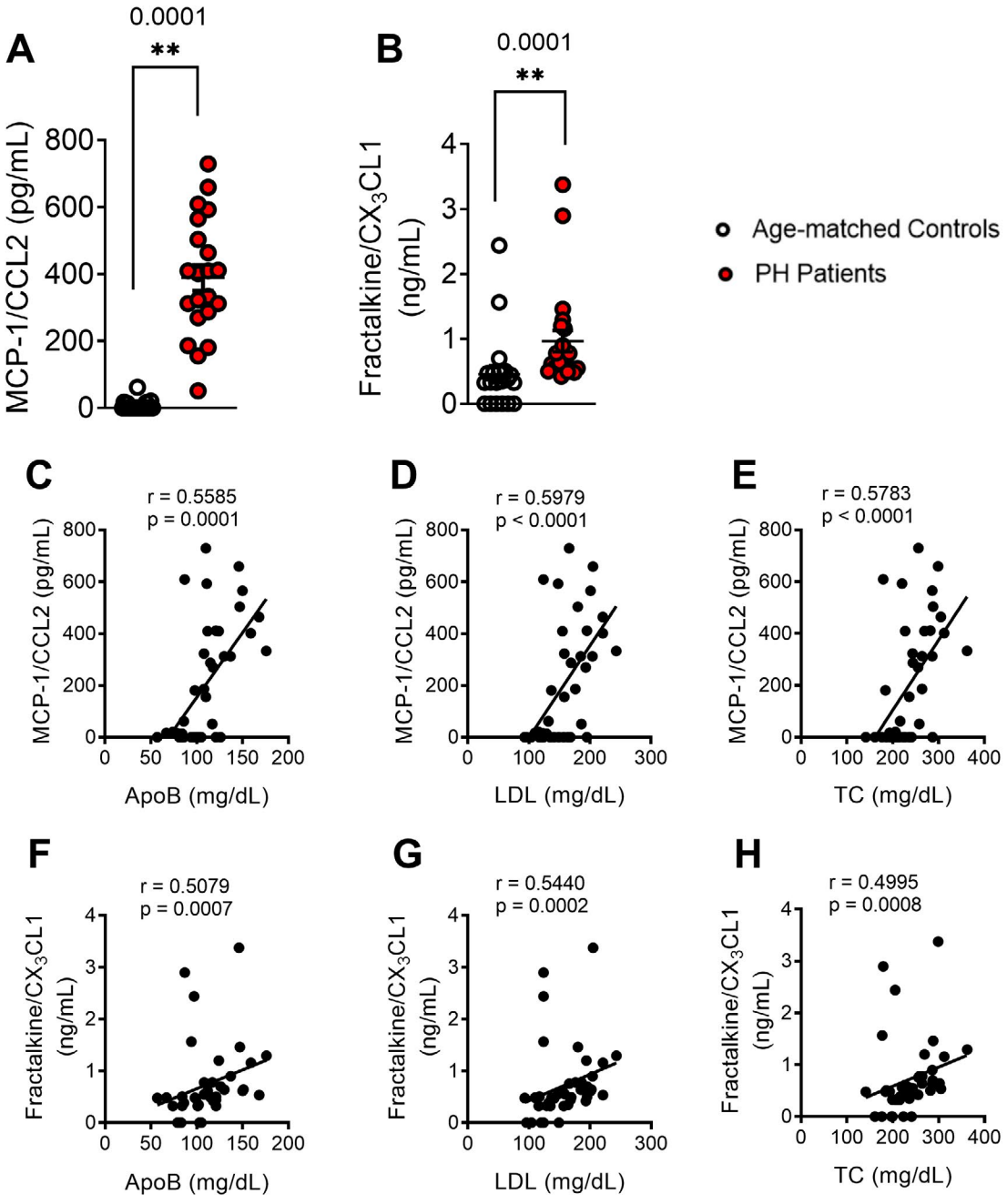

Figure 32. Plasma levels of CCL2 and CX_3CL1 are higher in patients than in controls.

MCP-1/CCL2 (**A**) and fractalkine/CX_3CL1 (**B**) plasma levels (pg or ng/mL) were measured by ELISA (n = 21 control subjects and n = 22 patients with PH). Values are expressed as mean ± SEM. * $p < 0.05$ or ** $p > 0.01$ relative to values in the control group. Correlations between circulating MCP-1/CCL2 or fractalkine/CX_3CL1 and ApoB (**C** and **F**), LDL (**D** and **G**) and TC (**E** and **H**) plasma levels.

8.5. Circulating $CD4^+$ lymphocytes, platelet-lymphocyte ($CD4^+$ and $CD8^+$) aggregates and lymphocyte ($CD4^+$ and $CD8^+$) activation are significantly increased in patients with PH

Mature T cells express the overall marker CD3, and depending on whether they are helper T cells or cytotoxic T cells, they also express CD4 or CD8 respectively. Peripheral blood analysis revealed that no significant differences were found in the number of CD3 and CD8 lymphocytes between patients and controls (**Figures 33A and J**). However, a significant increase in the number of CD4 lymphocytes was observed in patients with PH (**Figure 33D**) and a positive correlation with the three clinical parameters of the pathology (**Figures 33G - I**). In addition, the percentage of CD3, CD4, and CD8 bound to platelets and their activation status ($CD69^+$) was higher in patients tan in control subjects (**Figures 33B, C, E, F, K** and **L**). Interestingly, a positive correlation was found between the percentage of $CD69^+$ $CD8^+$ cells and the lipid profile (ApoB, LDL and TC levels) (**Figure 33M - O**).

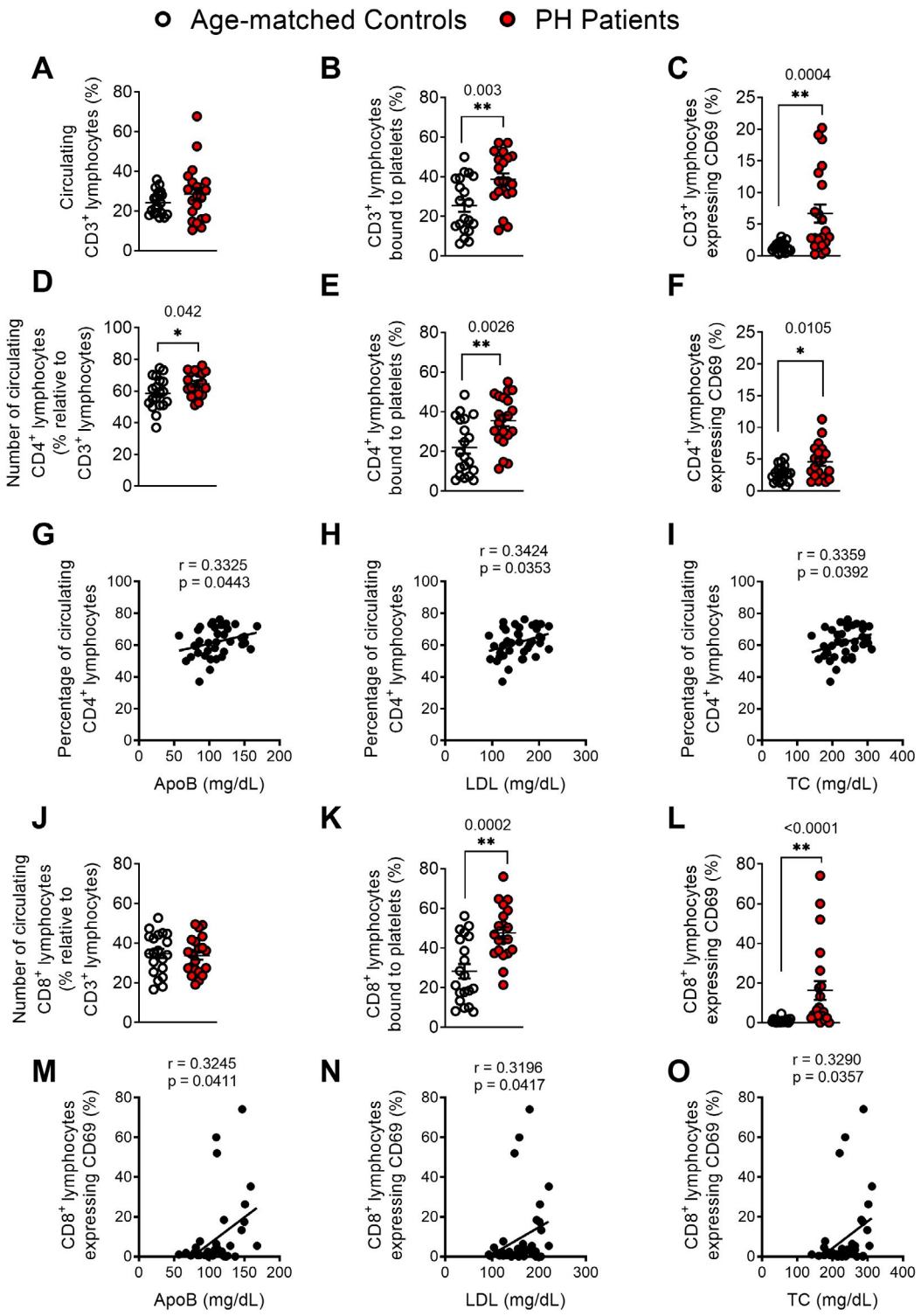

Figure 33. The percentage of circulating CD4⁺ lymphocytes, platelet-lymphocyte (CD4⁺ and CD8⁺) aggregates, and lymphocyte (CD4⁺ and CD8⁺) activation, are significantly elevated in patients with PH.

Heparinized whole blood was co-stained with specific markers for platelets and CD3⁺, CD4⁺ and CD8⁺ lymphocytes (**A**, **B**, **D**, **E**, **J** and **K**) as well as for CD69 (**C**, **F** and **L**). Results are expressed as the percentage of positive cells (n = 21 control subjects and n = 22 PH patients). Values are expressed as mean ± SEM. * $p < 0.05$ or ** $p < 0.01$ relative to values in the control group. Correlations between circulating CD4⁺ cells and activated CD8⁺ lymphocytes and ApoB (**G** and **M**), LDL (**H** and **N**) and TC (**I** and **O**) plasma levels.

An in-depth analysis of CD4 lymphocytes and their different subtypes showed a higher number of circulating Th2 and Th17 lymphocytes, but not Th1 in PH patients (**Figures 34A, D** and **G**). Furthermore, a decrease in the percentage of regulatory T lymphocytes (Treg) was found in patients with PH, whose function is to protect against the pathology (**Figure 34J**). However, the study of platelet-CD4 lymphocyte aggregates revealed an increase in the percentage of Th1, Th2, and Th17 lymphocytes, but not in Tregs (**Figures 34B, E, H** and **K**). In addition, the percentage of activated Th1, Th,2 and Th17 lymphocytes ($CD69^+$) was significantly increased in patients; by contrast, a decrease in the percentage of activated T regs was observed in the same patients (**Figures 34C, F, I** and **L**).

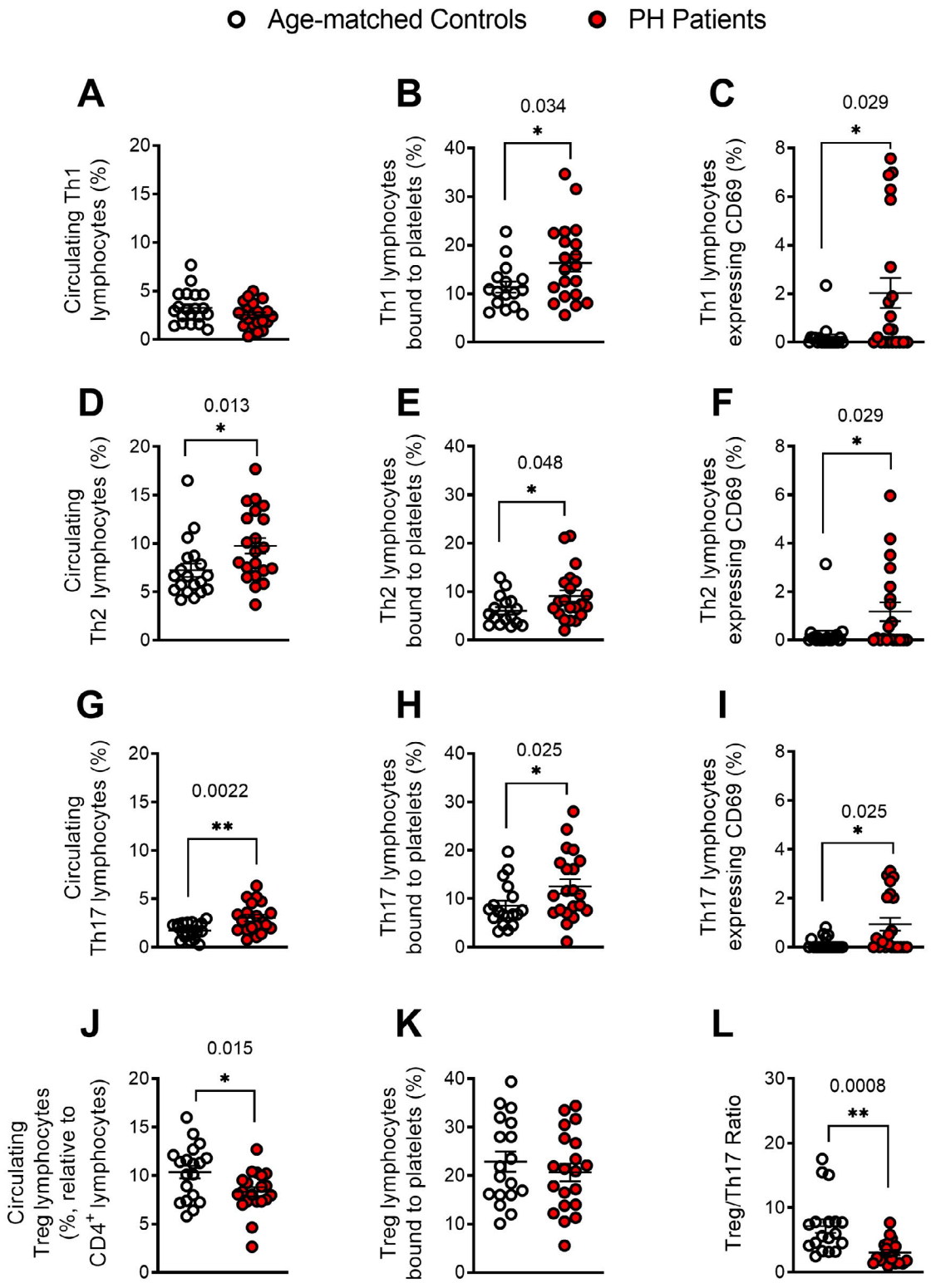

Figure 34. The percentage of circulating Th2 and Th17 lymphocytes, platelet-lymphocyte aggregates, and lymphocyte activation, are significantly increased in patients with PH whereas the percentage of circulating Treg cells and the Treg/Th17 ratio are decreased.

Heparinized whole blood was co-stained with specific markers for platelets and Th1, Th2, Th17 and Treg lymphocytes (**A**, **B**, **D**, **E**, **G, H, J** and **K**) as well as for CD69 (**C**, **F** and **I**). Results are expressed as the percentage of positive cells (n = 21 control subjects and n = 22 PH patients). Values are expressed as mean ± SEM. * $p < 0.05$ or ** $p < 0.01$ relative to values in the control group.

Regarding lymphocyte-related markers, plasma levels of IL-12, a cytokine involved in the differentiation of naïve T cells to Th1 cells, were significantly elevated in patients with PH. However, IFN-γ levels, a cytokine released by Th1 lymphocytes, were not different from those of control subjects (**Figures 35A** and **B**). By contrast, levels of the anti-inflammatory cytokines IL-4 and IL-10, which are mainly produced by Th2 and Treg lymphocytes, respectively, were significantly lower in the circulation of PH patients (**Figures 35C** and **G**). Indeed, an inverse correlation was found between IL-4 and IL-10 and the lipid profile associated with PH (**Figures 35D, E, F, H, I** and **J**).

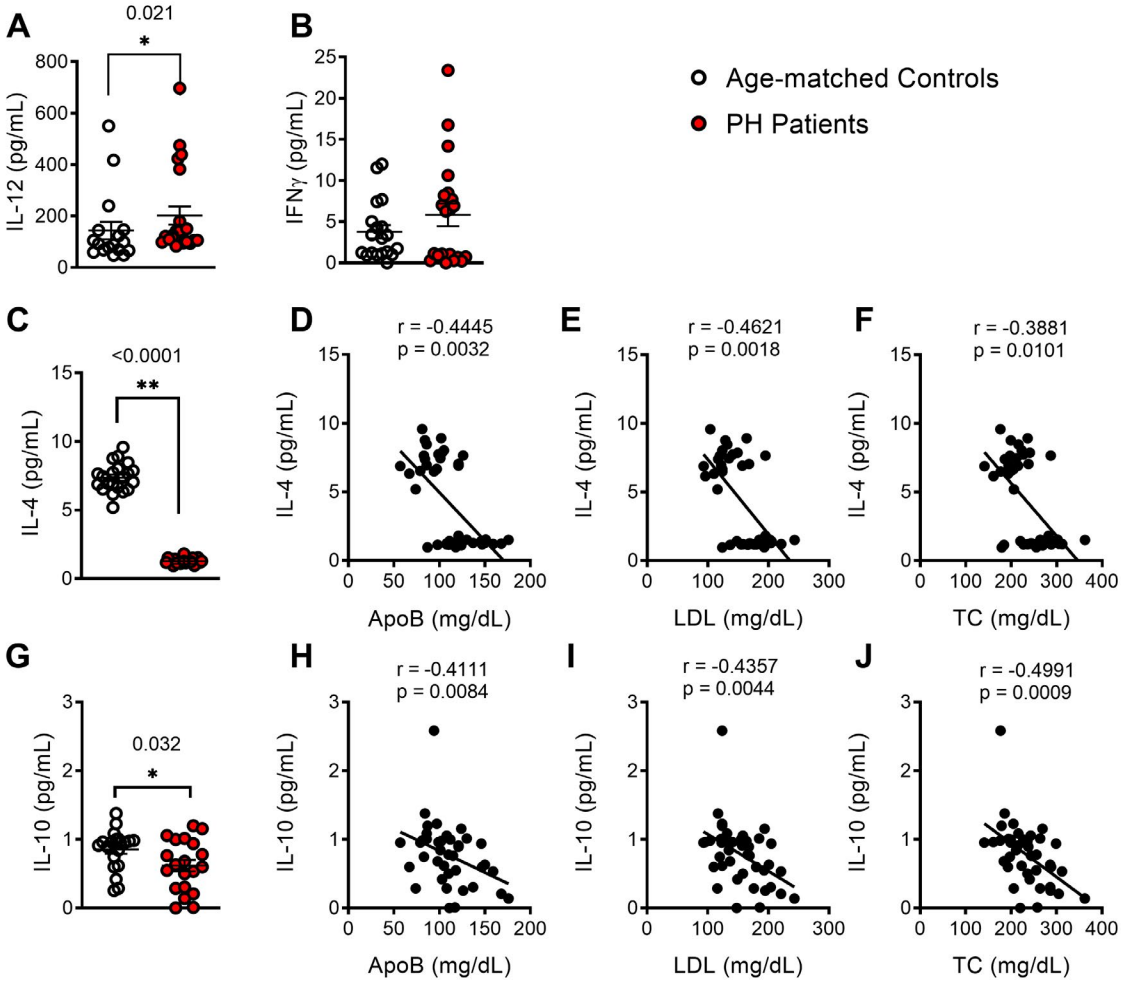

Figure 35. IL-12 circulating levels are significantly increased in patients with PH whereas IL-4 and IL-10 are decreased.

IL-12 (**A**), IFN-γ (**B**), IL-4 (**C**) and IL-10 (**G**) plasma levels were measured by ELISA (n = 21 control subjects and n = 22 PH patients). Values are expressed as mean ± SEM. * $p < 0.05$ or ** $p < 0.01$ relative to values in the control group. Correlations between circulating IL-4 and IL-10 and ApoB (**D** and **H**), LDL (**E** and **I**) and TC (**F** and **J**) plasma levels.

8.6. Circulating levels of pro-Inflammatory cytokines but not adipokines are increased in PH patients

Apart from the above mediators, other cytokines and chemokines were studied. Th17 lymphocytes produce TNF-α and IL-6 (Olson, Sallam, Doyle, Tracy, & Huber, 2013), and an increase in the plasma levels of these pro-inflammatory cytokines has been reported in patients with PH (Collado, Marques, Domingo, et al., 2018; Holven et al., 2014; Real et al., 2010; Sampietro et al., 1997). Similar results were found in our patients (**Figures 36A** and **B**); moreover, a positive association was found between IL-6 plasma levels and the levels of circulating ApoB, LDL and TC (**Figures 36C – E**). By contrast, no differences between patients and controls were found for the circulating levels of typical adipokines: adiponectin, leptin or ghrelin (**Figures 36F – H**).

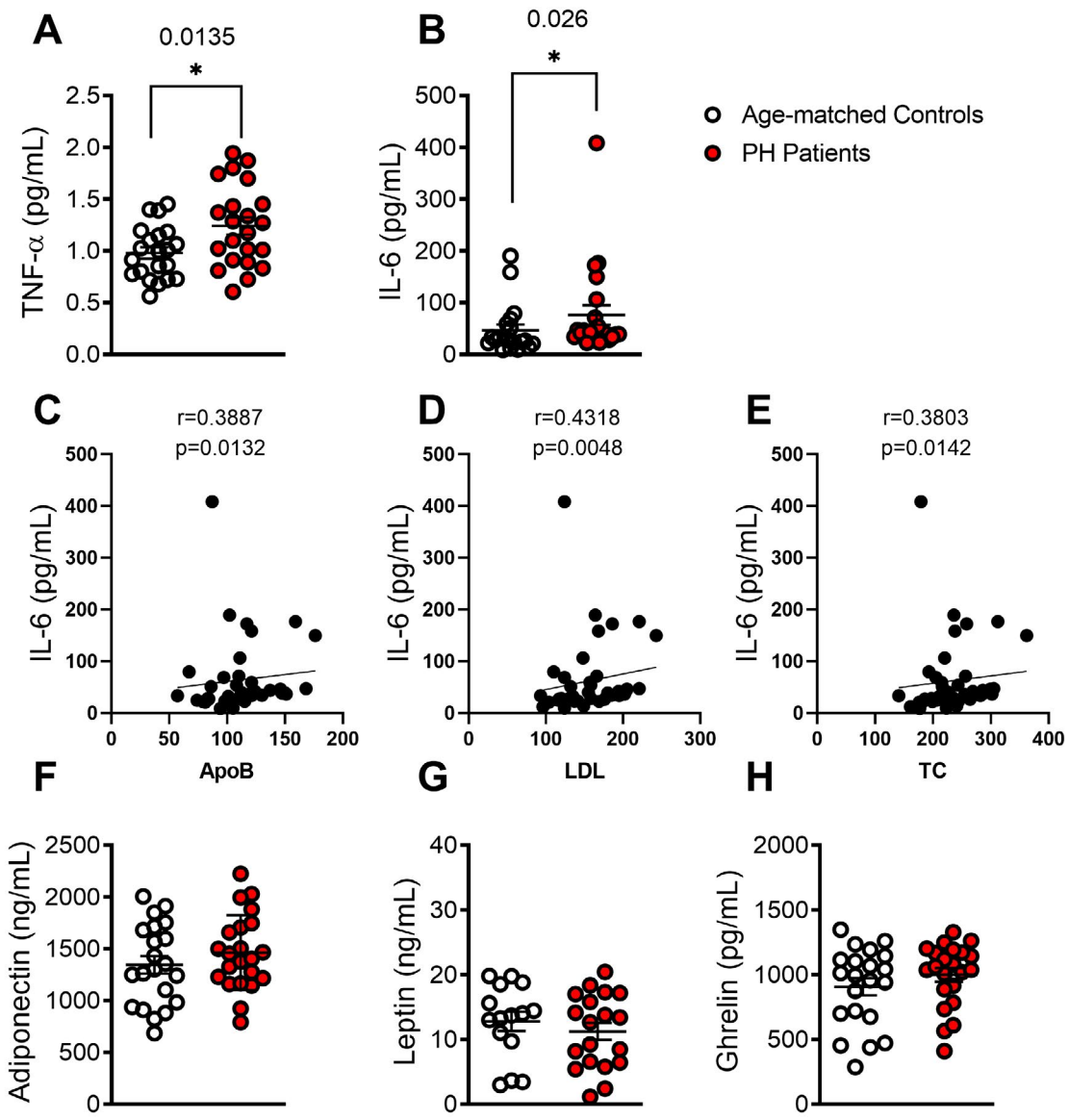

Figure 36. Increased circulating levels of pro-inflammatory cytokines but not adipokines in patients with PH.

TNF-α (**A**), IL-6 (**B**), adiponectin (**F**), leptin (**G**) and ghrelin (**H**) plasma levels (pg or ng/mL) were measured by ELISA (n = 21 control subjects and n = 22 PH patients). Values are expressed as mean ± SEM. * $p < 0.05$ or ** $p < 0.01$ relative to values in the control group. Correlations between circulating IL-6 and ApoB (**C**), LDL (**D**) and TC (**E**) plasma levels.

8.7. Circulating platelet-leukocytes and leukocytes from PH patients have increased adhesiveness to TNFα-stimulated HUAEC

Endothelial dysfunction is one of the earliest stages in atherogenesis that leads the leukocyte adhesion and transmigration to the inflammatory focus. Because TNF-α is a central cytokine in hypercholesterolemia, the functional role of elevated TNF-α levels in patients with PH was investigated. First, we evaluated the adhesion of platelet-leukocyte aggregates in heparinized blood to unstimulated or TNFα-stimulated arterial endothelial cells (HUAEC) under dynamic flow conditions. We next determined the leukocyte adhesion from EDTA-treated blood, which promotes the dissociation of platelets from leukocytes to the same unstimulated or TNFα-stimulated cells.

First, the diluted heparinized blood of patients and controls was perfused across unstimulated HUAEC. As a result, leukocyte adhesion was significantly higher in the PH group (**Figure 37B**). After HUAEC treatment with TNF-α for 24 hours, leukocyte adhesiveness increased in both groups and remained significantly higher in the patient group (**Figure 37B**). When platelets were disaggregated by EDTA treatment, adhesiveness remained significantly elevated in the PH group than in controls (**Figure 37C**), although the number of adhered leukocytes was lower in the stimulated endothelium after platelet disaggregation (**Figure 37C**).

Immunofluorescence studies revealed enhanced adherent platelet–leukocyte complexes to TNFα-stimulated endothelial cells from PH patients compared with age-matched controls (**Figure 37D** and **E**). Furthermore, when platelets were disaggregated from leukocytes with EDTA, leukocyte adhesion to TNFα-stimulated HUAEC was notably diminished but this parameter was markedly greater in the PH group than the control group (**Figure 37F** and **G**).

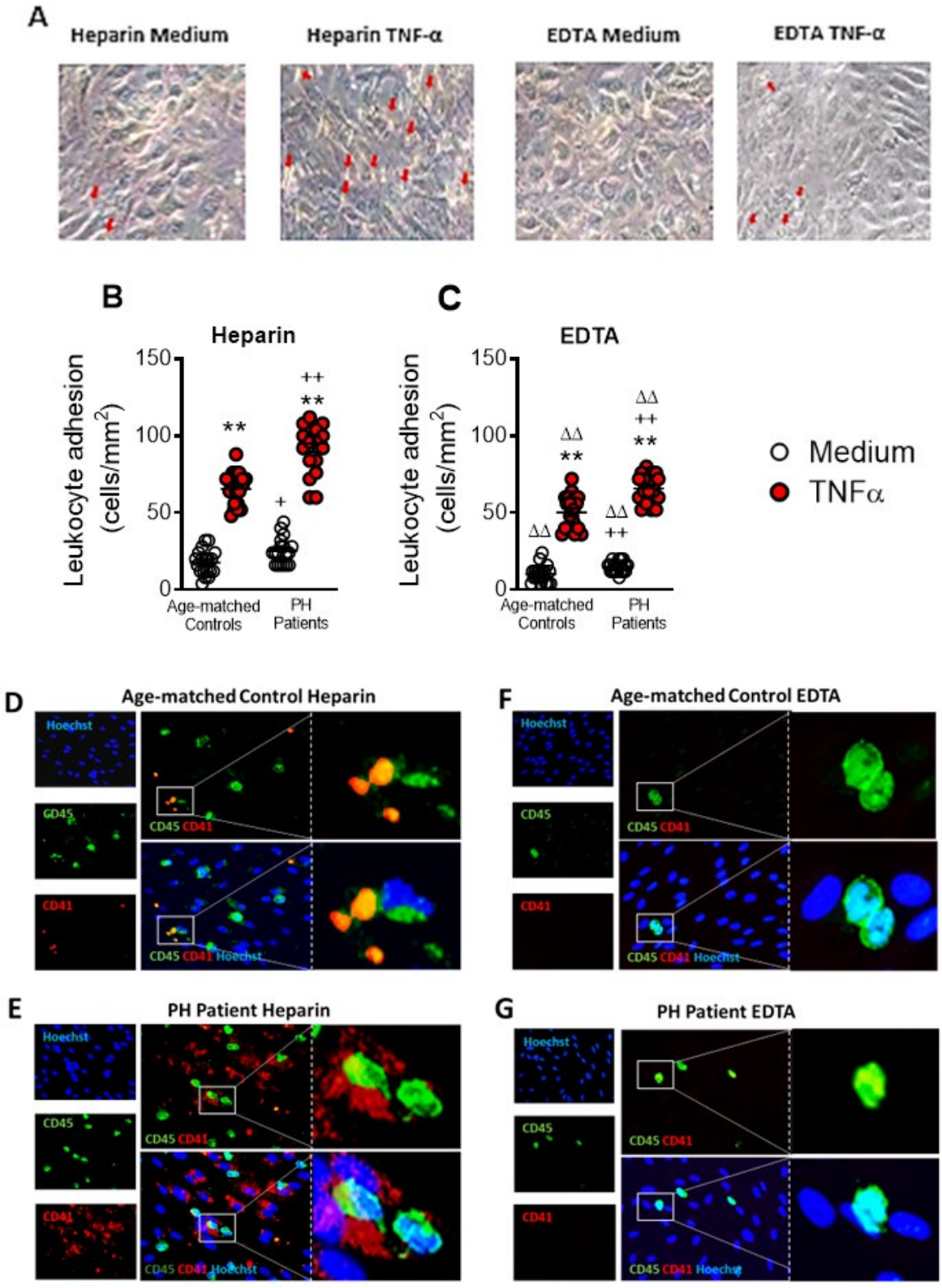

Figure 37. Circulating platelet-leukocyte aggregates and leukocytes from PH patients show increased adhesiveness to TNFα-stimulated HUAEC (20 ng/mL) for 24h.

Subsequently, whole blood from patients and controls, incubated without (**B**) or with EDTA (**C**), was perfused across endothelial monolayer for 7 min at 0.5 dyn/cm^2 and leukocyte adhesion quantified (cells/mm^2). Values are expressed as mean ± SEM (n = 21 control subjects and n= 22 PH patients). ** $p < 0,01$ relative values in the medium group; + $p< 0,05$ or ++ $p< 0,01$ relative to respective values in the control group; $p< 0,01$ relative to respective values in the heparin group. Immunofluorescence analysis showing

adherent platelet-leukocyte cell complexes to TNFα-stimulated HUAEC (**D-G**). Heparinized blood fromage-matched controls and patients with PH was incubated without or with EDTA. After the flow chamber assay, cells were fixed with 4% paraformaldehyde and blocked in phosphate-buffered saline (PBS) containing 1% bovine serum albumin (BSA). Then, cells were incubated for 2h with an Alexa-488 conjugated antibody against human CD45 (1:50 dilution, green) and allophycocyanin (APC)-conjugated antibody against human CD41 (1:50 dilution, red). Nuclei of endothelial cells and leukocytes were stained with Hoechst (blue). Images were captures with a Zeiss Axio Observer A1 fluorescence microscope.

9. STUDY OF SYSTEMIC INFLAMMATION IN PATIENTS WITH PH AND ITS MODULATION BY AN ORAL UNSATURATED FAT LOAD (OUFL)

In total, 20 patients (4 males and 16 females, aged 50.1 ± 3.0 years) and 10 age-matched controls (3 males and 7 females, aged 46.8 ± 4.2 years) were studied. Demographic, clinical and biochemical characteristics of subjects in fasting conditions are shown in **Table 25**. No statistically significant differences were found for age, gender, BMI, or waist circumference between the two groups (**Table 25**). By contrast, baseline levels of total cholesterol (TC), LDL, and apoB were significantly higher in patients than in controls (**Table 25**).

Table 25 – Clinical features of studied subjects

Parameters	Control volunteers (n = 10)	PH subjects (n = 20)
Age (years)	46.8 ± 4.2	50.1 ± 3.0
Gender M/F (%)	3/7 (30.0/70.0)	4/16 (20.0/80.0)
BMI (kg/m2)	25.9 ± 1.1	25.8 ± 0.8
Waist circumference (cm)	85.6 ± 2.9	86.1 ± 1.8
SBP (mmHg)	115.4 ± 2.6	124.8 ± 3.6
DBP (mmHg)	73.5 ± 3.1	78.5 ± 2.7
Glucose (mg/dL)	83.8 ± 1.7	88.1 ± 1.8
TC levels (mg/dL)	215.6 ± 12.9	266.6 ± 9.1**
LDL levels (mg/dL)	137.0 ± 10.2	184.0 ± 6.3**
TG (mg/dL)	93.5 ± 13.7	112.7 ± 8.5
HDL levels (mg/dL)	66.8 ± 3.6	63.6 ± 3.1
ApoB (mg/dL)	94.7 ± 7.0	128.4 ± 5.2**
GOT (U/L)	23.0 ± 1.0	22.8 ± 1.1
GPT (U/L)	23.0 ± 1.0	22.8 ± 1.1
Creatinine (mg/dL)	0.7 ± 0.0	0.7 ± 0.0
IgG (mg/dL)	959.6 ± 61.5	954.6 ± 31.2
IgM (mg/dL)	103.6 ± 10.6	123.5 ± 14.6
IgE total (IU/L)	36.8 ± 12.2	49.0 ± 17.2

*M, male; F, female; BMI, body mass index; SBP, systolic blood pressure; DBP, diastolic blood pressure; TC, total cholesterol; LDL, low-density lipoprotein; TG, triglycerides; HDL, high-density lipoprotein; ApoB, apolipoprotein B; GOT, glutamic-oxalacetic transaminase; GPT, glutamate- pyruvate transaminase; Ig, immunoglobulin. Data are presented as mean ± SEM. *p <0.05 or **p<0.01 relative to values in the control group.*

After the OUFL challenge to both groups, only the circulating levels of TG were significantly increased in patients (**Table 26**) and not the levels of the three clinical features of PH, apoB, LDL and TC, as described previously for other studies (Langsted, Freiberg, & Nordestgaard, 2008).

Table 26 – Effect of an oral unsaturated fat load test on different biochemical characteristics

Parameters	Study group	Fasting (t0)	T4
Glucose (mg/dL)	Control volunteers	83.8 ± 1.7	83.7 ± 1.4
	PH patients	88.1 ± 1.8	88.3 ± 1.6
TG (mg/dL)	Control volunteers	93.5 ± 13.7	133.0 ± 21.0
	PH patients	112.7 ± 8.5	177.5 ± 17.9**
IgG (mg/dL)	Control volunteers	959.6 ± 61.5	1002.1 ± 67.1
	PH patients	954.6 ± 31.2	958.6 ± 32.8
IgM (mg/dL)	Control volunteers	103.6 ± 10.6	105.9 ± 11.0
	PH patients	123.5 ± 14.6	123.3 ± 14.3
IgE total (IU/L)	Control volunteers	36.8 ± 12.2	37.3 ± 11.9
	PH patients	49.0 ± 17.2	50.0 ± 18.0

*Ig, immunoglobulin; PH, Primary Hypercholesterolemia; TG, Triglycerides. Data are presented as mean ± SEM. ** $p < 0.01$ relative to values in patients in fasting conditions*

9.1. Platelet activation and related soluble markers are reduced in patients with PH after an oral unsaturated fat load (OUFL)

After the OUFL, no changes were observed in the percentage of platelets in either group (**Figures 38A** and **B**). By contrast, the percentage of activated platelets expressing PAC-1 and CD62P was significantly lower after the OUFL in patients with PH, but not in the age-matched controls (**Figures 38C - F**).

Since P-selectin expression on the platelet surface can be cleaved and released into circulation as sP-selectin, we determined its circulating levels in plasma, finding that levels were significantly lower after OUFL administration in the PH group but not in the control group (**Figures 38G** and **H**). Similarly, plasma levels of PF-4/CXCL4 and RANTES/CCL5, chemokines released upon platelet activation, also showed a significant decrease in PH patients, but not in the age-matched control group (**Figures 38I** - **L**). Of note, we found positive correlations between circulating levels of PF-4/CXCL4 and RANTES/CCL5 and the percentage of activated platelets expressing PAC-1 in PH patients (**Figures 38M** and **N**).

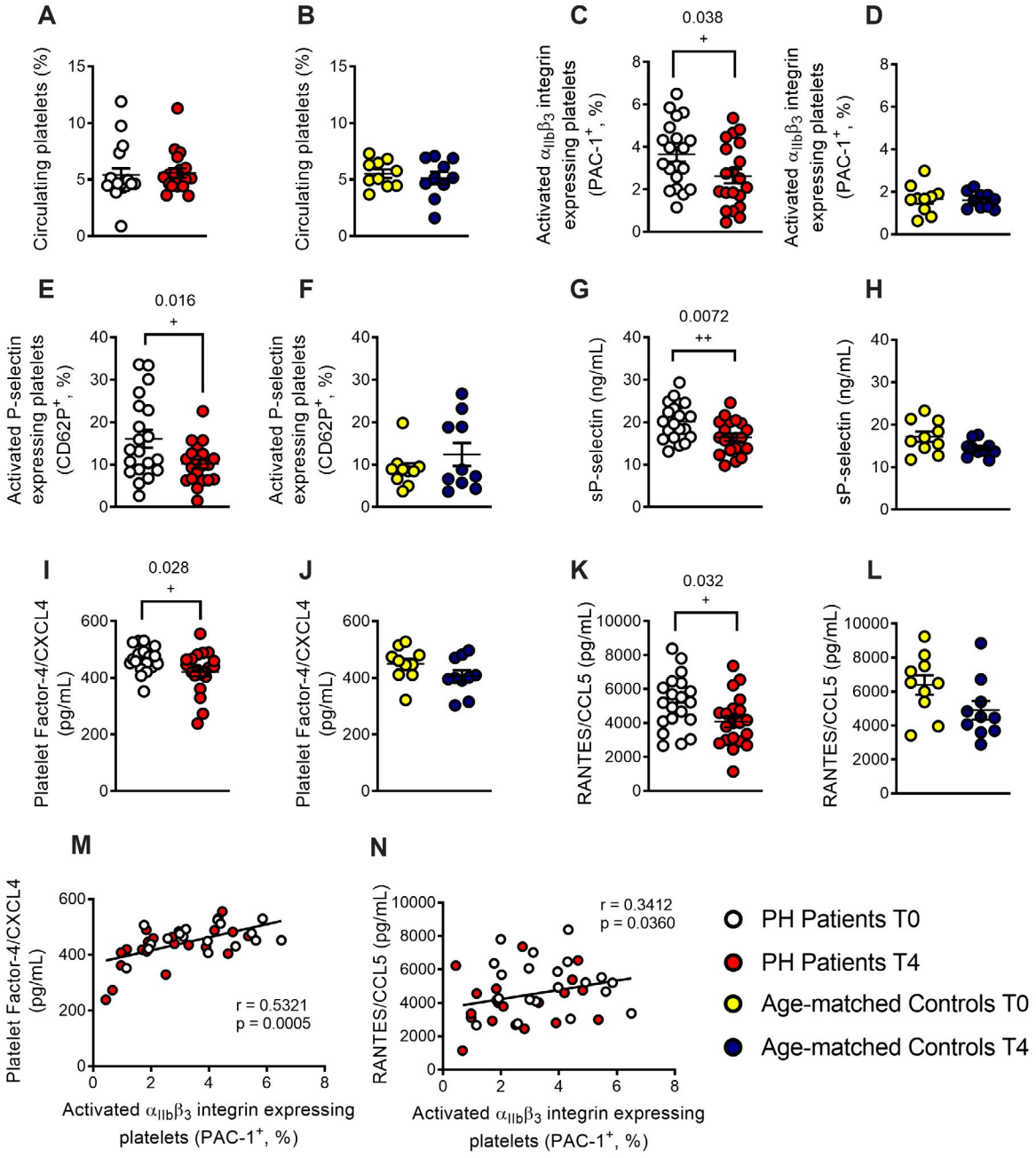

Figure 38. Platelet activation and related soluble markers are reduced in patients with Primary Hypercholesterolemia four hours after an oral unsaturated fat load but not in age-matched controls.

Flow cytometry analysis of platelets stained with conjugated antibodies against CD41 (**A** and **B**), CD41 and PAC-1 (**C** and **D**), and CD41 and CD62P (**E** and **F**). Results are expressed as the percentage of positive cells. sP-selectin (**G** and **H**), PF-4/CXCL4 (**I** and **J**) and RANTES/CCL5 (**K** and **L**) plasma levels (ng or pg/mL) were measured by ELISA (n= 10 age-matched controls and n=20 PH patients). Values are expressed as mean ± SEM. $^+$ $p < 0.05$ or $^{++}p < 0.01$ relative to values in the PH group at time 0 (T0). Positive correlations between the percentage of platelets expressing PAC-1 and plasma levels of PF-4/CXCL4 (**M**) and RANTES/CCL5 (**N**) in PH patients; T0: time 0; T4: time 4.

9.2. Neutrophil activation and circulating levels of IL-8/CXCL8 are reduced in patients with PH after an OUFL

Next, some parameters related to the activation of different leukocyte subsets were evaluated after the OUFL. Regarding circulation, no differences were found in the circulating percentage of neutrophils and in the platelet-neutrophil aggregates in either group before and after OUFL administration (**Figures 39A - D**). However, the percentage of activated neutrophils (CD11b expression and $CD69^{+}$) was significantly reduced in PH patients after the OUFL, but not in controls (**Figures 39E - H**). Regarding neutrophil-related mediators, as some chemokines GRO-α/CXCL1 and interleukin IL-8/CXCL8 can induce neutrophil activation, their levels were quantified in plasma. While no differences were found in plasma levels of GRO-α/CXCL1 (**Figures 39I** and **J**), a significant decrease in plasma levels of IL-8/CXCL8 was observed in patients with PH, but not in controls, after the OUFL (**Figures 39K** and **L**). Also, a positive correlation was also detected between the circulating levels of IL-8 and the activated platelets (CD11b expression and $CD69^{+}$) (**Figures 39M** and **N**).

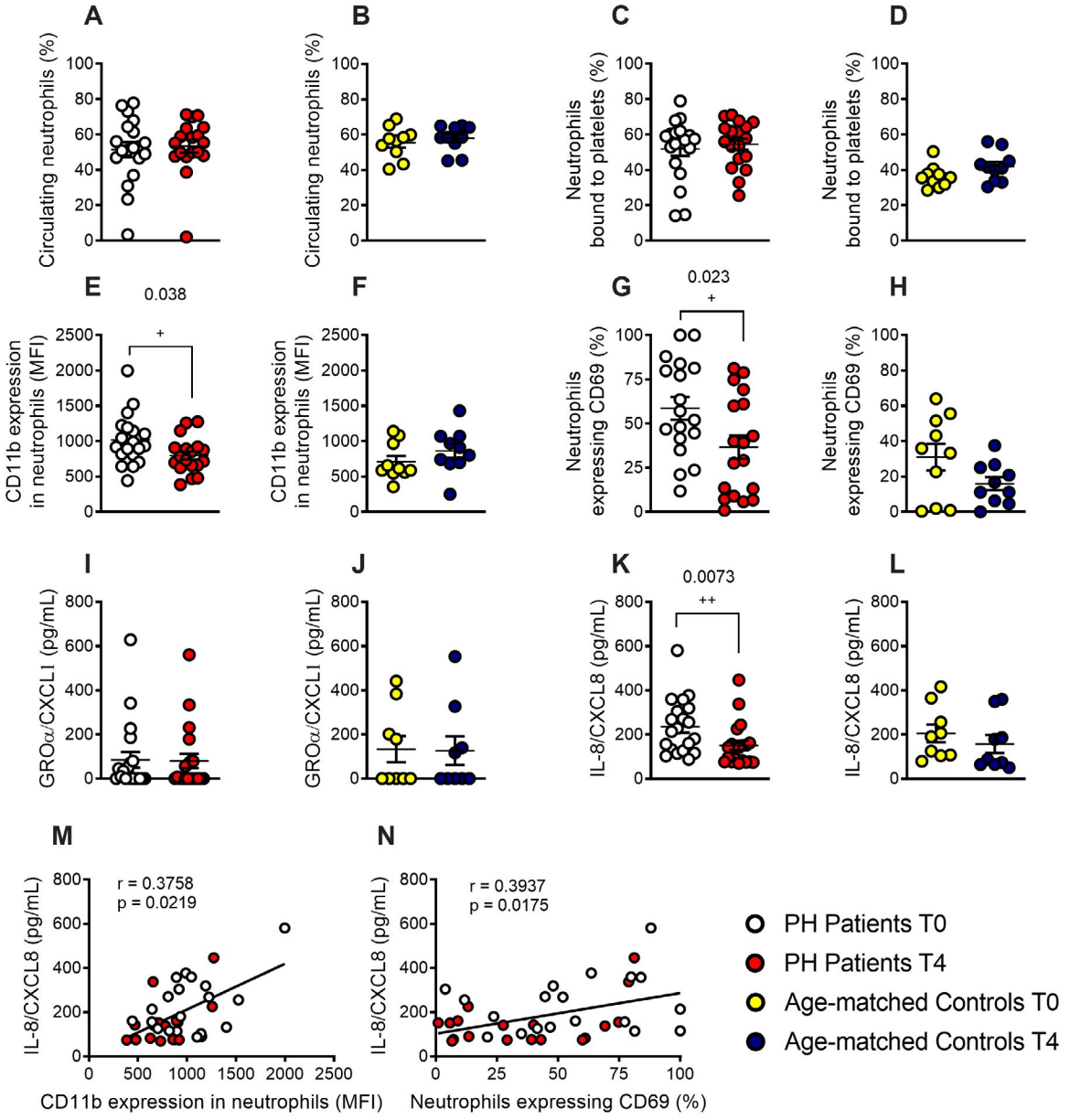

Figure 39. Neutrophil activation and circulating levels of IL-8/CXCL8 are reduced in patients with Primary Hypercholesterolemia after an oral unsaturated fat load but not in age-matched controls.

Flow cytometry analysis of heparinized whole blood co-stained with specific markers for platelets and neutrophils (**A, B, C** and **D**). Neutrophils were also stained for CD11b integrin (**E** and **F**) and CD69 (**G** and **H**). Results are expressed as the percentage of positive cells or median fluorescence intensity (MFI). GRO-α/CXCL1 (**I** and **J**) and IL-8/CXCL8 (**K** and **L**) plasma levels (ng or pg/mL) were measured by ELISA (n= 10 age-matched controls and n=20 PH patients). Values are expressed as mean ± SEM. $^{+}$ $p < 0.05$ or $^{++}p < 0.01$ relative to values in the PH group at time 0 (t0). Positive correlations between the IL-8/CXCL8 plasma levels and CD11b expression in neutrophils (**M**) and in neutrophils expressing CD69 (**N**); T0: time 0; T4: time 4.

9.3. Circulating Mon1 monocytes and MCP-1/CCL2 plasma levels are reduced in patients with PH after an oral unsaturated fat load

Three monocyte subpopulations have been described in peripheral blood based on their differential expression of the cell surface markers CD14, CD16 and CCR2 (***Section 5.3.4.2 Leukocyte studies. Monocytes***). Following the OUFL, a significant decrease in the percentage of circulating type 1 monocytes (Mon 1) was observed in patients but not in controls (**Figures 40A** and **B**), whereas the percentage of Mon 2 and 3 monocytes did not differ between groups before or after the OUFL (**Figures 40A** and **B**). Likewise, platelet-monocyte aggregates, CD11b integrin and CX_3CR1 expression and plasma concentrations of fractalkine/CX_3CL1 were unchanged by the OUFL in either group (**Figures 40C - J** and **Figure 40M** and **N**). Notably, the levels of MCP-1/CCL2 were significantly reduced by the OUFL in patients but not in controls (**Figure 40K** and **L**).

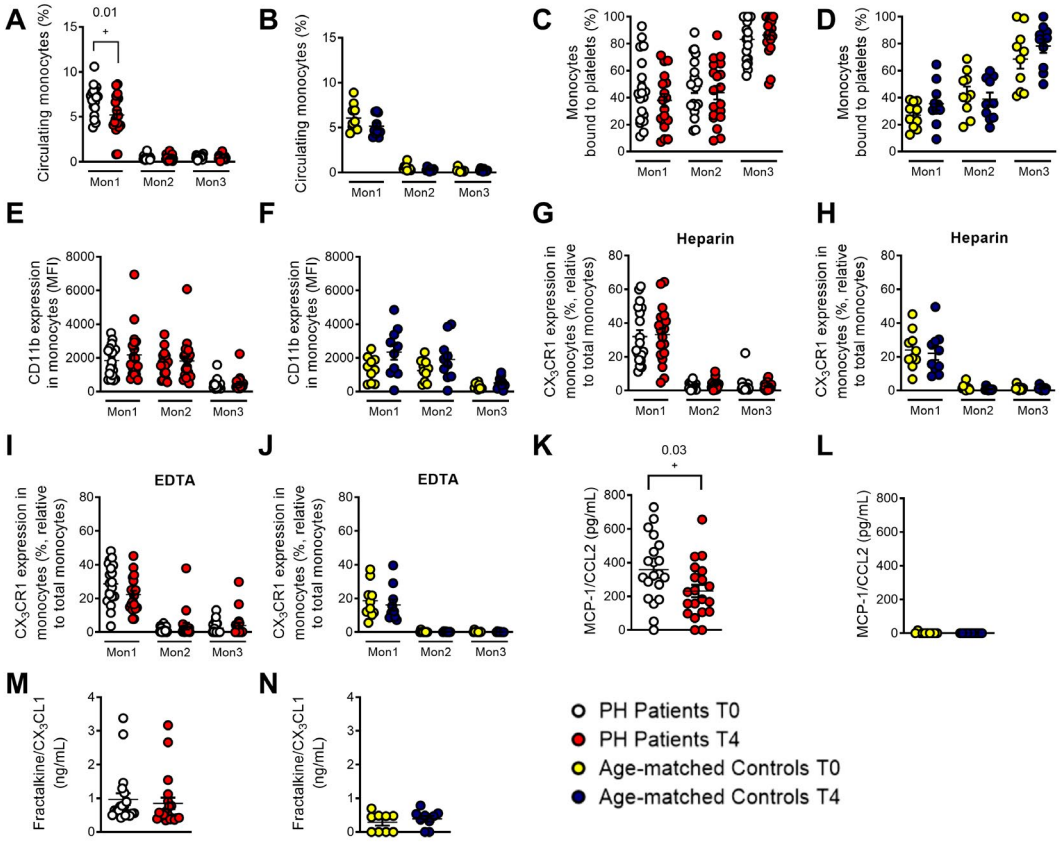

Figure 40. Circulating Mon1 monocytes and MCP-1/CCL2 plasma levels are reduced in patients with primary hypercholesterolemia after an oral unsaturated fat load.

Flow cytometry analysis of heparinized or EDTA-treated whole blood co-stained with specific markers for platelets and Mon 1, 2 and 3 monocytes (**A - D**), CD11b integrin (**E** and **F**), and CX_3CR1 in heparinized (**G** and **H**) and EDTA-treated whole blood (**I** and **J**). Results are presented as the percentage of positive cells or median fluorescence intensity (MFI). MCP-1/CCL2 (**K** and **L**) and fractalkine/CX_3CL1 (**M** and **N**) plasma levels (ng/mL or pg/mL) were measured by ELISA (n = 20 PH patients and n =10 controls). Values are expressed as mean ± SEM. +p <0.05 relative to values in the PH group at time 0 (T0); T0: time 0; T4: time 4.

9.4. The percentage of circulating Treg cells is increased in patients with PH after an oral unsaturated fat load

Mature T cells express the general marker CD3 and either CD4 or CD8 depending on the T cell type. Following the OUFL no significant differences were found in the percentage of circulating $CD3^+$, $CD3^+CD4^+$ or $CD3^+CD8^+$ cells, the percentage of platelet T lymphocyte aggregates, or the activation state of these cells in patients and controls (**Figures 41A - H**).

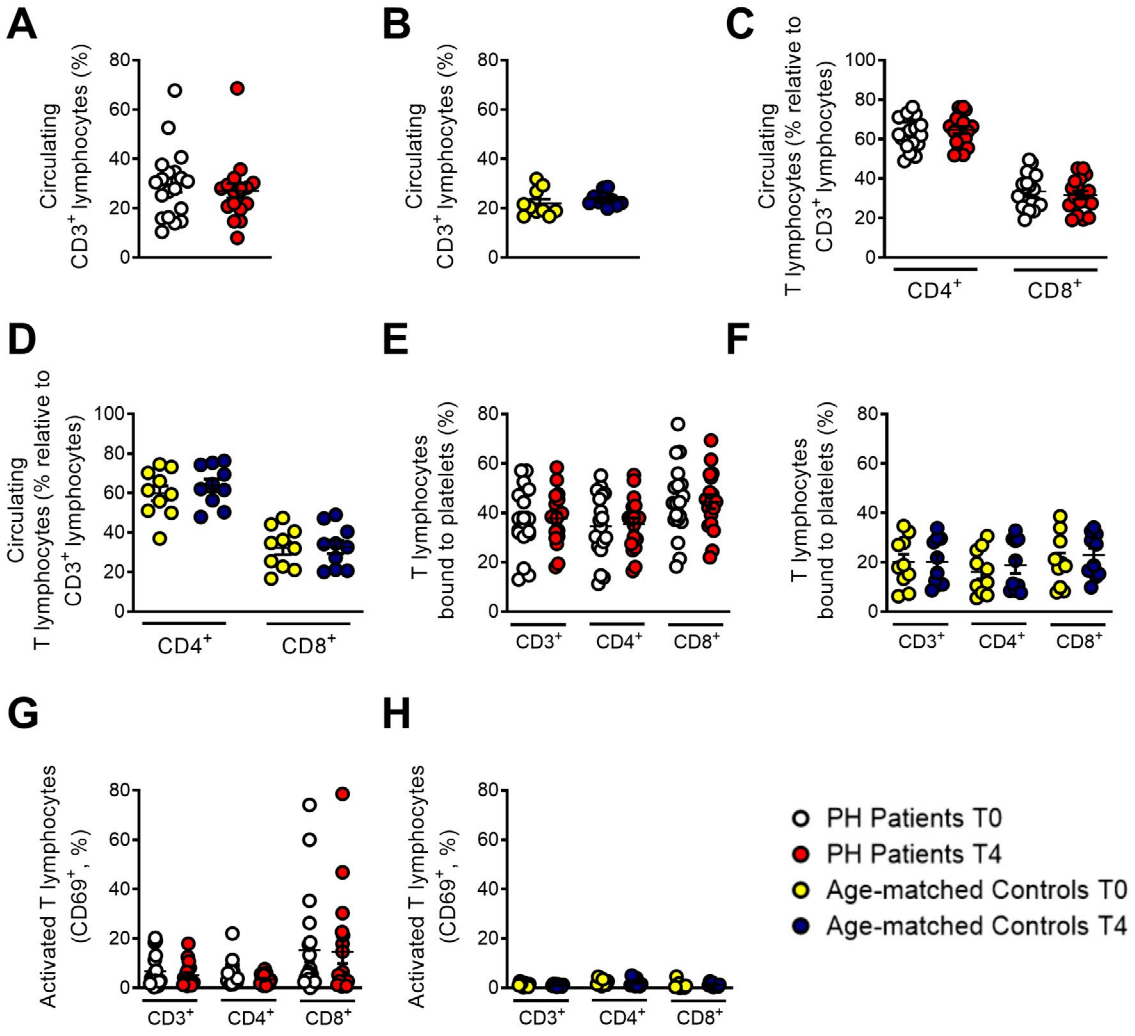

Figure 41. No changes in circulating T lymphocytes, platelet T lymphocyte aggregates and T lymphocyte activation in patients with primary hypercholesterolemia after an oral unsaturated fat load.

Heparinized whole blood was co-stained with specific markers for platelets, $CD3^+$, $CD4^+$ and $CD8^+$ lymphocytes (**A** - **F**), and activated lymphocytes ($CD69^+$) (**G** and **H**). Results are presented as the percentage of positive cells (n = 20 PH patients and 10 controls). Values are expressed as mean ± SEM.; T0: time 0; T4: time 4.

Similarly, no differences in these parameters were detected in the different Th lymphocyte subpopulations before or after the OUFL administration in either group (**Figures 42A - F**).

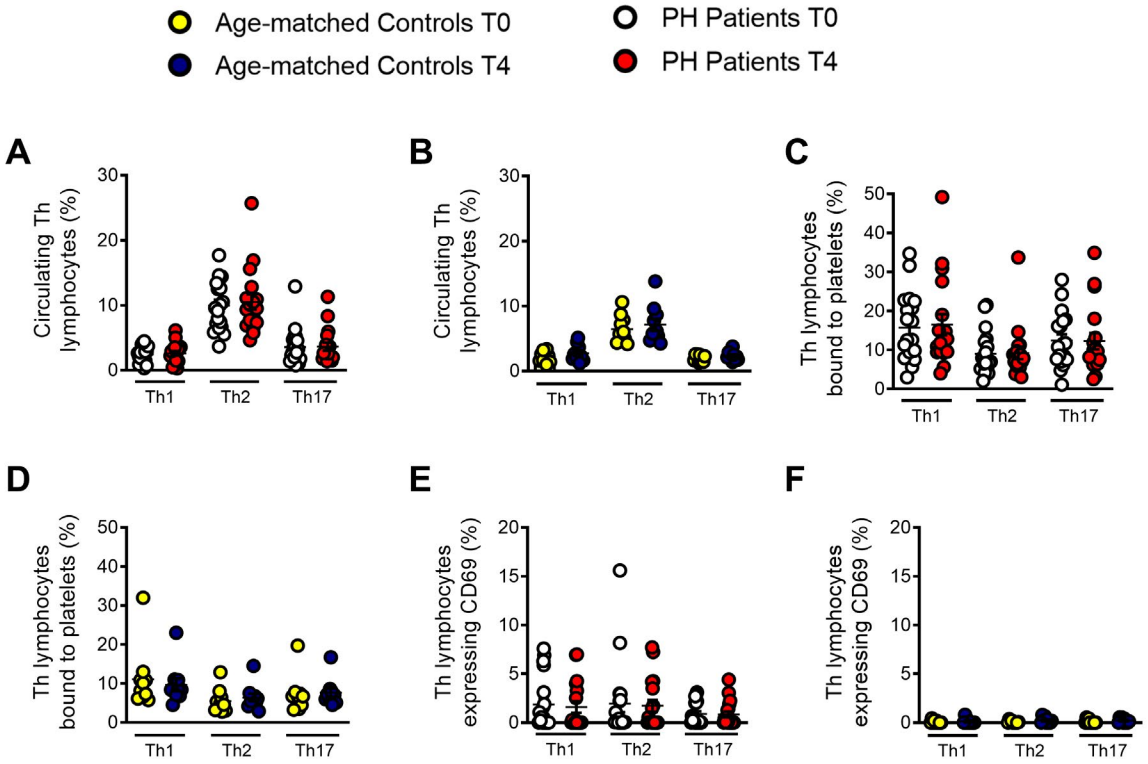

Figure 42. No differences are found in the percentage of circulating Th cells in either group after an oral unsaturated fat load.

Heparinized whole blood was co-stained with specific markers for platelets and Th1, Th2, Th17 lymphocytes (**A, B, C** and **D**) and for activated lymphocytes ($CD69^+$) (**E** and **F**) (n = 20 PH patients and 10 controls). Values are expressed as mean ± SEM. +p <0.05 relative to values in the PH group at time 0 (T0). T0: time 0; T4: time 4.

Interestingly, the percentage of circulating Treg lymphocytes after the OUFL was significantly higher in patients but not in controls (**Figures 43A** and **B**). No differences were observed in the percentage of Treg lymphocyte-platelet aggregates, the Treg/Th17 ratio or the plasma levels of different soluble markers associated with T lymphocytes (IL-12, IFN-γ, or IL-10) before or after the OUFL in either group (**Figures 43C - L**).

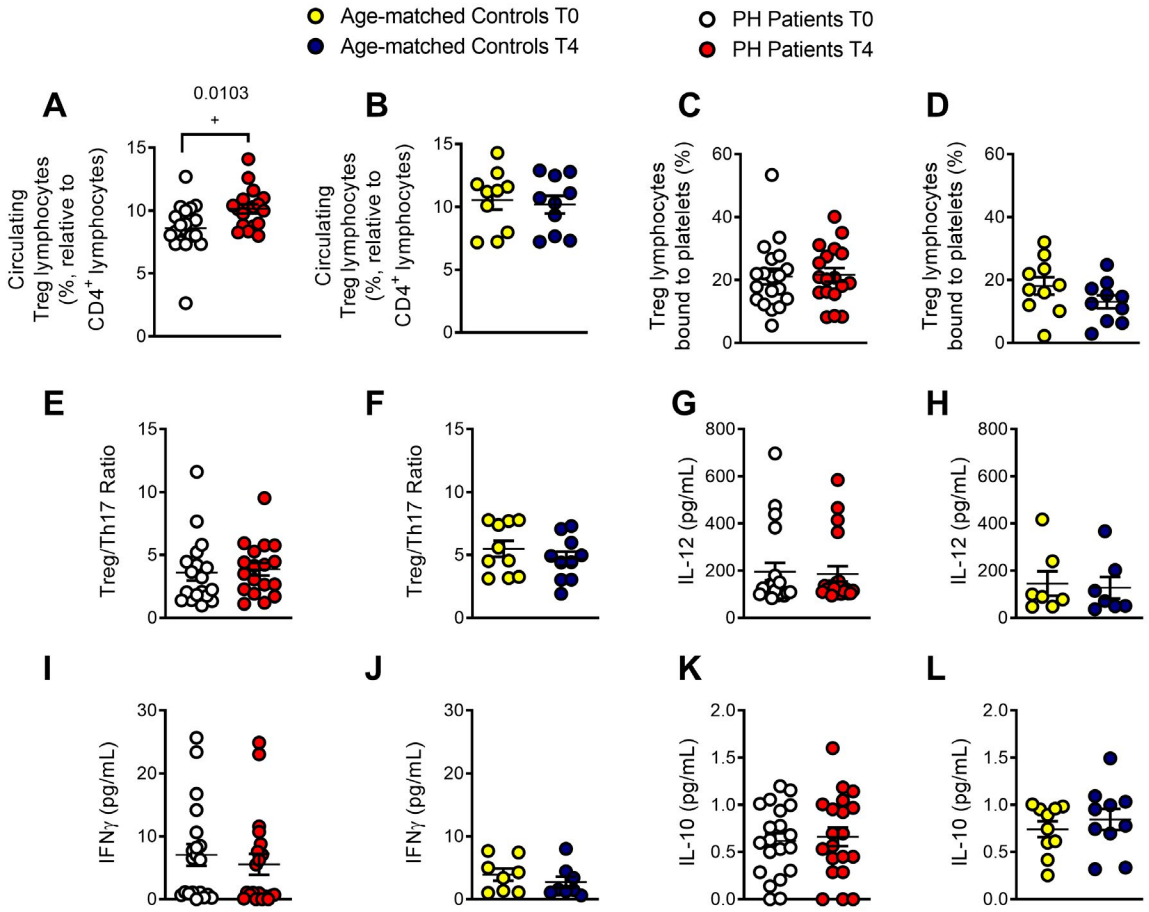

Figure 43. The percentage of circulating Treg cells is increased in patients with primary hypercholesterolemia after an oral unsaturated fat load.

Heparinized whole blood was co-stained with specific markers for platelets and Treg lymphocytes (**A**, **B**, **C** and **D**). The Treg/Th17 ratio was also determined (**E** and **F**). Results are presented as the percentage of positive cells. IL-12 (**G** and **H**), IFN-γ (**I** and **J**), and IL-10 (**K** and **L**) plasma levels (pg/mL) were measured by ELISA (*n* = 20 PH patients and 10 controls). Values are expressed as mean ± SEM. +*p* <0.05 relative to values in the PH group at time 0 (T0). T0: time 0; T4: time 4.

9.5. Circulating levels of TNF-α are reduced in patients with PH after an oral unsaturated fat load

Increased plasma levels of TNF-α and IL-6 have been reported in patients with PH (Collado, Marques, Domingo, et al., 2018; Holven et al., 2014; Real et al., 2010; Sampietro et al., 1997). We found that circulating plasma TNF-α levels were significantly lower after the OUFL in patients and similar to those found in controls, which did not change 4 h after the administration (**Figures 44A** and **B**) Conversely, plasma concentrations of IL-6, adiponectin, leptin or ghrelin were unchanged after the OUFL in both groups (**Figures 44C - J**).

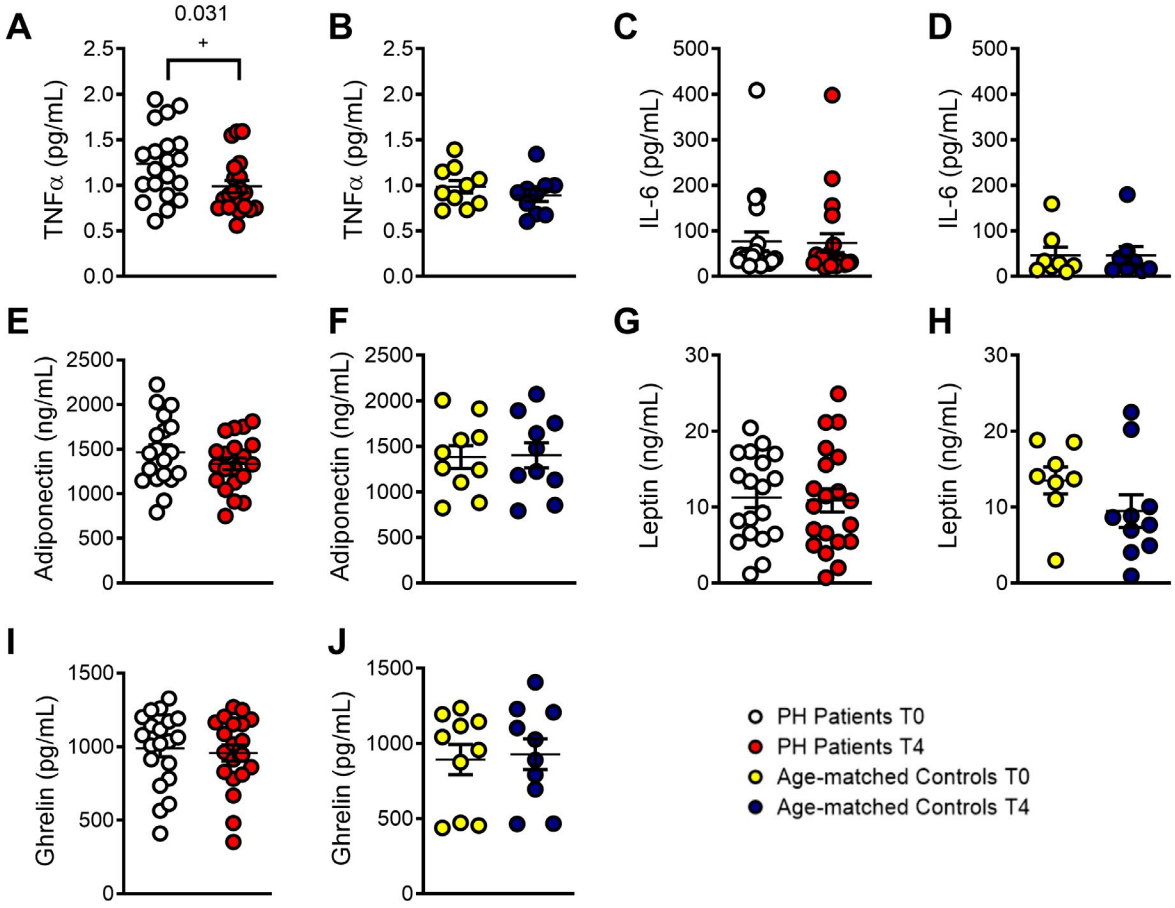

Figure 44. Circulating levels of TNF-α are reduced in patients with primary hypercholesterolemia after an oral unsaturated fat load.

TNF-α (**A** and **B**), IL-6 (**C** and **D**), adiponectin (**E** and **F**), leptin (**G** and **H**), and ghrelin (**I** and **J**) plasma levels (ng/mL or pg/mL) were measured by ELISA (n = 20 PH patients and 10 controls). Values are expressed as mean ± SEM. +p <0.05 relative to values in the PH group at time 0 (T0). T0: time 0; T4: time 4.

9.6. Circulating platelet-leukocyte aggregates and leukocytes from patients with PH show reduced adhesiveness to TNFα-stimulated endothelial cells after an oral unsaturated fat load

Endothelial dysfunction is the earliest stage of atherogenesis and is characterized by an increase in the adhesiveness of leukocytes to the endothelium, and their subsequent migration to the arterial subendothelial space (Landmesser et al., 2004). We previously demonstrated that the plasma levels of TNF-α are elevated in patients with PH and that the adhesion of platelet-leukocyte aggregates and leukocytes from these patients to dysfunctional arterial endothelium (TNFα-stimulated) is enhanced when compared with age-matched controls (Collado, Marques, Domingo, et al., 2018).

We performed the flow chamber adhesion analysis before and following the OUFL, finding that the number of platelet-leukocyte aggregates (heparin) or platelet-free leukocytes (EDTA) adhered to the unstimulated or TNFα-stimulated arterial endothelium was reduced after the OUFL in patients (**Figures 45A** and **C**) but not in controls (**Figures 45B** and **D**). Of note, we found positive correlations between patient leukocyte adhesion and MCP-1/CCL2 (**Figure 45E**), PF-4/CXCL4 (**Figure 45F**) and RANTES/CCL5 (**Figure 45G**) plasma levels.

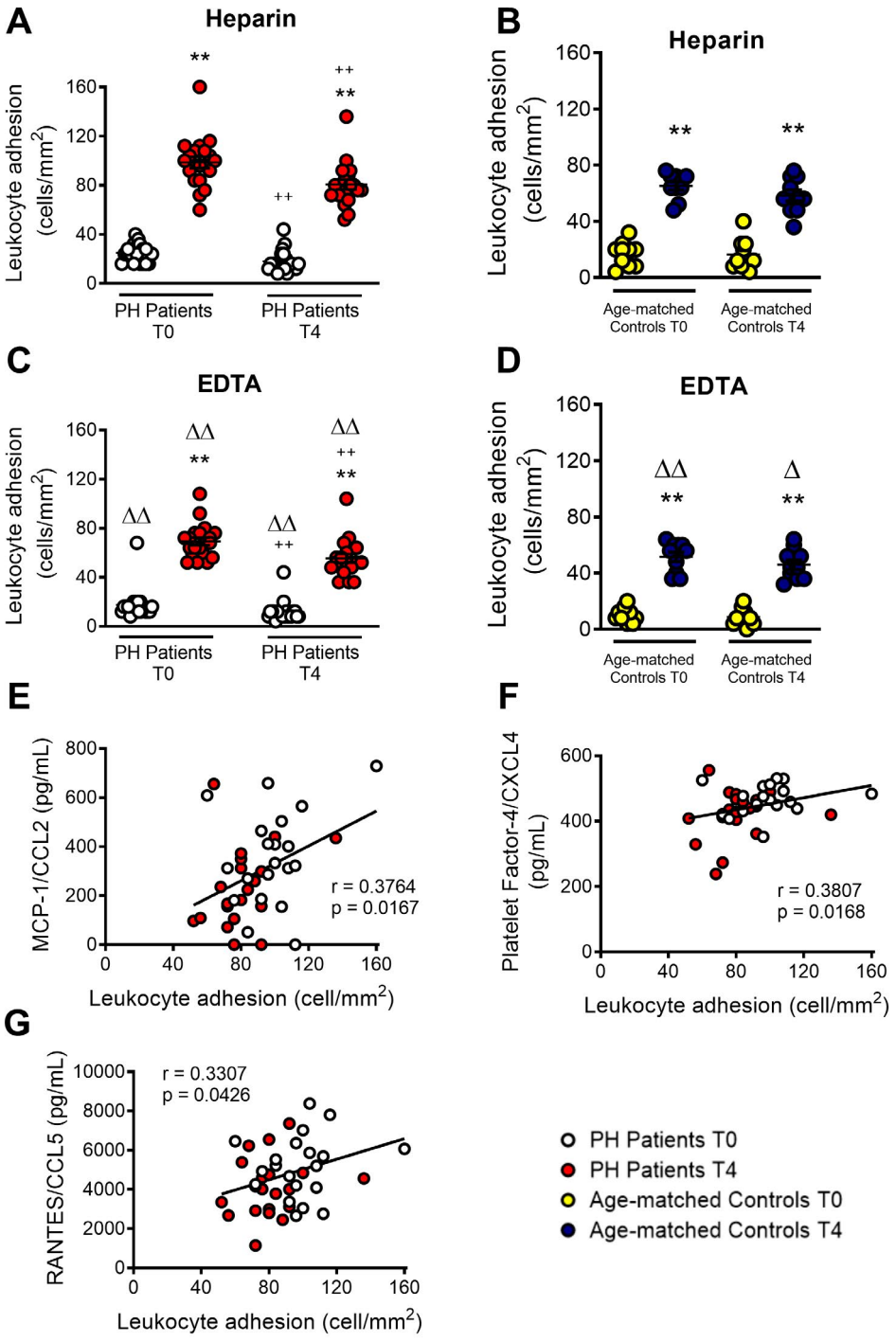

Figure 45. Circulating platelet-leukocyte aggregates and leukocytes from patients with primary hypercholesterolemia display lower adhesiveness to TNFα-stimulated HUAEC after an oral unsaturated fat load.

HUAEC were stimulated or not with TNF-α (20 ng/mL) for 24 h. Subsequently, whole blood from all patients, incubated without (**A** and **B**) or with EDTA (**C** and **D**), was perfused across the endothelial monolayers for 7 min at 0.5 dyn/cm^2 and leukocyte adhesion quantified (cells/mm^2). Values are expressed as mean ± SEM (n = 20 PH patients and 10 controls). $^{**}p<0.01$ relative to values in the medium-only group; $^{++}p<0.01$ relative to the respective values at time 0 (T0); $^{\Delta\Delta}p<0.01$ relative to the respective values in the heparin group. Positive correlations between leukocyte adhesion and plasma levels of MCP-1/CCL2 (**E**), PF-4/CXCL4 (**F**), and RANTES/CCL5 (**G**). T0: time 0; T4: time 4.

10. STUDY OF THE ROLE OF CCL11/CCR3 AXIS IN PH AND ATHEROSCLEROSIS DEVELOPMENT

10.1. Human studies

10.1.1. *Circulating plasma levels of eotaxin-1/CCL11 and the percentage of circulating eosinophils were significantly increased in PH patients compared with control subjects*

In the previous study carried out by our group, different cytokines and chemokines were detected in the plasma of patients with PH compared with age-matched controls (Collado, Marques, Domingo, et al., 2018). Surprisingly, in a in depth analysis, increased levels of circulating eotaxin-1/CCL11 were detected in PH patients compared to control subjects (**Figure 46A)** and its concentration positively correlated with two clinical features of PH such as apoB and LDL plasma content (**Figures 46B** and **C**). In contrast, no differences were found between groups in the circulating levels of eotaxin-2/CCL24 and eotaxin-3/CCL26 (**Figures 46D** and **E**). Since eotaxin-1/CCL11 signals exclusively through interaction with the CCR3 receptor, we next determined the percentage of CCR3-expressing platelets and leukocytes in peripheral blood by flow cytometry. Although platelets express functional CCR3 receptors (Clemetson et al., 2000), no differences between PH patients and age-matched controls were encountered in the percentage of circulating platelets (**Figure 46F**) or the percentage of CCR3-expressing platelets (**Figure 46G**). Unexpectedly, increased percentage of CCR3-expressing leukocytes was found in whole blood from PH patients compared with age–matched controls (**Figure 46H**). Dissecting evaluation of the leukocyte subpopulations that express CCR3 revealed that both the number and the percentage of circulating eosinophils were significantly enhanced in patients with PH (**Figures 46I - L**) and the latter positively correlated with apoB and LDL plasma levels (**Figures 46M** and **N**). Since a human subpopulation of Th2 lymphocytes also express the CCR3 receptor (Sallusto, Mackay, & Lanzavecchia, 1997), this population of leukocytes was next investigated. However, the percentage of circulating $CCR3^+$ Th2 lymphocytes did not differ between patients with PH and age-matched controls (**Figure 46O**).

Given that CCR3 receptor is constitutively expressed at high levels in eosinophils (Daugherty et al., 1996), we next determined circulating levels of other eosinophil-related cytokines. While IL-5 plasma concentrations were slightly lower in PH patients than in age-matched controls (**Figure 46P**), IL-13, IL-25 and IL-33 circulating levels did not differ between groups (**Figures 46Q - S**).

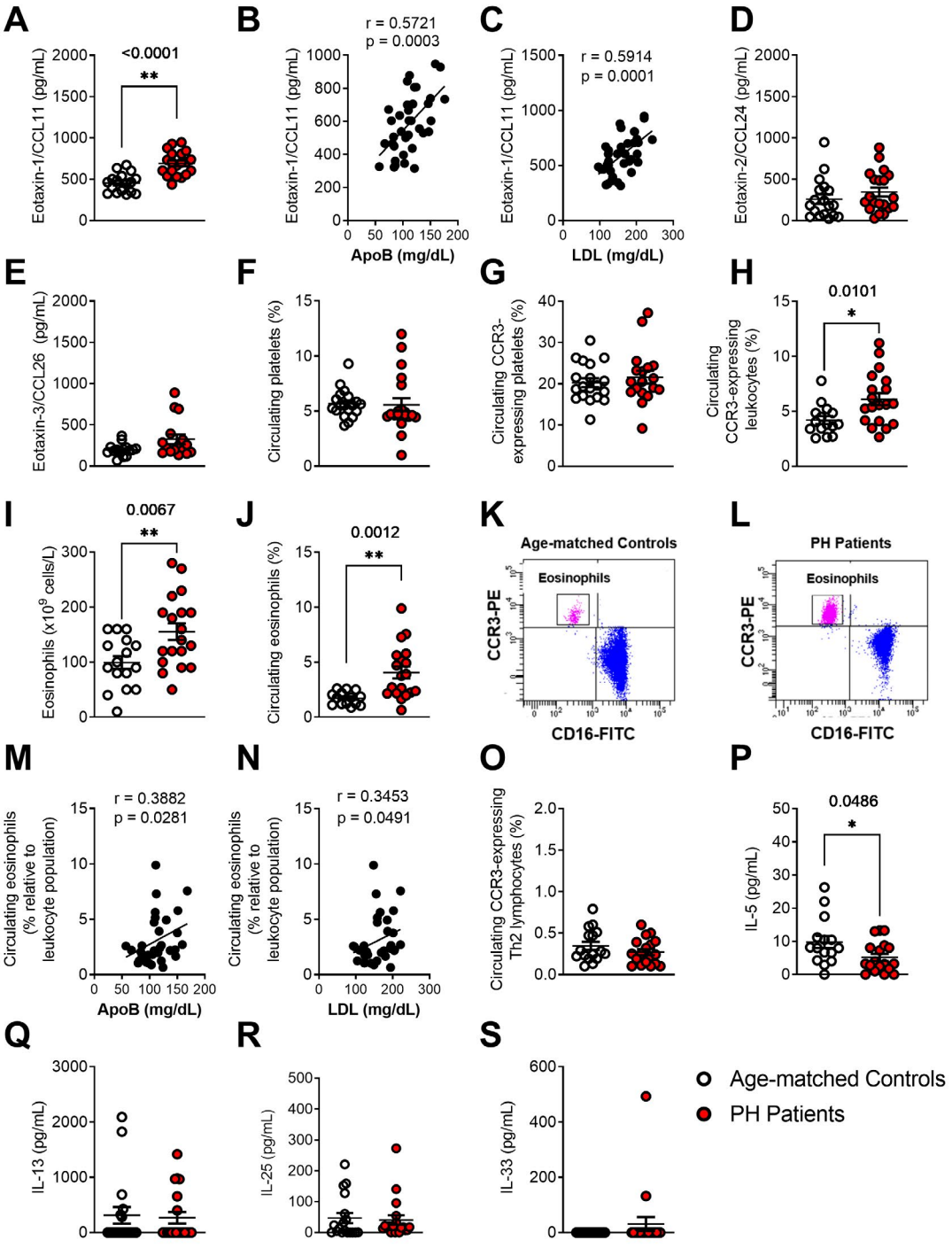

Figure 46. Circulating plasma levels of eotaxin-1/CCL11 and the percentage of circulating eosinophils were higher in PH patients compared to control group.

Plasma levels of eotaxin-1/CCL11 (**A**), eotaxin-2/CCL24 (**D**), eotaxin-3/CCL26 (**E**), IL-5 (**P**), IL-13 (**Q**), IL-25 (**R**) and IL-33 (**S**) were determined by ELISA. Results are presented as pg/mL (n=22 PH patients, n=21 age-matched controls). Percentage of platelets (**F** and **G**), CCR3-expressing leukocytes (**H**), eosinophils (**I** and **J**), and CCR3-expressing Th2 lymphocytes (**O**). Results are presented as cells/L (**I**) or percentage of positive populations. Values are expressed as mean ± SEM. *P < 0.05 or **P < 0.01 relative to values in the control group. Representative dot plots of the eosinophil population in PH patients and age-matched controls (**K** and **L**). Correlations with ApoB and LDL-cholesterol were performed **(B**, **C**, **M** and **N**).

10.2. Animal studies

First model: *apoE*$^{-/-}$

10.2.1. *ApoE*$^{-/-}$ *mice subjected to an atherogenic diet for two months had increased levels of TC, Non-HDLc and TG*

Based on the results found in humans, the animal model of mice deficient in apolipoprotein E (*apoE*$^{-/-}$) was used, a widely known model to carry out atherosclerosis formation studies (Li, C, Wang, & Liu, 2016). To accelerate the process of atherosclerotic plaque formation, *apoE*$^{-/-}$ mice were subjected or not to an atherogenic diet for two months. *ApoE*$^{-/-}$ mice subjected to an atherogenic diet for two months had significantly increased circulating levels of total cholesterol (TC), non-HDL cholesterol (LDL and VLDL) or TG but decreased plasma levels of HDL cholesterol than those animals under a control diet (**Table 27**).

Table 27 – Biochemical parameters of apoE$^{-/-}$ animals

Parameters	*apoE*$^{-/-}$ Control diet (*n* =10)	*apoE*$^{-/-}$ Atherogenic diet (*n* =11)
Weight (g)	29.5 ± 1.04	28.0 ± 1.02
Glucose (mg/dL)	82.0 ± 4.6	85.6 ± 5.58
TC levels (mg/dL)	296.8 ± 19.79	473.0 ± 24.74**
Non-HDLc levels (mg/dL)	251.4 ± 19.34	455.8 ± 24.35**
HDLc (mg/dL)	45.07 ± 2.18	17.25 ± 1.77**
TG (mg/dL)	101.2 ± 18.25	284.1 ± 18.14**
Ratio HDLc/non-HDLc	0.2 ± 0.0	0.0 ± 0.0**
Ratio HDLc/TC	0.2 ± 0.0	0.0 ± 0.0**
Ratio TG/HDLc	2.17 ± 0.49	17.74 ± 1.77**

*TC, total cholesterol; LDL, low-density lipoprotein; VLDL, very low-density lipoprotein; HDL, high-density lipoprotein; TG, triglycerides. Data are presented as mean ± SEM. *p <0.05 or **p<0.01 relative to values in the control group.*

10.2.2. *ApoE$^{-/-}$ mice subjected to an atherogenic diet for two months showed increased levels of circulating eotaxin-1/CCL11, percentage of eosinophils and eotaxin1/CCL11 and eosinophil infiltration within the atherosclerotic lesion*

Blood from *apoE$^{-/-}$* mice fed with control diet or atherogenic diet was extracted in 4 µL of sodium heparin (5,000 IU/mL)/ mL of blood. Interestingly, and in agreement with human data, elevated plasma levels of eotaxin-1/CCL11 were observed in *apoE$^{-/-}$* mice fed with a high-fat diet compared to those fed with a control diet for two months (**Figure 47A**).

This observation was accompanied by enhanced percentage of circulating CCR3-expressing leukocytes (**Figure 47B**) which were mainly eosinophils (**Figure 47C - E),** since murine Th2 lymphocytes do not express CCR3 receptor (Romagnani, 2002).

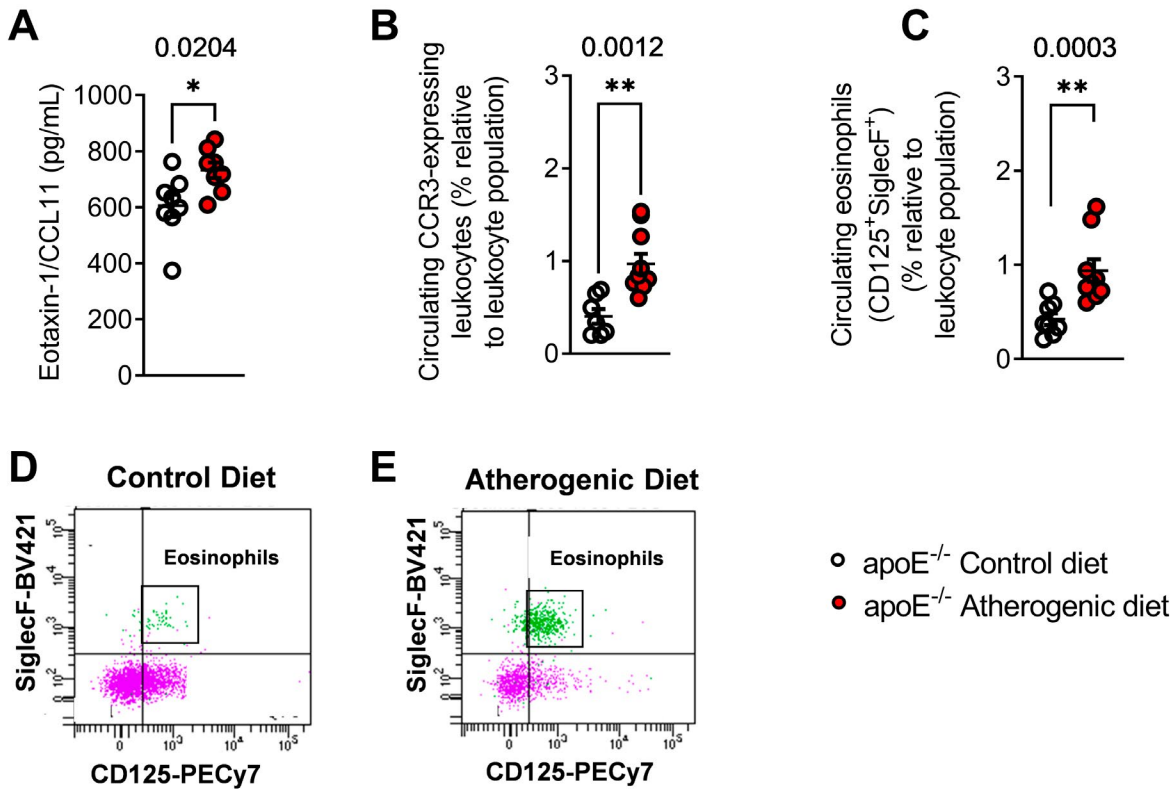

Figure 47. Circulating plasma levels of CCL11/eotaxin-1 and the percentage of eosinophils were elevated in apoE$^{-/-}$ mice fed with an atherogenic diet compared to their control.

Plasma levels of eotaxin-1/CCL11 (**A**), percentage of CCR3-expressing leukocytes (**B**) and eosinophils (**C - E**). Results are expressed as percentage of positive populations or pg/mL (n=8 *apoE$^{-/-}$* mice fed with a control diet, n=9 *apoE$^{-/-}$* mice fed with an atherogenic diet). Values are expressed as mean ± SEM. *P < 0.05 or **P < 0.01 relative to values in *apoE$^{-/-}$* mice fed with a control diet.

As expected, the study of the macroscopic lesion using Oil-Red staining revealed a significant development of an atheroma plaque (**Figures 48A - C**), both in the aortic arch (**Figures 48A** and **B**) and in the thoracic aorta (**Figures 48A** and **C**) of mice fed with an atherogenic diet compared to animals under a control diet. In parallel, the quantification of the atherogenic lesion in the sigmoidal aortic valves showed similar results (**Figures 48D - F**).

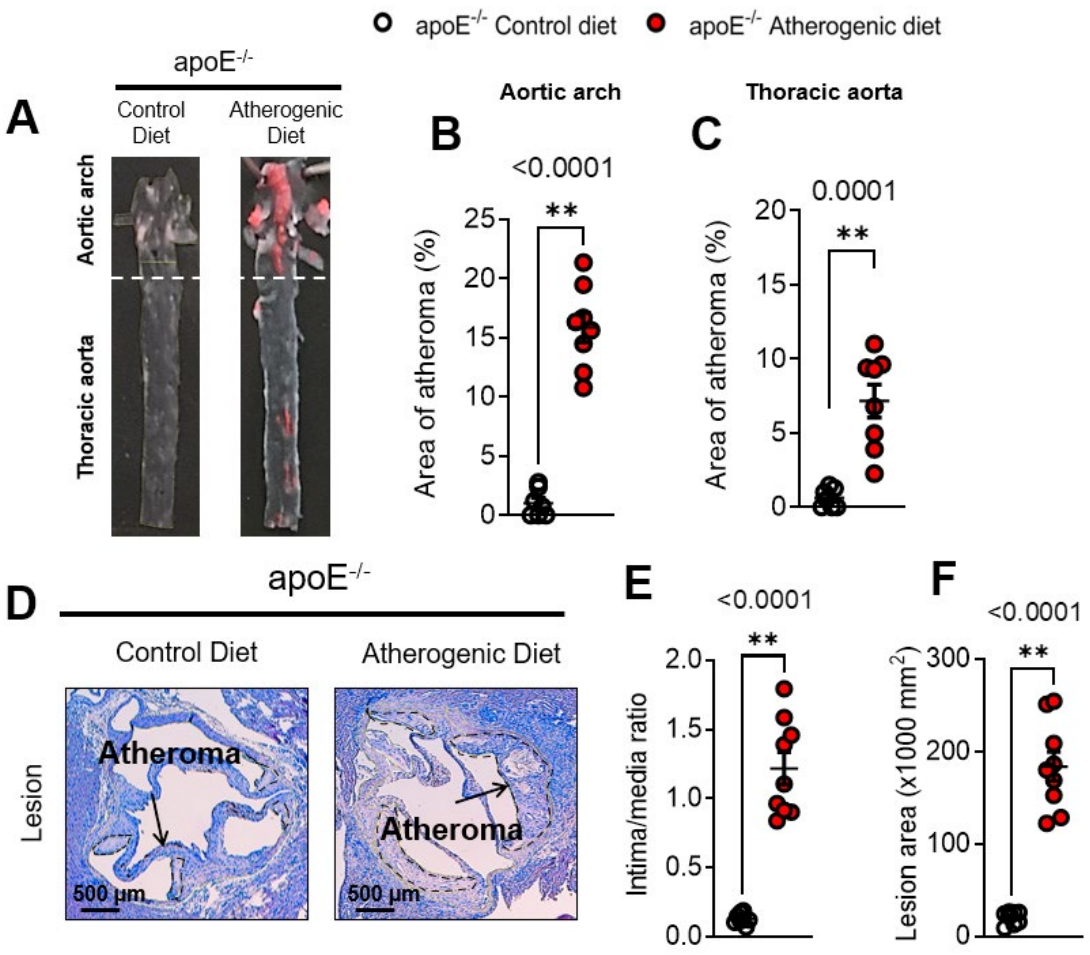

Figure 48. Two months with a high-fat diet markedly increased the atherosclerotic lesion formation.

Representative images of Oil-Red stained aortas (**A**), atheroma lesion in the aortic arch (**B**), and in the thoracic aorta (**C**). The discontinuous lines delineate the limits of the atherosclerotic lesion (**D**). Intima/media ratio (**E**), lesion area (**F**) was determined in the aortic sinus. Results are expressed as mean ± SEM (n=8 *apoE*$^{-/-}$ mice fed with a control diet, n=9 *apoE*$^{-/-}$ mice fed with an atherogenic diet). Values are expressed as mean ± SEM. **P < 0.01 relative to values in *apoE*$^{-/-}$ mice fed with a control diet.

Accordingly, increased infiltration of macrophages (Mac3^{+} cells), CD4^{+} and CD8^{+} lymphocytes were detected within the atherosclerotic lesion of *apoE*$^{-/-}$ mice subjected to an atherogenic diet for two months (**Figures 49A - G**).

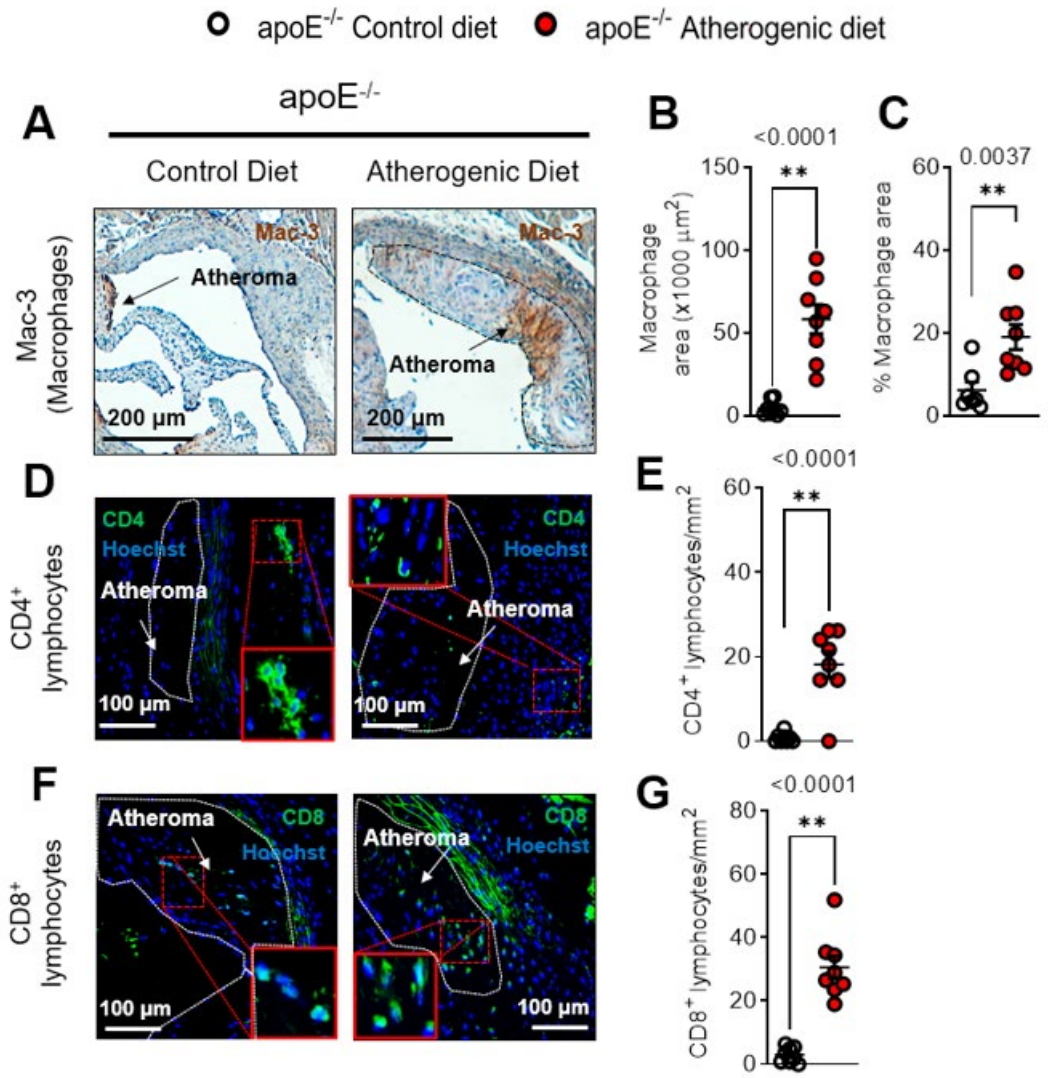

Figure 49. Two months with a high-fat diet markedly increased the macrophage and lymphocyte infiltration to the atherosclerotic plaque.

Representative images of immunohistology (**A, D** and **F**), and the quantification of macrophages (Mac-3$^+$, **B** and **C**), CD8$^+$ lymphocytes (**G**) and CD4$^+$ lymphocytes (**E**). The discontinuous lines delineate the limits of the atherosclerotic lesion. Results are expressed as mm^2 of positive populations. Values are expressed as mean ± SEM (n=8 *apoE*$^{-/-}$ mice fed with a control diet, n=9 *apoE*$^{-/-}$ mice fed with an atherogenic diet). Values are expressed as mean ± SEM. *P < 0.05 or **P < 0.01 relative to values in *apoE*$^{-/-}$ mice fed with a control diet.

In addition, an increase in the total percentage of circulating monocytes was observed (**Figure 50A - C**). This rise was largely due to the increase in pro-inflammatory monocytes (CCR2$^+$, **Figure 50B**). In contrast, the percentage of CD4$^+$ and CD8$^+$ lymphocytes were reduced when the animals were subjected to a hypercholesterolemic diet (**Figure 50D** and **E**).

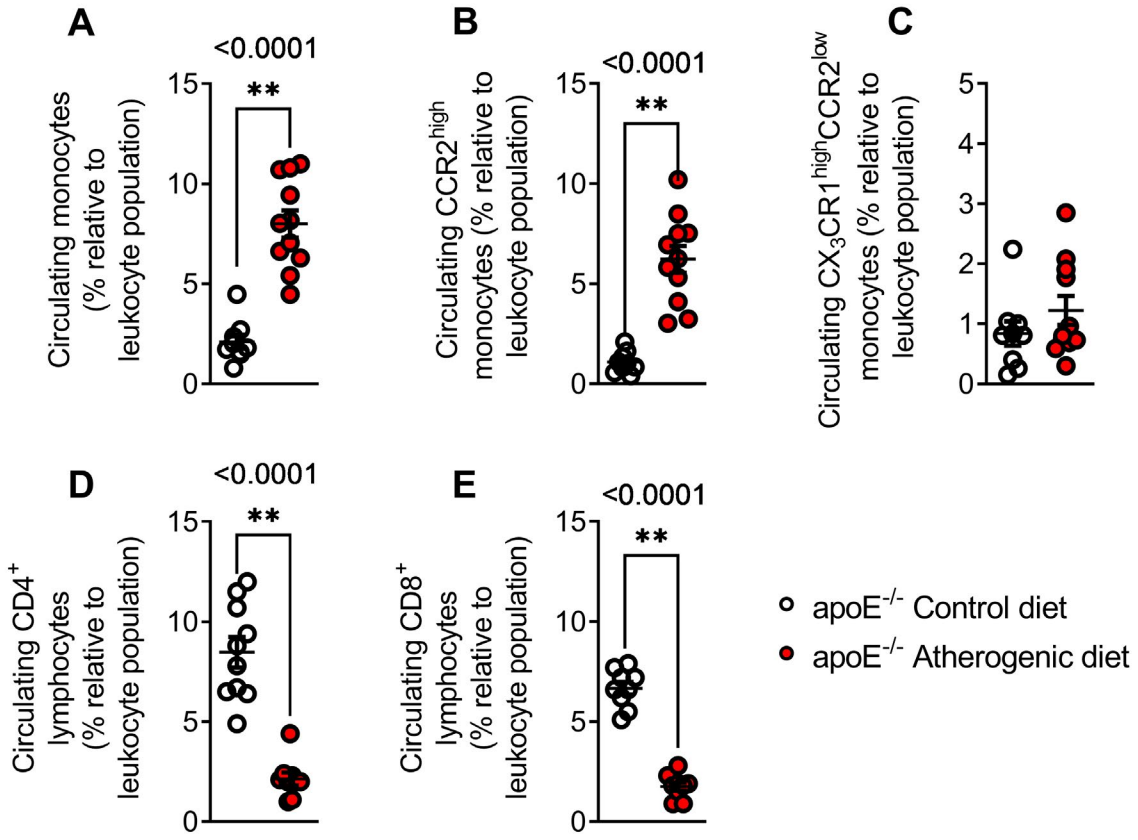

Figure 50. The percentage of circulating monocytes were elevated while the percentage of T lymphocytes were decreased in apoE$^{-/-}$ mice fed with an atherogenic diet compared to those under a control diet.

Percentage of total monocytes (**A**), pro-inflammatory monocytes (**B**), patrolling monocytes (**C**), CD4^{+} lymphocytes (**D**) and CD8^{+} lymphocytes (**E**). Results are expressed as percentage of positive populations. Values are expressed as mean ± SEM (n=10 *apoE*$^{-/-}$ mice fed with a control diet, n=11 *apoE*$^{-/-}$ mice fed with an atherogenic diet). *P < 0.05 or **P < 0.01 relative to values in *apoE*$^{-/-}$ mice fed with a control diet.

As found previously (Haley et al., 2000), eotaxin1/CCL11 expression was detected in the atherosclerotic lesion of the animals subjected to a high fat diet for two months but not in those under a control diet (**Figures 51A - C**).

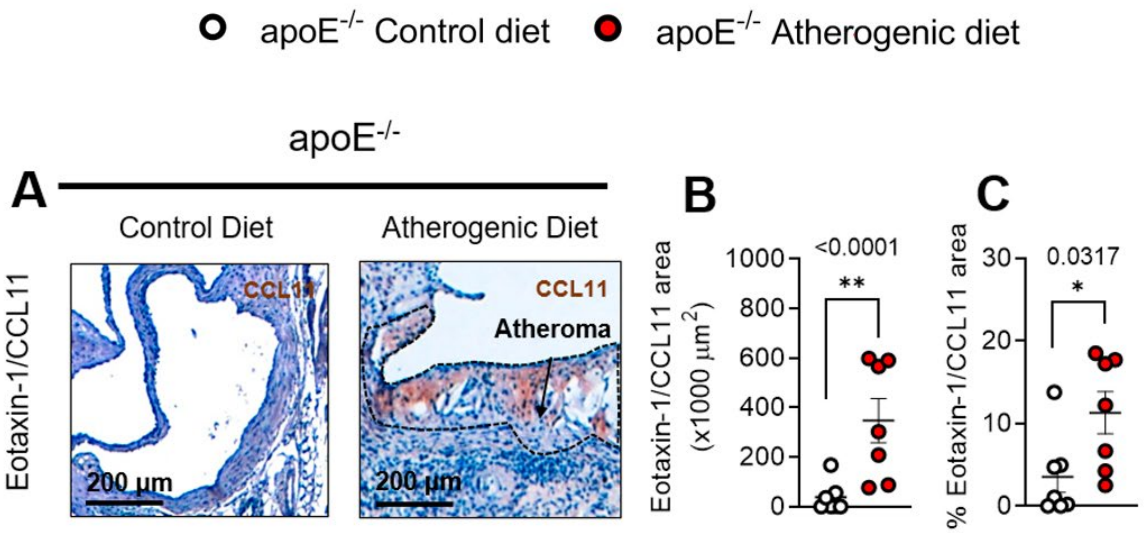

Figure 51. Two months with a high-fat diet markedly increased the expression of CCL11/eotaxin-1 within the lesion.

Representative images of immunohistology (**A**), and the quantification of eotaxin-1/CCL11 expression (**B** and **C**). The discontinuous lines delineate the limits of the atherosclerotic lesion. Results are expressed as mm^2 of positive staining. Values are expressed as mean ± SEM (n=8 *apoE*$^{-/-}$ mice fed with a control diet, n=7 *apoE*$^{-/-}$ mice fed with an atherogenic diet). *P < 0.05 or **P < 0.01 relative to values in *apoE*$^{-/-}$ mice fed with a control diet.

Unexpectedly and using three different approaches, CCR3/SiglecF, CD125/SiglecF or CCR3/epoperoxidase (EPX) double staining, we detected for first time a clear eosinophil infiltration in the atheroma of *apoE*$^{-/-}$ animals in a hypercholesterolemic environment and the three detection approaches yield similar results (**Figures 52A - F**).

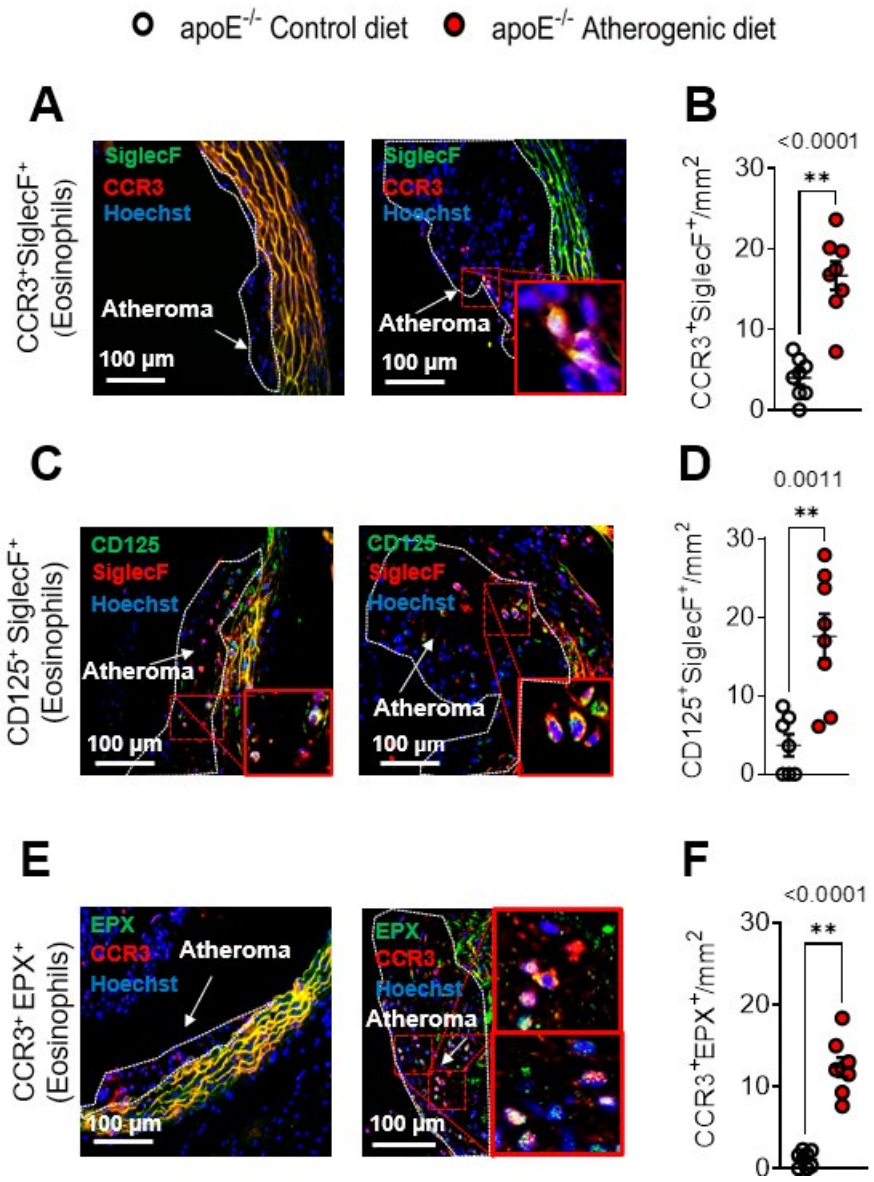

Figure 52. Two months with a high-fat diet markedly increased the eosinophil infiltration into the atherosclerotic plaque.

Representative images of immunohistology (**A, C** and **E**), and the quantification of eosinophils ($CCR3^+$/$SiglecF^+$, $CD125^+$/$SiglecF^+$ and $CCR3^+$/EPX^+ (**B, D** and **F**). The discontinuous lines delineate the limits of the atherosclerotic lesion. Results are expressed as mm^2 of positive populations. Values are expressed as mean ± SEM (n=8 *apoE*$^{-/-}$ mice fed with a control diet, n=8 *apoE*$^{-/-}$ mice fed with an atherogenic diet). **P < 0.01 relative to values in *apoE*$^{-/-}$ mice fed with a control diet.

In addition, while no eosinophils were detected in the subcutaneous fat, they were present in visceral fat, bone marrow or intestine (**Figures 53A - E**). However, no differences in the number of infiltrated eosinophils were encountered in these tissue/organs between animals subjected to control or hypercholesterolemic diet for 2 months (**Figures 53A - E**).

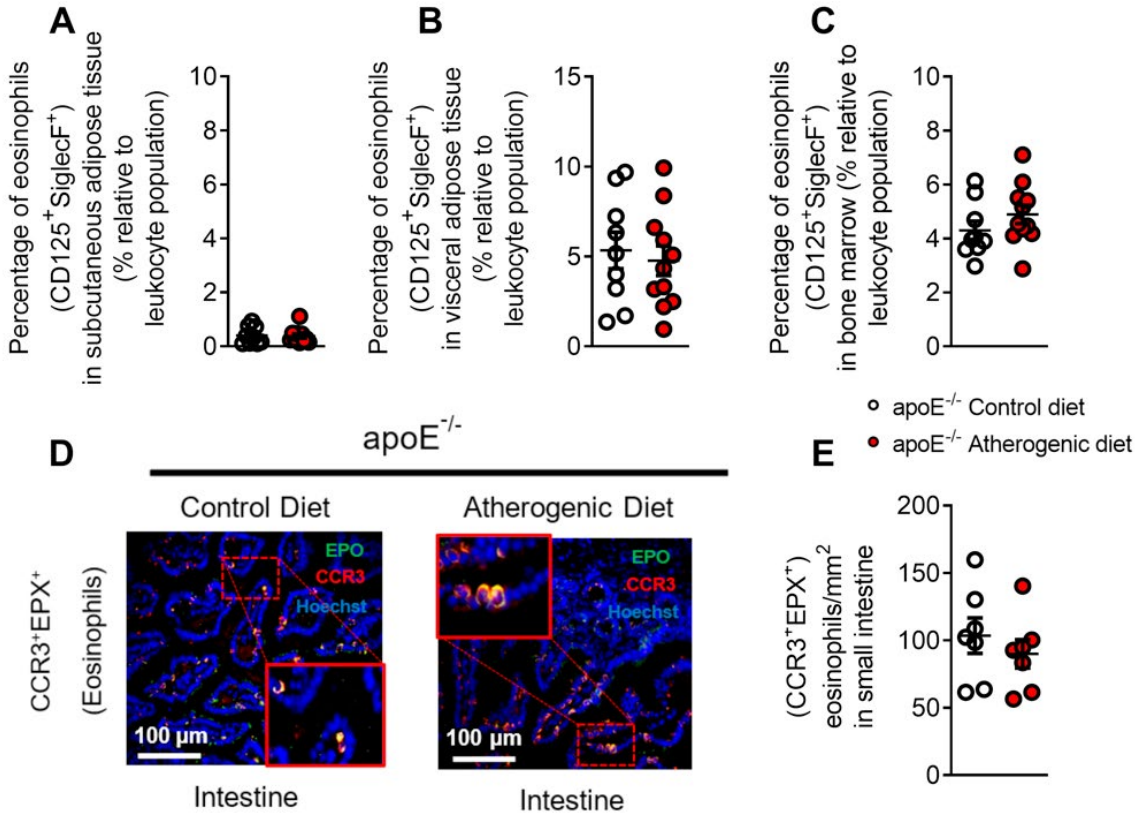

Figure 53. No significant differences were found in the eosinophil population present in the visceral adipose tissue, bone marrow or small intestine of apoE$^{-/-}$ mice fed or not with an atherogenic diet.

Percentage of eosinophils in subcutaneous adipose tissue (**A**), visceral adipose tissue (**B**), bone marrow (**C**) and intestine (**E**). Representative image of immunohistology (**D**). Results are expressed as mm^2 of positive populations. Values are expressed as mean ± SEM (n= 7-9 *apoE$^{-/-}$* mice fed with a control diet, n= 7-11 *apoE$^{-/-}$* mice fed with an atherogenic diet).

It is noteworthy that a population of CCR3$^-$/Ly6G$^+$/SiglecF$^+$ cells (neutrophils) was also encountered both in the circulation and the lesion of *apoE$^{-/-}$* animals subjected to an hypercholesterolemic diet (**Figures 54A - F**), indicating that not all SiglecF$^+$ cells are eosinophils.

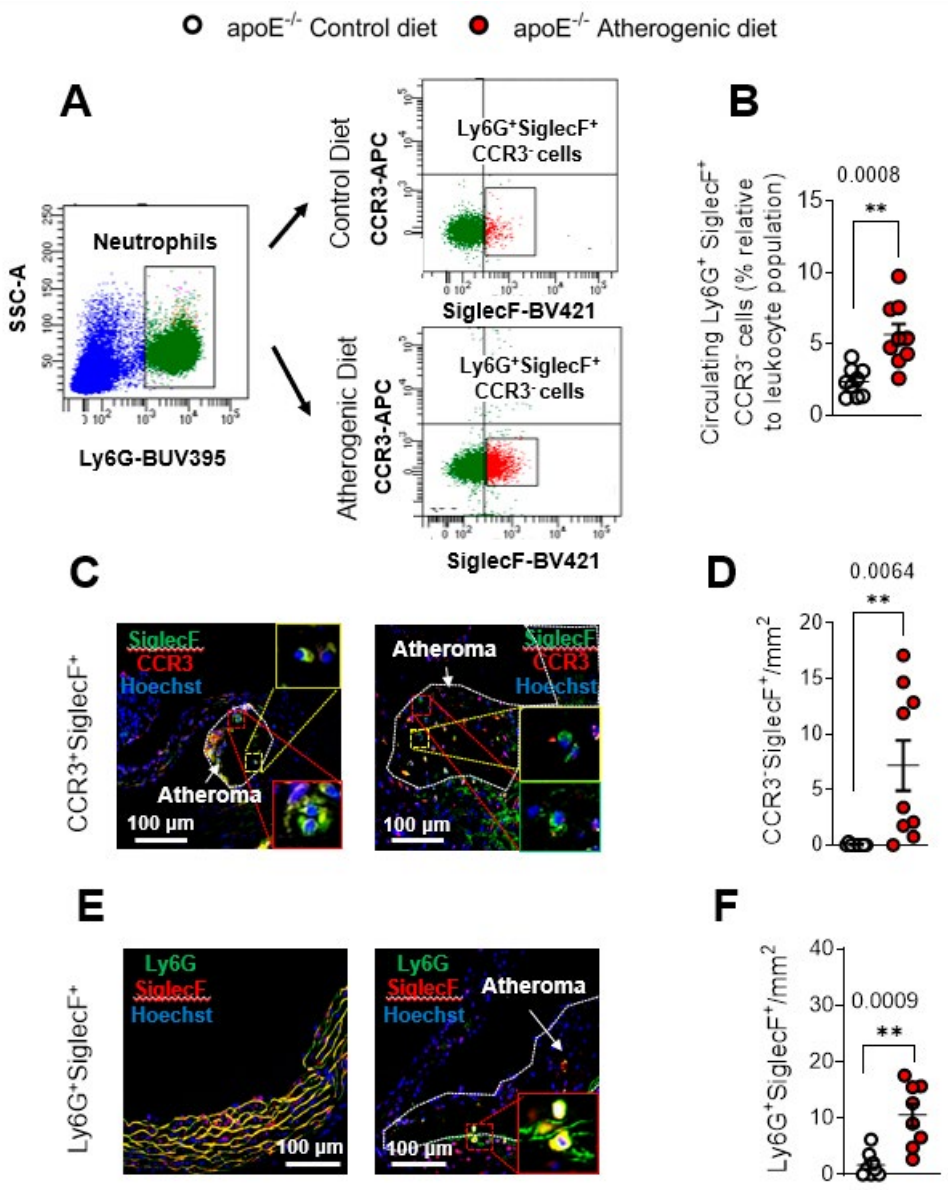

Figure 54. SiglecF⁺CCR3⁻ and SiglecF⁺Ly6G⁺ population was increased in peripheral blood and in atherosclerotic lesion.

Representative gating of flow cytometry (**A**), Ly6G⁺Siglec-F⁺CCR3⁻ cells in whole blood (**B**), CCR3⁻Siglec-F⁺ cells (**C** and **D**) and Ly6G⁺ Siglec-F⁺ cells (**E** and **F**) in the atherosclerotic lesion. Results are presented as percentage of total leukocytes (flow cytometry), mm^2 of positive populations (immunofluorescence)). Values are expressed as mean ± SEM (n=8 *apoE*$^{-/-}$ mice fed with a control diet, n=9 *apoE*$^{-/-}$ mice fed with an atherogenic diet). *P < 0.05 or **P < 0.01 relative to values in *apoE*$^{-/-}$ mice fed with a control diet.

Furthermore, plasma levels of IL-4 and IL-5 did not differ between groups regardless the diet administered (**Figures 55A** and **B**).

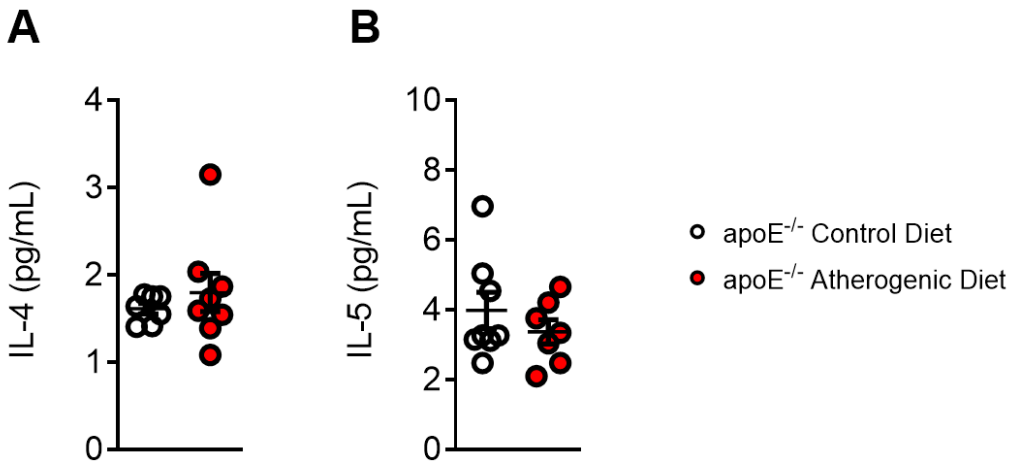

Figure 55. No differences were found in the plasma levels of eosinophil-related cytokines.

Plasma levels of IL-4 (**A**) and IL-5 (**B**) were measured by ELISA. Results are expressed as pg/mL. Values are expressed as mean ± SEM (n=8 *apoE*$^{-/-}$ mice fed with a control diet, n=8 *apoE*$^{-/-}$ mice fed with an atherogenic diet).

10.2.3. *Two-month high-fat diet led to an increased atherosclerotic lesion formation in apoE$^{-/-}$CCR3$^{-/-}$ animals with increased infiltration of macrophages and CD8^{+} lymphocytes compared to apoE$^{-/-}$CCR3$^{+/+}$ mice*

Since CCL11/CCR3 axis and eosinophil accumulation may play a role in atherosclerosis development, *apoE*$^{-/-}$ mice were crossbred with CCR3-deficient mice and *apoE*$^{-/-}$*CCR3*$^{+/+}$ and *apoE*$^{-/-}$*CCR3*$^{-/-}$ mice littermates were generated. Then, both mice genotypes were subjected to a high-fat or control diet for two months.

ApoE$^{-/-}$*CCR3*$^{+/+}$ and *apoE*$^{-/-}$*CCR3*$^{-/-}$ mice subjected to a control diet showed TC levels around 220 mg/dL. After two months with a high-fat diet, these levels significantly increased, reaching values close to 460 mg/dL (**Table 28**). A similar profile was found for plasma LDL, very low-density lipoprotein (VLDL) or TG (**Table 28**). HDL cholesterol levels decreased in both genotypes after two months of atherogenic diet (**Table 28**) but no differences were encountered between both phenotypes.

Table 28 – Biochemical parameters of apoE$^{-/-}$CCR3 animals

Parameters	*apoE*$^{-/-}$*CCR3*$^{+/+}$ Control diet	*apoE*$^{-/-}$*CCR3*$^{+/+}$ Atherogenic diet	*apoE*$^{-/-}$*CCR3*$^{-/-}$ Control diet	*apoE*$^{-/-}$*CCR3*$^{-/-}$ Atherogenic diet
Weight (g)	28.1 ± 0.5	29.4 ± 0.7	25.2 ± 0.5++	26.7 ± 0.4++
Glucose (mg/dL)	64.3 ± 4.6	97.2 ± 8.3*	79.3 ± 8.6	86.5 ± 5.4
TC (mg/dL)	214.5 ± 11.2	468.6 ± 23.7**	226.9 ± 19.9	466.3 ± 19.3**
Non-HDLc (mg/dL)	176.2 ± 14.3	445.1 ± 23.0**	188.0 ± 21.9	436.6 ± 19.3**
HDLc (mg/dL)	38.3 ± 5.2	24.9 ± 3.0*	38.8 ± 4.1	25.4 ± 1.8*
Ratio HDL/LDL	0.4 ± 0.1	0.1 ± 0.0*	0.3 ± 0.1	0.1 ± 0.0*
Ratio HDL/TC	0.2 ± 0.0	0.1 ± 0.0**	0.2 ± 0.0	0.1 ± 0.0**
Ratio TG/HDL	3.8 ± 0.6	12.5 ± 1.9**	3.8 ± 0.4	11.0 ± 1.2**
Triglycerides (mg/dL)	116.3 ± 8.8	236.1 ± 18.1**	131.9 ± 6.5	249.8 ± 19.3**

*TC, total cholesterol; HDLc, high-density lipoprotein-cholesterol; TG, triglycerides. Data are presented as mean ± SEM. *p <0.05 or **p<0.01 relative to values in the control group.*

Next, as found in *apoE*$^{-/-}$ mice, when *apoE*$^{-/-}$*CCR3*$^{+/+}$ or *apoE*$^{-/-}$*CCR3*$^{-/-}$ mice animals were subjected to an atherogenic diet, significant increases in eotaxin-1/CCL11 plasma levels were detected compared with the same animals fed with a control diet (**Figure 56A**). Similarly, when *apoE*$^{-/-}$*CCR3*$^{+/+}$ mice were fed with a high fat diet, increased percentages of circulating eosinophils, regardless the surface markers used for their identification (CCR3/Siglec-F or CD125/Siglec-F), were encountered compared with animals subjected to a control diet (**Figure 56B – D** and **Figure 57**). Surprisingly, no circulating eosinophils (CD125^{+}/Siglec-F^{+}) were detected in *apoE*$^{-/-}$*CCR3*$^{-/-}$ mice subjected or not to an atherogenic diet for two months (**Figures 56D** and **Figure 57**).

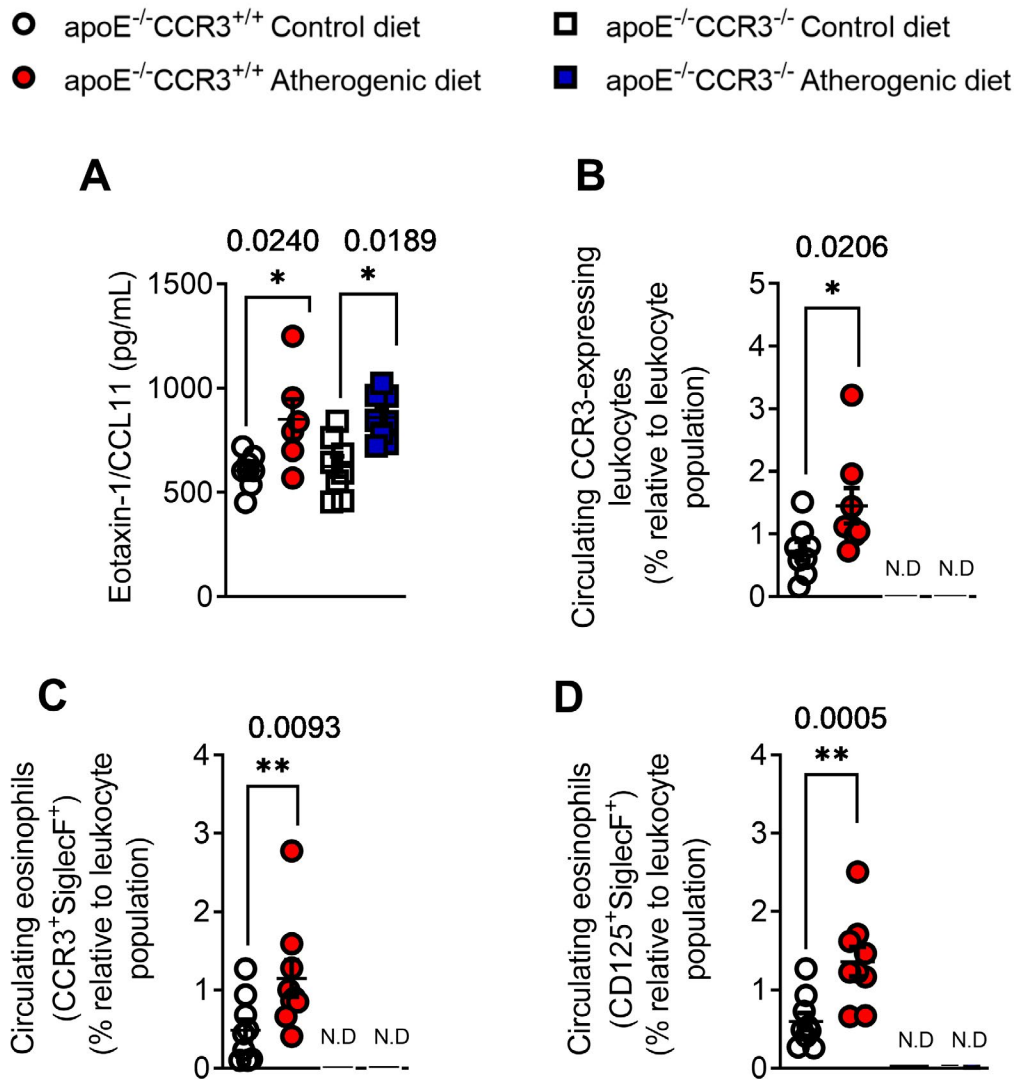

Figure 56. Increased plasma levels of eotaxin-1 (CCL11) and percentage of circulating eosinophils were detected apoE$^{-/-}$CCR3$^{+/+}$ fed with an atherogenic but no circulating eosinophils were found in apoE$^{-/-}$CCR3$^{-/-}$ mice fed with the same diet.

Plasma levels of eotaxin-1/CCL11 (**A**), percentage of circulating CCR3-expressing leukocytes (**B**), eosinophils (CD125^{+}SiglecF^{+} cells; **C** and **D**). Eotaxin-1/CCL11 plasma levels was measured by ELISA. Results are expressed as percentage of positive populations or pg/mL. Values are expressed as mean ± SEM (n=8 *apoE$^{-/-}$CCR3$^{+/+}$* mice fed with a control diet, n=8 *apoE$^{-/-}$CCR3$^{+/+}$* mice fed with an atherogenic diet; n=8 *apoE$^{-/-}$CCR3$^{-/-}$* mice fed with a control diet, n=8 *apoE$^{-/-}$CCR3$^{-/-}$* mice fed with an atherogenic diet). *P < 0.05 or **P < 0.01 relative to values in their respective genotype fed with a control diet. +p <0.05 or ++p <0.01 relative to values in *apoE$^{-/-}$CCR3$^{+/+}$* animals subjected to an atherogenic diet.

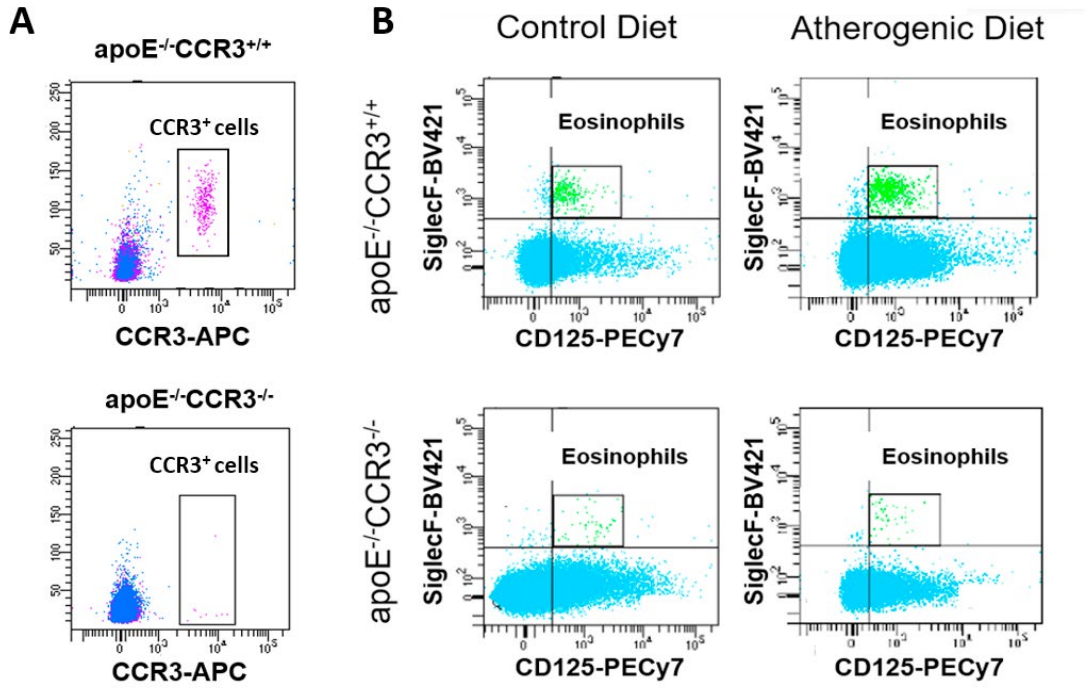

Figure 57. Representative images of flow cytometry in whole blood.

Representative dot plots confirming the absence of CCR3-expressing cells in *apoE*$^{-/-}$*CCR3*$^{-/-}$ (**A**). Representative gating of circulating eosinophils (CD125^{+}SiglecF^{+} cells) in both genotypes (**B**).

The analysis of the atheroma plaque revealed that although both genotypes showed increased lesion either in the aortic arch or in the thoracic aorta when they were fed with a fatty diet for two months, (**Figures 58A, C** and **D**), the lesion of *apoE*$^{-/-}$*CCR3*$^{-/-}$ animals was significantly greater than that developed in *apoE*$^{-/-}$*CCR3*$^{+/+}$ mice (**Figures 58A, C** and **D**). Likewise, the atherosclerotic lesion in the aortic sinus showed that *apoE*$^{-/-}$*CCR3*$^{+/+}$ and *apoE*$^{-/-}$*CCR3*$^{-/-}$ mice fed with an atherogenic diet had marked increases in both the intima/media ratio and the lesion area (**Figures 58B, E** and **F**). Again, either the intima/media ratio or the lesion area were clearly greater (45% and 26%, respectively) in *apoE*$^{-/-}$*CCR3*$^{-/-}$ mice fed with a high-fat diet than in *apoE*$^{-/-}$*CCR3*$^{+/+}$ mice mice equally fed but no differences were found between both genotypes when a control diet was administered for two months (**Figures 58B, E** and **F**).

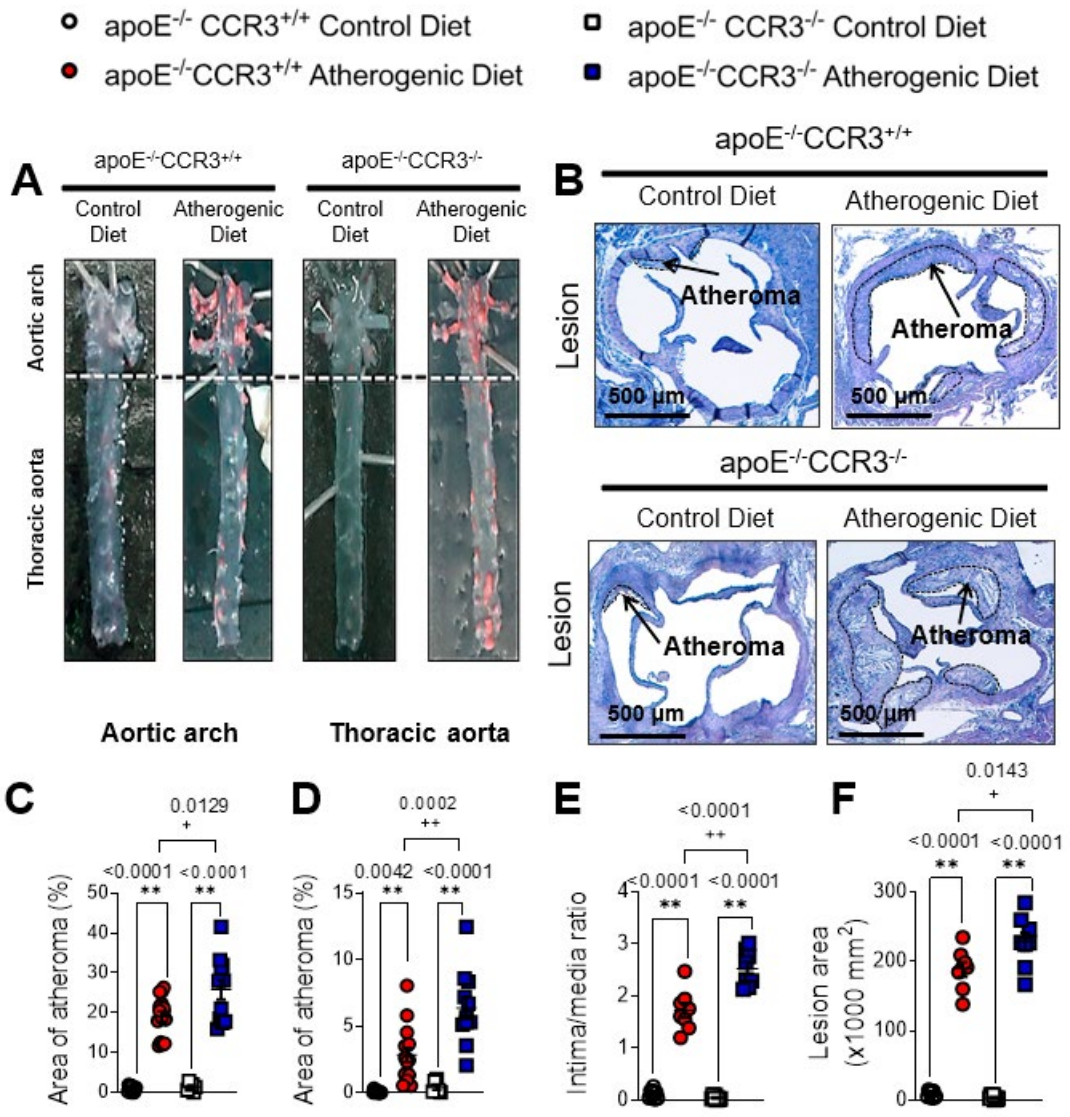

Figure 58. Two months with a high-fat diet markedly increased the atherosclerotic lesion formation in the aortic arch, thoracic aorta and the sigmoid aortic valves.

Representative images of Oil-Red stained aortas (**A**) and the atherosclerotic lesion in valves (**B**). Results of atheroma lesion in the aortic arch (**C**), in the thoracic aorta (**D**) and in the valves (**E** and **F**) are expressed as mean ± SEM (n=8 *apoE*$^{-/-}$*CCR3*$^{+/+}$ mice fed with a control diet, n=10 *apoE*$^{-/-}$*CCR3*$^{+/+}$ mice fed with an atherogenic diet; n=8 *apoE*$^{-/-}$*CCR3*$^{-/-}$ mice fed with a control diet, n=10 *apoE*$^{-/-}$*CCR3*$^{-/-}$ mice fed with an atherogenic diet). **P < 0.01 relative to values in their respective genotype fed with a control diet. +p <0.05 or ++p <0.01 relative to values in *apoE*$^{-/-}$*CCR3*$^{+/+}$ animals subjected to an atherogenic diet.

The unexpected enlargement of the atherosclerotic lesion in *apoE*$^{-/-}$*CCR3*$^{-/-}$ mice fed with a high-fat diet compared to *apoE*$^{-/-}$*CCR3*$^{+/+}$ animals under the same diet, led us to characterize the leukocyte subsets infiltrated into the atherosclerotic lesion of both genotypes.

Both, the number of infiltrated macrophages (Mac-3^{+} cells) and CD8^{+} T lymphocytes was significantly higher in *apoE*$^{-/-}$*CCR3*$^{-/-}$ mice fed with an atherogenic diet than in *apoE*$^{-/-}$*CCR3*$^{+/+}$ animals fed under the same

conditions (**Figures 59A, B, E and F**) while the numbers of $CD4^+$ T lymphocytes was not affected (**Figures 59C** and **D**).

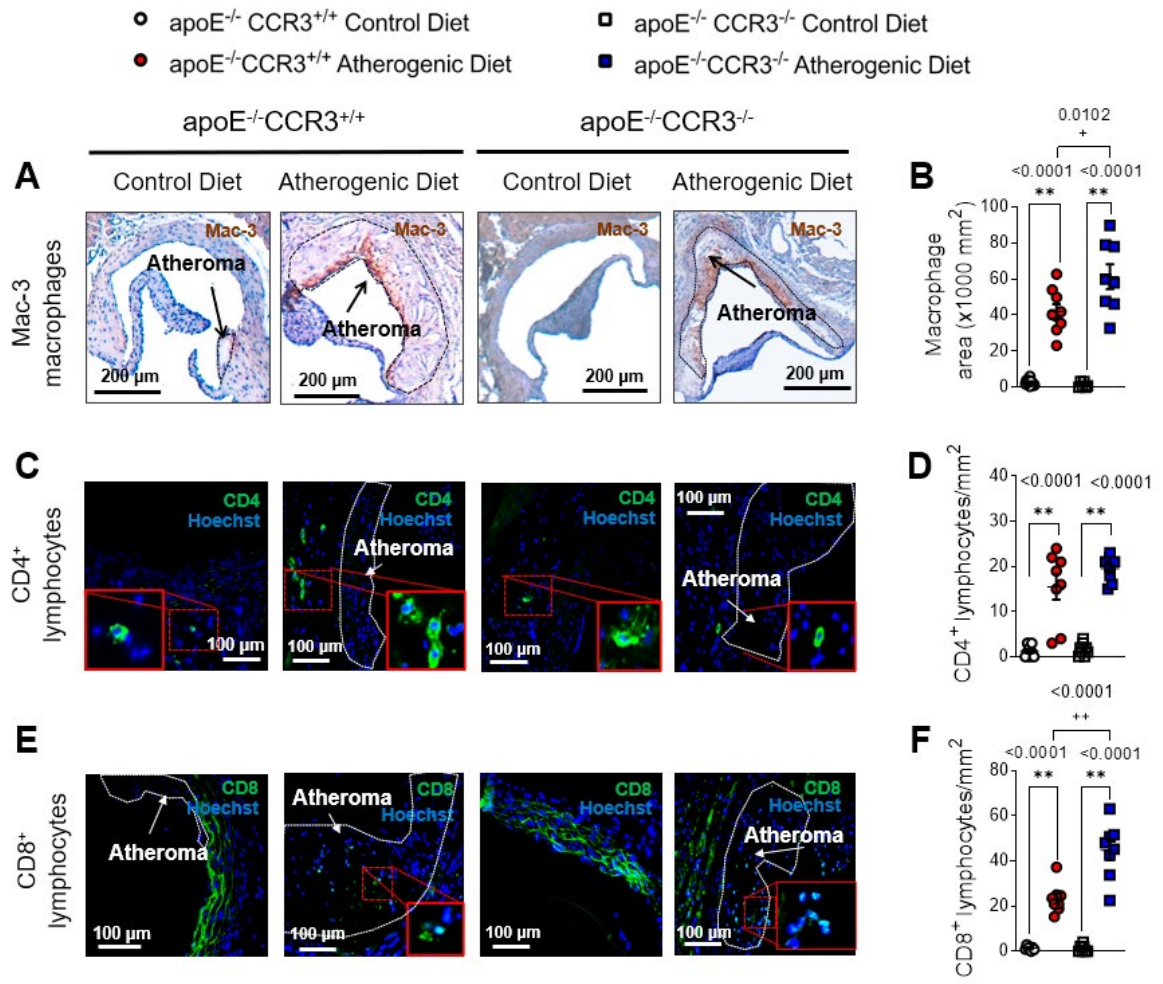

Figure 59. Two months with a high-fat diet markedly increased inflammatory infiltrates in $apoE^{-/-}CCR3^{-/-}$ animals compared with $apoE^{-/-}CCR3^{+/+}$ mice fed with the same diet.

Representative images of macrophages (**A**), $CD4^+$ lymphocytes (**C**) and $CD8^+$ lymphocytes (**E**). Results are presented as macrophage area (**B**), $CD4^+$ (**D**) or $CD8^+$ (**F**) cells/mm^2. Values are expressed as mean ± SEM (n=8 *apoE*$^{-/-}$*CCR3*$^{+/+}$ mice fed with a control diet, n=8 *apoE*$^{-/-}$*CCR3*$^{+/+}$ mice fed with an atherogenic diet; n=8 *apoE*$^{-/-}$*CCR3*$^{-/-}$ mice fed with a control diet, n=8 *apoE*$^{-/-}$*CCR3*$^{-/-}$ mice fed with an atherogenic diet). *P < 0.05 or **P < 0.01 relative to values in their respective genotype fed with a control diet. +p <0.05 or ++p <0.01 relative to values in *apoE*$^{-/-}$*CCR3*$^{+/+}$ animals subjected to an atherogenic diet.

Similarly, a significant increase in the collagen content was observed in the atherosclerotic lesion from *apoE*$^{-/-}$*CCR3*$^{-/-}$ mice compared to *apoE*$^{-/-}$*CCR3*$^{+/+}$ mice fed an atherogenic diet (**Figures 60A** and **C**). However, the necrotic core area and smooth muscle cell (SMC) infiltration were not affected by the genotype (**Figures 60A, B, D** and **E**).

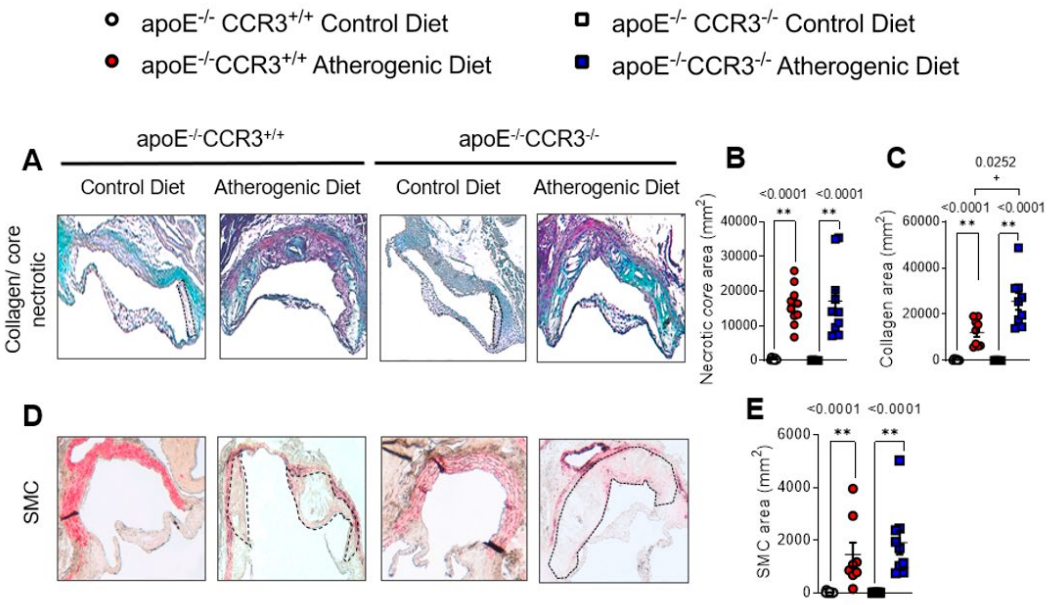

Figure 60. Two months with a high-fat diet markedly increased the synthesis of collagen fibers in apoE$^{-/-}$CCR3$^{-/-}$ animals compared with apoE$^{-/-}$CCR3$^{+/+}$ mice fed with the same diet.

Representative images of Masson stained (**A**) and α-actin immunohistochemistry (**D**). Quantification of necrotic area (**B**), collagen area (**C**) and SMC area (**E**). Results are expressed as mean ± SEM (n=8 *apoE$^{-/-}$CCR3$^{+/+}$* mice fed with a control diet, n=10 *apoE$^{-/-}$CCR3$^{+/+}$* mice fed with an atherogenic diet; n=8 *apoE$^{-/-}$CCR3$^{-/-}$* mice fed with a control diet, n=10 *apoE$^{-/-}$CCR3$^{-/-}$* mice fed with an atherogenic diet).**P < 0.01 relative to values in their respective genotype fed with a control diet. +p <0.05 relative to values in *apoE$^{-/-}$CCR3$^{+/+}$* animals subjected to an atherogenic diet.

In addition, an increase in the total percentage of circulating monocytes was observed in those animals subjected to an atherogenic diet but the percentage of CCR2^{+} circulating monocytes was significantly greater in *apoE$^{-/-}$CCR3$^{-/-}$* mice than in *apoE$^{-/-}$CCR3$^{+/+}$* animals (**Figures 61A - C**). Conversely, no differences between genotypes were detected in the percentage of CD4^{+} and CD8^{+} circulating lymphocytes under a control diet but were significantly reduced when the animals were subjected to a hypercholesterolemic diet (**Figures 61D** and **E**).

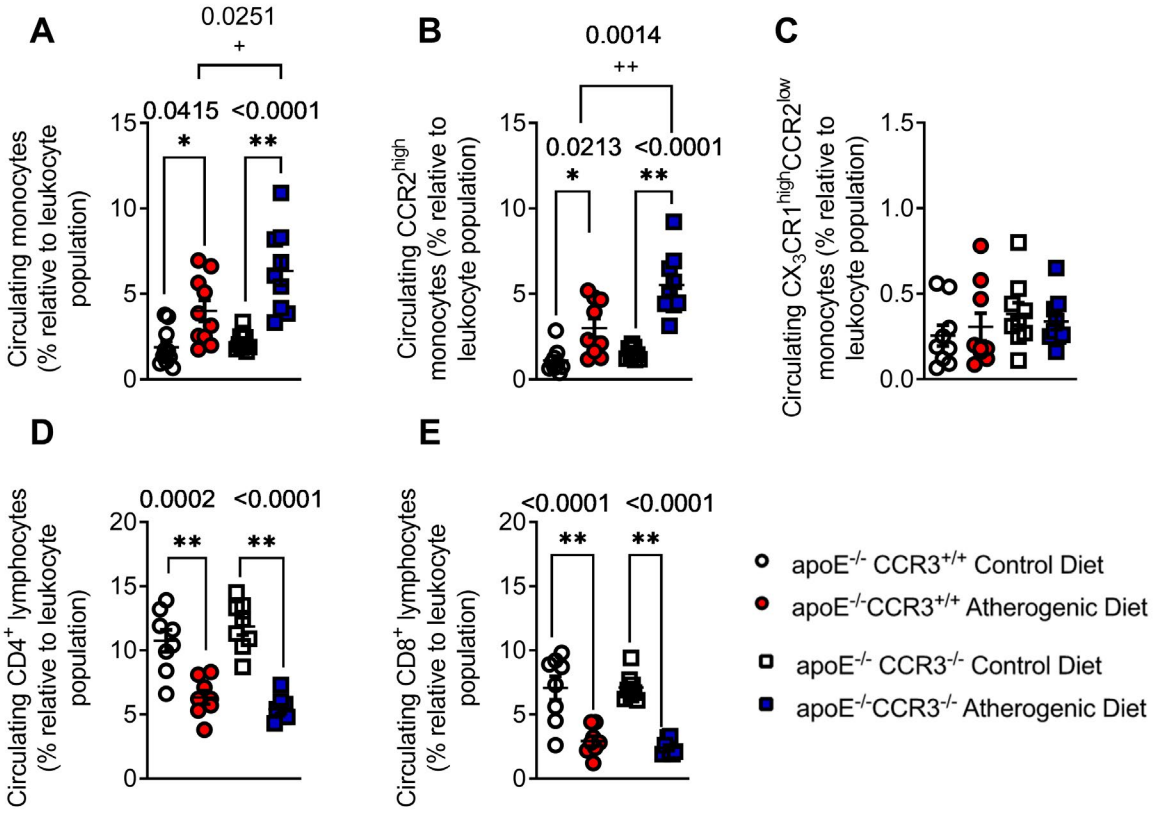

Figure 61. The percentage of monocytes in peripheral blood were increased in apoE$^{-/-}$CCR3$^{-/-}$ mice fed with an atherogenic diet compared with apoE$^{-/-}$CCR3$^{+/+}$ fed with the same diet.

Percentage of total monocytes (**A**), pro-inflammatory monocytes (**B**), patrolling monocytes (**C**), CD4^{+} lymphocytes (**D**) and CD8^{+} lymphocytes (**E**). Results are presented as percentage of positive populations. Values are expressed as mean ± SEM (n=9 *apoE$^{-/-}$CCR3$^{+/+}$* mice fed with a control diet, n=10 *apoE$^{-/-}$CCR3$^{+/+}$* mice fed with an atherogenic diet; n=9 *apoE$^{-/-}$CCR3$^{-/-}$* mice fed with a control diet, n=10 *apoE$^{-/-}$CCR3$^{-/-}$* mice fed with an atherogenic diet). *P < 0.05 or **P < 0.01 relative to values in their respective genotype fed with a control diet. +p <0.05 or ++p <0.01 relative to values in *apoE$^{-/-}$CCR3$^{+/+}$* animals subjected to an atherogenic diet.

10.2.4. *After two-month of high-fat diet, apoE$^{-/-}$CCR3$^{-/-}$ animals had decreased eotaxin-1/CCL11 expression and no eosinophil infiltration in the atherosclerotic lesion*

To try to understand the role of eotaxin-1/CCL11 and eosinophils in the atherosclerotic lesion formation, we next found that while in the atheroma of *apoE$^{-/-}$CCR3$^{+/+}$* mice fed with the hypercholesterolemic diet, a significant enhanced staining for eotaxin-1/CCL11 (**Figures 62A - C**) was detected, no significant expression of the chemokine was found neither in animals fed with a control diet nor in *apoE$^{-/-}$CCR3$^{-/-}$* animals fed with the atherogenic diet (**Figures 62A - C**).

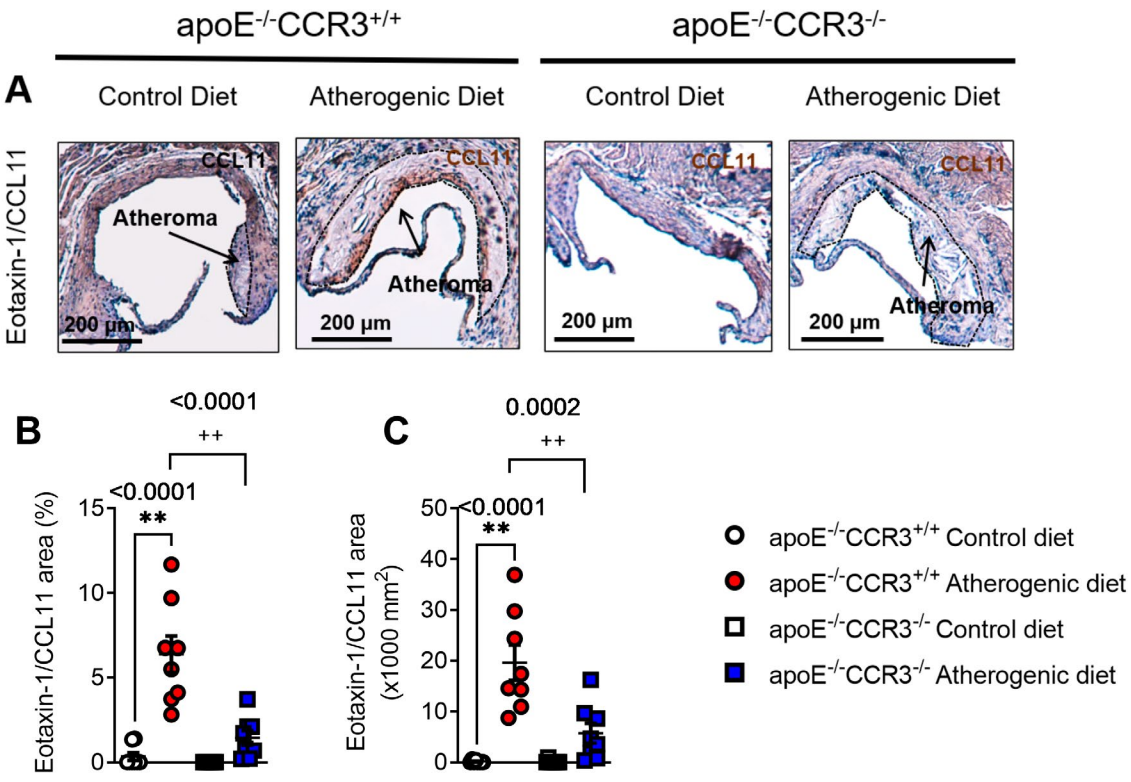

Figure 62. Two months with a high-fat diet markedly increased the expression of CCL11/eotaxin-1 in apoE$^{-/-}$CCR3$^{+/+}$, but not in apoE$^{-/-}$CCR3$^{-/-}$ animals.

Representative images of immunohistology (**A**), and the quantification of eotaxin-1/CCL11 expression (**B** and **C**). The discontinuous lines delineate the limits of the atherosclerotic lesion. Results are presented as mm^2 of positive populations. Values are expressed as mean ± SEM (n=8 *apoE$^{-/-}$CCR3$^{+/+}$* mice fed with a control diet, n=8 *apoE$^{-/-}$CCR3$^{+/+}$* mice fed with an atherogenic diet; n=8 *apoE$^{-/-}$CCR3$^{-/-}$* mice fed with a control diet, n=8 *apoE$^{-/-}$CCR3$^{-/-}$* mice fed with an atherogenic diet). **P < 0.01 relative to values in their respective genotype fed with a control diet. ++p <0.01 relative to values in *apoE$^{-/-}$CCR3$^{+/+}$* animals subjected to an atherogenic diet.

More relevant, while a significant increase of eosinophil infiltration (CCR3$^+$/SiglecF$^+$, CD125$^+$/ SiglecF$^+$ or CCR3$^+$/EPX$^+$ cells) was observed in the atherosclerotic lesion of those *apoE$^{-/-}$CCR3$^{+/+}$* mice subjected to an atherogenic diet (**Figures 63A - F**), no eosinophils were encountered in the atheroma developed in *apoE$^{-/-}$CCR3$^{-/-}$* animals under the same diet regardless the immunofluorescence approach (**Figures 63A - F**).

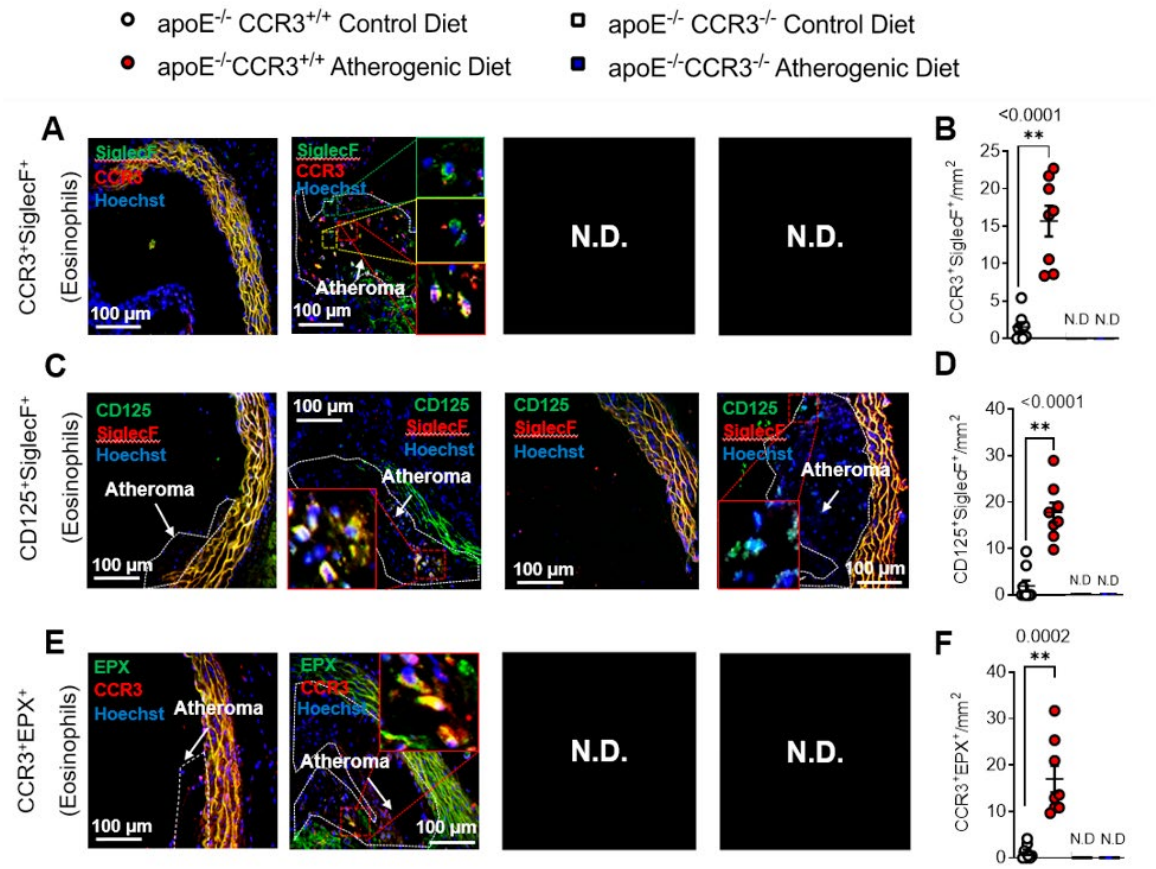

Figure 63. Two months with a high-fat diet markedly increased the infiltration of eosinophils in apoE$^{-/-}$ CCR3$^{+/+}$, but not in apoE$^{-/-}$CCR3$^{-/-}$ animals.

Representative images of immunohistology (**A, C** and **E**), and quantification of eosinophils (CCR3$^+$/SiglecF$^+$, CD125$^+$/SiglecF$^+$ and CCR3$^+$/EPX$^+$ (**B, D** and **F**). The discontinuous lines delineate the limits of the atherosclerotic lesion. Results are presented as mm^2 of positive populations. Values are expressed as mean ± SEM (n=8 *apoE$^{-/-}$CCR3$^{+/+}$* mice fed with a control diet, n=8 *apoE$^{-/-}$CCR3$^{+/+}$* mice fed with an atherogenic diet; n=8 *apoE$^{-/-}$CCR3$^{-/-}$* mice fed with a control diet, n=8 *apoE$^{-/-}$CCR3$^{-/-}$* mice fed with an atherogenic diet). **P < 0.01 relative to values in their respective genotype fed with a control diet.

Since eosinophils can release IL-4 (D. Wu et al., 2011) and IL-4 provokes the generation of eotaxin-1/CCL11 (Sanz et al., 1998), the expression of IL-4 was investigated in the lesion of both genotypes. While no expression of IL-4 was identified in the atheroma of animals subjected to a control diet (**Figures 64A** and **B**), significant expression of IL-4 was detected in *apoE$^{-/-}$CCR3$^{+/+}$* mice when they were exposed to an atherogenic diet for 2 months (**Figures 64A** and **B**) but barely no expression of the cytokine was found in the lesion of *apoE$^{-/-}$CCR3$^{-/-}$* animals similarly fed (**Figures 64A** and **B)**.

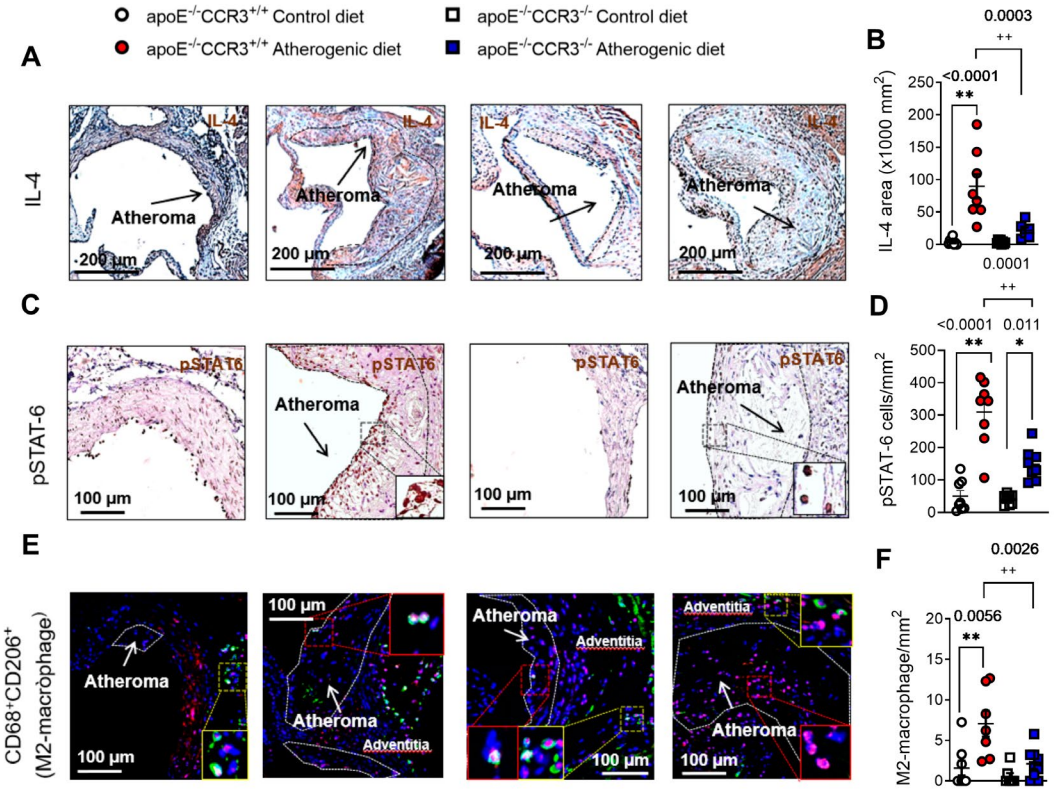

Figure 64. Two months with a high-fat diet markedly increased the expression of IL-4, the activation of STAT-6 and the infiltration of M2-macrophage in apoE$^{-/-}$CCR3$^{+/+}$ animals fed with an atherogenic diet but it was barely or no detected in apoE$^{-/-}$CCR3$^{-/-}$ mice fed with the same diet.

Representative images of IL-4 (**A**) and pSTAT-6 immunohistochemistry (**C**) as well as M2-like macrophage infiltration (**E**). Quantification of IL-4 area (**B**), pSTAT-6 cells (**D**) and M2-macrophages (**F**). Results are expressed as mean ± SEM (n=8 *apoE$^{-/-}$CCR3$^{+/+}$* mice fed with a control diet, n=8 *apoE$^{-/-}$CCR3$^{+/+}$* mice fed with an atherogenic diet; n=8 *apoE$^{-/-}$CCR3$^{-/-}$* mice fed with a control diet, n=8 *apoE$^{-/-}$CCR3$^{-/-}$* mice fed with an atherogenic diet). *P < 0.05 or **P < 0.01 relative to values in their respective genotype fed with a control diet, ++p <0.01 relative to values in *apoE$^{-/-}$CCR3$^{+/+}$* animals subjected to an atherogenic diet.

In this line and given that IL-4-induced eotaxin-1/CCL11 generation is mediated via signal transducer and activator of transcription 6 (STAT6)-dependent signaling (Heller et al., 2004), we found basal STAT6 phosphorylation in those animals under a control diet for 2 months (**Figures 64C** and **D**). In contrast, in an hypercholesterolemic environment, clear increase of STAT6 phosphorylation was detected in the lesion of *apoE$^{-/-}$CCR3$^{+/+}$* mice (**Figures 64C** and **D**) but a reduction of activation of this signalling pathway was encountered in *apoE$^{-/-}$CCR3$^{-/-}$* animals (**Figures 64C** and **D**)**.** Furthermore, the release of IL-4 additionally results in the polarization of macrophages from a proinflammatory M1-like phenotype to an anti-inflammatory M2-like phenotype albeit in adipose tissue, and this effect seems to be due to an eosinophil-mediated release of IL-4 (D. Wu et al., 2011). In regard to this, a significant increase in the number of anti-inflammatory M2-like macrophages was encountered in the atheroma of those *apoE$^{-/-}$CCR3$^{+/+}$* mice subjected to an atherogenic diet but not in those under a control diet (**Figures 64E** and **F**). Interestingly, in *apoE$^{-/-}$CCR3$^{-/-}$* animals the number of M2-like macrophages was markedly reduced in the lesion regardless the diet administered (**Figures 64E** and **F**).

Deeper analysis of both genotype littermates revealed that eosinophils were present in the visceral fat, bone marrow and intestine of animals but not in the subcutaneous fat of *apoE*$^{-/-}$*CCR3*$^{+/+}$ subjected or not to a high-fat diet without differences in their content (**Figures 65A** - **E**). In contrast, while eosinophils were not encountered in the visceral or the gut of *apoE*$^{-/-}$*CCR3*$^{-/-}$ mice (**Figures 65B, D** and **E**), higher eosinophil content was detected in the bone marrow of these animals than in control *apoE*$^{-/-}$*CCR3*$^{+/+}$ irrespective of the subjected diet (**Figures 65C**).

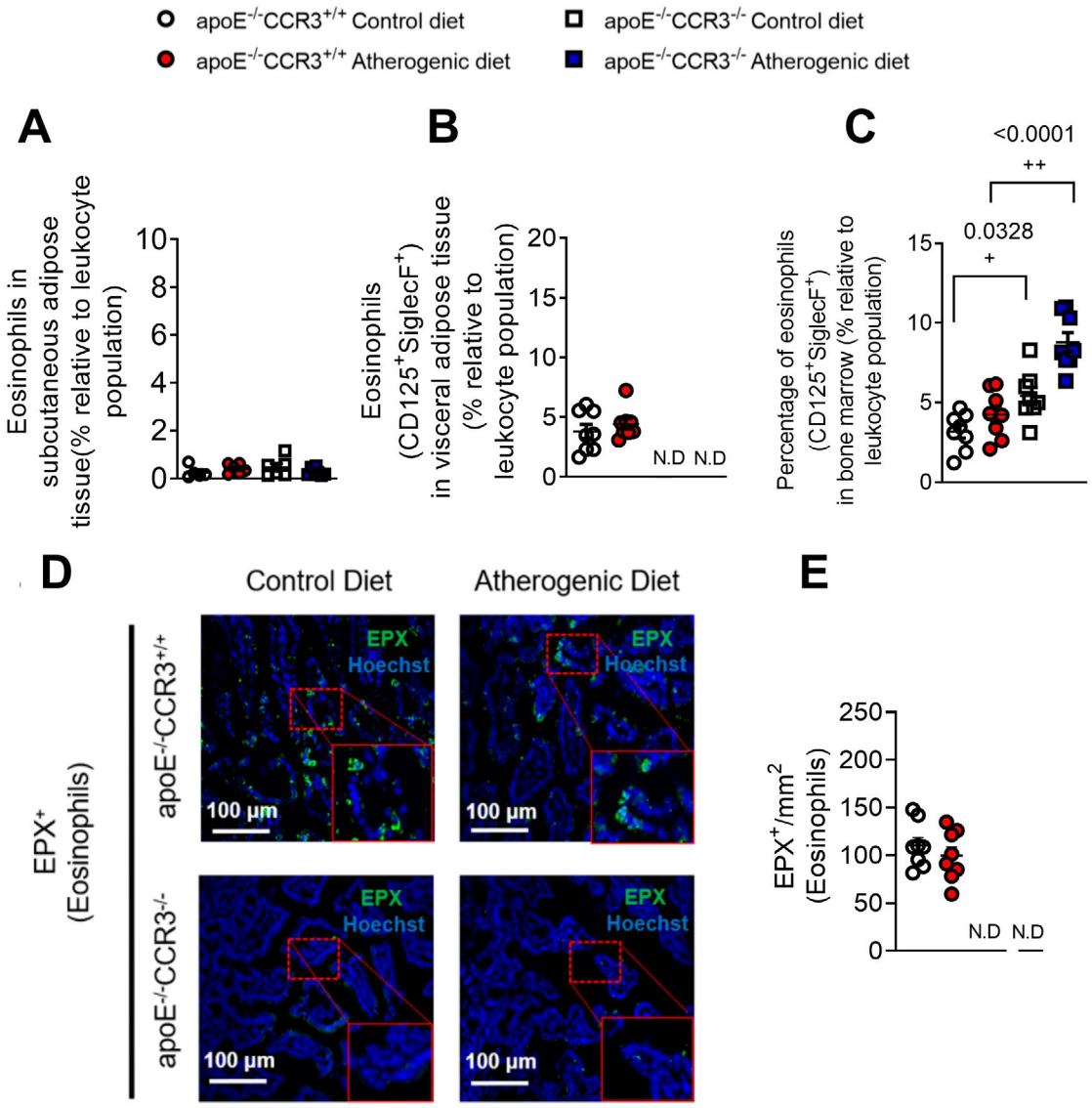

Figure 65. The percentage of eosinophils in bone marrow were increased in apoE$^{-/-}$CCR3$^{-/-}$ mice fed with an atherogenic diet compared with apoE$^{-/-}$CCR3$^{+/+}$ fed with the same diet.

Percentage of eosinophils in subcutaneous adipose tissue (**A**), visceral fat (**B**), bone marrow (**C**) and intestine (**E**). Representative image of immunohistology (**D**). Results are presented as mm^2 of positive populations. Results are expressed as mean ± SEM (n=8 *apoE*$^{-/-}$*CCR3*$^{+/+}$ mice fed with a control diet, n=8 *apoE*$^{-/-}$*CCR3*$^{+/+}$ mice fed with an atherogenic diet; n=8 *apoE*$^{-/-}$*CCR3*$^{-/-}$ mice fed with a control diet, n=8 *apoE*$^{-/-}$*CCR3*$^{-/-}$ mice fed with an atherogenic diet). +p <0.05 or ++p <0.01 relative to values in *apoE*$^{-/-}$*CCR3*$^{+/+}$ animals.

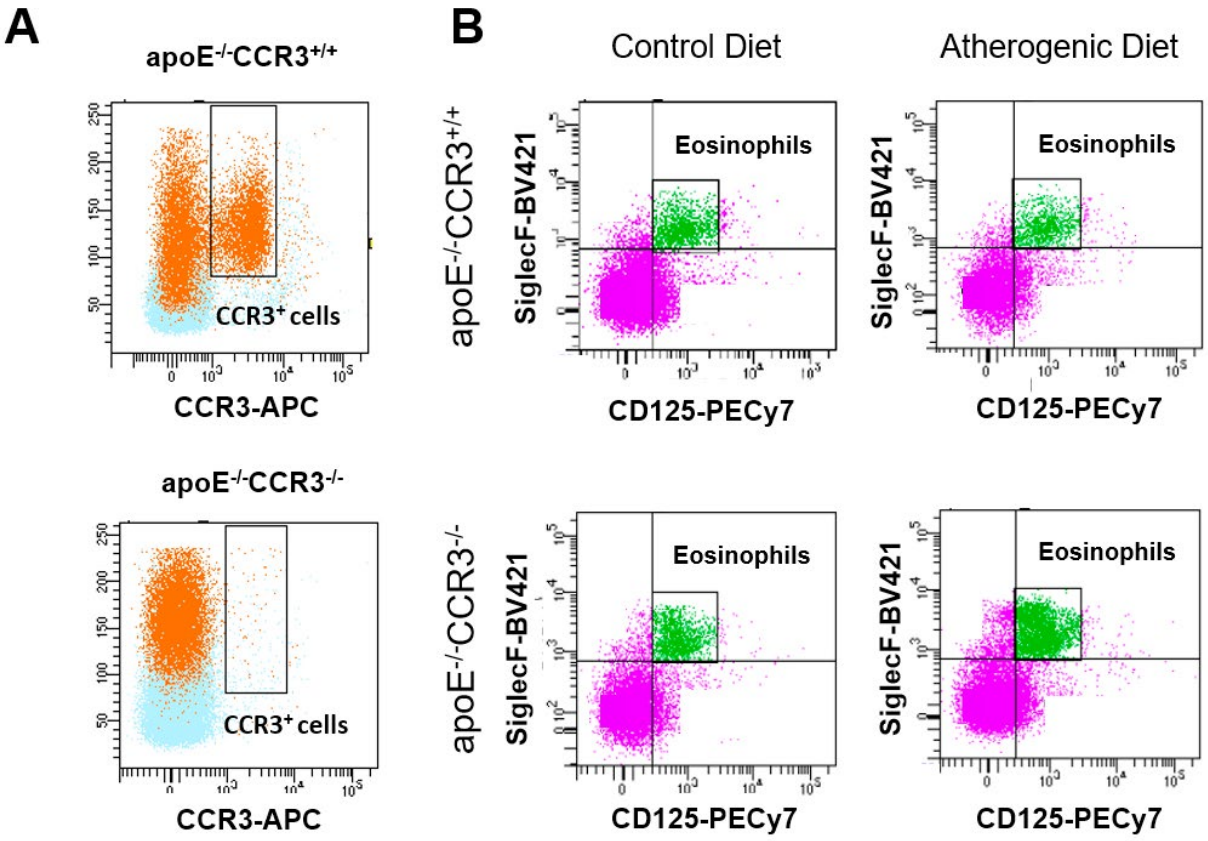

Figure 66. Representative images of flow cytometry in bone marrow.

Representative dot plot showing the absence of CCR3-expressing cells in *apoE$^{-/-}$CCR3$^{-/-}$* (**A**). Representative gating of circulating eosinophils (CD125^{+}Siglec-F^{+}) in both genotypes (**B**).

10.2.5. *Two months with a high-fat diet provoked greater atherosclerotic lesion formation in apoE$^{-/-}$ Ly5.1 mice transplanted with the bone marrow (BM) from apoE$^{-/-}$CCR3$^{-/-}$ animals than apoE$^{-/-}$CCR3$^{-/-}$ mice with bone marrow from apoE$^{-/-}$ Ly5.1 animals*

To confirm the results obtained, we generated BM chimeras by transferring whole BM from *apoE$^{-/-}$ Ly5.1* or *apoE$^{-/-}$CCR3$^{-/-}$* mice to whole-body irradiated *apoE$^{-/-}$ Ly5.1* or *apoE$^{-/-}$CCR3$^{-/-}$* mice. Recipient mice were irradiated with two 5.5Gy doses and blood was obtained to confirm their depletion (**Figure 67A** and **Table 29**).

Table 29 – Depletion of leukocytes

Group	Before irradiation	After irradiation
BM *apoE*$^{-/-}$ *Ly5.1*	11.79 ± 1.11	0.4 ± 0.07
BM *apoE*$^{-/-}$*CCR3*$^{-/-}$	7.90 ± 1.03	0.42 ± 0.1
Both genotypes	9.87 ± 0.88	0.41 ± 0.06

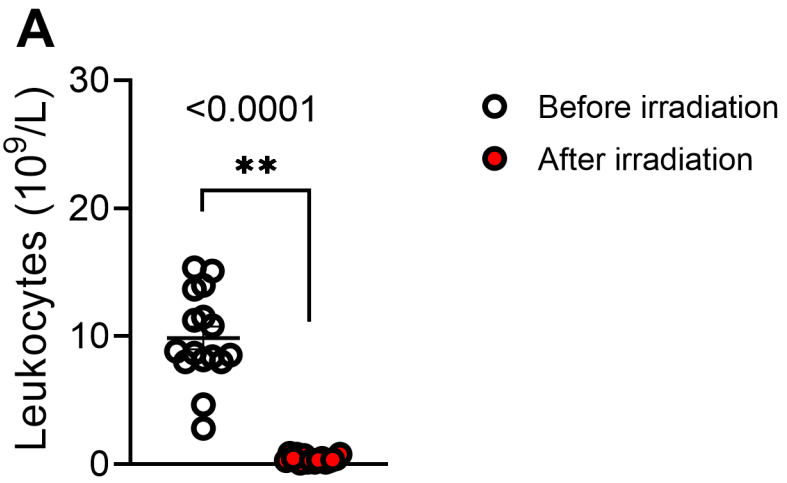

Figure 67. Leukocytes before and after irradiation.

Results are presented as number of leukocytes. Values are expressed as mean ± SEM (n=11 animals before irradiation, n=11 animals after irradiation). *P < 0.05 or **P < 0.01 relative to values in the group before irradiation.

Bone marrow (BM) was obtained from *apoE*$^{-/-}$ *Ly5.1* donor mice and transferred to irradiated *apoE*$^{-/-}$ *CCR3*$^{-/-}$ recipient mice. Similarly, BM was transplanted from *apoE*$^{-/-}$*CCR3*$^{-/-}$ mice to irradiated *apoE*$^{-/-}$ *Ly5.1* animals. After three weeks of recovery, confirmed by the hemocytometer, recipient mice were subjected to a control or an atherogenic diet for 2 months.

After two months of diet administration, a trend of increased atherosclerotic lesion formation was observed in both, the aortic arch and the thoracic aorta of those animals subjected to an atherogenic diet (**Figures 68A, B** and **C**). It seems that those animals transplanted with BM of *apoE*$^{-/-}$*CCR3*$^{-/-}$, presented greater lesion than thos transplanted with BM from *apoE*$^{-/-}$ Ly5.1. Nevertheless, we require to performe additional experiments to reach conclusive results.

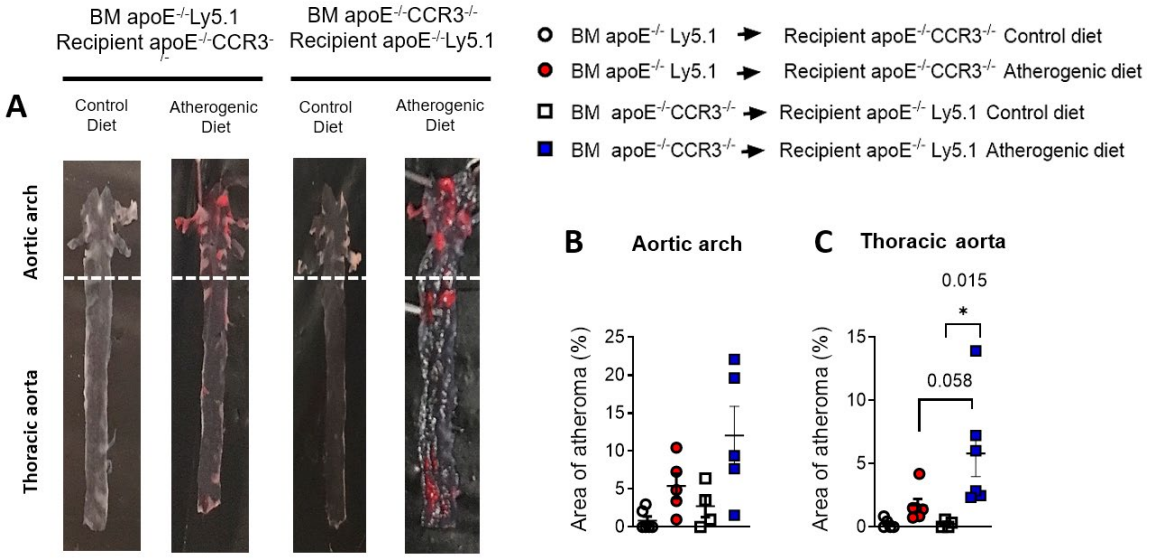

Figure 68. Two months with a high-fat diet markedly increased the atherosclerotic lesion formation in the aortic arch, and the thoracic aorta.

Representative images of Oil-Red stained aortas (**A**) Atheroma lesion in the aortic arch (**B**), and in the thoracic aorta (**C**) are expressed as mean ± SEM (n = 4-5 animals per group). *p <0.05 or **p <0.01 relative to values in animals subjected to a control diet.

10.2.6. *Two months with a high-fat diet markedly increased the circulating percentage of eosinophils in apoE$^{-/-}$CCR3$^{-/-}$ transplanted with the BM of apoE$^{-/-}$ Ly5.1 animals compared with apoE$^{-/-}$ Ly5.1 animals transplanted with the BM of apoE$^{-/-}$CCR3$^{-/-}$ mice*

After administration of an atherogenic diet or a control diet, *apoE$^{-/-}$Ly5.1* and *apoE$^{-/-}$CCR3$^{-/-}$* recipients were sacrificed and their peripheral blood was obtained. A tendency towards increased percentage of circulating CCR3-expressing leukocytes was observed in *apoE$^{-/-}$CCR3$^{-/-}$* mice transplanted with BM from *apoE$^{-/-}$Ly5.1.* In contrast, no circulating CCR3-expressing leukocytes were detected in the *apoE$^{-/-}$Ly5.1* mice transplanted with the BM from *apoE$^{-/-}$CCR3$^{-/-}$* animals (**Figure 69A** and **D**). Therefore suggesting that in absence of CCR3 receptors, eosinophils can not circulate and are retained in the BM of the recipient animal (**Figures 69B, C** and **E**).

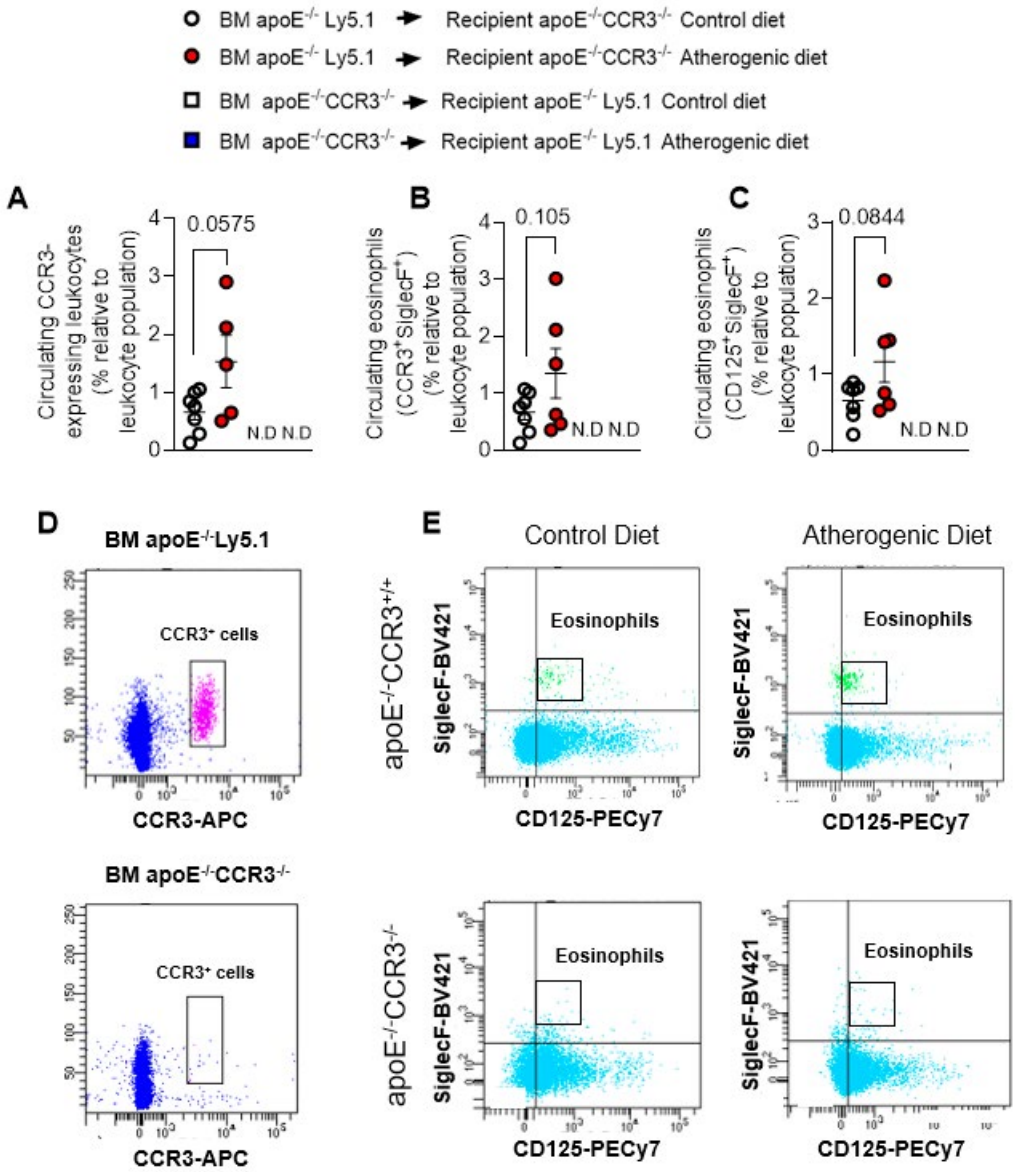

Figure 69. After two months with a high-fat diet, circulating eosinophils were not detected in the peripheral blood of apoE$^{-/-}$ Ly5.1 mice transplanted with the BM of apoE$^{-/-}$CCR3$^{-/-}$ animals.

The percentage of CCR3-expressing leukocytes (**A**) and eosinophils (CCR3^{+}SiglecF^{+} or CD125^{+}SiglecF^{+}; **B** and **C**)**.** Representative dot plots of *apoE$^{-/-}$Ly5.1* mice transplanted with BM of *apoE$^{-/-}$CCR3$^{-/-}$* animals and *apoE$^{-/-}$CCR3$^{-/-}$* mice transplanted with BM of *apoE$^{-/-}$Ly5.1* animals (**D**). Representative gating of circulating eosinophils (CCR3^{+}SiglecF^{+} or CD125^{+}SiglecF^{+}) in both genotypes (**E**). Results are presented as percentage of positive populations. Values are expressed as mean ± SEM (n=4-6 per group).

10.2.7. *The percentage of eosinophils was higher in the BM of apoE$^{-/-}$ Ly5.1 transplanted with the BM of apoE$^{-/-}$CCR3$^{-/-}$ donors than apoE$^{-/-}$CCR3$^{-/-}$ animals transplanted with BM from apoE$^{-/-}$ Ly5.1 donors regardless the diet*

Similarly, the bone marrow of all recipients was analyzed and a greater percentage of eosinophils was observed in the BM of *apoE$^{-/-}$Ly5.1* mice transplanted with BM from *apoE$^{-/-}$CCR3$^{-/-}$* animals (**Figure 70C**) than in *apoE$^{-/-}$CCR3$^{-/-}$* mice transplanted with BM from *apoE$^{-/-}$Ly5.1* animals. As previously indicated, additional experiments are required to reach conclusive results.

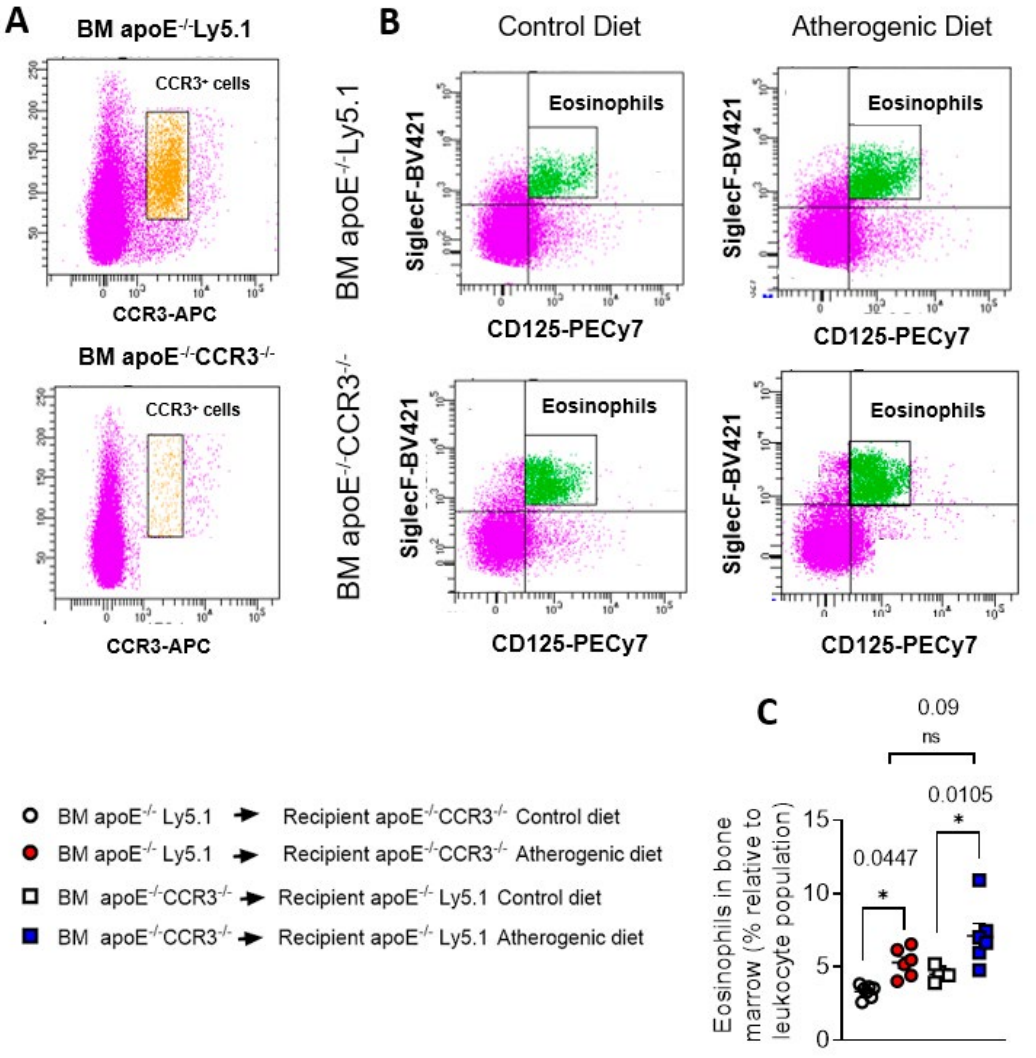

Figure 70. After two months with a high-fat diet, greater percentage of BM eosinophils were detected in apoE$^{-/-}$ Ly5.1 mice transplanted with the BM of apoE$^{-/-}$CCR3$^{-/-}$ animals than in apoE$^{-/-}$CCR3$^{-/-}$ mice transplanted with the BM from apoE$^{-/-}$ Ly5.1 animals.

Representative dot plots of *apoE$^{-/-}$Ly5.1* mice transplanted with BM of *apoE$^{-/-}$CCR3$^{-/-}$* animals and *apoE$^{-/-}$CCR3$^{-/-}$* mice transplanted with BM of *apoE$^{-/-}$Ly5.1* animals (**A**). Representative gating of BM eosinophils (CCR3^{+}SiglecF^{+} or CD125^{+}SiglecF^{+}) in both genotypes (**B**). Results are presented as percentage of positive populations (**C**). Values are expressed as mean ± SEM (n=4-6 per group). *P < 0.05 relative to values in their control-diet group.

DISCUSSION

11. STUDY OF SYSTEMIC INFLAMMATION IN PATIENTS WITH PH

PH is associated with risk of developing arteriosclerosis and the likelihood of future serious ischemic events. Previous studies have provided evidence of low systemic inflammation in patients with hypercholesterolemia (Chironi et al., 2006; Cortes et al., 2016; Hansen et al., 2019; Holven et al., 2014; Real et al., 2010; Sampietro et al., 1997). Here, we carried out a detailed characterization of different immune players and soluble inflammatory markers in PH and correlated these data with the circulating levels of key lipid components. The enhanced inflammatory status of PH reported herein has functional consequences, as illustrated for circulating platelet-bound leukocytes, which have increased adhesiveness to dysfunctional arterial endothelium, a prominent feature of the atherogenic process.

Platelet activation is known to be associated with atherogenesis and cardiovascular morbidity (von Hundelshausen & Schmitt, 2014). Indeed, upon their activation, platelets express specific cell adhesion molecules such as P-selectin, and release several inflammatory chemokines including PF-4/CXCL4 or RANTES/CCL5 (von Hundelshausen & Schmitt, 2014). We show that patients with PH present a pro-thrombotic state characterized by increased platelet activation (P-selectin^{+} and PAC-1^{+} platelets). While hypercholesterolemia has been previously associated with platelet activation (Barale et al., 2018; Chironi et al., 2006), we found that patients have both increased circulating levels of sP-selectin and PF-4/CXCL4, which are involved in multiple atherogenic processes. Indeed, different platelet surface molecules such as GPIIb/IIIa (recognized by PAC-1) or P-selectin are critically involved in the interaction of platelets to endothelial cells and leukocytes (von Hundelshausen & Schmitt, 2014), all of which are central for atherosclerotic lesion formation.

To gain insight into the immune state of the hypercholesterolemic environment of PH, we examined different leukocyte subtypes. An increase in leukocyte activation *in vitro* has been reported in subjects at high cardiovascular risk (hyperlipidemia) (Mazor et al., 2008). In our study, whereas no differences in the percentage of circulating neutrophils were detected between patients and controls, a clear increase in the percentage of activated cells (CD69^{+}) was observed, suggesting the existence of a proatherogenic state. This is consistent with our finding of increased circulating levels of CXCL8, which is involved in neutrophil activation, in the PH group, as has been reported previously, albeit in patients with FH patients (Cortes et al., 2016). Also, the plasma concentrations of this chemokine positively correlated with the circulating levels of key lipids in PH, apoB, LDL and TC. Overall, these results indicate that IL-8 might have utility as biomarker of atherosclerotic risk in PH.

Human monocytes are a heterogeneous cell population that are commonly classified into three subtypes: classical $CD14^+CD16^-CCR2^+$ (Mon 1), intermediate $CD14^+CD16^+CCR2^+$ (Mon 2), and nonclassical $CD14^+CD16^+CCR2^-$ (Mon 3) (C. Weber et al., 2016). There is evidence to support that adults with FH have a pro-inflammatory imbalance in circulating monocyte subpopulations (Mon 1) (Fadini et al., 2014), although another study indicated that the levels of Mon 2 and/or Mon 3 subtypes were increased in hyperlipidemia and associated with atherosclerosis development (H. Wu & Ballantyne, 2017). We found that only the percentage of the nonclassical/Mon 3 subtype was increased in patients over controls, and this positively correlated with the circulating levels of apoB, LDL and TC. By contrast, Mon 1 and Mon 2 subtypes, both of which express the CCR2 receptor, were significantly activated in patients. We also show for the first time an increase in the percentage of fractalkine/CX_3CL1 receptor (CX_3CR1) expression on Mon 1 monocytes in heparinized whole blood, and on all monocyte subsets when platelets were dissociated. In line with these observation, studies of atherosclerosis in mice suggest that both inflammatory (similar to human Mon 1) and patrolling (similar to human Mon 3) monocytes are involved in disease progression (Kratofil et al., 2017). In humans, different studies have noted increases in circulating $CD16^+$ monocytes in cardiovascular disease (Kratofil et al., 2017), which are possibly linked to disease outcome (Urra et al., 2009). There is also evidence to support that mobilized classical monocytes from the bone marrow mature into nonclassical monocytes through an intermediate subset. How these different monocyte subtypes correlate with disease pathogenesis and clinical outcomes in PH is, however, unknown. Nevertheless, it is likely that those subtypes expressing both CCR2 and CX_3CR1 are more prone to migrate from the circulation into arterial walls through the interaction with their cognate ligands CCL2 and CX_3CL1, the circulating levels of which were significantly elevated in patients and correlated positively with plasma apoB, LDL and TC content.

To the best of our knowledge, the associations we found between T lymphocytes and PH have not previously been reported. Four findings are worthy of mention. First, the percentage of circulating $CD4^+$ cells was significantly higher in patients with PH than controls, and directly correlated with levels of apoB, LDL and TC. Of note, this increase was likely due to the increased numbers of circulating Th2 and Th17 cells. Second, most of the T cell subpopulations in patients displayed an activated state and positive correlations were found between the percentage of $CD8^+$ $CD69^+$ cells and key lipid features of the disease. Third, the percentage of circulating Treg cells and the Treg/Th17 ratio was decreased in PH patients. Finally, whereas IL-12, TNF-α and IL-6 plasma levels were increased in patients, levels of the anti-inflammatory cytokines IL-4 or IL-10 were decreased and inversely correlated with the levels of apoB, LDL and TC. These observations, overall, link the cellular and molecular inflammatory profile to a possible pro-atherogenic enviroment. Along this line, it is well known that both $CD4^+$ and $CD8^+$ T cells are involved in atherosclerosis development (Ketelhuth & Hansson, 2016). While the role of Th2 cells in atherogenesis remains debated (Ketelhuth & Hansson, 2016), it has recently been shown that patients with coronary artery atherosclerosis had an impaired Treg/Th17 ratio together with reduced serum levels of IL-10 (Ding et al., 2016). Th17 cells repress the function of Treg cells, contributing to an inflammatory milieu. Moreover, whereas Th17 cells can produce the inflammatory cytokines TNF-α and IL-6 (Olson et

al., 2013), Treg cells generate and release the anti-inflammatory cytokine IL-10. It is therefore tempting to speculate that there is a conversion of Treg cells into Th17 cells in PH. Finally, although IL-4 is a clasical Th2 cytokine, the decreased levels found in patients suggest an alternative cellular origin of this cytokine. Indeed, potential sources of IL-4 are double-positive CD4/CD8 lymphocytes, basophils or natural killer T cells (Quandt, Rothe, Scholz, Baerwald, & Wagner, 2014; Yoshimoto, 2018) whose circulating levels may be decreased in this pathology, although this requires further investigation.

We used a dynamic flow chamber model to explore the functional consequences of platelet-leukocyte-endothelium (heparin) or leukocyte-endothelium (EDTA) interactions, finding that adhesion of platelet-leukocyte aggregates to HUAEC, stimulated or not with TNF-α, was significantly higher in the patient group. The increased adhesion to functional (nonstimulated) endothelium was likely due to neutrophil and monocyte activation and consequent over-expression of CD11b/CD18 integrin, which interacts with the constitutively expressed intercellular cell adhesion molecule-1 in endothelium. Furthermore, platelets seem to be critical for leukocyte adhesion to dysfunctional (stimulated) arterial endothelium, as leukocyte-endothelium interactions were significantly impaired when platelets were dissociated with EDTA. It is widely accepted that activated platelets can mediate the endothelial adhesion of circulating leukocytes, a characteristic feature of the dysfunctional endothelium (Furio et al., 2018; Landmesser et al., 2004; Marques et al., 2017; Rius, Company, et al., 2013; Rius, Piqueras, et al., 2013). We also found a significant enhancement in the percentage of platelet-leukocyte aggregates, which were established with almost all the leukocyte subsets investigated in a background of PH. The increased number of these aggregates have been detected in the peripheral circulation of patients with unstable angina or other coronary diseases, and they have been considered a predictive factor of acute myocardial infarction (Michelson, Barnard, Krueger, Valeri, & Furman, 2001). This platelet-leukocyte interaction is in all probability due to the interaction of platelet P-selectin with its ligand, P-selectin glycoprotein ligand-1, present on leukocyte surfaces, which in turns facilitates the interaction between these aggregates and dysfunctional endothelium, a key event in arteries prone to arteriosclerotic lesion development (Landmesser et al., 2004).

In conclusion, we report that the low grade systemic inflammation associated with PH is accompanied by a pro-thrombotic state with heightened platelet activation and associated circulating soluble markers. This platelet activation state in PH, together with the activation of different leukocyte subsets, results in the formation of platelet-leukocyte aggregates and their adhesion to dysfunctional arterial endothelium, suggesting a potential link between systemic inflammation and CVD development in this metabolic disorder. Finally, the positive correlations between key lipid features of PH and different circulating inflammatory mediators (IL-8, MCP-1, fractalkine or IL-6) and the negative correlations between these lipids and anti-inflammatory cytokines (IL-4 and IL-10) might be used as potential markers of CVD. Overall, the modulation of the cellular and molecular inflammatory components in PH, as well as the lipid profile, might be crucial to prevent further cardiovascular complications.

12. STUDY OF SYSTEMIC INFLAMMATION IN PATIENTS WITH PH AND ITS MODULATION BY AN ORAL UNSATURATED FAT LOAD (OUFL)

PH is characterized by elevated plasma levels of cholesterol – specifically, LDL and apoB – which contribute to the development of atherosclerosis and associated ischemic events (Chironi et al., 2006; Collado, Marques, Domingo, et al., 2018; Cortes et al., 2016; Hansen et al., 2019; Holven et al., 2014; Real et al., 2010; Sampietro et al., 1997). In addition, there is increasing evidence that systemic inflammation is the main driver of premature atherosclerosis (Catapano, Pirillo, & Norata, 2017) and is a component of PH (Barale et al., 2018; Collado, Marques, Domingo, et al., 2018; Langslet et al., 2015). In the present study, we have extensively analyzed the acute impact (4 hours) of an OUFL containing 58% oleic acid and 20% linoleic acid (**Table 6**) on the systemic inflammatory response associated with PH. We show that an OUFL challenge beneficially modulates different immune players, reduces the levels of inflammatory cytokines and chemokines and impairs a prominent feature of the atherogenesis – the adhesiveness of leukocytes to the dysfunctional arterial endothelium. In agreement with our findings, oleic acid has been shown to protect against CVD and insulin resistance, and to improve endothelial dysfunction in response to pro-inflammatory signals (Perdomo et al., 2015). And in the same line, dietary intake of linoleic acid is inversely associated with the risk of coronary heart disease (Farvid et al., 2014).

Inflammation triggers platelet activation, which in turn plays an important role in several processes such as homeostasis (Manne, Xiang, & Rondina, 2017; Periayah, Halim, & Mat Saad, 2017) and thrombosis (Mancuso & Santagostino, 2017). Activated platelets are now also recognized as essential immune-modulators (Lam, Vijayan, & Rumbaut, 2015) by their expression of specific cell adhesion molecules such as P-selectin, which plays a crucial role in the recruitment of leukocytes to the inflammatory site. Additionally, they can release various inflammatory chemokines, including PF-4/CXCL4 or RANTES/CCL5 which can be deposited in the endothelium to stimulate monocyte and lymphocyte recruitment (von Hundelshausen & Schmitt, 2014). Patients with PH show a pro-thrombotic state characterized by increased platelet activation, which is reflected by the presence of P-selectin^{+} and PAC-1^{+} platelets (Collado, Marques, Domingo, et al., 2018). We found that a lipid OUFL challenge significantly reduced platelet activation in patients, pointing to the potential anti-thrombotic effects of the intervention. Additionally, OUFL reduced the circulating levels of several inflammatory mediators linked to platelet activation including sP-selectin, PF-4/CXCL4 and RANTES/CCL5, again suggesting that in postprandial state this treatment may impair the pro-thrombotic state associated with PH and the progression of atherogenesis (von Hundelshausen & Schmitt, 2014).

To understand the immune state of the PH environment, we surveyed different leukocyte subtypes following OUFL challenge. Neutrophils are known to be one of the major players in acute inflammation (Kolaczkowska & Kubes, 2013), as they express integrin CD11b/CD18 that is up-regulated upon activation and promotes leukocyte adhesion and transmigration across the vascular endothelium through its interaction with its cognate ligands intercellular adhesion molecule (ICAM)-1 and ICAM-2 (Diacovo, Roth, Buccola, Bainton, & Springer, 1996). Our analysis showed that while there no differences were evident in the percentage of circulating neutrophils and neutrophil-platelet aggregates after the OUFL in patients, there was a significant reduction in their activation state (CD11b expression and $CD69^{+}$). This was accompanied by a clear reduction in the circulating levels of IL-8/CXCL8, which induces neutrophil activation and chemotaxis (Kolaczkowska & Kubes, 2013). Both outcomes were positively correlated, thus indicating an improvement in the immune state of patients with PH and ameliorating the proatherogenic status.

Human circulating monocytes comprise a heterogeneous cell population that is commonly classified into three subtypes: classical $CD14^{+}CD16^{-}CCR2^{+}$ (Mon 1), intermediate $CD14^{+}CD16^{+}CCR2^{+}$ (Mon 2), and non-classical $CD14^{+}CD16^{+}CCR2^{-}$ (Mon 3) (C. Weber et al., 2016), with the Mon1 subtype more commonly known as classical or inflammatory monocytes. We found that an OUFL led to a significant reduction in the percentage of circulating Mon1 monocytes. Interestingly, there is evidence to support that adults with FH have a pro-inflammatory imbalance in circulating monocyte subpopulations (Mon 1) (Fadini et al., 2014). Although different studies in humans have noted increases in circulating $CD16^{+}$ monocytes in CVD (Kratofil et al., 2017), we observed no changes in Mon2 and Mon3 populations, monocyte activation state (CD11b expression) or CX_3CR1 expression after the OUFL. By contrast, MCP-1/CCL2 circulating levels were significantly reduced in patients with PH after the OUFL, confirming a previous report in patients with FH (Cortes et al., 2016). MCP-1/CCL2 mainly recruits Mon1 and Mon2 monocytes to inflammatory sites through interaction with its CCR2 receptor (Deshmane, Kremlev, Amini, & Sawaya, 2009; K. S. Weber, Nelson, Gröne, & Weber, 1999), and this inflammatory axis has been widely associated with CVD development (França et al., 2017).

T lymphocyte analysis revealed no changes in total T or Th lymphocytes after the OUFL in patients with PH but a significant increase in the percentage of Treg lymphocytes, which might contribute to the anti-inflammatory environment created by this intervention. However, neither the Treg/Th17 ratio nor the circulating levels of IL-10 were improved by the OUFL, although it is tempting to speculate that changes in these parameters might be evident at later time points. Of note, plasma levels of TNF-α were significantly reduced in patients after the OUFL being normalized to control subjects' levels. In this regard, a prior study in FH found that a similar intervention decreased the circulating levels of several inflammatory chemokines including macrophage inflammatory protein (MIP)-1α, MIP-1β, and interferon γ-induced protein 10 (IP-10)/CXCL10, among others, with values close to those found in control subjects (Cortes et al., 2016).

Finally, we used the dynamic flow chamber to explore the functional consequences of platelet-leukocyte-endothelium (heparin) or leukocyte-endothelium (EDTA) interactions. We previously showed that adhesion of platelet-leukocyte aggregates to HUAEC stimulated or not with TNF-α is significantly higher in patients with PH than in controls (Collado, Marques, Domingo, et al., 2018) . When these parameters were evaluated after the OUFL challenge, we found lowered adhesion of both platelet-leukocyte aggregates (heparin) and platelet-free leukocytes (EDTA) to dysfunctional arterial endothelium. The reduction in leukocyte adhesion is likely the consequence of several of the aforementioned experimental observations. First, the reduced activation state of neutrophils (CD11b/CD18 integrin down-regulation) can lead to decreased interactions with the constitutively or inducible (TNFα-stimulated) expressed endothelial ICAM-1. Second, since activated platelets can mediate the endothelial adhesion of circulating leukocytes – a characteristic feature of the dysfunctional endothelium (Collado, Marques, Domingo, et al., 2018; Collado, Marques, Escudero, et al., 2018; Furio et al., 2018; Landmesser et al., 2004; Marques et al., 2017; Rius, Company, et al., 2013) – their decreased activation may alter leukocyte arrest. Third, a reduction in the percentage of circulating inflammatory (classical) monocytes (Mon 1) results in diminished monocyte adhesion. Finally, the decreased levels of circulating chemokines may also affect the adhesion of leukocytes to endothelium in patients with PH. Supporting this concept, neutralization of CCL2 activity was found to decrease the endothelial arrest of Mon1 monocytes (Marques et al., 2019). Likewise, platelet deposition of RANTES/CCL5 in the endothelium can trigger monocyte arrest (von Hundelshausen et al., 2001) and PF-4/CXCL4 has multiple atherogenic activities and synergizes with CCL5 (von Hundelshausen & Schmitt, 2014). Leukocyte adhesion in this setting positively correlates with the plasma levels of these chemokines.

Our study has limitations. First, to date the acute intervention of the OUFL do not allow us to extrapolate these results to those with a long-term intervention and second, Supracal® cannot be considered a physiological ingestion of fat. Nevertheless, preclinical studies in animal models of hypercholesterolemia will be designed to evaluate the long-term effects of the OUFL.

In summary, administration of an OUFL has beneficial acute effects on the postprandial pro-thrombotic and pro-inflammatory state of PH patients. Further long-term studies are, however, warranted. Our findings indicate that the modulation of the cellular and soluble inflammatory components in PH might be crucial to prevent further cardiovascular complications.

13. STUDY OF THE ROLE OF CCL11/CCR3 AXIS IN PH AND ATHEROSCLEROSIS DEVELOPMENT

PH is a metabolic disorder which is associated with the risk of developing early arteriosclerosis and the likelihood of suffering further ischemic severe events. Although previous studies in PH patients have provided evidence of signs of low grade systemic inflammation (Collado, Marques, Domingo, et al., 2018; Cortes et al., 2016; Holven et al., 2014; Real et al., 2010; Sampietro et al., 1997), in this study and for the first time, we found that the circulating levels of eotaxin-1/CCL11, not yet linked to this metabolic disease, were significantly elevated in PH patients compared with age-matched controls and its plasma concentrations positively correlated with the altered circulating levels of key lipid components of this disease (apoB and LDL). Of note, since eotaxin-1/CCL11 only signals through the CCR3 receptor (Combadiere, Ahuja, & Murphy, 1995; Kitaura et al., 1996; Petkovic, Moghini, Paoletti, Uguccioni, & Gerber, 2004) we also found increased circulating percentages of CCR3-expressing leukocytes which were mainly eosinophils, a hematological feature not previously described in PH patients which again their percentage positively correlated with plasma apoB and LDL levels. Next, we first found that some of these findings were reproduced in *apoE*$^{-/-}$ mice under a hypercholesterolemic environment such as the higher plasma levels of eotaxin-1/CCL11 and percentage of circulating eosinophils. As expected, in addition to significant development of an atheroma plaque, eotaxin-1/CCL11 was detected in the atherosclerotic lesion which was in agreement with previous human and mice observations (Haley et al., 2000; Kraaijeveld, de Jager, van Berkel, Biessen, & Jukema, 2007). Surprisingly, and using three different approaches with double immunofluorescence staining, now we have shown a clear eosinophil infiltration in the atheroma of *apoE*$^{-/-}$ animals in this hypercholesterolemic setting. These results suggests that eotaxin-1 (CCL11)/CCR3 axis is probably involved in eosinophil recruitment within the lesion and plays a yet unknown role.

Therefore, a double-deficient mice in *apoE* and eotaxin receptor, CCR3 (*apoE*$^{-/-}$*CCR3*$^{-/-}$*)* was generated to try to clarify the function of CCL11/CCR3 axis in this pathological condition. Of note, when both *apoE*$^{-/-}$*CCR3*$^{+/+}$ and *apoE*$^{-/-}$*CCR3*$^{-/-}$ mice were subjected for 2 months to an atherogenic diet, the lesion in the *apoE*$^{-/-}$*CCR3*$^{-/-}$ group was significantly higher than that detected in *apoE*$^{-/-}$*CCR3*$^{+/+}$ mice and had higher and significant infiltration of macrophages and CD8^{+} T lymphocytes. However, although *apoE*$^{-/-}$*CCR3*$^{+/+}$ and *apoE*$^{-/-}$*CCR3*$^{-/-}$ mice showed similar increases in circulating levels of eotaxin-1/CCL11 compared with their respective control-diet genotypes, no circulating eosinophils were detected in *apoE*$^{-/-}$*CCR3*$^{-/-}$ regardless the diet administered. Inasmuch, immunodetection of eotaxin-1/CCL11 was only present in the lesion of *apoE*$^{-/-}$*CCR3*$^{+/+}$ mice but not in those animals subjected to a control diet or in *apoE*$^{-/-}$*CCR3*$^{-/-}$ mice fed with a hypercholesterolemic diet. Lastly, as found in the peripheral circulation, no eosinophils were present in the lesion of *apoE*$^{-/-}$*CCR3*$^{-/-}$ animals after 2 months in an atherogenic milieu. Taken together, these findings

also suggest that within the atherosclerotic lesion, eosinophils are likely the source of eotaxin1/CCL11 and exert an anti-atherogenic effect.

In regard to this, IL-4 can be generated and released by eosinophils (D. Wu et al., 2011) and IL-4 is one of the main drivers of eotaxin-1/CCL11 generation of (Sanz et al., 1998). Accordingly, in the absence of eosinophils a drastic reduction in IL-4 expression was detected in *apoE*$^{-/-}$*CCR3*$^{-/-}$ mice. Inasmuch, since IL4-induced eotaxin-1/CCL11 generation is mediated via STAT6-dependent signaling (Heller et al., 2004), we have now provided additional evidence that eotaxin-1/CCL11 generation within the atherosclerotic lesion occurs through an IL-4/STAT6-dependent activation pathway.

All the above-mentioned findings were endorsed with the studies carried out with bone marrow (BM) transplants, where myeloablated *apoE*$^{-/-}$*CCR3*$^{-/-}$ CD45.2 mice and reconstituted with of BM from *apoE*$^{-/-}$ CD45.1 mice, yielded similar observations to *apoE*$^{-/-}$*CCR3*$^{+/+-}$ animals. Conversely, myeloablated *apoE*$^{-/-}$ CD45.1 animals reconstituted with BM from *apoE*$^{-/-}$*CCR3*$^{-/-}$ CD45.2 mice resembled the results obtained in *apoE*$^{-/-}$*CCR3*$^{-/-}$ animals. The provided data from all these studies support the hypothesis that increased activation of eotaxin-1 (CCL11)/CCR3 axis results in enhanced eosinophil-infiltrated atheroma and circulating eosinophils leading to a compensatory mechanism to attenuate atherosclerotic lesion formation in hypercholesterolemia.

Based on these findings, the next question is: how eosinophils exert their protective effect? Firstly, they can limit macrophage infiltration within the lesion since eotaxin-1 /CCL11 acts as a natural antagonist of CCR2 receptor, which is expressed on the surface of proinflammatory monocytes (Ogilvie et al., 2001), and both CCR2 receptor and its cognate ligand (MCP-1/CCL2) are widely known to be involved in the mononuclear cell infiltration into the atherosclerotic lesion (Reape & Groot, 1999). Accordingly, *apoE*$^{-/-}$*CCR3*$^{-/-}$ mice subjected to an atherogenic diet showed increased circulating numbers of CCR2^{+} monocytes and infiltrated pro-inflammatory macrophages within the atherosclerotic lesion compared to *apoE*$^{-/-}$*CCR3*$^{+/+}$ animals under the same diet. Thus indicating that the absence of eotaxin1/CCL11 in the lesion can account for the enhanced atheroma in *apoE*$^{-/-}$*CCR3*$^{-/-}$ *vs*. *apoE*$^{-/-}$*CCR3*$^{+/+}$ animals. And, secondly, since IL-4 is one of the main stimuli for macrophage switching from a proinflammatory M1-like to an anti-inflammatory M2-like phenotype (D. Wu et al., 2011) and this response also requires STAT6 activation (Huber, Hoffmann, Muskens, & Voehringer, 2010), in the atherosclerotic milieu, eosinophils could promote macrophage switching through IL-4/STAT6 activation pathway. In fact, increased M2-like macrophages (CD68^{+}/CD206^{+} cells) were found in the lesions of *apoE*$^{-/-}$*CCR3*$^{+/+}$ but not in those animals in which eosinophils were absent (*apoE*$^{-/-}$*CCR3*$^{-/-}$ mice).

So, who triggers the initial eosinophil infiltration in the atheroma? In that sense, eosinophils can initially infiltrate into the atherosclerotic lesion in response to RANTES/CCL5 which is a potent eosinophil chemoattractant through its interaction with their CCR3 receptor (Kameyoshi, Dörschner, Mallet, Christophers, & Schröder, 1992). Indeed, it is well accepted that platelets store RANTES in their α-granules

and different studies have shown that the deposition and immobilization of platelet-derived RANTES can trigger enhanced recruitment of monocytes and lymphocytes on the initially activated atherosclerotic endothelium (Danese et al., 2004; Kameyoshi et al., 1992; Kameyoshi, Schröder, Christophers, & Yamamoto, 1994; Schober et al., 2002; von Hundelshausen et al., 2001). Hence, in addition to these immune players, platelet-deposited RANTES may also recruit and activate eosinophils. Once activated, the release of IL-4 and the subsequent production of eotaxin-1/CCL11 may amplify peripheral eosinophil recruitment within the atherosclerotic lesion from the peripheral circulation.

Until recently, eosinophils were solely envisaged as driving force of parasite defence and as mediators of allergic disease. However, an increasing amount of data suggests a broader and rather homeostatic role of these cells. In this regard, previous reports suggest that eosinophils play an unexpected role in metabolic homeostasis through maintenance of adipose alternatively activated macrophages (AAMs or M2-like macrophages) (D. Wu et al., 2011). Similarly, mobilization of adipose tissue eosinophils seems to play a role in promoting healthy aging (Brigger et al., 2020). Interestingly and as opposed to the latter observations, in the current study, no differences in the number of homing eosinophils were encountered in key tissues/organs where eosinophils are usually resident such as visceral fat, intestine or bone marrow between *apoE*$^{-/-}$ animals subjected or not to an atherogenic diet. In consequence, circulating and lesion-infiltrated eosinophils do not seem to be mobilized from the fat tissue or the gut in a hypercholesterolemic environment. In contrast, they are likely eotaxin-1/CCL11-dependent released from the bone marrow since this chemokine is involved in their mobilization and trafficking from the bone marrow into the blood stream and in their transit to their dwelling tissue/organs (Palframan, Collins, Williams, & Rankin, 1998). In support of this contention, no eosinophils were encountered in the visceral fat, intestine or atheroma of *apoE*$^{-/-}$*CCR3*$^{-/-}$ mice under a high-fat diet but eosinophil numbers were much greater in the bone marrow than those found in *apoE*$^{-/-}$*CCR3*$^{+/+}$. These findings suggest that in the absence of CCR3 receptor, eosinophils are retained in this hematopoyetic organ without being capable of transiting reagardless the increased circulating levels of eotaxin-1 /CCL11 induced by the atherogenic environment.

On the other hand, controversial published observations can be encountered regarding the role of eosinophils in some metabolic and cardiovascular diseases. While some studies have found a protective role of these immune players such as in cardiac function after myocardial infarction, abdominal aortic aneurism or age-related disorders (Brigger et al., 2020; C. L. Liu et al., 2021; J. Liu et al., 2020), others did not in close experimental settings (Diny et al., 2017; Marx et al., 2019). These discrepancies may rely on differences in the experimental protocol applied or even in the staining approach to detect eosinophils. It is noteworthy that in some of these publications Siglec-F was the exclusive marker used to detect murine eosinophils (Diny et al., 2017; Marx et al., 2019). It is well known that different macrophages can express Siglec-F (Bolden et al., 2018; Huggins et al., 2021; Khalsa et al., 2020) and, more relevant, previous studies have detected a neutrophil population that express Siglec-F (Pfirschke et al., 2020; Ryu et al., 2022; Vafadarnejad et al., 2020). Inasmuch, we have detected a neutrophil population that express Siglec-F but not CCR3 or CD125 receptor both in the atheroma and the circulation of *apoE*$^{-/}$ mice subjected

to an atherogenic diet. In regard to this, it is widely accepted that neutrophils exert a deleterious effect in cardiomyopathy and atherosclerosis (Sreejit et al., 2022).

Collectively, all of these evidences suggest that eotaxin-1 (CCL11)/CCR3 axis exerts a protective effect against the development of atherosclerosis under hypercholesterolemic conditions. The increased eotaxin-1/CCL11 circulating levels in this environment promotes the CCR3-dependent eosinophil release from the bone marrow and their mobilization and infiltration into the atheroma plaque. Eosinophils exert a beneficial role mitigating $CCR2^{+}$ monocyte infiltration through additional eotaxin-1/CCL11 generation within the atheroma and increasing the numbers of M2-like anti-inflammatory macrophages being both events mediated through the activation of IL-4/STAT6 signalling pathway. These results shed mechanistic light to a yet unexplored and favourable effects of eosinophils in atherosclerosis lesion formation.

CONCLUSIONS

CONCLUSIONS

1. PH is accompanied by a low-grade of systemic inflammation and associated to platelet and leukocyte activation which results in the formation of platelet-leukocyte aggregates and their adhesion to the dysfunctional arterial endothelium, suggesting a possible link between systemic inflammation and cardiovascular disease development in this metabolic disorder.

2. The positive correlations between key lipid features of PH and different circulating pro-inflammatory mediators (IL-6, IL-8/CXCL8, MCP-1/CCL2 or fractalkine/CX_3CL1) and the negative correlation between these lipids and anti-inflammatory cytokines (IL-4 and IL-10) might be used as potential markers of cardiovascular disease.

3. The administration of a lipid OUFL has a beneficial impact on the pro-thrombotic and inflammatory status of PH patients. Therefore, the modulation of the cellular and inflammatory components in PH, as well as the lipid profile, might be crucial to prevent futher cardiovascular complications.

4. Circulating levels of eotaxin-1/CCL11 and eosinophils were significantly elevated in PH patients compared with age-matched controls and its plasma concentrations positively correlated with the altered circulating levels of key lipid components of this disease (apoB and LDL), features not previously described in this metabolic disorder. These findings were reproduced in *apoE*$^{-/-}$ mice subjected to a hypercholesterolemic diet.

5. Generation of *apoE*$^{-/-}$*CCR3*$^{-/-}$ and *apoE*$^{-/-}$*CCR3*$^{+/+}$ mice revealed that eotaxin-1 (CCL11)/CCR3 axis exerts a protective effect against the development of atherosclerosis under hypercholesterolemic conditions through eosinophil mobilization from the BM. These cells exert a beneficial role limiting $CCR2^+$ monocyte infiltration through IL-4 release, STAT6 activation and eotaxin-1/CCL11 generation within the atheroma and increasing the numbers of M2-like anti-inflammatory macrophages. These results suggests a favourable effects of eosinophils in atherosclerosis lesion formation.

REFERENCES

REFERENCES

Aggarwal, B. B., Gupta, S. C., & Kim, J. H. (2012). Historical perspectives on tumor necrosis factor and its superfamily: 25 years later, a golden journey. *Blood, 119*(3), 651-665. doi:10.1182/blood-2011-04-325225

Ahotupa, M. (2017). Oxidized lipoprotein lipids and atherosclerosis. *Free Radic Res, 51*(4), 439-447. doi:10.1080/10715762.2017.1319944

Ahrens, R., Waddell, A., Seidu, L., Blanchard, C., Carey, R., Forbes, E., . . . Hogan, S. P. (2008). Intestinal macrophage/epithelial cell-derived CCL11/eotaxin-1 mediates eosinophil recruitment and function in pediatric ulcerative colitis. *J Immunol, 181*(10), 7390-7399. doi:10.4049/jimmunol.181.10.7390

Avogaro, A., & de Kreutzenberg, S. V. J. C. c. a. (2005). Mechanisms of endothelial dysfunction in obesity. *360*(1-2), 9-26.

Bäck, M., Yurdagul, A., Jr., Tabas, I., Öörni, K., & Kovanen, P. T. (2019). Inflammation and its resolution in atherosclerosis: mediators and therapeutic opportunities. *Nat Rev Cardiol, 16*(7), 389-406. doi:10.1038/s41569-019-0169-2

Badimon, L., & Vilahur, G. (2014). Thrombosis formation on atherosclerotic lesions and plaque rupture. *J Intern Med, 276*(6), 618-632. doi:10.1111/joim.12296

Barale, C., Frascaroli, C., Senkeev, R., Cavalot, F., & Russo, I. (2018). Simvastatin Effects on Inflammation and Platelet Activation Markers in Hypercholesterolemia. *Biomed Res Int, 2018*, 6508709. doi:10.1155/2018/6508709

Barrett, T. J. (2020). Macrophages in Atherosclerosis Regression. *Arterioscler Thromb Vasc Biol, 40*(1), 20-33. doi:10.1161/atvbaha.119.312802

Bartlett, B., Ludewick, H. P., Misra, A., Lee, S., & Dwivedi, G. (2019). Macrophages and T cells in atherosclerosis: a translational perspective. *Am J Physiol Heart Circ Physiol, 317*(2), H375-h386. doi:10.1152/ajpheart.00206.2019

Baum, S. J., & Cannon, C. P. (2018). PCSK9 inhibitor valuation: A science-based review of the two recent models. *Clin Cardiol, 41*(4), 544-550. doi:10.1002/clc.22924

Bednarczyk, M., Stege, H., Grabbe, S., & Bros, M. (2020). β2 Integrins-Multi-Functional Leukocyte Receptors in Health and Disease. *Int J Mol Sci, 21*(4). doi:10.3390/ijms21041402

Bennett, M. R., Sinha, S., & Owens, G. K. (2016). Vascular Smooth Muscle Cells in Atherosclerosis. *Circ Res, 118*(4), 692-702. doi:10.1161/circresaha.115.306361

Bhargava, P., & Lee, C. H. (2012). Role and function of macrophages in the metabolic syndrome. *Biochem J, 442*(2), 253-262. doi:10.1042/bj20111708

Biosciences, B. D. J. M. P. (2000). Introduction to Flow Cytometry: A learning guide. *1*(1).

Blanchet, X., Langer, M., Weber, C., Koenen, R. R., & von Hundelshausen, P. (2012). Touch of chemokines. *Front Immunol, 3*, 175. doi:10.3389/fimmu.2012.00175

Bochner, B. S. (2009). Siglec-8 on human eosinophils and mast cells, and Siglec-F on murine eosinophils, are functionally related inhibitory receptors. *Clin Exp Allergy, 39*(3), 317-324. doi:10.1111/j.1365-2222.2008.03173.x

Bolden, J. E., Lucas, E. C., Zhou, G., O'Sullivan, J. A., de Graaf, C. A., McKenzie, M. D., . . . Fairfax, K. A. (2018). Identification of a Siglec-F+ granulocyte-macrophage progenitor. *J Leukoc Biol, 104*(1), 123-133. doi:10.1002/jlb.1ma1217-475r

Brigger, D., Riether, C., van Brummelen, R., Mosher, K. I., Shiu, A., Ding, Z., . . . Eggel, A. (2020). Eosinophils regulate adipose tissue inflammation and sustain physical and immunological fitness in old age. *Nat Metab, 2*(8), 688-702. doi:10.1038/s42255-020-0228-3

Butt, W. Z., & Yee, J. K. (2022). The Role of Non-statin Lipid-Lowering Medications in Youth with Hypercholesterolemia. *Curr Atheroscler Rep, 24*(5), 379-389. doi:10.1007/s11883-022-01013-x

Camaré, C., Pucelle, M., Nègre-Salvayre, A., & Salvayre, R. (2017). Angiogenesis in the atherosclerotic plaque. *Redox Biol, 12*, 18-34. doi:10.1016/j.redox.2017.01.007

Carlens, J., Wahl, B., Ballmaier, M., Bulfone-Paus, S., Förster, R., & Pabst, O. (2009). Common gamma-chain-dependent signals confer selective survival of eosinophils in the murine small intestine. *J Immunol, 183*(9), 5600-5607. doi:10.4049/jimmunol.0801581

Cartier, J. L., & Goldberg, A. C. (2016). Familial Hypercholesterolemia: Advances in Recognition and Therapy. *Prog Cardiovasc Dis, 59*(2), 125-134. doi:10.1016/j.pcad.2016.07.006

Catapano, A. L., Pirillo, A., & Norata, G. D. (2017). Vascular inflammation and low-density lipoproteins: is cholesterol the link? A lesson from the clinical trials. *Br J Pharmacol, 174*(22), 3973-3985. doi:10.1111/bph.13805

Chen, L., Deng, H., Cui, H., Fang, J., Zuo, Z., Deng, J., . . . Zhao, L. (2018). Inflammatory responses and inflammation-associated diseases in organs. *Oncotarget, 9*(6), 7204-7218. doi:10.18632/oncotarget.23208

Chen, P. Y., Qin, L., Li, G., Tellides, G., & Simons, M. (2016). Smooth muscle FGF/TGFβ cross talk regulates atherosclerosis progression. *EMBO Mol Med, 8*(7), 712-728. doi:10.15252/emmm.201506181

Chen, Y., Song, Y., Du, W., Gong, L., Chang, H., & Zou, Z. (2019). Tumor-associated macrophages: an accomplice in solid tumor progression. *J Biomed Sci, 26*(1), 78. doi:10.1186/s12929-019-0568-z

Cheng, S. S., Lukacs, N. W., & Kunkel, S. L. (2002). Eotaxin/CCL11 suppresses IL-8/CXCL8 secretion from human dermal microvascular endothelial cells. *J Immunol, 168*(6), 2887-2894. doi:10.4049/jimmunol.168.6.2887

Chironi, G., Dosquet, C., Del-Pino, M., Denarie, N., Megnien, J. L., Drouet, L., . . . Simon, A. (2006). Relationship of circulating biomarkers of inflammation and hemostasis with preclinical atherosclerotic burden in nonsmoking hypercholesterolemic men. *Am J Hypertens, 19*(10), 1025-1031. doi:10.1016/j.amjhyper.2006.03.016

Chistiakov, D. A., Orekhov, A. N., & Bobryshev, Y. V. (2015). Contribution of neovascularization and intraplaque haemorrhage to atherosclerotic plaque progression and instability. *Acta Physiol (Oxf), 213*(3), 539-553. doi:10.1111/apha.12438

Chlebus, K., Cybulska, B., Dobrowolski, P., Romanowska-Kocejko, M., Żarczyńska-Buchowiecka, M., Gilis-Malinowska, N., . . . Gruchała, M. (2022). Effectiveness and safety of PCSK9 inhibitor therapy in patients with familial hypercholesterolemia within a therapeutic program in Poland: Preliminary multicenter data. *Cardiol J, 29*(1), 62-71. doi:10.5603/CJ.a2022.0003

Cho, J. G., Lee, A., Chang, W., Lee, M. S., & Kim, J. (2018). Endothelial to Mesenchymal Transition Represents a Key Link in the Interaction between Inflammation and Endothelial Dysfunction. *Front Immunol, 9*, 294. doi:10.3389/fimmu.2018.00294

Cicero, A. F., & Cincione, I. R. (2022). Secondary (acquired) hypercholesterolemia. In *Cholesterol* (pp. 609-621): Elsevier.

Clemetson, K. J., Clemetson, J. M., Proudfoot, A. E., Power, C. A., Baggiolini, M., & Wells, T. N. (2000). Functional expression of CCR1, CCR3, CCR4, and CXCR4 chemokine receptors on human platelets. *Blood, 96*(13), 4046-4054.

Collado, A., Domingo, E., Piqueras, L., & Sanz, M. J. (2021). Primary hypercholesterolemia and development of cardiovascular disorders: Cellular and molecular mechanisms involved in low-grade systemic inflammation and endothelial dysfunction. *Int J Biochem Cell Biol, 139*, 106066. doi:10.1016/j.biocel.2021.106066

Collado, A., Marques, P., Domingo, E., Perello, E., González-Navarro, H., Martinez-Hervás, S., . . . Sanz, M. J. (2018). Novel Immune Features of the Systemic Inflammation Associated with Primary Hypercholesterolemia: Changes in Cytokine/Chemokine Profile, Increased Platelet and Leukocyte Activation. *J Clin Med, 8*(1). doi:10.3390/jcm8010018

Collado, A., Marques, P., Escudero, P., Rius, C., Domingo, E., Martinez-Hervás, S., . . . Sanz, M. J. (2018). Functional role of endothelial CXCL16/CXCR6-platelet-leucocyte axis in angiotensin II-associated metabolic disorders. *Cardiovasc Res, 114*(13), 1764-1775. doi:10.1093/cvr/cvy135

Combadiere, C., Ahuja, S. K., & Murphy, P. M. (1995). Cloning and functional expression of a human eosinophil CC chemokine receptor. *J Biol Chem, 270*(28), 16491-16494. doi:10.1074/jbc.270.28.16491

Conroy, D. M., & Williams, T. J. (2001). Eotaxin and the attraction of eosinophils to the asthmatic lung. *Respir Res, 2*(3), 150-156. doi:10.1186/rr52

Cortes, R., Ivorra, C., Martínez-Hervás, S., Pedro, T., González-Albert, V., Artero, A., . . . Chaves, F. J. (2016). Postprandial Changes in Chemokines Related to Early Atherosclerotic Processes in Familial Hypercholesterolemic Subjects: A Preliminary Study. *Arch Med Res, 47*(1), 33-39. doi:10.1016/j.arcmed.2016.01.002

Crijns, H., Vanheule, V., & Proost, P. (2020). Targeting Chemokine-Glycosaminoglycan Interactions to Inhibit Inflammation. *Front Immunol, 11*, 483. doi:10.3389/fimmu.2020.00483

Croft, M., & Siegel, R. M. (2017). Beyond TNF: TNF superfamily cytokines as targets for the treatment of rheumatic diseases. *Nat Rev Rheumatol, 13*(4), 217-233. doi:10.1038/nrrheum.2017.22

Cyr, A. R., Huckaby, L. V., Shiva, S. S., & Zuckerbraun, B. S. (2020). Nitric Oxide and Endothelial Dysfunction. *Crit Care Clin, 36*(2), 307-321. doi:10.1016/j.ccc.2019.12.009

Danese, S., de la Motte, C., Reyes, B. M., Sans, M., Levine, A. D., & Fiocchi, C. (2004). Cutting edge: T cells trigger CD40-dependent platelet activation and granular RANTES release: a novel pathway for immune response amplification. *J Immunol, 172*(4), 2011-2015. doi:10.4049/jimmunol.172.4.2011

Daugherty, B. L., Siciliano, S. J., DeMartino, J. A., Malkowitz, L., Sirotina, A., & Springer, M. S. (1996). Cloning, expression, and characterization of the human eosinophil eotaxin receptor. *J Exp Med, 183*(5), 2349-2354. doi:10.1084/jem.183.5.2349

De Castro-Orós, I., Pocoví, M., & Civeira, F. (2010). The genetic basis of familial hypercholesterolemia: inheritance, linkage, and mutations. *Appl Clin Genet, 3*, 53-64. doi:10.2147/tacg.s8285

de Vries, M. R., & Quax, P. H. (2016). Plaque angiogenesis and its relation to inflammation and atherosclerotic plaque destabilization. *Curr Opin Lipidol, 27*(5), 499-506. doi:10.1097/mol.0000000000000339

Deshmane, S. L., Kremlev, S., Amini, S., & Sawaya, B. E. (2009). Monocyte chemoattractant protein-1 (MCP-1): an overview. *J Interferon Cytokine Res, 29*(6), 313-326. doi:10.1089/jir.2008.0027

Diacovo, T. G., Roth, S. J., Buccola, J. M., Bainton, D. F., & Springer, T. A. (1996). Neutrophil rolling, arrest, and transmigration across activated, surface-adherent platelets via sequential action of P-selectin and the beta 2-integrin CD11b/CD18. *Blood, 88*(1), 146-157.

Dimitrov, S., Shaikh, F., Pruitt, C., Green, M., Wilson, K., Beg, N., & Hong, S. (2013). Differential TNF production by monocyte subsets under physical stress: blunted mobilization of proinflammatory monocytes in prehypertensive individuals. *Brain Behav Immun, 27*(1), 101-108. doi:10.1016/j.bbi.2012.10.003

Ding, J. W., Zheng, X. X., Zhou, T., Tong, X. H., Luo, C. Y., & Wang, X. A. (2016). HMGB1Modulates the Treg/Th17 Ratio in Atherosclerotic Patients. *J Atheroscler Thromb, 23*(6), 737-745. doi:10.5551/jat.31088

Diny, N. L., Baldeviano, G. C., Talor, M. V., Barin, J. G., Ong, S., Bedja, D., . . . Čiháková, D. (2017). Eosinophil-derived IL-4 drives progression of myocarditis to inflammatory dilated cardiomyopathy. *J Exp Med, 214*(4), 943-957. doi:10.1084/jem.20161702

Erin, E. M., Williams, T. J., Barnes, P. J., & Hansel, T. T. (2002). Eotaxin receptor (CCR3) antagonism in asthma and allergic disease. *Curr Drug Targets Inflamm Allergy, 1*(2), 201-214. doi:10.2174/1568010023344715

Fadini, G. P., Simoni, F., Cappellari, R., Vitturi, N., Galasso, S., Vigili de Kreutzenberg, S., . . . Avogaro, A. (2014). Pro-inflammatory monocyte-macrophage polarization imbalance in human hypercholesterolemia and atherosclerosis. *Atherosclerosis, 237*(2), 805-808. doi:10.1016/j.atherosclerosis.2014.10.106

Farvid, M. S., Ding, M., Pan, A., Sun, Q., Chiuve, S. E., Steffen, L. M., . . . Hu, F. B. (2014). Dietary linoleic acid and risk of coronary heart disease: a systematic review and meta-analysis of prospective cohort studies. *Circulation, 130*(18), 1568-1578. doi:10.1161/circulationaha.114.010236

Filippi, M. D. (2019). Neutrophil transendothelial migration: updates and new perspectives. *Blood, 133*(20), 2149-2158. doi:10.1182/blood-2018-12-844605

França, C. N., Izar, M. C. O., Hortêncio, M. N. S., do Amaral, J. B., Ferreira, C. E. S., Tuleta, I. D., & Fonseca, F. A. H. (2017). Monocyte subtypes and the CCR2 chemokine receptor in cardiovascular disease. *Clin Sci (Lond), 131*(12), 1215-1224. doi:10.1042/cs20170009

Furio, E., García-Fuster, M. J., Redon, J., Marques, P., Ortega, R., Sanz, M. J., & Piqueras, L. (2018). CX3CR1/CX3CL1 Axis Mediates Platelet-Leukocyte Adhesion to Arterial Endothelium in Younger Patients with a History of Idiopathic Deep Vein Thrombosis. *Thromb Haemost, 118*(3), 562-571. doi:10.1055/s-0038-1629897

Gavriilaki, E., Anyfanti, P., Gavriilaki, M., Lazaridis, A., Douma, S., & Gkaliagkousi, E. (2020). Endothelial Dysfunction in COVID-19: Lessons Learned from Coronaviruses. *Curr Hypertens Rep, 22*(9), 63. doi:10.1007/s11906-020-01078-6

Gencer, B., & Nanchen, D. (2016). Identifying familial hypercholesterolemia in acute coronary syndrome. *Curr Opin Lipidol, 27*(4), 375-381. doi:10.1097/mol.0000000000000311

Germic, N., Hosseini, A., Stojkov, D., Oberson, K., Claus, M., Benarafa, C., . . . Simon, H. U. (2021). ATG5 promotes eosinopoiesis but inhibits eosinophil effector functions. *Blood, 137*(21), 2958-2969. doi:10.1182/blood.2020010208

Germolec, D. R., Shipkowski, K. A., Frawley, R. P., & Evans, E. (2018). Markers of Inflammation. *Methods Mol Biol, 1803*, 57-79. doi:10.1007/978-1-4939-8549-4_5

Gevaert, P., Han, J. K., Smith, S. G., Sousa, A. R., Howarth, P. H., Yancey, S. W., . . . Bachert, C. (2022). The roles of eosinophils and interleukin-5 in the pathophysiology of chronic rhinosinusitis with nasal polyps. *Int Forum Allergy Rhinol, 12*(11), 1413-1423. doi:10.1002/alr.22994

Giagulli, C., Ottoboni, L., Caveggion, E., Rossi, B., Lowell, C., Constantin, G., . . . Berton, G. (2006). The Src family kinases Hck and Fgr are dispensable for inside-out, chemoattractant-induced signaling regulating beta 2 integrin affinity and valency in neutrophils, but are required for beta 2 integrin-mediated outside-in signaling involved in sustained adhesion. *J Immunol, 177*(1), 604-611.

Ginsberg, M. H., Partridge, A., & Shattil, S. J. (2005). Integrin regulation. *Curr Opin Cell Biol, 17*(5), 509-516.

Gisterå, A., & Hansson, G. K. (2017). The immunology of atherosclerosis. *Nat Rev Nephrol, 13*(6), 368-380. doi:10.1038/nrneph.2017.51

Grozdanovic, M., Laffey, K. G., Abdelkarim, H., Hitchinson, B., Harijith, A., Moon, H. G., . . . Ackerman, S. J. (2019). Novel peptide nanoparticle-biased antagonist of CCR3 blocks eosinophil recruitment and airway hyperresponsiveness. *J Allergy Clin Immunol, 143*(2), 669-680.e612. doi:10.1016/j.jaci.2018.05.003

Guenther, C. (2022). β2-Integrins - Regulatory and Executive Bridges in the Signaling Network Controlling Leukocyte Trafficking and Migration. *Front Immunol, 13*, 809590. doi:10.3389/fimmu.2022.809590

Guthier, H. E., & Zimmermann, N. (2022). Targeting Eosinophils in Mouse Models of Asthma. *Methods Mol Biol, 2506*, 211-222. doi:10.1007/978-1-0716-2364-0_15

Haley, K. J., Lilly, C. M., Yang, J. H., Feng, Y., Kennedy, S. P., Turi, T. G., . . . Lee, R. T. (2000). Overexpression of eotaxin and the CCR3 receptor in human atherosclerosis: using genomic technology to identify a potential novel pathway of vascular inflammation. *Circulation, 102*(18), 2185-2189. doi:10.1161/01.cir.102.18.2185

Hansen, M., Kuhlman, A. C. B., Sahl, R. E., Kelly, B., Morville, T., Dohlmann, T. L., . . . Dela, F. (2019). Inflammatory biomarkers in patients in Simvastatin treatment: No effect of co-enzyme Q10 supplementation. *Cytokine, 113*, 393-399. doi:10.1016/j.cyto.2018.10.011

Hassani, M., van Staveren, S., van Grinsven, E., Bartels, M., Tesselaar, K., Leijte, G., . . . Koenderman, L. (2020). Characterization of the phenotype of human eosinophils and their progenitors in the bone marrow of healthy individuals. *Haematologica, 105*(2), e52-e56. doi:10.3324/haematol.2019.219048

Hedrick, C. C. (2015). Lymphocytes in atherosclerosis. *Arterioscler Thromb Vasc Biol, 35*(2), 253-257. doi:10.1161/atvbaha.114.305144

Heller, N. M., Matsukura, S., Georas, S. N., Boothby, M. R., Rothman, P. B., Stellato, C., & Schleimer, R. P. (2004). Interferon-gamma inhibits STAT6 signal transduction and gene expression in human airway epithelial cells. *Am J Respir Cell Mol Biol, 31*(5), 573-582. doi:10.1165/rcmb.2004-0195OC

Hilger, D., Masureel, M., & Kobilka, B. K. (2018). Structure and dynamics of GPCR signaling complexes. *Nat Struct Mol Biol, 25*(1), 4-12. doi:10.1038/s41594-017-0011-7

Hintermann, E., & Christen, U. (2019). The Many Roles of Cell Adhesion Molecules in Hepatic Fibrosis. *Cells, 8*(12). doi:10.3390/cells8121503

Holven, K. B., Narverud, I., Lindvig, H. W., Halvorsen, B., Langslet, G., Nenseter, M. S., . . . Retterstøl, K. (2014). Subjects with familial hypercholesterolemia are characterized by an inflammatory phenotype despite long-term intensive cholesterol lowering treatment. *Atherosclerosis, 233*(2), 561-567. doi:10.1016/j.atherosclerosis.2014.01.022

Huber, S., Hoffmann, R., Muskens, F., & Voehringer, D. (2010). Alternatively activated macrophages inhibit T-cell proliferation by Stat6-dependent expression of PD-L2. *Blood, 116*(17), 3311-3320. doi:10.1182/blood-2010-02-271981

Huggins, D. N., LaRue, R. S., Wang, Y., Knutson, T. P., Xu, Y., Williams, J. W., & Schwertfeger, K. L. (2021). Characterizing Macrophage Diversity in Metastasis-Bearing Lungs Reveals a Lipid-Associated Macrophage Subset. *Cancer Res, 81*(20), 5284-5295. doi:10.1158/0008-5472.Can-21-0101

Hughes, C. E., & Nibbs, R. J. B. (2018). A guide to chemokines and their receptors. *Febs j, 285*(16), 2944-2971. doi:10.1111/febs.14466

Humbles, A. A., Lu, B., Friend, D. S., Okinaga, S., Lora, J., Al-Garawi, A., . . . Gerard, C. (2002). The murine CCR3 receptor regulates both the role of eosinophils and mast cells in allergen-induced airway inflammation and hyperresponsiveness. *Proc Natl Acad Sci U S A, 99*(3), 1479-1484. doi:10.1073/pnas.261462598

Incalza, M. A., D'Oria, R., Natalicchio, A., Perrini, S., Laviola, L., & Giorgino, F. (2018). Oxidative stress and reactive oxygen species in endothelial dysfunction associated with cardiovascular and metabolic diseases. *Vascul Pharmacol, 100*, 1-19. doi:10.1016/j.vph.2017.05.005

Jacobsen, E. A., Jackson, D. J., Heffler, E., Mathur, S. K., Bredenoord, A. J., Pavord, I. D., . . . Rothenberg, M. E. (2021). Eosinophil Knockout Humans: Uncovering the Role of Eosinophils Through Eosinophil-Directed Biological Therapies. *Annu Rev Immunol, 39*, 719-757. doi:10.1146/annurev-immunol-093019-125918

Jaipersad, A. S., Lip, G. Y., Silverman, S., & Shantsila, E. (2014). The role of monocytes in angiogenesis and atherosclerosis. *J Am Coll Cardiol, 63*(1), 1-11. doi:10.1016/j.jacc.2013.09.019

Jarauta, E., Bea-Sanz, A. M., Marco-Benedi, V., & Lamiquiz-Moneo, I. (2020). Genetics of Hypercholesterolemia: Comparison Between Familial Hypercholesterolemia and Hypercholesterolemia Nonrelated to LDL Receptor. *Front Genet, 11*, 554931. doi:10.3389/fgene.2020.554931

Jung, Y., & Rothenberg, M. E. (2014). Roles and regulation of gastrointestinal eosinophils in immunity and disease. *J Immunol, 193*(3), 999-1005. doi:10.4049/jimmunol.1400413

Kameyoshi, Y., Dörschner, A., Mallet, A. I., Christophers, E., & Schröder, J. M. (1992). Cytokine RANTES released by thrombin-stimulated platelets is a potent attractant for human eosinophils. *J Exp Med, 176*(2), 587-592. doi:10.1084/jem.176.2.587

Kameyoshi, Y., Schröder, J. M., Christophers, E., & Yamamoto, S. (1994). Identification of the cytokine RANTES released from platelets as an eosinophil chemotactic factor. *Int Arch Allergy Immunol, 104 Suppl 1*(1), 49-51. doi:10.1159/000236751

Kamstrup, P. R. (2021). Lipoprotein(a) and Cardiovascular Disease. *Clin Chem, 67*(1), 154-166. doi:10.1093/clinchem/hvaa247

Kanda, A., Yun, Y., Bui, D. V., Nguyen, L. M., Kobayashi, Y., Suzuki, K., . . . Iwai, H. (2021). The multiple functions and subpopulations of eosinophils in tissues under steady-state and pathological conditions. *Allergol Int, 70*(1), 9-18. doi:10.1016/j.alit.2020.11.001

Kawano, Y., Kikukawa, Y., Nakamura, M., Okuno, Y., Yuki, H., Fujiwara, S., . . . Hata, H. (2010). CD125-Expressing Myeloma: A Subgroup of Multiple Myeloma (MM) with Immature Phenotype, Endoplasmic Reticulum Stress Response and Low Sensitivity to Bortezomib. *Blood, 116*(21), 616-616. doi:10.1182/blood.V116.21.616.616 %J Blood

Ketelhuth, D. F., & Hansson, G. K. (2016). Adaptive Response of T and B Cells in Atherosclerosis. *Circ Res, 118*(4), 668-678. doi:10.1161/circresaha.115.306427

Khalsa, J. K., Cheng, N., Keegan, J., Chaudry, A., Driver, J., Bi, W. L., . . . Shah, K. (2020). Immune phenotyping of diverse syngeneic murine brain tumors identifies immunologically distinct types. *Nat Commun, 11*(1), 3912. doi:10.1038/s41467-020-17704-5

Kitaura, M., Nakajima, T., Imai, T., Harada, S., Combadiere, C., Tiffany, H. L., . . . Yoshie, O. (1996). Molecular cloning of human eotaxin, an eosinophil-selective CC chemokine, and identification of a specific eosinophil eotaxin receptor, CC chemokine receptor 3. *J Biol Chem, 271*(13), 7725-7730. doi:10.1074/jbc.271.13.7725

Kodali, R. B., Kim, W. J., Galaria, II, Miller, C., Schecter, A. D., Lira, S. A., & Taubman, M. B. (2004). CCL11 (Eotaxin) induces CCR3-dependent smooth muscle cell migration. *Arterioscler Thromb Vasc Biol, 24*(7), 1211-1216. doi:10.1161/01.ATV.0000131654.90788.f5

Kolaczkowska, E., & Kubes, P. (2013). Neutrophil recruitment and function in health and inflammation. *Nat Rev Immunol, 13*(3), 159-175. doi:10.1038/nri3399

Korbecki, J., Kojder, K., Simińska, D., Bohatyrewicz, R., Gutowska, I., Chlubek, D., & Baranowska-Bosiacka, I. (2020). CC Chemokines in a Tumor: A Review of Pro-Cancer and Anti-Cancer Properties of the Ligands of Receptors CCR1, CCR2, CCR3, and CCR4. *Int J Mol Sci, 21*(21). doi:10.3390/ijms21218412

Kraaijeveld, A. O., de Jager, S. C., van Berkel, T. J., Biessen, E. A., & Jukema, J. W. (2007). Chemokines and atherosclerotic plaque progression: towards therapeutic targeting? *Curr Pharm Des, 13*(10), 1039-1052. doi:10.2174/138161207780487584

Kratofil, R. M., Kubes, P., & Deniset, J. F. (2017). Monocyte Conversion During Inflammation and Injury. *Arterioscler Thromb Vasc Biol, 37*(1), 35-42. doi:10.1161/atvbaha.116.308198

Lacy, P., Rosenberg, H. F., & Walsh, G. M. (2021). Molecular Biology of Eosinophils: Introduction. *Methods Mol Biol, 2241*, 1-14. doi:10.1007/978-1-0716-1095-4_1

Lam, F. W., Vijayan, K. V., & Rumbaut, R. E. (2015). Platelets and Their Interactions with Other Immune Cells. *Compr Physiol, 5*(3), 1265-1280. doi:10.1002/cphy.c140074

Landmesser, U., Hornig, B., & Drexler, H. (2004). Endothelial function: a critical determinant in atherosclerosis? *Circulation, 109*(21 Suppl 1), II27-33.

Langer, H. F., & Chavakis, T. (2009). Leukocyte-endothelial interactions in inflammation. *J Cell Mol Med, 13*(7), 1211-1220. doi:10.1111/j.1582-4934.2009.00811.x

Langslet, G., Emery, M., & Wasserman, S. M. (2015). Evolocumab (AMG 145) for primary hypercholesterolemia. *Expert Rev Cardiovasc Ther, 13*(5), 477-488. doi:10.1586/14779072.2015.1030395

Langsted, A., Freiberg, J. J., & Nordestgaard, B. G. (2008). Fasting and nonfasting lipid levels: influence of normal food intake on lipids, lipoproteins, apolipoproteins, and cardiovascular risk prediction. *Circulation, 118*(20), 2047-2056. doi:10.1161/circulationaha.108.804146

Ley, K., Laudanna, C., Cybulsky, M. I., & Nourshargh, S. (2007). Getting to the site of inflammation: the leukocyte adhesion cascade updated. *Nat Rev Immunol, 7*(9), 678-689. doi:10.1038/nri2156

Li, Y., C, G. Z., Wang, X. H., & Liu, D. H. (2016). Progression of atherosclerosis in ApoE-knockout mice fed on a high-fat diet. *Eur Rev Med Pharmacol Sci, 20*(18), 3863-3867.

Li, Y., Zhao, Y., Qiu, C., Yang, Y., Liao, G., Wu, X., . . . Wang, Z. (2020). Role of eotaxin-1/CCL11 in sepsis-induced myocardial injury in elderly patients. *Aging (Albany NY), 12*(5), 4463-4473. doi:10.18632/aging.102896

Libby, P. (2021). The changing landscape of atherosclerosis. *Nature, 592*(7855), 524-533. doi:10.1038/s41586-021-03392-8

Libby, P., Buring, J. E., Badimon, L., Hansson, G. K., Deanfield, J., Bittencourt, M. S., . . . Lewis, E. F. (2019). Atherosclerosis. *Nat Rev Dis Primers, 5*(1), 56. doi:10.1038/s41572-019-0106-z

Libby, P., Ridker, P. M., & Hansson, G. K. (2011). Progress and challenges in translating the biology of atherosclerosis. *Nature, 473*(7347), 317-325. doi:10.1038/nature10146

Lieschke, S., Zechmeister, B., Haupt, M., Zheng, X., Jin, F., Hein, K., . . . Doeppner, T. R. (2019). CCL11 Differentially Affects Post-Stroke Brain Injury and Neuroregeneration in Mice Depending on Age. *Cells, 9*(1). doi:10.3390/cells9010066

Liu, C. L., Liu, X., Zhang, Y., Liu, J., Yang, C., Luo, S., . . . Shi, G. P. (2021). Eosinophils Protect Mice From Angiotensin-II Perfusion-Induced Abdominal Aortic Aneurysm. *Circ Res, 128*(2), 188-202. doi:10.1161/circresaha.120.318182

Liu, J., Yang, C., Liu, T., Deng, Z., Fang, W., Zhang, X., . . . Shi, G. P. (2020). Eosinophils improve cardiac function after myocardial infarction. *Nat Commun, 11*(1), 6396. doi:10.1038/s41467-020-19297-5

Loktionov, A. (2019). Eosinophils in the gastrointestinal tract and their role in the pathogenesis of major colorectal disorders. *World J Gastroenterol, 25*(27), 3503-3526. doi:10.3748/wjg.v25.i27.3503

Luo, Y., Cui, D., Yu, X., Chen, S., Liu, X., Tang, H., . . . Liu, L. J. P. o. (2016). Modeling of mechanical stress exerted by cholesterol crystallization on atherosclerotic plaques. *11*(5), e0155117.

Mancuso, M. E., & Santagostino, E. (2017). Platelets: much more than bricks in a breached wall. *Br J Haematol, 178*(2), 209-219. doi:10.1111/bjh.14653

Manne, B. K., Xiang, S. C., & Rondina, M. T. (2017). Platelet secretion in inflammatory and infectious diseases. *Platelets, 28*(2), 155-164. doi:10.1080/09537104.2016.1240766

Marichal, T., Mesnil, C., & Bureau, F. (2017). Homeostatic Eosinophils: Characteristics and Functions. *4*. doi:10.3389/fmed.2017.00101

Marques, P., Collado, A., Escudero, P., Rius, C., González, C., Servera, E., . . . Sanz, M. J. (2017). Cigarette Smoke Increases Endothelial CXCL16-Leukocyte CXCR6 Adhesion In Vitro and In Vivo. Potential Consequences in Chronic Obstructive Pulmonary Disease. *Front Immunol, 8*, 1766. doi:10.3389/fimmu.2017.01766

Marques, P., Collado, A., Martinez-Hervás, S., Domingo, E., Benito, E., Piqueras, L., . . . Sanz, M. J. (2019). Systemic Inflammation in Metabolic Syndrome: Increased Platelet and Leukocyte Activation, and Key Role of CX(3)CL1/CX(3)CR1 and CCL2/CCR2 Axes in Arterial Platelet-Proinflammatory Monocyte Adhesion. *J Clin Med, 8*(5). doi:10.3390/jcm8050708

Marx, C., Novotny, J., Salbeck, D., Zellner, K. R., Nicolai, L., Pekayvaz, K., . . . Stark, K. (2019). Eosinophil-platelet interactions promote atherosclerosis and stabilize thrombosis with eosinophil extracellular traps. *Blood, 134*(21), 1859-1872. doi:10.1182/blood.2019000518

Matthews, A. N., Friend, D. S., Zimmermann, N., Sarafi, M. N., Luster, A. D., Pearlman, E., . . . Rothenberg, M. E. (1998). Eotaxin is required for the baseline level of tissue eosinophils. *Proc Natl Acad Sci U S A, 95*(11), 6273-6278. doi:10.1073/pnas.95.11.6273

Mazor, R., Shurtz-Swirski, R., Farah, R., Kristal, B., Shapiro, G., Dorlechter, F., . . . Sela, S. (2008). Primed polymorphonuclear leukocytes constitute a possible link between inflammation and oxidative stress in hyperlipidemic patients. *Atherosclerosis, 197*(2), 937-943. doi:10.1016/j.atherosclerosis.2007.08.014

McBrien, C. N., & Menzies-Gow, A. (2017). The Biology of Eosinophils and Their Role in Asthma. *Front Med (Lausanne), 4*, 93. doi:10.3389/fmed.2017.00093

McEver, R. P. (2010). Rolling back neutrophil adhesion. *Nat Immunol, 11*(4), 282-284. doi:10.1038/ni0410-282

Medzhitov, R. (2008). Origin and physiological roles of inflammation. *Nature, 454*(7203), 428-435. doi:10.1038/nature07201

Mehta, A. K., Gracias, D. T., & Croft, M. (2018). TNF activity and T cells. *Cytokine, 101*, 14-18. doi:10.1016/j.cyto.2016.08.003

Menzies-Gow, A., Ying, S., Sabroe, I., Stubbs, V. L., Soler, D., Williams, T. J., & Kay, A. B. (2002). Eotaxin (CCL11) and eotaxin-2 (CCL24) induce recruitment of eosinophils, basophils, neutrophils, and macrophages as well as features of early- and late-phase allergic reactions following cutaneous injection in human atopic and nonatopic volunteers. *J Immunol, 169*(5), 2712-2718. doi:10.4049/jimmunol.169.5.2712

Michelson, A. D., Barnard, M. R., Krueger, L. A., Valeri, C. R., & Furman, M. I. (2001). Circulating monocyte-platelet aggregates are a more sensitive marker of in vivo platelet activation than platelet surface P-selectin: studies in baboons, human coronary intervention, and human acute myocardial infarction. *Circulation, 104*(13), 1533-1537. doi:10.1161/hc3801.095588

Miller, M. C., & Mayo, K. H. (2017). Chemokines from a Structural Perspective. *Int J Mol Sci, 18*(10). doi:10.3390/ijms18102088

Moore, K. J. (2019). Targeting inflammation in CVD: advances and challenges. *Nat Rev Cardiol, 16*(2), 74-75. doi:10.1038/s41569-018-0144-3

Moro-García, M. A., Mayo, J. C., Sainz, R. M., & Alonso-Arias, R. (2018). Influence of Inflammation in the Process of T Lymphocyte Differentiation: Proliferative, Metabolic, and Oxidative Changes. *Front Immunol, 9*, 339. doi:10.3389/fimmu.2018.00339

Murugappa, S., & Kunapuli, S. P. J. F. i. B.-L. (2006). The role of ADP receptors in platelet function. *11*(2), 1977-1986.

Mytilinaiou, M., Kyrou, I., Khan, M., Grammatopoulos, D. K., & Randeva, H. S. (2018). Familial Hypercholesterolemia: New Horizons for Diagnosis and Effective Management. *Front Pharmacol, 9*, 707. doi:10.3389/fphar.2018.00707

Nourshargh, S., & Alon, R. (2014). Leukocyte migration into inflamed tissues. *Immunity, 41*(5), 694-707. doi:10.1016/j.immuni.2014.10.008

O'Sullivan, J. A., & Bochner, B. S. (2018). Eosinophils and eosinophil-associated diseases: An update. *J Allergy Clin Immunol, 141*(2), 505-517. doi:10.1016/j.jaci.2017.09.022

Ogilvie, P., Bardi, G., Clark-Lewis, I., Baggiolini, M., & Uguccioni, M. (2001). Eotaxin is a natural antagonist for CCR2 and an agonist for CCR5. *Blood, 97*(7), 1920-1924. doi:10.1182/blood.v97.7.1920

Olson, N. C., Sallam, R., Doyle, M. F., Tracy, R. P., & Huber, S. A. (2013). T helper cell polarization in healthy people: implications for cardiovascular disease. *J Cardiovasc Transl Res, 6*(5), 772-786. doi:10.1007/s12265-013-9496-6

Onorato, A., & Sturm, A. C. (2016). Heterozygous Familial Hypercholesterolemia. *Circulation, 133*(14), e587-589. doi:10.1161/circulationaha.115.020701

Ozga, A. J., Chow, M. T., & Luster, A. D. (2021). Chemokines and the immune response to cancer. *Immunity, 54*(5), 859-874. doi:10.1016/j.immuni.2021.01.012

Palange, A. L., Di Mascolo, D., Singh, J., De Franceschi, M. S., Carallo, C., Gnasso, A., & Decuzzi, P. (2012). Modulating the vascular behavior of metastatic breast cancer cells by curcumin treatment. *Front Oncol, 2*, 161. doi:10.3389/fonc.2012.00161

Palframan, R. T., Collins, P. D., Williams, T. J., & Rankin, S. M. (1998). Eotaxin induces a rapid release of eosinophils and their progenitors from the bone marrow. *Blood, 91*(7), 2240-2248.

Pan, H., Xue, C., Auerbach, B. J., Fan, J., Bashore, A. C., Cui, J., . . . Reilly, M. P. (2020). Single-Cell Genomics Reveals a Novel Cell State During Smooth Muscle Cell Phenotypic Switching and Potential Therapeutic Targets for Atherosclerosis in Mouse and Human. *Circulation, 142*(21), 2060-2075. doi:10.1161/circulationaha.120.048378

Park, J. Y., Kang, Y. W., Choi, B. Y., Yang, Y. C., Cho, B. P., & Cho, W. G. (2017). CCL11 promotes angiogenic activity by activating the PI3K/Akt pathway in HUVECs. *J Recept Signal Transduct Res, 37*(4), 416-421. doi:10.1080/10799893.2017.1298132

Pease, J. E. (2006). Asthma, allergy and chemokines. *Curr Drug Targets, 7*(1), 3-12. doi:10.2174/138945006775270204

Pedro, T., Martinez-Hervas, S., Tormo, C., García-García, A. B., Saez-Tormo, G., Ascaso, J. F., . . . Real, J. T. (2013). Oxidative stress and antioxidant enzyme values in lymphomonocytes after an oral unsaturated fat load test in familial hypercholesterolemic subjects. *Transl Res, 161*(1), 50-56. doi:10.1016/j.trsl.2012.09.002

Pello, O. M., Silvestre, C., De Pizzol, M., & Andrés, V. (2011). A glimpse on the phenomenon of macrophage polarization during atherosclerosis. *Immunobiology, 216*(11), 1172-1176. doi:10.1016/j.imbio.2011.05.010

Perdomo, L., Beneit, N., Otero, Y. F., Escribano, Ó., Díaz-Castroverde, S., Gómez-Hernández, A., & Benito, M. (2015). Protective role of oleic acid against cardiovascular insulin resistance and in the early and late cellular atherosclerotic process. *Cardiovasc Diabetol, 14*, 75. doi:10.1186/s12933-015-0237-9

Periayah, M. H., Halim, A. S., & Mat Saad, A. Z. (2017). Mechanism Action of Platelets and Crucial Blood Coagulation Pathways in Hemostasis. *Int J Hematol Oncol Stem Cell Res, 11*(4), 319-327.

Petkovic, V., Moghini, C., Paoletti, S., Uguccioni, M., & Gerber, B. (2004). Eotaxin-3/CCL26 is a natural antagonist for CC chemokine receptors 1 and 5. A human chemokine with a regulatory role. *J Biol Chem, 279*(22), 23357-23363. doi:10.1074/jbc.M309283200

Petri, B., & Sanz, M. J. (2018). Neutrophil chemotaxis. *Cell Tissue Res, 371*(3), 425-436. doi:10.1007/s00441-017-2776-8

Pfirschke, C., Engblom, C., Gungabeesoon, J., Lin, Y., Rickelt, S., Zilionis, R., . . . Pittet, M. J. (2020). Tumor-Promoting Ly-6G(+) SiglecF(high) Cells Are Mature and Long-Lived Neutrophils. *Cell Rep, 32*(12), 108164. doi:10.1016/j.celrep.2020.108164

Pirillo, A., Catapano, A. L., & Norata, G. D. (2021). Monoclonal Antibodies in the Management of Familial Hypercholesterolemia: Focus on PCSK9 and ANGPTL3 Inhibitors. *Curr Atheroscler Rep, 23*(12), 79. doi:10.1007/s11883-021-00972-x

Polosukhina, D., Singh, K., Asim, M., Barry, D. P., Allaman, M. M., Hardbower, D. M., . . . Coburn, L. A. (2021). CCL11 exacerbates colitis and inflammation-associated colon tumorigenesis. *Oncogene, 40*(47), 6540-6546. doi:10.1038/s41388-021-02046-3

Postea, O., Vasina, E. M., Cauwenberghs, S., Projahn, D., Liehn, E. A., Lievens, D., . . . Koenen, R. R. (2012). Contribution of platelet CX(3)CR1 to platelet-monocyte complex formation and vascular recruitment during hyperlipidemia. *Arterioscler Thromb Vasc Biol, 32*(5), 1186-1193. doi:10.1161/atvbaha.111.243485

Poznyak, A. V., Bezsonov, E. E., Popkova, T. V., Starodubova, A. V., & Orekhov, A. N. (2021). Immunity in Atherosclerosis: Focusing on T and B Cells. *Int J Mol Sci, 22*(16). doi:10.3390/ijms22168379

Propper, D. J., & Balkwill, F. R. (2022). Harnessing cytokines and chemokines for cancer therapy. *Nat Rev Clin Oncol, 19*(4), 237-253. doi:10.1038/s41571-021-00588-9

Quandt, D., Rothe, K., Scholz, R., Baerwald, C. W., & Wagner, U. (2014). Peripheral CD4CD8 double positive T cells with a distinct helper cytokine profile are increased in rheumatoid arthritis. *PLoS One, 9*(3), e93293. doi:10.1371/journal.pone.0093293

Rabin, R. L. (2003). CC, C, and CX3C Chemokines. In H. L. Henry & A. W. Norman (Eds.), *Encyclopedia of Hormones* (pp. 255-263). New York: Academic Press.

Rafieian-Kopaei, M., Setorki, M., Doudi, M., Baradaran, A., & Nasri, H. (2014). Atherosclerosis: process, indicators, risk factors and new hopes. *Int J Prev Med, 5*(8), 927-946.

Rahman, M. J. A. s. (2006). Introduction to flow cytometry. *7*.

Rahman, T., Hamzan, N. S., Mokhsin, A., Rahmat, R., Ibrahim, Z. O., Razali, R., . . . Nawawi, H. (2017). Enhanced status of inflammation and endothelial activation in subjects with familial hypercholesterolaemia and their related unaffected family members: a case control study. *Lipids Health Dis, 16*(1), 81. doi:10.1186/s12944-017-0470-1

Rajendran, P., Rengarajan, T., Thangavel, J., Nishigaki, Y., Sakthisekaran, D., Sethi, G., & Nishigaki, I. (2013). The vascular endothelium and human diseases. *Int J Biol Sci, 9*(10), 1057-1069. doi:10.7150/ijbs.7502

Real, J. T., Martínez-Hervás, S., García-García, A. B., Civera, M., Pallardó, F. V., Ascaso, J. F., . . . Carmena, R. (2010). Circulating mononuclear cells nuclear factor-kappa B activity, plasma xanthine oxidase, and low grade inflammatory markers in adult patients with familial hypercholesterolaemia. *Eur J Clin Invest, 40*(2), 89-94. doi:10.1111/j.1365-2362.2009.02218.x

Reape, T. J., & Groot, P. H. (1999). Chemokines and atherosclerosis. *Atherosclerosis, 147*(2), 213-225. doi:10.1016/s0021-9150(99)00346-9

Reichman, H., Rozenberg, P., & Munitz, A. (2017). Mouse Eosinophils: Identification, Isolation, and Functional Analysis. *Curr Protoc Immunol, 119*, 14.43.11-14.43.22. doi:10.1002/cpim.35

Rius, C., Company, C., Piqueras, L., Cerdá-Nicolás, J. M., González, C., Servera, E., . . . Sanz, M. J. (2013). Critical role of fractalkine (CX3CL1) in cigarette smoke-induced mononuclear cell adhesion to the arterial endothelium. *Thorax, 68*(2), 177-186. doi:10.1136/thoraxjnl-2012-202212

Rius, C., Piqueras, L., González-Navarro, H., Albertos, F., Company, C., López-Ginés, C., . . . Sanz, M. J. (2013). Arterial and venous endothelia display differential functional fractalkine (CX3CL1) expression by angiotensin-II. *Arterioscler Thromb Vasc Biol, 33*(1), 96-104. doi:10.1161/atvbaha.112.254870

Romagnani, S. (2002). Cytokines and chemoattractants in allergic inflammation. *Mol Immunol, 38*(12-13), 881-885. doi:10.1016/s0161-5890(02)00013-5

Rosenberg, H. F., Dyer, K. D., & Foster, P. S. (2013). Eosinophils: changing perspectives in health and disease. *Nat Rev Immunol, 13*(1), 9-22. doi:10.1038/nri3341

Rothenberg, M. E., & Hogan, S. P. (2006). The eosinophil. *Annu Rev Immunol, 24*, 147-174. doi:10.1146/annurev.immunol.24.021605.090720

Roy, I., Evans, D. B., & Dwinell, M. B. (2014). Chemokines and chemokine receptors: update on utility and challenges for the clinician. *Surgery, 155*(6), 961-973. doi:10.1016/j.surg.2014.02.006

Ryu, S., Shin, J. W., Kwon, S., Lee, J., Kim, Y. C., Bae, Y. S., . . . Kim, H. Y. (2022). Siglec-F-expressing neutrophils are essential for creating a profibrotic microenvironment in renal fibrosis. *J Clin Invest, 132*(12). doi:10.1172/jci156876

Saigusa, R., Winkels, H., & Ley, K. (2020). T cell subsets and functions in atherosclerosis. *Nat Rev Cardiol, 17*(7), 387-401. doi:10.1038/s41569-020-0352-5

Salcedo, R., Young, H. A., Ponce, M. L., Ward, J. M., Kleinman, H. K., Murphy, W. J., & Oppenheim, J. J. (2001). Eotaxin (CCL11) induces in vivo angiogenic responses by human CCR3+ endothelial cells. *J Immunol, 166*(12), 7571-7578. doi:10.4049/jimmunol.166.12.7571

Sallusto, F., Mackay, C. R., & Lanzavecchia, A. (1997). Selective expression of the eotaxin receptor CCR3 by human T helper 2 cells. *Science, 277*(5334), 2005-2007. doi:10.1126/science.277.5334.2005

Sampietro, T., Tuoni, M., Ferdeghini, M., Ciardi, A., Marraccini, P., Prontera, C., . . . Bionda, A. (1997). Plasma cholesterol regulates soluble cell adhesion molecule expression in familial hypercholesterolemia. *Circulation, 96*(5), 1381-1385. doi:10.1161/01.cir.96.5.1381

Sanz, M. J., Ponath, P. D., Mackay, C. R., Newman, W., Miyasaka, M., Tamatani, T., . . . Jose, P. J. (1998). Human eotaxin induces alpha 4 and beta 2 integrin-dependent eosinophil accumulation in rat skin in vivo: delayed generation of eotaxin in response to IL-4. *J Immunol, 160*(7), 3569-3576.

Schnoor, M., Alcaide, P., Voisin, M. B., & van Buul, J. D. (2015). Crossing the Vascular Wall: Common and Unique Mechanisms Exploited by Different Leukocyte Subsets during Extravasation. *Mediators Inflamm, 2015*, 946509. doi:10.1155/2015/946509

Schober, A., Manka, D., von Hundelshausen, P., Huo, Y., Hanrath, P., Sarembock, I. J., . . . Weber, C. (2002). Deposition of platelet RANTES triggering monocyte recruitment requires P-selectin and is involved in neointima formation after arterial injury. *Circulation, 106*(12), 1523-1529. doi:10.1161/01.cir.0000028590.02477.6f

Shantsila, E., Wrigley, B., Tapp, L., Apostolakis, S., Montoro-Garcia, S., Drayson, M. T., & Lip, G. Y. (2011). Immunophenotypic characterization of human monocyte subsets: possible implications for cardiovascular disease pathophysiology. *J Thromb Haemost, 9*(5), 1056-1066. doi:10.1111/j.1538-7836.2011.04244.x

Sharifi, M., Futema, M., Nair, D., & Humphries, S. E. (2019). Polygenic Hypercholesterolemia and Cardiovascular Disease Risk. *Curr Cardiol Rep, 21*(6), 43. doi:10.1007/s11886-019-1130-z

Sharma, M., Schlegel, M. P., Afonso, M. S., Brown, E. J., Rahman, K., Weinstock, A., . . . Moore, K. J. (2020). Regulatory T Cells License Macrophage Pro-Resolving Functions During Atherosclerosis Regression. *Circ Res, 127*(3), 335-353. doi:10.1161/circresaha.119.316461

Sherwood, E. R., & Toliver-Kinsky, T. (2004). Mechanisms of the inflammatory response. *Best Pract Res Clin Anaesthesiol, 18*(3), 385-405. doi:10.1016/j.bpa.2003.12.002

Soehnlein, O., & Lindbom, L. (2010). Phagocyte partnership during the onset and resolution of inflammation. *Nat Rev Immunol, 10*(6), 427-439. doi:10.1038/nri2779

Sreejit, G., Johnson, J., Jaggers, R. M., Dahdah, A., Murphy, A. J., Hanssen, N. M. J., & Nagareddy, P. R. (2022). Neutrophils in cardiovascular disease: warmongers, peacemakers, or both? *Cardiovasc Res, 118*(12), 2596-2609. doi:10.1093/cvr/cvab302

Suzuki, Y., Yamaguchi, M., Mori, M., Sugimoto, N., Suzukawa, M., Iikura, M., . . . Ohta, K. (2021). Eotaxin (CCL11) enhances mediator release from human basophils. *Allergy, 76*(11), 3549-3552. doi:10.1111/all.14975

Tabas, I., García-Cardeña, G., & Owens, G. K. (2015). Recent insights into the cellular biology of atherosclerosis. *J Cell Biol, 209*(1), 13-22. doi:10.1083/jcb.201412052

Tao, Z., Zhu, H., Zhang, J., Huang, Z., Xiang, Z., & Hong, T. (2022). Recent advances of eosinophils and its correlated diseases. *Front Public Health, 10*, 954721. doi:10.3389/fpubh.2022.954721

Taylan, C., & Weber, L. T. (2022). An update on lipid apheresis for familial hypercholesterolemia. *Pediatr Nephrol*. doi:10.1007/s00467-022-05541-1

Tian, M., Chen, L., Ma, L., Wang, D., Shao, B., Wu, J., . . . Jin, Y. (2016). Expression and prognostic significance of CCL11/CCR3 in glioblastoma. *Oncotarget, 7*(22), 32617-32627. doi:10.18632/oncotarget.8958

Tokgozoglu, L., & Kayikcioglu, M. (2021). Familial Hypercholesterolemia: Global Burden and Approaches. *Curr Cardiol Rep, 23*(10), 151. doi:10.1007/s11886-021-01565-5

Trinder, M., Francis, G. A., & Brunham, L. R. (2020). Association of Monogenic vs Polygenic Hypercholesterolemia With Risk of Atherosclerotic Cardiovascular Disease. *JAMA Cardiol, 5*(4), 390-399. doi:10.1001/jamacardio.2019.5954

Tse, K., Tse, H., Sidney, J., Sette, A., & Ley, K. (2013). T cells in atherosclerosis. *International Immunology, 25*(11), 615-622. doi:10.1093/intimm/dxt043 %J International Immunology

Urra, X., Villamor, N., Amaro, S., Gómez-Choco, M., Obach, V., Oleaga, L., . . . Chamorro, A. (2009). Monocyte subtypes predict clinical course and prognosis in human stroke. *J Cereb Blood Flow Metab, 29*(5), 994-1002. doi:10.1038/jcbfm.2009.25

Vafadarnejad, E., Rizzo, G., Krampert, L., Arampatzi, P., Arias-Loza, A. P., Nazzal, Y., . . . Cochain, C. (2020). Dynamics of Cardiac Neutrophil Diversity in Murine Myocardial Infarction. *Circ Res, 127*(9), e232-e249. doi:10.1161/circresaha.120.317200

van Duijn, J., Kritikou, E., Benne, N., van der Heijden, T., van Puijvelde, G. H., Kröner, M. J., . . . Slütter, B. (2019). CD8+ T-cells contribute to lesion stabilization in advanced atherosclerosis by limiting macrophage content and CD4+ T-cell responses. *Cardiovasc Res, 115*(4), 729-738. doi:10.1093/cvr/cvy261

Vass, M., Kooistra, A. J., Yang, D., Stevens, R. C., Wang, M. W., & de Graaf, C. (2018). Chemical Diversity in the G Protein-Coupled Receptor Superfamily. *Trends Pharmacol Sci, 39*(5), 494-512. doi:10.1016/j.tips.2018.02.004

von Hundelshausen, P., & Schmitt, M. M. (2014). Platelets and their chemokines in atherosclerosis-clinical applications. *Front Physiol, 5*, 294. doi:10.3389/fphys.2014.00294

von Hundelshausen, P., Weber, K. S., Huo, Y., Proudfoot, A. E., Nelson, P. J., Ley, K., & Weber, C. (2001). RANTES deposition by platelets triggers monocyte arrest on inflamed and atherosclerotic endothelium. *Circulation, 103*(13), 1772-1777. doi:10.1161/01.cir.103.13.1772

Wakabayashi, K., Isozaki, T., Tsubokura, Y., Fukuse, S., & Kasama, T. (2021). Eotaxin-1/CCL11 is involved in cell migration in rheumatoid arthritis. *Sci Rep, 11*(1), 7937. doi:10.1038/s41598-021-87199-7

Wakefield, P. E., James, W. D., Samlaska, C. P., & Meltzer, M. S. (1991). Tumor necrosis factor. *J Am Acad Dermatol, 24*(5 Pt 1), 675-685. doi:10.1016/0190-9622(91)70102-8

Weber, C., Shantsila, E., Hristov, M., Caligiuri, G., Guzik, T., Heine, G. H., . . . Lip, G. Y. (2016). Role and analysis of monocyte subsets in cardiovascular disease. Joint consensus document of the European Society of Cardiology (ESC) Working Groups “Atherosclerosis & Vascular Biology” and “Thrombosis”. *Thromb Haemost, 116*(4), 626-637. doi:10.1160/th16-02-0091

Weber, K. S., Nelson, P. J., Gröne, H. J., & Weber, C. (1999). Expression of CCR2 by endothelial cells : implications for MCP-1 mediated wound injury repair and In vivo inflammatory activation of endothelium. *Arterioscler Thromb Vasc Biol, 19*(9), 2085-2093. doi:10.1161/01.atv.19.9.2085

Willems, L. I., & Ijzerman, A. P. (2010). Small molecule antagonists for chemokine CCR3 receptors. *Med Res Rev, 30*(5), 778-817. doi:10.1002/med.20181

Wolf, D., & Ley, K. (2019). Immunity and Inflammation in Atherosclerosis. *Circ Res, 124*(2), 315-327. doi:10.1161/circresaha.118.313591

Wolfs, I. M., Donners, M. M., & de Winther, M. P. (2011). Differentiation factors and cytokines in the atherosclerotic plaque micro-environment as a trigger for macrophage polarisation. *Thromb Haemost, 106*(5), 763-771. doi:10.1160/th11-05-0320

World Health Organization cardiovascular disease risk charts: revised models to estimate risk in 21 global regions. (2019). *Lancet Glob Health, 7*(10), e1332-e1345. doi:10.1016/s2214-109x(19)30318-3

Wu, D., Molofsky, A. B., Liang, H. E., Ricardo-Gonzalez, R. R., Jouihan, H. A., Bando, J. K., . . . Locksley, R. M. (2011). Eosinophils sustain adipose alternatively activated macrophages associated with glucose homeostasis. *Science, 332*(6026), 243-247. doi:10.1126/science.1201475

Wu, H., & Ballantyne, C. M. (2017). Dyslipidaemia: PCSK9 inhibitors and foamy monocytes in familial hypercholesterolaemia. *Nat Rev Cardiol, 14*(7), 385-386. doi:10.1038/nrcardio.2017.75

Xenakis, J. J., Howard, E. D., Smith, K. M., Olbrich, C. L., Huang, Y., Anketell, D., . . . Spencer, L. A. (2018). Resident intestinal eosinophils constitutively express antigen presentation markers and include two phenotypically distinct subsets of eosinophils. *Immunology, 154*(2), 298-308. doi:10.1111/imm.12885

Xing, Y., Tian, Y., Kurosawa, T., Matsui, S., Touma, M., Yanai, T., . . . Sugimoto, K. (2016). CCL11-induced eosinophils inhibit the formation of blood vessels and cause tumor necrosis. *Genes Cells, 21*(6), 624-638. doi:10.1111/gtc.12371

Xu, J. Y., Xiong, Y. Y., Tang, R. J., Jiang, W. Y., Ning, Y., Gong, Z. T., . . . Yang, Y. J. (2022). Interleukin-5-induced eosinophil population improves cardiac function after myocardial infarction. *Cardiovasc Res, 118*(9), 2165-2178. doi:10.1093/cvr/cvab237

Yoshimoto, T. (2018). The Hunt for the Source of Primary Interleukin-4: How We Discovered That Natural Killer T Cells and Basophils Determine T Helper Type 2 Cell Differentiation In Vivo. *Front Immunol, 9*, 716. doi:10.3389/fimmu.2018.00716

Zernecke, A., & Weber, C. (2010). Chemokines in the vascular inflammatory response of atherosclerosis. *Cardiovasc Res, 86*(2), 192-201. doi:10.1093/cvr/cvp391

Zhang, J. M., & An, J. (2007). Cytokines, inflammation, and pain. *Int Anesthesiol Clin, 45*(2), 27-37. doi:10.1097/AIA.0b013e318034194e

Zhang, J. Q., Biedermann, B., Nitschke, L., & Crocker, P. R. (2004). The murine inhibitory receptor mSiglec-E is expressed broadly on cells of the innate immune system whereas mSiglec-F is restricted to eosinophils. *Eur J Immunol, 34*(4), 1175-1184. doi:10.1002/eji.200324723

Zhang, M., Angata, T., Cho, J. Y., Miller, M., Broide, D. H., & Varki, A. (2007). Defining the in vivo function of Siglec-F, a CD33-related Siglec expressed on mouse eosinophils. *Blood, 109*(10), 4280-4287. doi:10.1182/blood-2006-08-039255

Zhang, M., Zhu, Z. L., Gao, X. L., Wu, J. S., Liang, X. H., & Tang, Y. L. (2018). Functions of chemokines in the perineural invasion of tumors (Review). *Int J Oncol, 52*(5), 1369-1379. doi:10.3892/ijo.2018.4311

Zhao, Y., Vanhoutte, P. M., & Leung, S. W. (2015). Vascular nitric oxide: Beyond eNOS. *J Pharmacol Sci, 129*(2), 83-94. doi:10.1016/j.jphs.2015.09.002

Zieske, A. W., Tracy, R. P., McMahan, C. A., Herderick, E. E., Homma, S., Malcom, G. T., . . . Strong, J. P. (2005). Elevated serum C-reactive protein levels and advanced atherosclerosis in youth. *Arterioscler Thromb Vasc Biol, 25*(6), 1237-1243. doi:10.1161/01.Atv.0000164625.93129.64

Zlotnik, A., & Yoshie, O. (2012). The chemokine superfamily revisited. *Immunity, 36*(5), 705-716. doi:10.1016/j.immuni.2012.05.008